SYNTHESIS AND CRYSTAL CHEMISTRY OF LANTHANIDE ALLANITES

by

Kathleen Ann Affholter

Dissertation submitted to the Faculty of the

Virginia Polytechnic Institute and State University

in partial fulfillment of the requirements for the degree of

DOCTOR OF PHILOSOPHY

in

Geological Sciences

APPROVED:

_____

D. A. Hewitt, Chairman

F. D. Bloss	G. V. Gibbs
P. H. Ribbe	J. A. Speer

December, 1987

Blacksburg, Virginia

SYNTHESIS AND CRYSTAL CHEMISTRY OF LANTHANIDE ALLANITES

by

Kathleen Ann Affholter

(ABSTRACT)

Metamictization and complex chemistry are major obstacles to the crystal chemical characterization of natural allanites. To overcome these problems, allanites, $Ca(REE)Fe^{2+}Al_2Si_3O_{12}(OH)$, where REE = La, La-Ce, Ce, Nd, Sm, Eu, Gd, Er, Dy, Yb and Y have been synthesized hydrothermally from unbuffered and buffered oxide mixes at 500 to 650°C, 5.5 kbar (550 MPa), and 700 to 725°C, 4 kbar (400 MPa). Although allanite is readily synthesized, high yields are obtained only for allanite-(LREE) compositions, and end-member composition is obtained only for allanite-(La). Er and Yb ions are too small to substitute at the A(2) site in allanite, but a small amount can substitute at the VI-coordinated M(3) site. Fe^{2+} in the M(3) site favors LREE substitution, which supports the contention that allanite is Ce-selective.

At 800°C, 1 kbar, and 0.25 $X(H_2O)$, synthetic allanite-(Ce) decomposes to britholite, anorthite, magnetite, quartz and a Ce-silicate (cheralite?). At T > 800°C and P = 1 atmosphere, natural allanite decomposes to britholite, anorthite, magnetite, quartz and cerianite. At higher pressure, cerianite may combine with quartz to form cheralite. An example of allanite after britholite occurs at Jamestown, Colorado, where britholite from a vein cutting aplite-pegmatite was previously misidentified as cerite.

Infrared absorption spectra were measured in the range 4000 to 200 cm^{-1} for the synthetic allanites, where REE = La, Ce, Nd, Sm, Gd, Y, Er, Yb. The OH band positions (in wavenumbers) depend on the valence of the cation substituting in the A(2) and M(3)

sites, not M(3) only, as in the case of zoisite, clinozoisite and epidote. Divalent cations in the M(3) site yield a lower frequency OH band (3150) while divalent cations in the A(2) site or trivalent cations in the M(3) site yield a higher frequency vibration (3380). The band at 2160, which has been reported to be present in zoisite but not clinozoisite - epidote, is present in those allanites with a 3150 peak. Allanite-(La) has one band at 3150, while Er and Yb compositions have a strong band at 3380 similar to that of epidote. Oxyallanite if totally deprotonated has no OH stretching band. With partial oxidation, a higher frequency band (3380) is present, similar to that of epidote. The higher thermal stability observed for allanite as compared to epidote is consistent with the stronger OH bond measured in allanite. The stability of these similar structures is determined by their weakest bonds.

Site occupation of ferrous and ferric iron in the synthetic allanites with REE = La, La-Ce, Ce, Sm, Gd, Dy and Yb and two natural epidotes have been analyzed by ^{57}Fe Mössbauer spectroscopy. Substitution of trivalent REE into the A site of the allanite structure is compensated by substitution of ferrous iron in the M(3) site. Distortion of this site is sensitive to compositional changes giving rise to large variations of the Fe^{3+} quadrupole splittings. Ferrous iron also occupies an A site and the amount increases as the size and amount of REE decreases.

ACKNOWLEDGMENTS

As Bertrand Russell said, "The good life is one inspired by love and guided by knowledge." First, I would like to thank those people I love the most: my lifemate, , whose creativity, sense of humor, and patience sustained me through this project; my creative and shining mother, , whose confidence in her children never fails; my father, , who inspired my interest in learning and discovery, and discouraged my tendencies to be less than I am capable; my sister and best friend, , always there to share her perceptive view of life; and my brothers, , and , who taught me to fight back. Special thanks go to the family, all of my students, and all of my other friends who were my sounding boards. Many, many thanks also go to , who let me share her apartment, wear her clothes, drive her car and eat her peanut butter; to , who typed many of the tables and much of the text, , who helped with photographs and slides, and who skillfully drafted several figures. Most of the figures were drafted on a computer using the program Telagraf. Other clerical assistance was provided by , , , , and .

I benefited greatly from my principal advisor, Dr. David A. Hewitt. Dave shared his knowledge of high pressure and temperature synthesis techniques and geochemistry. The relentless Dr. Jerry Gibbs skillfully answered my many questions concerning the mineralogy of allanite. Dr. F. D. Bloss provided personal qualities for which I strive, and Dr. Alex Speer encouraged me and offered sound advice when I needed it most. Dr. David Wones shared his enthusiasm for science, which was his trademark. After Dr. Wones tragic death, Dr. Ribbe kindly accepted to become a committee member. I thank all my committee members for reading this manuscript and making positive suggestions.

Dr. Jurgen Abrecht first showed me around the hydrothermal laboratory while he was doing research with Dr. Hewitt at VPI&SU. Dr. Hans Annersten provided the ^{57}Fe Mossbauer data on my synthetic and natural allanite samples. supplied the natural epidote and Dr. Cech supplied the natural allanite. provided the sample of "cerite" rock from Jamestown, Colorado, and provided literature tabulations of allanite chemical analyses. guided me through the electron microprobe analytical techniques which were a special problem with the fine particles I synthesized. Drs. Zelazny and Graybeal generously allowed me to freely use equipment in agronomy and chemistry to obtain the infrared spectra. instructed me in some techniques of IR spectroscopy. The Analytical Electron Microscopy was completed in the Electron Microbeam Analysis Facility in the Department of Geology and Institute of Meteoritics at the University of New Mexico, courtesy of .

Finally, I want to thank the Department of Geological Sciences, and two other departments on campus. I thank the VPI&SU geology department, secretaries and staff, for stressing a professional attitude, offering me numerous opportunities to go to professional meetings, providing me scholarship monies, and encouraging me to reach my own personal goals. I thank the Learning Resources Center and Physical Education department with their outstanding staffs, for keeping me sane and healthy.

CONTENTS

Appendix page

Chapter I

REVIEW OF THE EPIDOTE GROUP NOMENCLATURE AND CRYSTAL CHEMISTRY

INTRODUCTION

Epidotes are important rock-forming minerals, exhibiting wide chemical variation and a variety of parageneses. Some epidote group minerals are common constituents of acid plutonic rocks, while others are important in low-to-medium grade metamorphic rocks. Less commonly, they occur in eclogites and rhyolites.

The epidotes crystallize in two crystal systems, monoclinic and orthorhombic. The wide chemical variations within the group result from "flexible" geometry of the crystal structure, i.e., several crystallographically unique sites are available to accommodate cations of formal charge 1+ to 4+ and ionic radius 0.70 to 1.80 A.

Because of the chemical and structural complexities, considerable attention has been given to most members of this mineral group. The application of improved x-ray diffraction, mineral analysis, and spectroscopic techniques has resulted in a proliferation of predominantly chemical and some structural data. A review of the nomenclature and crystal chemistry of the epidote group minerals is presented in this chapter to provide background for the research presented in the remaining chapters.

NOMENCLATURE

There are several names assigned to the epidote group minerals because of the many chemical substitutions that may occur, and because of the existence of distinct monoclinic and orthorhombic structures. In general, the nomenclature gives no clue to the chemical nature of the phases. It neglects divalent and tetravalent ionic substitutions and has

ambiguous prefixes such as α and ß (which are more properly used to imply a structural phase change as in α- and ß-quartz). In the case of α- and ß-zoisite, the same name is defined in two different ways.

Fleischer (1987) lists eight mineral species for the epidote group (Table 1). In the literature, at least 30 names may be classified under these species headings. These include varieties, synonyms, discredited mineral names, and miscellaneous names given by authors to suit their particular needs. Epidote compositions in the literature are commonly referred to as combinations of the hypothetical iron end-member, pistacite, Ps ($Ca_2Fe^{3+}_3Si_3O_{12}(OH)$), the aluminum end-member, clinozoisite, Cz ($Ca_2Al^{3+}_3Si_3O_{12}(OH)$), and/or the manganese end-member, piemontite, Pm ($Ca_2Mn^{3+}_3Si_3O_{12}(OH)$). In this manner, common epidote is approximately $Cz_{70}Ps_{30}$, clinozoisite $Cz_{89}Ps_{11}$, ß-zoisite $Cz_{95}Ps_5$, α-zoisite $Cz_{95\text{-}100}Ps_{0\text{-}5}$, and piemontite $Cz_{40\text{-}75}Ps_{13\text{-}23}Pm_{47\text{-}2}$ (Strens, 1963, 1964a). This chemical classification of zoisite was originally based on four chemical analyses (Tempel, 1938). Other workers (Bloss, 1985; Enami and Banno, 1977; Meyer, 1966; Deer et al., 1966; Wolff, 1941) prefer to describe zoisite according to its optical properties: α-zoisite has the optic plane parallel to the (100) cleavage, ß-zoisite has the optic plane perpendicular to the (100) cleavage. They report that iron-rich zoisite (Fe > 0.30 atoms/12.5 anions) has the optical properties of α-zoisite whereas iron-poor zoisite (Fe ≤ 0.30 atoms/12.5 anions) has the optical properties of ß-zoisite, the opposite of the above chemical classification. Based on current data, the optical definition of α and ß-zoisite is more appropriate than the chemical one of Strens (1963, 1964a).

The uncertainty about a complete solid solution between epidote and allanite has led authors to assign various names to the intermediate compositions, such as "brithionite" or

Table 1. Epidote group nomenclature.

name	crystal system	space group	optic sign	ideal chemical formula
epidote	mon	$P2_1/m$	B(-)	$Ca_2Fe^{3+}Al_2O{\cdot}OH(Si_2O_7)(SiO_4)$
pistacite*	mon	$P2_1/m$	B(-)	$Ca_2Fe^{3+}Al_2O{\cdot}OH(Si_2O_7)(SiO_4)$
tawmanite*	mon	$P2_1/m$	B(-)	$Ca_2(Fe^{3+},Cr^{3+})Al_2O{\cdot}OH(Si_2O_7)(SiO_4)$
hancockite	mon	$P2_1/m$	B(-)	$(Ca,Mn^{2+},Sr,Pb)_2Fe^{3+}Al_2O{\cdot}OH(Si_2O_7)(SiO_4)$
clinozoisite	mon	$P2_1/m$	B(+)	$Ca_2Al^{3+}Al_2O{\cdot}OH(Si_2O_7)(SiO_4)$
mukhinite	mon	$P2_1/m$	B(+)	$Ca_2V^{3+}Al_2O{\cdot}OH(Si_2O_7)(SiO_4)$
zoisite	orth	Pnma	B(+)	$Ca_2Al^{3+}Al_2O{\cdot}OH(Si_2O_7)(SiO_4)$
α -zoisite**	orth	Pnma	B(+)	$Ca_2Al^{3+}Al_2O{\cdot}OH(Si_2O_7)(SiO_4)$
β-zoisite***	orth	Pnma	B(+)	$Ca_2Al^{3+}Al_2O{\cdot}OH(Si_2O_7)(SiO_4)$
tanzanite*	orth	Pnma	B(+)	$Ca_2V^{3+}Al_2O{\cdot}OH(Si_2O_7)(SiO_4)$
thulite*	mon orth	$P2_1/m$ Pnma	B(+) B(+)	$(Ca,Mn^{2+})_2Al^{3+}Al_2O{\cdot}OH(Si_2O_7)(SiO_4)$
piemontite	mon	$P2_1/m$	B(+)	$Ca_2Al^{3+}(Mn^{3+},Fe^{3+},Al^{3+})_2O{\cdot}OH(Si_2O_7)(SiO_4)$
withamite*	mon	$P2_1/m$	B(+)	$Ca_2Al^{3+}(Mn^{3+},Fe^{3+},Al^{3+})_2O{\cdot}OH(Si_2O_7)(SiO_4)$
allanite-(Ce)	mon	$P2_1/m$	B(+/-)	$(Ca,Ce,La,Y)_2Fe^{2+}Al_2O{\cdot}OH(Si_2O_7)(SiO_4)$
allanite-(La)	mon	$P2_1/m$	B(+/-)	$(Ca,La,Ce,Y)_2Fe^{2+}Al_2O{\cdot}OH(Si_2O_7)(SiO_4)$
allanite-(Y) (yttro-orthite)	mon	$P2_1/m$	B(+/-)	$(Ca,Y,Ce,La)_2Fe^{2+}Al_2O{\cdot}OH(Si_2O_7)(SiO_4)$
oxyallanite*	mon	$P2_1/m$	B(+)	$(Ca,REE^{3+})_2(Fe^{3+},Fe^{2+})Al_2O{\cdot}O(Si_2O_7)(SiO_4)$

*varietal name
**optic axial plane (100)
***optic axial plane (010)

"REE epidote," and to suggest values to delimit "REE epidote" from allanite. Cech and Povondra (1972) propose a boundary between epidote and allanite based on REE composition. Using the general formula $Ca(Ca_{0.5}REE_{0.5})(Fe^{2+},Fe^{3+},Al^{3+})_3Si_3O_{12}(OH)$, they suggest that compositions with REE less than 0.5 be named REE-bearing epidote and those with REE greater than 0.5, allanite. They do not propose a boundary between epidote and REE-bearing epidote.

Within the larger set of silicates, the epidote group minerals are considered sorosilicates with mixed silicate anions (Strunz, 1986, 1966), mixed anion silicates (with isolated SiO_4 and Si_2O_7 groups) (Liebau, 1980), and silicates with isolated tetrahedra and a sharing coefficient of 1.162 (Zoltai, 1960). The first two classifications are essentially the same, giving qualitative information about the silicate tetrahedra in the structure. Zoltai's classification is more useful for quantitative information. The sharing coefficient of 1.162 means that 16.2 percent of the corners in the silicate tetrahedra are bridging and 83.8 percent are non-bridging. In a more comprehensive classification of oxyanion compounds being developed by Hawthorne (1987), the epidote group minerals are considered framework structures because of their 3-dimensional linkage of octahedra and tetrahedra.

Throughout this work, the nomenclature for rare earth minerals proposed by Levinson (1966) is adopted. The name for each rare earth mineral has a suffix "-(REE)".

CRYSTAL STRUCTURE

Members of the epidote group crystallize with both monoclinic $P2_1/m$ and orthorhombic Pnma symmetry. The epidote structure consists of two large coordination (VII-XI) polyhedra occupied by A cations [A(1) = Ca; A(2) = Ca, REE, Pb, Sr, Mn^{2+}, and others], three octahedral sites occupied by M cations (M(1), M(2) = Fe^{3+}, Al^{3+}, Mn^{3+}, and

others, M(3) = Fe^{2+}, Fe^{3+}), and the silicate polyanions, SiO_4^{4-} and $Si_2O_7^{6-}$ (Fig. 1). Chain of the M octahedra share edges and are parallel to the **b**-axis. The orthorhombic epidotes have one type of chain (Fig. 2) composed of two nonequivalent octahedra, M(1,2) = M(3). The number of shared edges per octahedron is three for M(1,2) and two for M(3). The monoclinic epidotes have two types of chains (Fig. 2), one chain with a single type of octahedron, M(2), and one with two nonequivalent octahedra, M(1) and M(3). The number of shared edges per octahedron is four for M(1), two for M(2) and M(3). In both orthorhombic and monoclinic epidotes, the chains of octahedra are connected by corner-sharing SiO_4 and Si_2O_7 groups. The A cations within the large irregular polyhedral cavities have been assigned various coordination numbers (A-O bond lengths vary from 2.30 to 3.13 A). These range from VII for A(1) and A(2) for an orthorhombic epidote to VII-XI for A(1) and VIII-XI for A(2) in monoclinic epidotes (Dollase, 1971). Based on bond strength calculations for oxygen atoms (Dollase, 1968; Gabe et al., 1973) and infrared spectroscopy (Hanisch and Zemann, 1966; Linke, 1970), it was concluded that hydrogen atoms are bonded in both structure types to O(10) so as to form a hydrogen bond to O(4) (see Fig. 1). This conclusion was based on crystal chemical arguments (Ito, et al., 1954), bond strength calculations for oxygen atoms (Dollase, 1968; Gabe et al., 1973), and IR experiments with oriented crystal sections using polarized radiation (Hanisch and Zemann, 1966; Linke, 1970), Langer and Raith (1974) suggest that some of the H atoms in zoisite are bonded to oxygens other than O(10) and O(4); however, they could not make a conclusive statement. In allanite, the H position has not been determined by single-crystal x-ray structure refinement, and IR spectra collected (Cech et al., 1972) in the appropriate regions to elucidate H bonding are not interpretable. Neutron diffraction has not been used to determine the H positions in any of the epidote structures.

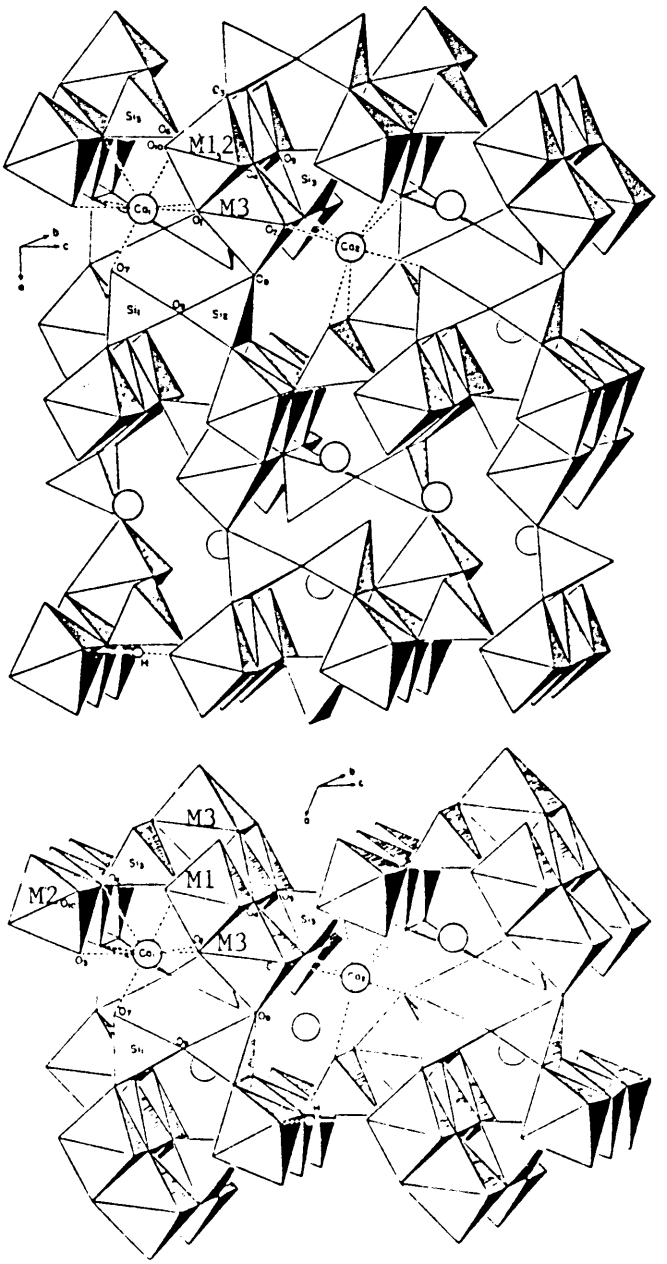

Figure 1. Polyhedral structure drawings for (a) zoisite and (b) clinozoisite as viewed nearly along the **b**-axis (Dollase, 1968). In zoisite and clinozoisite, the M sites are occupied by Al and the A sites by Ca.

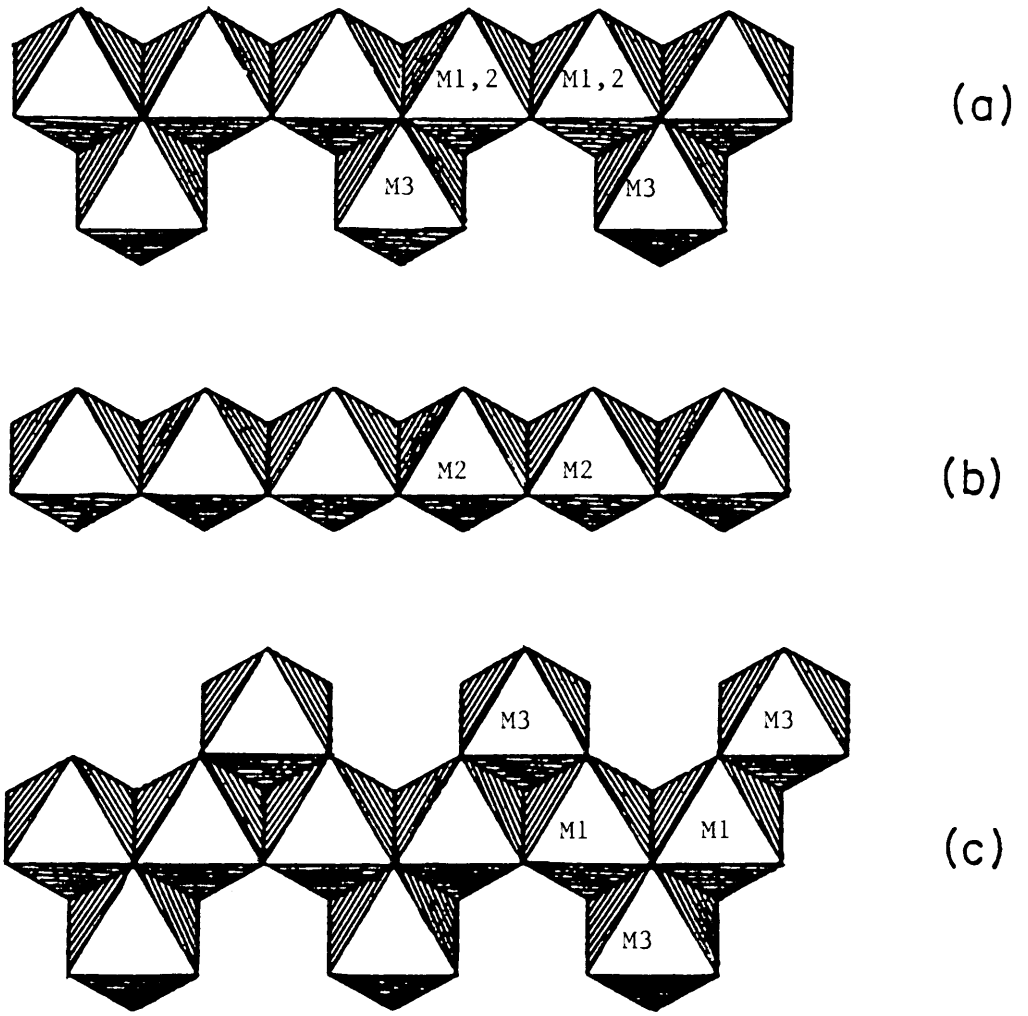

Figure 2. Idealized octahedral chains in zoisite (a) and clinozoisite (b) and (c) (after Dollase, 1968).

Allanite has $P2_1/m$ space group symmetry with two formula units per cell. The cell for a typical natural allanite-(Ce) is slightly larger than for the other epidotes (Dollase, 1971). Three of the 10 oxygens are in general positions, M(1) and M(2) are on inversion centers, and all other atoms are on the mirror planes perpendicular to **b**. Four structure refinements (Dollase, 1971; Pudovkina and Pyatenko, 1963; Rumanova and Nikolaeva, 1959; Ueda, 1955) have been made on natural allanites with complex compositions. The refinements of Ueda (1955), Pudovkina and Pyatenko (1963) and Rumanova and Nikolaeva (1959) report cell dimensions only to 0.01 A. Rumanova and Nikolaeva (1959) describe their sample as metamict, exhibiting weak reflections from x-ray analysis. The Si(2)-O(9) interatomic distance of 1.836 A calculated from the data of Ueda is unreasonably long. Dollase (1971) reports cell dimensions to 0.001 A and believes the allanite he used to be the most crystalline of the allanites previously examined by Frondel (1963). Of the above studies, errors in the atom positions were reported only by Dollase (1971).

Structure refinements on the other members of the epidote group include: zoisite, clinozoisite (Dollase, 1968); piemontite (Dollase, 1969); hancockite (Dollase, 1971); epidote (Carbonin and Molin, 1980; Gabe et al., 1973; Dollase, 1971; Ito, 1950; Ito et al., 1954; Belov and Rumanova, 1953). The epidote cell parameters of Belov and Rumanova (1953) and Ito et al. (1954) were reported only to 0.01 A and errors in the atom positions were not reported.

In the epidote group, the bond distances increase most dramatically in the M(3) octahedron as the composition changes from zoisite to allanite, and this is reflected in the distortion of the M(3) octahedra (Fig. 3). This distortion also appears to affect the Si(1)-O(9)-Si(2) angle in the epidote group, because M(3) is bonded to O(8) which in turn is bonded to Si(2). According to Dollase (1968), the substitution at the M(3) site accounts for

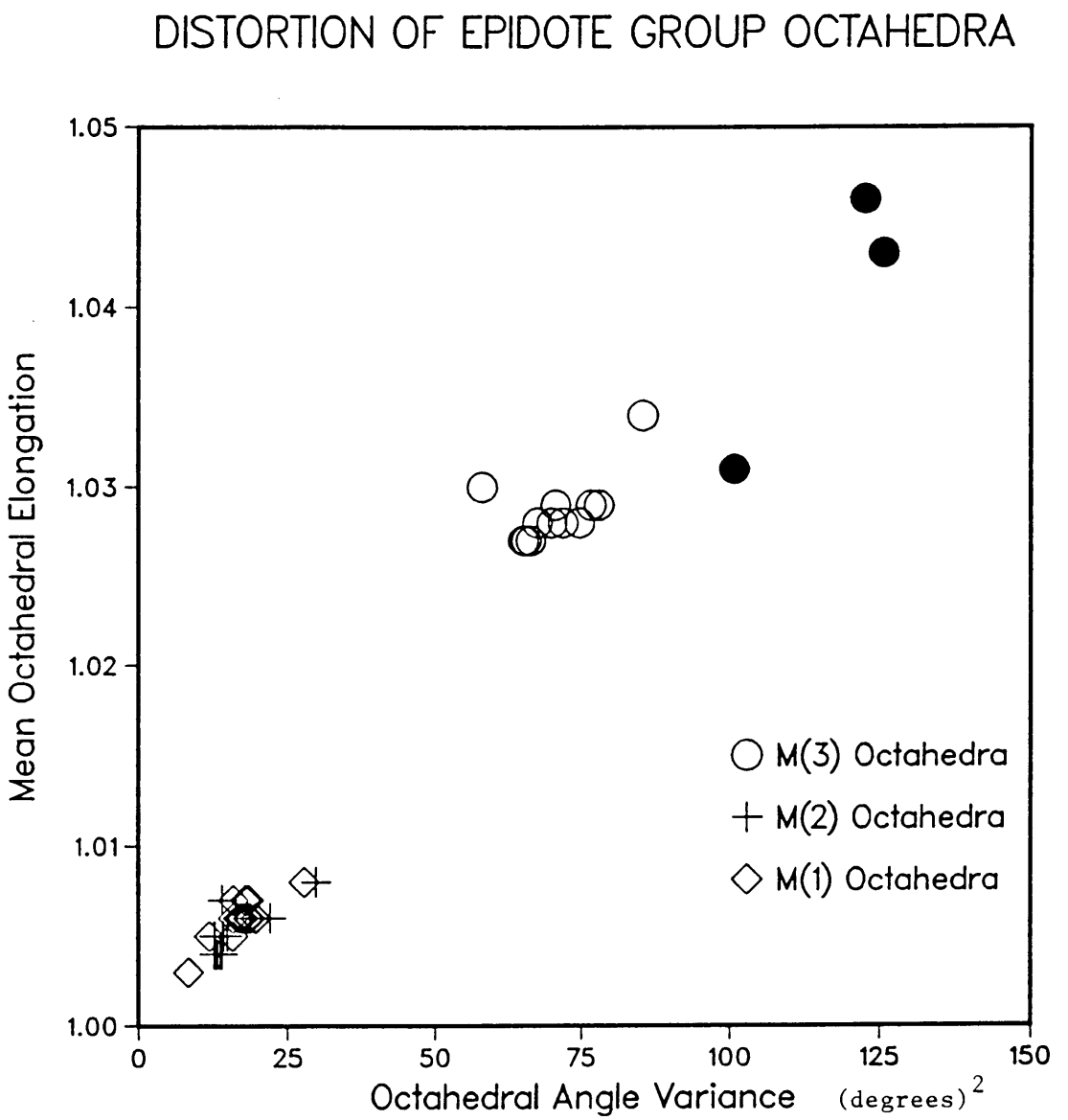

Figure 3. Distortion of octahedra in the epidote minerals whose structures have been refined. The solid circles are allanite octahedra.

the change in structure from orthorhombic to monoclinic.

The well-established inverse correlation of Si-O bond length with Si-O-Si angle observed for many silicates (Gibbs, 1982) is also observed for the disilicate anion in the epidote group (Fig. 4b). Interestingly, within the epidote group, the Si(1)-O(9)-Si(2) angle decreases as the amount and size of the ions substituting in the M(3) site increases (Fig. 4a). A change of Fe^{3+} occupancy from 0.04 (clinozoisite) to 0.86 (epidote) corresponds to a decrease in the Si-O-Si angle of 11°. An allanite with 0.83 Fe^{2+} per 12.5 anions (the same iron occupany as an epidote with an Si-O-Si angle of 155° on Fig. 4a) corresponds to an Si-O-Si angle of about 165°; the increase in angle is probably due to the larger size of the M(3) octahedra when Fe^{2+} substitutes for Fe^{3+} (of epidote). A natural mukhinite, a vanadium member of the epidote group, is predicted to have an Si-O-Si bond angle of 153° based on the reported Fe^{3+} + V^{3+} M(3) occupancy of 0.90 atoms.

Another factor that may effect changes in the Si-O-Si angle is substitution at A(2). In hancockite, Pb^{2+} (CN = X) and Sr^{2+} (CN = X) (ionic radii = 1.40, 1.36 A, respectively) substitute for Ca^{2+} (CN = X) (ionic radius = 1.23 A) at this site. Since A(2) is bonded to O(7) which is in turn bonded to Si(1), a larger ion in A(2) may cause a decrease in the Si(1) O(9)-Si(2) angle.

CHEMISTRY

Allanite, $Ca(REE)Fe^{2+}Al^{3+}{}_2Si_3O_{12}(OH)$, is the only member of the epidote group in which Fe^{2+} and REE^{3+} are essential components. Conceptually, it may be obtained from epidote, $Ca_2Al_2Fe^{3+}Si_3O_{12}(OH)$, by the coupled substitution Ca^{2+} + Fe^{3+} = REE^{3+} + Fe^{2+} although all intermediate compositions between epidote and allanite have not been

Figure 4. (a) The Si-O-Si angle variation as a function of the M(3)-O bond length in epdiote group minerals, i.e., as the amount of larger ions substitute at the M(3) site. The M(3) site occupancy changes from Al^{3+} for zoisite to Fe^{2+} for allanite. For the epidotes plotted the Fe^{3+} occupancy in M(3) ranges from 0.30 to 0.86. (b) The Si-O-Si angle variation as a function of mean SiO bond length for the same structures as in (a). Points with error bars that do not intersect the fitted line are pre-1960 data, which have cell parameters reported to 0.01 A. Data were generated or used directly from the following sources: allanite- Rumanova et al. (1959) [open circle], Pudovkina et al. (1963) [half-solid circle], Dollase (1971) [solid circle]; piemontite- Dollase (1969); mukhinite- Shepel and Karpenko (1969); epidote- Dollase (1971), Gabe et al. (1973), Carbonin and Molin (1980), Belov and Rumanova (1953), Ito et al. (1954); hancockite - Dollase (1971); clinozoisite- Dollase (1968); zoisite- Dollase (1968).

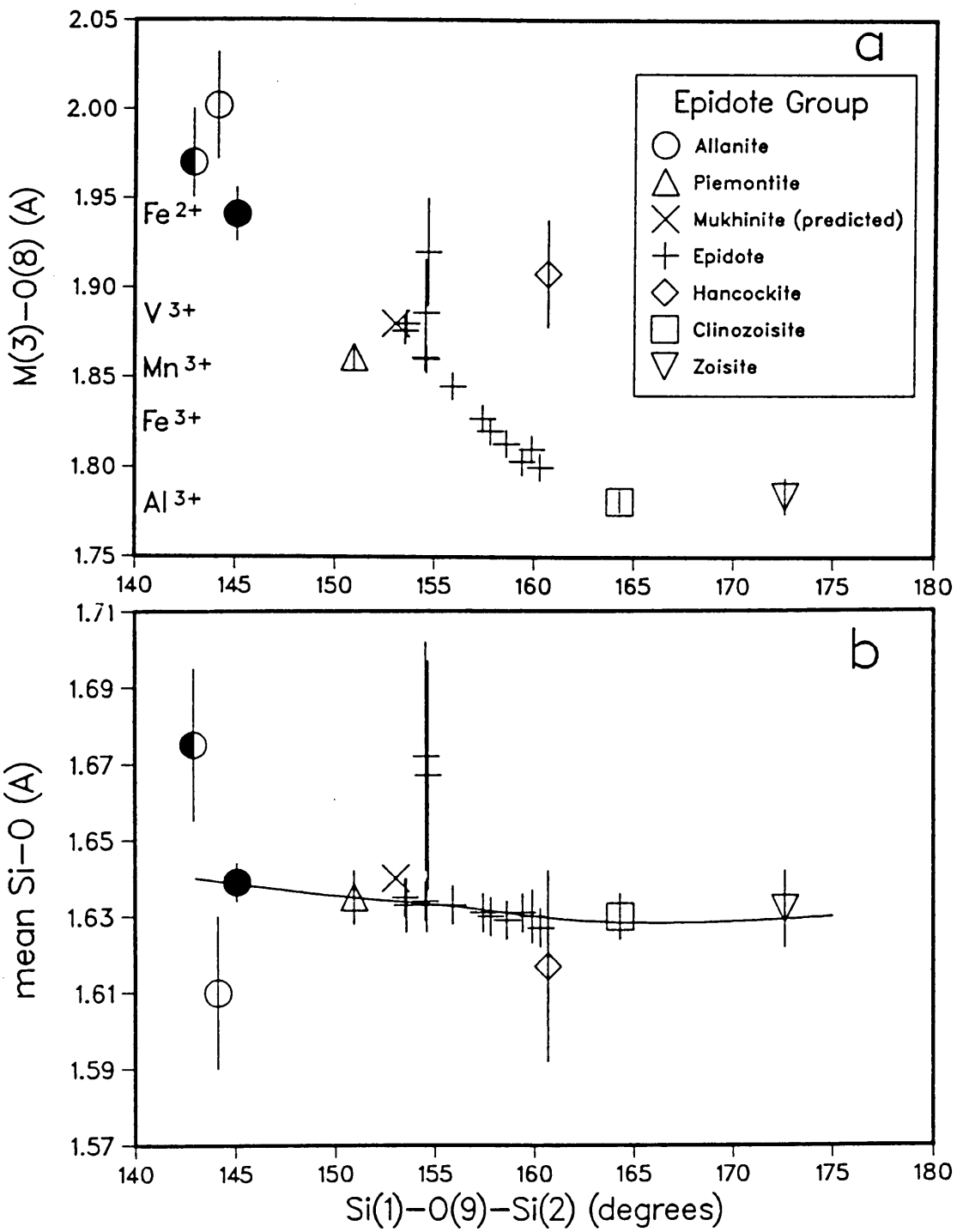
a
Epidote Group
Allanite
Piemontite
Mukhinite (predicted)
Epidote
Hancockite
Clinozoisite
Zoisite
Fe 2+
V 3+
Mn 3+
Fe 3+
Al 3+
M(3)–O(8) (A)
2.05
2.00
1.95
1.90
1.85
1.80
1.75
b
mean Si–O (A)
1.71
1.69
1.67
1.65
1.63
1.61
1.59
1.57
140
145
150
155
160
165
170
175
180
Si(1)–O(9)–Si(2) (degrees)

observed. The oxide Ce_2O_3, present up to 25 weight percent (0.88 a.f.u.), is more abundant than La_2O_3; Y_2O_3 is seldom present in amounts greater than Ce_2O_3 or La_2O_3. Tl other lanthanides occur in minor or trace amounts. Cerium has two stable oxidation states, 3+ and 4+, in nature; however, cerium in allanite is trivalent as inferred from structural formulas and redox equilibrium studies in silicate systems (Schreiber and Balazs, 1985; Schreiber et al., 1980). Other substitutions for Ca^{2+} and REE^{3+} include U^{4+}, U^{6+}(?), Th^{4+} Mn^{2+}, Pb^{2+}, Sr^{2+}, K^{+}, and Na^{+}. The amount of ThO_2 present is commonly 0.30 to 1.30 weight percent (0.007 to 0.028 a.f.u.) and U from 30 to 65 ppm (Deer et al., 1966). Brooks et al. (1981) suggests allanite fractionates thorium from uranium and that uranium is predominately in a high oxidation state (U^{6+}) in both allanite and the melt. The alpha-recoil events associated with the decay chains of ^{238}U, ^{235}U, and ^{232}Th account for the lac of crystallinity or metamict state of allanite (Headley et al., 1982; Ewing et al., 1987). The ionic radii (Shannon, 1976) for cations in the A sites range from 0.8 to 1.8 A.

Numerous substitutions occur at the M sites. Iron substitution in epidote group minerals has been investigated by optical absorption spectroscopy studies of epidotes (Fe^{3+} only) (Burns and Strens, 1967), ^{57}Fe Mossbauer spectroscopy studies of epidote and allanite (Fe^{3+}, Fe^{2+}) (Bancroft et al., 1967; Remy et al., 1969; Dollase, 1973), and site refinements from crystal structure analysis of epidote and allanite (Fe^{3+}, Fe^{2+}) (Gabe et al., 1973; Dollase, 1971, 1973).

Remy et al. (1969) studied the process of iron oxidation in a natural allanite which originally contained 10.6 atomic percent Fe^{2+} and 0.7 atomic percent Fe^{3+}. They found tha up to 300°C, most of the iron was divalent, between 400 and 700°C more was trivalent,

and above 1100°C, the allanite decomposed to Fe_2O_3 and presumably other products.

Dollase (1973) studied 33 samples of synthetic epidotes, natural and heat-treated natural samples of epidote, clinozoisite, allanite, and oxyallanite by ^{57}Fe Mössbauer spectroscopy. All four of his allanite samples were annealed at various temperatures (in H_2) to improve the spectral pattern that was otherwise difficult to interpret due to the metamict nature of the allanites. Still the spectrum was of low quality, presumably due to the extreme positional disorder of the Fe in the metamict state. In iron-rich epidote, piemontite and oxyallanite, most of the Fe^{3+} is found in the M(3) site with minor amounts in the M(1) site (Dollase, 1973). In allanite, nearly all of the Fe^{2+} is in M(3) site. Other reported substitutions in the M sites include Mn^{2+}, Mn^{3+}, Mg^{2+}, Ti^{4+}, and Zr^{4+}. The ionic radii (Shannon, 1976) for these cations in the M site range from 0.7 to 1.0 A.

Fluorine substitutes for hydroxyl. Although fluorine is not routinely determined, up to 3.3 weight percent (0.98 a.f.u.) is reported in allanite from carbonatites (Zdorik et al., 1964) and from a quartz-molybdenite deposit related to subalkaline granites (Kupriyanova et al., 1964).

Compositional zoning of REE is common; the rims of individual grains may be enriched or depleted in REE (Lee and Bastron, 1967; Black, 1970; Ghent, 1972; Sawka et al., 1984). Allanite is also frequently reported with rims of epidote partially or completely surrounding it (Lee and Bastron, 1967; Hickling et al., 1970).

PHYSICAL PROPERTIES

As expected, the physical properties of the epidote group minerals are similar, the main distinction being the color in hand sample, and the refractive index and 2V in thin section. Allanite is black to brown, with a Mohs hardness of 5-6.5 and a density of 3.4-

4.2 g/cm^3 (Deer et al., 1966). Optically, α = 1.690-1.791, β = 1.700-1.815, γ = 1.706-1.828, and 2V = 0-130° (Holmqvist, 1975; Deer et al., 1966; Wahlstrom, 1955; Phillips and Griffen, 1981). Crystals are tabular with poor (001) cleavage. Twinning may occur on (100) (Kokkinakis, 1980; Holmqvist, 1975; Bocquet, 1975; Cech et al., 1972; Ghent, 1972; Zimmerle, 1971; Deer et al., 1966; Volborth, 1962).

Allanite is often metamict as a result of the alpha-decay of small amounts of constitutent U and Th. The extent of structural damage preserved depends on the age of the sample, the amount of U and Th initially present, and the thermal history of the sample. The accumulation of alpha-decay damage correlates with changes in physical properties: decreasing density, refractive indices, birefringence, and lattice diffraction intensity; and increasing macroscopic volume, cell volume, and solubility (Smith et al., 1957; Pellas, 1962; Ewing et al., 1987). Radiation effects in allanite, as measured by birefringence, have been used to interpret age relations among magmatic rocks in the Boulder Creek Batholith, Colorado (Hickling et al., 1970).

Chapter II

SYNTHESIS OF LANTHANIDE AND YTTRIUM ALLANITES

INTRODUCTION

Allanite, a rare earth element (REE) epidote, is an important accessory rock-forming mineral, common in igneous rocks and also occurring in metamorphic rocks. Because of varying amounts of constituent U and Th, allanite can occur in a wholly crystalline, partly crystalline (partly metamict) or noncrystalline state (metamict). Metamictization and complex chemistry have been major obstacles to complete crystal chemical descriptions of natural samples.

The P-T stability relations of allanite have not been defined experimentally. In addition, there is a paucity of literature dealing with P-T conditions of the rock in which allanite has been reported. Hildreth (1979), in his investigation of the Bishop Tuff, has limited the crystallization of allanite to T = 720 to 763°C and oxidative conditions either close to or more reducing than the nickel-nickel oxide (NNO) buffer. Izett (1981) reports allanite is pervasive in biotite-bearing ash beds, and is present in biotite-absent ash beds formed from magmas with temperatures of 695 to 830°C and 870 to 1000°C, respectively. Because allanite is widespread and common in granitic pegmatites, it must be stable at their conditions of formation determined by Jahns (1982) to be P = 0.1 to 10 kbar and T = 550 to 1000°C.

Previous syntheses of epidote group minerals have been successful for zoisite, clinozoisite, epidote and piemontite (Rapp, 1960; Merrin, 1962; Strens, 1964a; Liou, 1973; Anastasiou and Langer, 1977; Prunier, 1978). All of these were synthesized in the P-T range 400 to 800°C and 2.1 to 15 kbar (210 to 1500 MPa) using Tuttle "cold seal" bombs or a piston-cylinder apparatus. Similar methods can be used to synthesize allanite

compositions. As determined by hydrothermal synthesis studies (Liou, 1973), epidote compositions are stable over the range of pressure and temperature up to T = 648°C and P = 5 kbar at the fO_2 values of the NNO buffer. At higher temperatures and pressures, epidote decomposes to garnet, anorthite, magnetite, and vapor.

As a first step towards determining the stability of allanite, and to overcome certain problems posed by natural allanites with complex composition and metamict properties, end-member compositions, $CaAFe^{2+}Al_2Si_3O_{12}(OH)$ where A = La, Ce, Ce-La, Nd, Sm, Eu, Gd, Dy, Er, Yb and Y have been hydrothermally synthesized. These end members were selected for the following reasons:

(1) Ce, La and Y are the most abundant REE in natural allanites. Therefore, the natural allanite compositions are mimicked.

(2) To determine what controls the REE patterns in allanite, i.e. whether the incorporation of REEs in natural allanite is dependent on the geometry of the crystal or paragenetic factors.

(3) La and Yb span the lanthanides (excluding Lu). Consequently, the magnitudes of any crystal structural changes due to the decreasing relative ionic size are magnified.

EXPERIMENTAL PROCEDURES

Hydrothermal Apparatus

Experiments were carried out in 12" horizontally mounted Rene 41 "cold seal" pressure vessels (Tuttle, 1949). The temperatures were measured with external chromel-alumel thermocouples calibrated against the melting point of NaCl; water pressure was measured with a Harwood manganin cell calibrated against a Heise Bourdon tube gauge. The temperatures recorded by the thermocouple varied less than ± 10°C; usually the variation was ± 5°C. Filler rods were used in the calibration and in the experimental runs.

Pressure measurements are accurate to within 50 bars (0.5 MPa). The pressure varied less than 50 bars in all runs unless otherwise noted. All runs were brought to temperature at pressure and quenched at nearly constant pressure.

Starting Materials

The end-member compositions were made from stoichiometric proportions of oxide mixes prepared from reagent grade $CaCO_3$ (fired 5 hours at 900°C in air), optical grade silica glass from Corning Glass Works, fired for 4 hours at 1200°C, Fe_2O_3 (fired 24 hours at 1200°C in air), γ-Al_2O_3 (prepared from $AlCl_3 \cdot 6H_2O$ heated to constant weight at 700°C, then fired 5 hours at 900°C) and CeO_2 or REE_2O_3. The oxide mix was then heated 1 hour at 560°C in an H-atmosphere to reduce the iron. Thermodynamic calculations indicate the Ce in the CeO_2 would be reduced to Ce^{3+} at these conditions. The REE end-member compositions were prepared with 1.0 REE per formula unit. For allanite-(Yb), additional compositions of 0.33 and 0.25 Yb atoms per formula unit (a.f.u.) were prepared.

Charge Capsules and Run Conditions

Fifty to seventy milligrams of the above mixtures plus ten to 15 milligrams H_2O were enclosed in $Ag_{70}Pd_{30}$ capsules and placed in the pressure vessel (which is close to the NNO buffer). When a solid oxygen buffer was used, there were two different capsule configurations. The NNO buffer requires use of a Pt capsule, but because Fe diffuses into Pt (and the charge contains Fe), an additional inner capsule of $Ag_{70}Pd_{30}$ was needed. For fayalite-magnetite-quartz (FMQ) buffered runs, the sealed $Ag_{70}Pd_{30}$ capsule, 45 to 55 mg fayalite and 10 to 15 mg H_2O were then sealed in a gold outer capsule. The crimping and

welding technique used is called the "milk carton" weld described by Sneeringer and Watson (1985). The inner $Ag_{70}Pd_{30}$ capsule was 2 cm long, 1.5 mm O.D., 0.1 mm wall thickness; the outer gold capsule was 4 cm long, 2.5 mm O.D., 0.4 mm wall thickness. The capsules were reweighed after heating to 110°C to detect any weight loss that would indicate a faulty seal.

Synthesis runs were made at T = 450 to 725°C and P = 4 to 5.5 kbar (40 to 55 MPa) to explore the allanite stability field suggested by the occurrence of natural allanite, and the experimentally determined stability of epidote.

Run Product Characterization

Most of the phases obtained in the run charges and in the buffers were identified by x-ray powder diffraction and optical microscopy. Microscopic examination was most useful for determining the presence or absence of magnetite. After the initial analysis of the diffraction patterns and identification of allanite and other phases, peaks still remained that were not readily identifiable. Consequently, analytical electron microscopy (AEM) was used to elucidate further the composition of the run products. Electron microprobe analysis was performed on the run products from the charges which contained the largest crystals (determined optically) for each composition.

Chemical analysis. Most of the compositions of the run products were determined with a nine-spectrometer, automated ARL-SEMQ electron microprobe using 15 kV operating voltage and 10 or 20 nA beam current, depending on particle size. The standards used were $Ca_5(PO_4)_3(OH)$ for Ca, $LaVO_4$ for La, CeO_2 for Ce, $Nd_2Si_2O_7$ for Nd $Sm_2Si_2O_7$ for Sm, $GdDy(MoO_3)_4$ for Gd and Dy, $Y_2Si_2O_7$ for Y, $YbVO_4$ for Yb, Al_2SiO_5 for Al and Si, and Fe_2SiO_4 for Fe. The pyrosilicates and $LaVO_4$ were grown by

J. A. Speer and their preparations are described in Speer and Solberg (1982) and Brixner and Abramson (1965), respectively. Suitable probe mounts were prepared by dispersing fine particles (40 μm and less in size) onto graphite wafers and coating them with a 200 A carbon film. A modified Bence-Albee data reduction scheme was used (Bence and Albee, 1968). When the particle size was less than 5 μm a method for probing small particles (Solberg et al., 1981) was used.

Some analyses of the run products and all analyses of the natural samples from Jamestown, Colorado were made at the University of New Mexico (UNM) using a JEOL 733 electron microprobe operated at 15 kV and a sample current of 20 nA with a 1 μm beam diameter (G. R. Lumpkin, analyst). For the synthetic allanites the standards used were anorthite for Al, Si and Ca, olivine for Fe, and $(REE)PO_4$ for REE. For the natural REE silicates the standards used were the synthetic allanite-(Ce) for Si, Al, Ca, Fe and Ce, synthetic allanite-(La) for La, synthetic allanite-(Y) for Y, gadolinite for Sm, Gd, Dy, Er and Yb, $(REE)PO_4$ for Pr and Nd, $ThSiO_4$ for Th, UO_2 for U, cerussite for Pb, albite for Na, $SrMoO_4$ for Sr, olivine for Mg, and diopside for Mg and Ti. A Bence-Albee analytical scheme was used.

All iron in allanite was initially calculated as FeO, but was later divided into ferric and ferrous contributions based upon ^{57}Fe Mossbauer spectroscopy (See Chapter III). An assumed stoichiometric amount of (OH) was included for the hydrous minerals. Replicate electron microprobe analyses on allanite-(La), allanite-(Ce) and allanite-(Y) obtained at VPI&SU and UNM indicate that the data from both sources are comparable.

X-ray powder diffraction. For run product identification, the allanites were analyzed with an automated Philips powder diffractometer employing a graphite monochromator set for Cu $K\alpha$ radiation (wavelength = 1.5418 A) at 40 kV, 20 mA. The

finely ground allanite run product and a small amount of internal standard (CaF_2, **a** = 5.4632 A) were blended thoroughly by grinding under acetone. Sixty-three allanite-(Ce) peaks were indexed in space group $P2_1/m$ by comparison with published patterns of natural allanite having known structure and composition. Allanites of other compositions were identified by using the synthetic allanite-(Ce) pattern as a guide. Scans were made from 10 to 75° 2Θ at 0.5°/min. Run products with the highest allanite yields were selected to obtain accurate d-spacings for cell dimension measurement on a Scintag diffractometer with a graphite monochromator set for

Cu Kα radiation at 40 kV, 30 mA. For these runs, BaF_2 (**a** = 6.1971 A) was used as an external standard, and typical scan ranges were 5 to 75° 2Θ at 1°/min. Only those reflections that could be indexed unambiguously and that did not overlap significantly with neighboring peaks were used in the cell dimension calculations. These requirements restricted usable allanite reflections between 20°and 65° 2Θ from 17 to as few as 7. The smaller number of reflections was a subset of the 17 reflections. Cell dimensions were refined using the program of Burnham (1962).

Analytical electron microscopy. This technique proved useful to identify phases in which the most intense x-ray diffraction peaks overlapped with peaks of other phases, or for phases that were present in smaller amounts than can be detected by x-ray diffraction (~5 volume percent). From a single grain (< 1 μm), a composition can be determined and an electron diffraction pattern obtained. With the new knowledge provided by the chemical constraints and electron diffraction, the JCPDS file was searched to identify additional phases in the x-ray diffraction patterns. The AEM analyses were made using a JEOL 2000FX AEM operated at an accelerating voltage of 200 kV, and equipped with a Tracor Northern TN-5500 energy dispersive spectrometer (EDS). Nominal beam

size in the TEM mode at the specimen using a LaB_6 filament is 20 nm (FWHM; JEOL specifications). All AEM analyses were performed under the same lens conditions at a vacuum <2.0 X 10^{-5} Pa. Each run product was placed in a vial with acetone and ultrasonically vibrated for 1 to 5 minutes to break up clumps of grains. The samples were then dispersed on holey carbon films supported by copper grids. Phases were characterized through a combination of standard imaging, selected area diffraction, and EDS analysis following the procedures outlined by Mackinnon et al. (1986).

Optical techniques. Refractive indices (α, ß, γ for N_d) were determined using the central focal masking technique (Wilcox, 1983) with Cargille immersion oils. The allanite-(Ce) was sufficiently large to examine by using a spindle stage (Bloss, 1981). Other compositions were examined as grain mounts on glass slides; however, because of the complexity of some of the run products and similar habits of the minerals, optical properties were difficult to establish.

Extinction measurements obtained with the spindle stage (with Na light) were used in the computer program EXCALIBR (Bloss, 1981) to obtain the optic axial angle of allanite-(Ce) and to locate the principal vibration directions X, Y and Z with respect to the crystallographic axes **a**, **b**, and **c**.

RESULTS

Synthesis Products

The conditions and results of hydrothermal synthesis experiments are compiled in Table 2. Abbreviations for mineral names in the table are taken from Kretz (1983). The synthetic run products contained different combinations of the following phases: allanite-(REE), britholite-(REE), anorthite, magnetite, quartz, pyrosilicate-(REE), garnet-(REE),

hedenbergite, Ce-Al-silicate (törnebohmite?), Fe-Al-silicate (chlorite?), epidote-(Er), epidote-(Yb). One hundred volume percent yield was obtained for allanite-(La) starting compositions. Greater than 90 volume percent allanite-(REE) was present in all the run products with the starting compositions: REE = La, La-Ce, Ce, Nd, Sm, Eu, Gd. Between 70 and 90 volume percent allanite was present in the run products from starting compositions with Dy, and approximately 50 volume percent allanite was present with Y. For the allanite-(Er) starting composition, epidote-(Er) was present up to ~10 volume percent. Epidote-(Yb) crystallized from the allanite-(Yb) starting composition; however, pyrosilicate-(Yb) was present in much greater amounts than the epidote-(Yb). In reporting the run products, the name epidote-(Yb) (and epidote-(Er)) rather than allanite-(Yb) is used to emphasize the greater amount of Ca (1.64 atoms/12.5 O) than Yb (0.24 atoms/12.5 O) present (see Table 4). Garnet appears in the run products for which the starting compositions are Yb = 0.33 a.f.u. (Ca = 1.67 a.f.u.) and Yb = 0.25 a.f.u. (Ca = 1.75 a.f.u.), and the run conditions are P = 4.0 kbar (40 MPa), T = 700 to 703°C, and P = 5.5 kbar (55 MPa), T = 650°C, respectively. This is consistent with the stability relationships for epidote, which decomposes to garnet, anorthite, magnetite and vapor under such conditions (Liou, 1973). Percentage estimates of the major phases are included in Table 2. The percentages were estimated by identifying the composition of 50 to 100 grains in a sample, or by visually estimating the number of each type of grain after identifying (using the EDS capability of the AEM) approximately 20 grains in the sample.

The synthetic allanites are distinct, euhedral, slender, prismatic crystals (Fig. 5). Despite run durations of more than three months, seeding the runs with previously crystallized allanite, and repeating the experiment at P and T after recrushing the run products, the synthetic allanite crystals generally were small - 10 to 40 μm or less in greatest dimension (Fig. 6). The largest crystals (up to 120 X 66 X 16 μm) were obtained

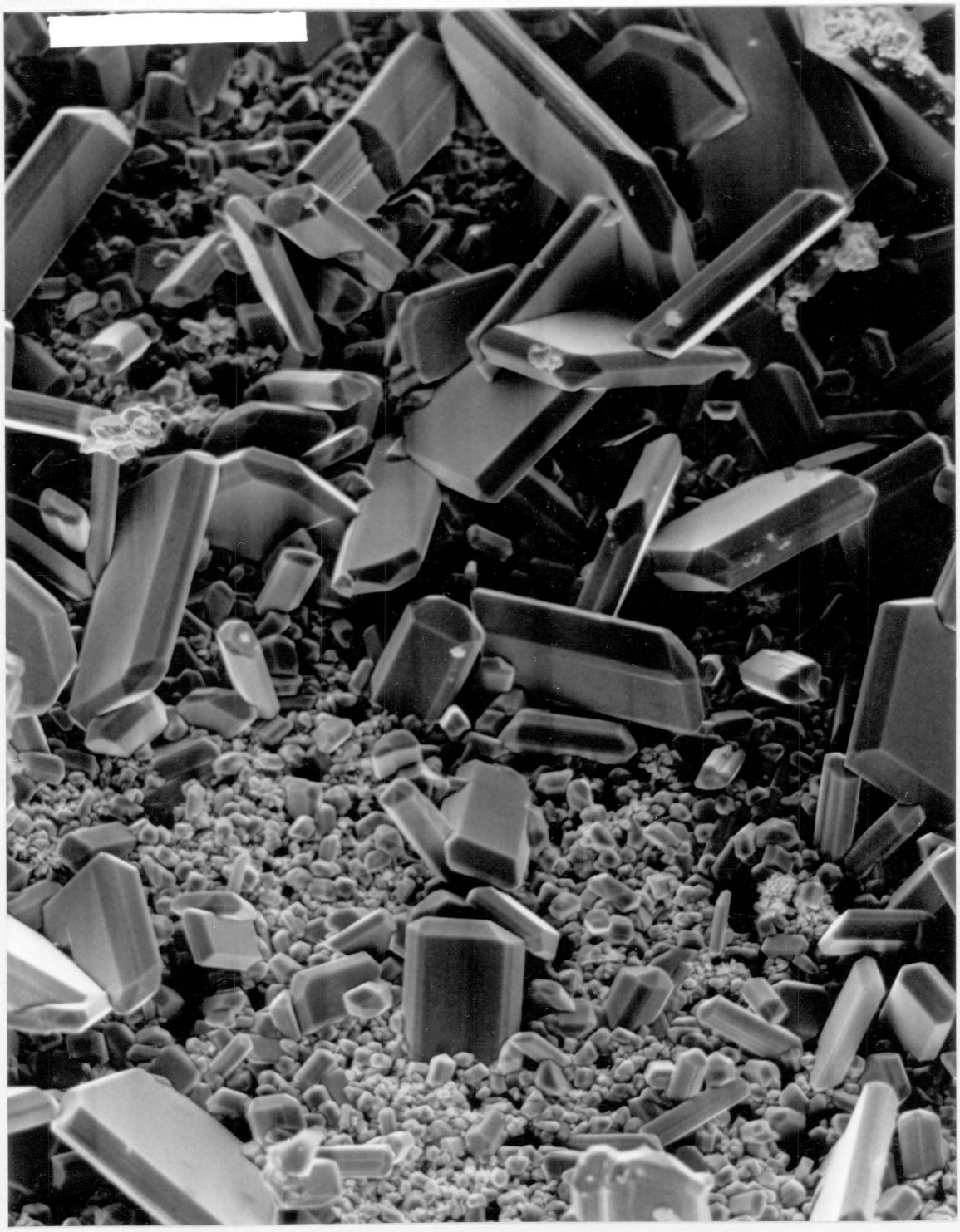

Figure 5. SEM micrograph (400X, 15 keV) of allanite-(Ce) synthesized at 700°C, and 4 kbar (400 MPa). The scale bar is 50 μm.

Figure 6. TEM micrographs of selected run products. Scale bar is one micron. (A) allanite-(La), 610°, 5.5 kbar, 61 days. (B) allanite-(Ce), 700°C, 4.0 kbar, 21 days; "a" = allanite, "t" = Ce-Al-silicate (tornebohmite?). (C) allanite-(Nd), 723°C, 4 kbar, 11 days. (D) allanite-(Sm), 650°C, 5.5 kbar, 8 days. (E) allanite-(Gd), 560°C, 5.5 kbar, 5 days. (F) allanite-(Dy), 650°C, 5.6 kbar, 35 days; "a" = allanite, "b" = britholite.

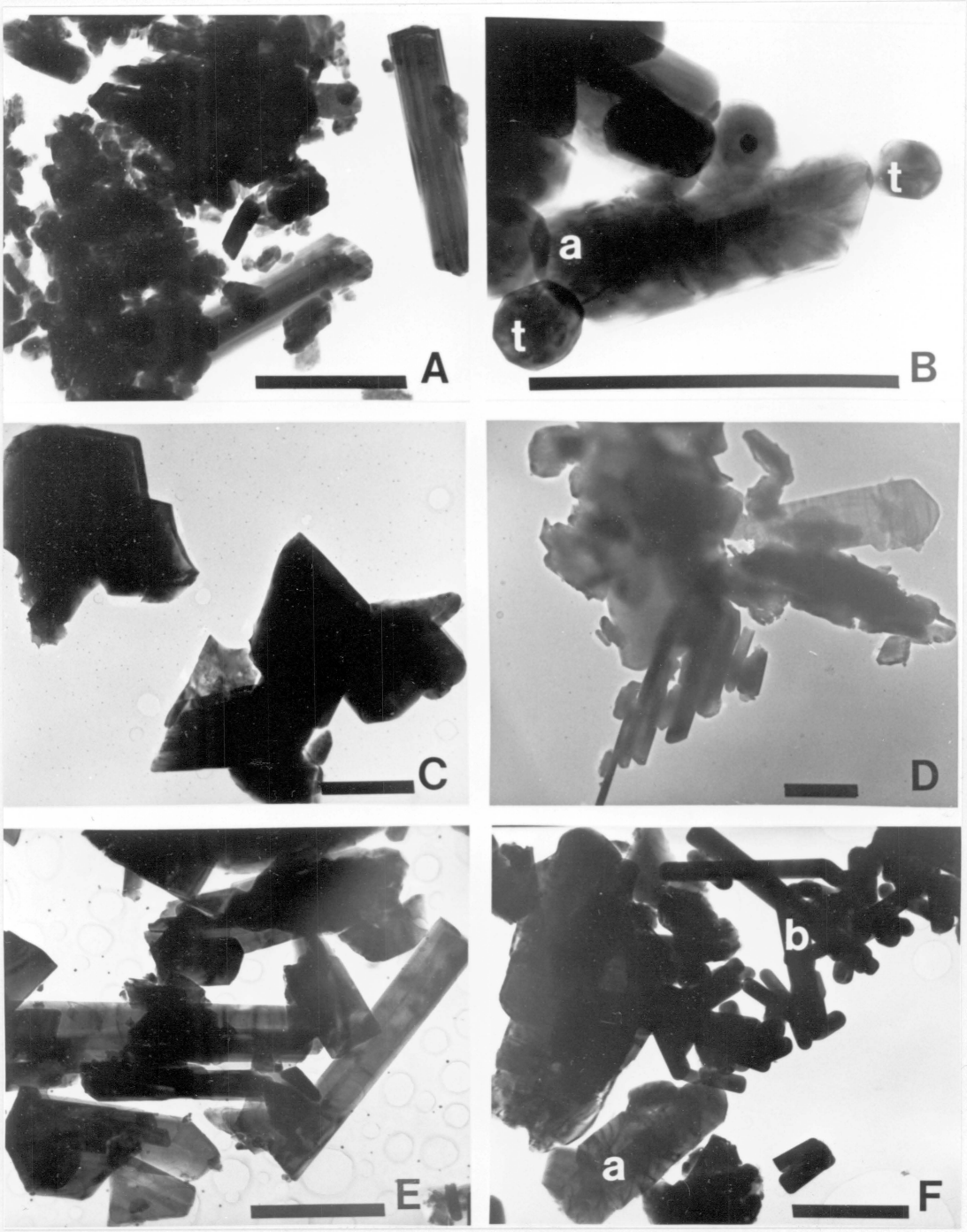
A
t
a
t
B
C
D
E
b
a
F

from runs at 700°C, 4 kbar (run no. 153 in Table 2, and Fig. 5).

Minor phases. A Ce-Al-silicate (~3 volume percent) (Fig. 6b), and quartz (~2 volume percent) crystallized with allanite-(Ce). The Ce-Al-silicate phase could be cheralite (Ca,REE)[(Al,Si)O_4] or törnebohmite, $REE_2Al[SiO_4]_2(OH)$. Unfortunately, the majority of the diffraction peaks for both of these phases overlap with allanite peaks, including the most intense peak at d = 3.073 A (cheralite) and d = 3.08 A (törnebohmite). Moreover, because these phases are present in small amounts, they produce weak diffraction peaks which are indistinguishable from the general diffraction pattern. The chemical analyses obtained through electron microprobe and TEM EDS are consistent with tornebohmite. Törnebohmite is reported to have a monoclinic (Shen and Moore, 1982) or a hexagonal structure (Povarennykh, 1972). The electron diffraction patterns suggest that the phase reported here is monoclinic. The formula determined from qualitative TEM analysis is $(Ce_{1.81}Ca_{.02}Fe^{2+}_{.05})_{1.88}Al_{.934}Si_{1.9}O_8(OH)$.

Britholite occurred in the run products of allanite-(Nd), -(Sm), -(Gd) and -(Dy) starting compositions. Britholite-(REE) is noticeably smaller than allanite and occurs as long, slender needles (1 to 10 μm), the length to width ratio being ~6 (Fig. 6f). It was identified on the TEM by its composition. Identification by x-ray diffraction was precluded because the three most intense x-ray diffraction peaks of britholite overlap with diffraction peaks of other phases in the run products. The britholites were more abundant in the Dy and Gd runs than in the Nd runs. Electron microprobe analyses indicate that the britholites are of the type $A_2B_8[SiO_4]_6O_2$. In the run products, britholite-(Nd) has the structural formula $(Ca_{1.9}Fe^{2+}_{.18})_{2.08}(Nd_{3.0}Fe^{2+}_{1.92}Al_{3.28})_{8.20}Si_{6.24}O_{26}$; britholite-(Gd) has the stuctu formula $Ca_2(Gd_{5.57}Al_{.940}Fe^{2+}_{1.46})_{7.97}(Si_{5.20}Al_{.80})_{6.0}O_{26}$; and britholite-(Dy) has the

structural formula $(Ca_{1.93}Fe^{2+}_{.07})_{2.0}(Dy_{7.5}Fe^{2+}_{.66})_{8.16}(Al_{.23}Si_{5.79})_{6.02}O_{26}$. The increase of REEs in the britholites with increasing atomic number and decreasing radii corresponds to a decrease of REEs in the allanites with increasing atomic number.

The allanite-(Er) and allanite-(Yb) runs were dominated by pyrosilicate, anorthite and magnetite. In the lower temperature, shorter duration runs, an Fe-Al-silicate was also present. The pyrosilicates have the same crystal habit as allanite and are usually 20 μm or less and thus smaller than the allanite crystals. Indexing the x-ray powder diffraction pattern for the pyrosilicates confirmed that their structure belongs to the space group C2/m, i.e., the type C polymorph (Felsche, 1973).

The Fe-Al-silicate phase has a platy crystal habit; the electron diffraction pattern is always the same for every grain indicating the same orientation. The measured diffraction pattern obtained on the TEM indicates that this mineral is hexagonal and may be a chlorite. Qualitative TEM analysis of a single grain yields the form $(Fe^{2+}_{1.64},Al^{3+}_{1.0})_{2.64}(Si_{1.52},Al_{0.55})_{2.07}O_5(OH)_4$.

Hedenbergite, $CaFeSi_2O_6$, identified using the AEM, was found only in run products synthesized from the Yb allanite starting compositions. Qualitative analysis gave the formula: $Ca_{1.07}(Fe^{2+}_{.76}Al_{.15})_{.91}(Si_{1.89}Al_{.11})_{2.0}O_6$. Liou (1973) found that hedenbergit with anorthite, garnet and fluid replaced epidote in the presence of excess quartz, when the fO_2 was lower than that defined by the QFM buffer. In this study, the Yb run products at T = 700°C and P = 4 kbar were the same, but included magnetite as well.

In summary, 70 - 100 volume percent allanite is found in the run products of starting compositions where REE = La, Ce, Nd, Sm, Gd and Dy. About 50 volume percent allanite-(Y) occurs with pyrosilicate, britholite, anorthite and magnetite.

Pyrosilicate, anorthite, and magnetite are abundant in run products from the heavy rare earth (HREE) starting compositions, Er and Yb. To summarize the run product REE phases: allanite-(La) occurs alone, allanite-(Ce) occurs with trace amounts of tornebohmite; allanite-(Nd), -(Sm), -(Gd), -(Dy) occur with trace amounts of britholite; and pyrosilicate-(Er) and pyrosilicate-(Yb) occur with major amounts of epidote-(Er) and epidote-(Yb). EDS spectra for selected runs representing the different REE starting compositions are shown in Appendix A.

Allanite and Epidote-(REE) Characterizations

Compositions. The compositions and structural formulas of the synthetic allanite-(REE) based on electron microprobe analysis and Mossbauer analysis are compiled in Tables 3 and 4. The amount of calcium increases with increasing atomic number of the REEs, and is greatest in allanite-(Yb), 1.64 atoms per formula unit (a.f.u.). The REEs decrease ranging from 0.93 a.f.u. in allanite-(La) to as little as 0.24 a.f.u. in allanite-(Yb). The Fe^{2+} content increases with a decrease in REE content. The greatest amount of Fe^{2+} (0.69 a.f.u.) and the least amount of REE (0.24 a.f.u.) occurs in allanite-(Yb). The amount of Fe^{3+} is nearly constant for all compositions, 0.14 to 0.16 a.f.u. The Al content ranges from 1.95 a.f.u. in allanite-(La) to 2.11 in allanite-(Dy); in allanite-(Yb) it increases to 2.55 a.f.u.. All of the allanites have Fe^{2+} in the A site except for allanite-(La); the amount of Fe^{2+} is greater in the HREE allanites than in the LREE allanites. Allanite-(La) is close to an ideal allanite formula, whereas allanite-(Yb) is close to an epidote formula and should be referred to as "epidote-(Yb)".

Space group and cell parameters. The lattice constants of eight synthetic allanite samples obtained by the method of least-squares refinement for powder x-ray

Table 3. Compositions and cell dimensions of synthetic allanites.

REE	La	Ce	Nd	Sm	Gd	Dy	Y	Er	Yb
Number of ions based on 12.5 oxygens									
Si	3.05(10)	2.90(7)	3.03(22)	2.97(10)	2.95(13)	2.94(23)	2.91(21)	-	2.95(7)
Al	1.95(13)	2.18(9)	1.99(16)	2.19(17)	2.13(19)	2.11(32)	2.24(17)	-	2.55(6)
Fe^{2+}**	0.88(4)	0.90(7)	1.10(11)	0.85(23)	0.93(7)	0.97(13)	0.90(16)	-	0.69(13)
Fe^{3+}	0.15	0.15		0.16	0.15	0.14	0.14		0.16
Ca	1.04(3)	1.09(7)	1.07(11)	1.08(11)	1.11(8)	1.12(7)	1.01(11)	-	1.64(10)
REE	0.93(4)	0.84(6)	0.81(24)	0.77(12)	0.78(8)	0.81(12)	0.80(18)	-	0.24(3)
Total*	8.00	8.06	7.91	8.02	8.05	8.09	8.00	-	8.23
Σ A site	1.97	2.07	1.98	2.05	2.05	2.08	2.00	-	2.14
Σ M site	2.98	3.00	2.99	3.00	3.00	3.01	3.00	-	3.09
Cell dimensions (space group $P2_1/m$)									
a (A)	8.916(4)	8.904(3)	8.878(5)	8.861(4)	8.849(6)	8.861(4)	8.888(11)	8.859(9)	-
b (A)	5.746(4)	5.748(3)	5.729(8)	5.704(5)	5.702(8)	5.700(5)	5.681(5)	5.679(6)	-
c (A)	10.123(7)	10.100(5)	10.066(9)	10.063(10)	10.051(11)	10.075(7)	10.036(7)	10.081(9)	-
ß (°)	114.66(3)	114.74(2)	114.97(4)	115.19(4)	115.29(7)	115.27(3)	115.43(4)	115.88(7)	-
V (A^3)	471.3(6)	469.5(4)	464.2(8)	460.3(7)	458.5(1.0)	460.2(5)	457.6(9)	456.3(1.2)	-

** Errors for Fe^{2+} and Fe^{3+} are given for total Fe. Fe^{2+} and Fe^{3+} were determined by Mossbauer analysis, see Chapter 3. Only total iron was determined for allanite-(Nd).

* See Table 4 for the assignment of cations in the A and M sites.

Table 4. Structural formulas of synthetic allanites and a natural allanite and epidote with ferrous/ferric ratios from Mossbauer analysis.

	$^{VII-XI}A_2$	$^{VI}M_3$	$^{IV}T_3$	$O_{12}(OH)$
La	$(Ca_{1.04}La_{0.93})_{1.97}$	$(Fe^{2+}_{0.88}Fe^{3+}_{0.15}Al_{1.95})_{2.98}$	$Si_{3.05}$	$O_{12}(OH)$
Ce	$(Ca_{1.09}Ce_{0.84}Fe^{2+}_{0.14})_{2.07}$	$(Fe^{2+}_{0.76}Fe^{3+}_{0.15}Al_{2.09})_{3.00}$	$(Si_{2.9}Al_{0.09})_{2.99}$	$O_{12}(OH)$
Sm	$(Ca_{1.08}Sm_{0.77}Fe^{2+}_{0.20})_{2.05}$	$(Fe^{2+}_{0.65}Fe^{3+}_{0.16}Al_{2.19})_{3.00}$	$Si_{2.97}$	$O_{12}(OH)$
Gd	$(Ca_{1.11}Gd_{0.71}Fe^{2+}_{0.23})_{2.05}$	$(Fe^{2+}_{0.70}Fe^{3+}_{0.15}Gd_{0.07}Al_{2.08})_{3.00}$	$(Si_{2.95}Al_{0.05})_{3.00}$	$O_{12}(OH)$
Dy	$(Ca_{1.12}Dy_{0.75}Fe^{2+}_{0.21})_{2.08}$	$(Fe^{2+}_{0.76}Fe^{3+}_{0.14}Dy_{0.06}Al_{2.05})_{3.01}$	$(Si_{2.94}Al_{0.06})_{3.00}$	$O_{12}(OH)$
Y[1]	$(Ca_{1.01}Y_{0.80}Fe^{2+}_{0.19})_{2.00}$	$(Fe^{2+}_{0.71}Fe^{3+}_{0.14}Al_{2.15})_{3.00}$	$(Si_{2.91}Al_{0.09})_{3.00}$	$O_{12}(OH)$
Yb	$(Ca_{1.64}Fe^{2+}_{0.50})_{2.14}$	$(Fe^{2+}_{0.19}Fe^{3+}_{0.16}Yb_{0.24}Al_{2.5})_{3.09}$	$(Si_{2.95}Al_{0.05})_{3.00}$	$O_{12}(OH)$
allanite[2]	$(Ca_{1.05}REE_{0.89}Mn_{0.07})_{2.01}$	$(Fe^{2+}_{0.74}Fe^{3+}_{0.76}Mg_{0.09}Al_{1.41})_{3.0}$	$(Si_{2.9}Al_{0.05})_{2.95}$	$O_{12}(OH)$
epidote[2]	$Ca_{2.0}$	$(Fe^{3+}_{0.81}Al_{2.15})_{2.96}$	$Si_{3.00}$	$O_{12}(OH)$

[1] The ferrous/ferric ratio was not determined for this composition by Mossbauer spectroscopy, but it is included for completeness.

[2] Allanite composition reported by Cech et al. (1972) and epidote composition reported by Dollase (1971).

diffraction data (Burnham, 1962) are listed in Table 4. Indexed peaks used in each refinement are listed in Appendix B.

Additional information was acquired for the allanite-(Ce) composition, because large crystals of it were obtained. The x-ray powder diffraction pattern for allanite-(Ce) has the largest number of sharp, well-defined peaks. The unit cell dimensions for allanite-(Ce) analyzed with the Philips powder diffractometer and CaF_2 internal standard are as follows: **a** = 8.909(5), **b** = 5.743(3), **c** = 10.123(5) A, ß = 114.80(3)°, V = 470.2(6) A^3 (standard errors, in parentheses, refer to the last digit).

As an additional check on the identification of the synthetic allanite, whose ideal formula is $CaCeFe^{2+}Al_2Si_3O_{12}(OH)$, a theoretical powder diffraction pattern was calculated for allanite-(Ce) (Table 5) by using the POWD10 program (Smith and Zolensky, 1983) and the positional and isotropic thermal parameters of a natural allanite (Dollase, 1971). The calculated intensities are in fair agreement with the synthetic and natural allanite patterns (JCPDS card 25-169) with the exception of (100) peak. The strip chart recordings for the synthetic and natural allanites are presented in Fig. 7. For the synthetic allanite-(Ce), hkl, d spacing (A), and intensities of the strongest lines are: -211, 3.53, 53; -113, 2.920, 100; 020, 2.886, 49; 013, 2.714, 65; -311, 2.627, 54; -401, 2.182, 22.

Precession photographs obtained for allanite-(Ce) and allanite-(La) confirm the monoclinic symmetry. The photographs were exposed for 5 days because of the small allanite crystal size. The systematic absences (h + k = 2n + 1 for (h0l) reflections) are consistent with the space group $P2_1/m$, and lattice constants measured from the zero level photographs agree with the published results of Dollase (1971).

Optical Parameters. The synthetic allanite crystals are elongated along **b** and flattened on the (100) plane (Fig. 5) similar to that observed for synthetic zoisite and

TABLE 5.

Indexed x-ray powder diffraction patterns for synthetic Ce-allanite (measured and theoretical) and natural allanite.

				synthetic Ce-allanite[1]				natural allanite[2]		Ce-allanite[3]	
h	k	l		d(obs)	d(calc)	I/I_1		d(calc)	I/I_1	d(calc)	I/I_1
0	0	1	*	9.1855	9.1830	2	7	9.23	8	9.192	7
1	0	0	*	8.0742	8.0815	6	11	8.11	11	8.088	49
-1	0	1	*	8.0002	7.9941	4	8	7.96	17	7.948	100
1	0	1		5.0911	5.0969	2	4	5.12	13	5.102	40
-1	0	2		4.9885	4.9939	.3	1	5.02	10	4.997	6
0	1	1	*	4.8688	4.8634		9	4.89	5	4.870	32
1	1	0		4.6787	4.6762	8	14	4.70	15	4.682	60
0	0	2	*	4.6106	4.5915	1	3	4.61	10	4.596	9
-2	0	1								4.454	1
2	0	0						4.06	1	4.044	1
-2	0	2						3.98	3	3.974	2
1	1	1		3.8061	3.8093		4	3.83	4	3.814	1
-1	1	2		3.7643	3.7657	2	4	3.79	8	3.770	2
0	1	2		3.5829	3.5839	4	6	3.60	9	3.588	21
-2	1	1	*	3.5164	3.5163	39	53	3.53	45	3.520	36
1	0	2								3.426	1
2	1	0		3.3027	3.3029	6	11	3.32	7	3.306	29
-2	1	2		3.2689	3.2650	1	3	3.28	6		
2	0	1		3.2317	3.2316	8	12	3.25	13	3.235	8
-2	0	3						3.17	2	3.164	7
0	0	3								3.064	2
1	1	2		2.9387	2.9384	2	7			2.942	17
-1	1	3		2.9049	2.9051	100	100	2.920	100	2.908	69
0	2	0		2.8698	2.8667	38	49	2.886	30	2.871	40
2	1	1		2.8172	2.8152	5	9	2.829	16	2.818	18
-2	1	3								2.771	4
0	2	1	*	2.7620	2.7365		6	2.753	5	2.740	12
0	1	3		2.7004	2.7002	61	65	2.714	65	2.706	44
-3	0	3		2.6444	2.6480	2	4	2.658	5	2.649	5
-3	1	1		2.6160	2.6161	47	54	2.627	40	2.618	24
2	0	2		2.5747	2.5484	12	16	2.561	20	2.551	16
1	0	3								2.534	6
-2	0	4		2.4951	2.4969	7	9	2.506	10	2.499	8
-1	2	2								2.489	7
3	1	0		2.4390	2.4381	2	4	2.447	8	2.435	3
-3	1	3		2.4035	2.4040	10	13	2.413	14	2.406	4
-2	2	2		2.3253	2.3245	7	9	2.337	13	2.327	8
-1	1	4	*	2.3042	2.2931		4	2.301	8	2.291	18
-2	1	4		2.2852	2.2842	11	11	2.291	5	2.291	18
-4	0	2		2.2272	2.2259		3	2.233	2	2.227	3
1	2	2		2.1971	2.1975	3	5	2.210	7	2.200	6
-1	2	3		2.1880	2.1835		15	2.193	12	2.186	10
-4	0	1		2.1735	2.1742	19	22	2.182	35	2.176	20
3	1	1								2.164	11
2	2	1		2.1447	2.1445	20	20	2.158	25	2.147	27
0	1	4		2.1299	2.1312		20	2.141	13	2.133	7
-2	2	3		2.1244	2.1237	27	24	2.135	19	2.126	13
0	2	3		2.0927	2.0924	4	8	2.105	11	2.095	13
-4	1	2								2.076	2

Table 5. Continued.

h	k	l	d(obs)	d(calc)	I/I_1		d(calc)	I/I_1	d(calc)	I/I_1
2	0	3	2.0577	2.0588	3	6	2.070	5	2.061	5
-3	2	1							2.055	4
-3	2	2	2.0490	2.0456		4	2.056	3	2.048	3
-4	1	1							2.035	2
-2	0	5	2.0207	2.0225		4	2.030	2	2.024	3
1	0	4							2.001	1
-4	0	4	1.9841	1.9860		3	1.992	1	1.9870	3
3	2	0							1.9653	1
-3	2	3	1.9430	1.9451		4	1.951	2	1.9470	5
2	2	2	1.9043	1.9046	11	13	1.916	11	1.9070	11
1	2	3	1.8982	1.8976		8	1.909	7	1.9000	8
-2	2	4	1.8823	1.8828	21	18	1.892	14	1.8848	11
3	1	2							1.8797	13
1	3	0	1.8632	1.8598		4	1.871	5	1.8626	7
-3	1	5	1.8420	1.8417		3	1.849	2	1.8429	3
0	0	5							1.8383	4
3	2	1							1.8118	1
0	2	4	1.7907	1.7919		6	1.801	4	1.7881	4
-4	0	5	1.7834	1.7818		6	1.783	5	1.7828	3
-5	0	2	1.7769	1.7864	.2	2			1.7773	3
0	3	2							1.7669	8
-4	2	2	1.7569	1.7581	1	8	1.767	11	1.7585	8
4	1	1	1.7331	1.7340	.6	7			1.7300	5
2	0	4							1.7128	1
-4	1	5							1.7026	7
-5	1	2							1.6978	5
-2	0	6							1.6861	5
2	2	3							1.6742	4
1	3	2							1.6709	4
-1	3	3	1.6663	1.6646	4	6			1.6646	7
4	2	0	1.6520	1.6526	27	48			1.6531	4
2	3	1							1.6472	6
2	1	4							1.6413	6
-4	2	4	1.6359	1.6355	35	29			1.6339	19
-5	1	4							1.6307	18
-2	1	6							1.6178	
-3	2	5	1.6058	1.6093	2	4			1.6108	4
-3	3	1							1.6043	5
-3	1	6							1.5997	7
1	1	5	1.5847	1.5835	6	7			1.5851	5
-4	0	6							1.5818	6
4	1	2	1.5574	1.5587	3	7			1.5568	9
0	2	5							1.5482	6
-5	1	5							1.5320	2
-4	1	6							1.5250	1
-2	3	4							1.5194	3
-4	2	5							1.5145	2
-5	2	2							1.5111	1
-5	2	3							1.5065	1
0	1	6							1.4802	3
-5	2	1							1.4762	5
0	3	4							1.4707	3
-5	2	4	1.4622	1.4615	.5	2			1.4633	2

Table 5. Continued.

h	k	l	d(obs)	d(calc)	I/I_1		d(calc)	I/I_1	d(calc)	I/I_1
-6	0	4	1.4603	1.4599	1	3			1.4607	2
-2	2	6	1.4514	1.4525	.9	3			1.4539	3
-6	1	3	1.4358	1.4366	7	10			1.4355	9
1	2	5	1.4301	1.4284	3	7			1.4301	6
-6	1	2							1.4249	3
-1	2	6							1.4214	3
2	1	5	1.4120	1.4122	1	3			1.4156	4
4	2	2	1.4091	1.4105	1	3			1.4091	4
-3	1	7							1.3993	1
-2	1	7							1.3957	2
4	1	3							1.3908	1
1	4	1							1.3819	3
3	3	2							1.3793	3
0	4	2							1.3702	1
1	1	6	1.3635	1.3644	3	7			1.3615	3
0	2	6							1.3516	1
5	2	1							1.3224	3
4	3	1							1.3193	2
0	0	7							1.3131	2
2	4	1							1.3121	3
-6	2	2	1.3080	1.3080	.4	1			1.3091	4
-4	3	5	1.3029	1.3032	.5	2			1.3045	4
-5	3	2							1.3024	4
-5	1	7							1.2940	1
-6	1	6							1.2907	3
4	3	3							1.2825	3
0	1	7							1.2800	3
-5	3	1	1.2775	1.2784	.3	2			1.2798	0
2	3	4							1.2764	2
-7	0	3							1.2716	3
-5	3	4	1.2733	1.2701	.6	2			1.2714	0

[1] $CuK_{\alpha 1}$ radiation (λ=1.54050 A), graphite monochromator. Internal standard, CaF_2. Intensities are integrated peak areas. Indexing based on space group $P2_1/m$. Refined cell parameters from 62 reflections: a = 8.908(4), b = 5.742(3), c = 10.123(5), β = 114.80(2). Reflections not used for cell refinement are starred. The first column under I/I_1 is the integrated area of each peak, and the second column is the peak height.

[2] natural allanite (crystalline), Zambia. JCPDS card 25-169 (Cech et al., 1972).

[3] Ce-allanite, theoretically calculated using POWD10 (Smith and Zolensky, 1983). Positional and isotropic thermal parameters used are from the structure refinement of a natural allanite (Dollase, 1968), and the cell parameters are of the synthetic Ce-allanite. Ionic scattering factors were employed, except for Ce.

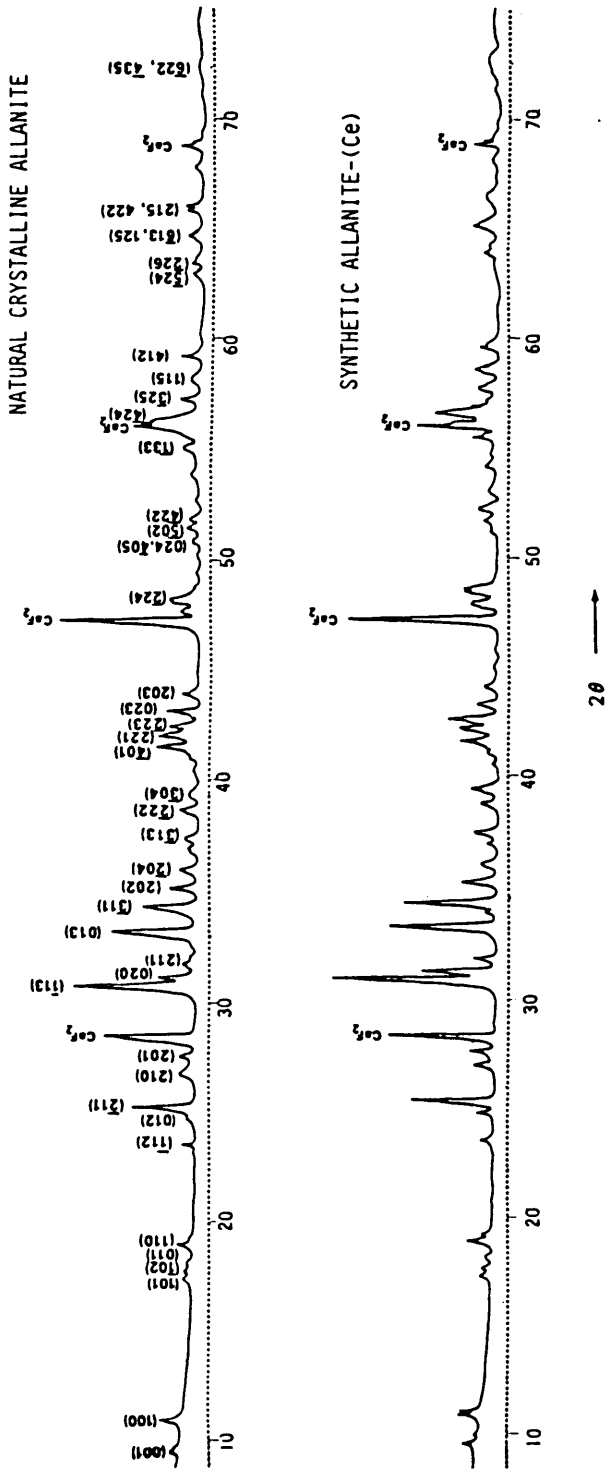

Figure 7. X-ray powder diffraction patterns for synthetic allanite-(Ce) and natural allanite from Zambia (JCPDS 25-169).

clinozoisite by Prunier (1978). In plane light the crystals are clear or slightly golden colored. The larger crystals are slightly pleochroic, light gold to dark gold. The allanite is biaxial negative with $2V_X = 62°$, X:**c** = 54° and Z = **b**. Although Deer et al. (1966) reported that most allanites have their O.A.P. parallel to (010), the orientation of the optic plane in the synthetic allanite-(Ce) (O.A.P. perpendicular to (010)) is similar to some natural crystalline allanites (Cech et al., 1972; Izett and Wilcox, 1968; Holmqvist, 1975).

Twinning. A precession photograph taken with allanite-(Ce) mounted on the **c**-axis reveals a twinned crystal with (100) as the composition plane. The angle between the **c*** axes of each twin is 47°. A possible way to twin the monoclinic allanite on (100) is with an n-glide parallel to (100) through the O(7) atoms. Using an n-glide with (**b**+**c**)/2 translation component is the same procedure described by Ito (1950) and Dollase (1968) to obtain zoisite from clinozoisite. The twinning requires distortion of the M(1,2) octahedron at the twin plane because the inclination of M(1) to the twin plane differs from that of M(2). Distortion of the octahedra would also occur during the twinning of allanite, because the inclination of the M(1) and M(2) octahedra to the (100) plane are slightly different. The difference in orientation of these octahedra relative to (100) is 10.42°, plane M(1)-O(1) ^ (100) = 72.24°; M(1)-O(4)-O(5)-O(4)'-O(5)' ^ (100) = 17.76°; plane M(2)-O(3) = 61.82°; M(2)-O(6)-O(10)-O(6)'-O(10)' ^ (100) = 28.18° (see Fig. 4 of Dollase (1968)).

DISCUSSION

Cell Parameters And Volume Changes In Allanites

The lanthanides, La to Lu, exhibit a monotonic decrease in the ionic radii, a 10% reduction from La^{3+} (1.216 A) to Lu^{3+} (1.032 A) for IX coordination (Shannon, 1976). This decrease in ionic radius should be reflected in a plot of volume (A^3) vs. REE cation

radius cubed (r^3) if there is a simple substitution at the A(2) site of REE^{3+} for Ca^{2+} in the synthetic allanite-(REE). Electron microprobe and ^{57}Fe Mossbauer analyses (see Chapter III) show less than one REE per formula unit in A(2), and other substitution at the A sites as well. The data from ^{57}Fe Mossbauer analysis suggest Fe^{2+} at an A site, the amount increasing from La to Yb. The increase in Fe^{2+} in the A site correlates with a decrease in REEs in the A(2) site. Fe^{2+} probably substitutes into A(1), which is smaller than the A(2) site. Based on stoichiometry, there could also be some REE^{3+} on an M site for the HREE runs. Since it is assumed that the Fe^{2+} will prefer the smaller site, the A(2) site is left with REE^{3+} and Ca^{2+}, the Ca in that site increasing with decreasing REE. Thus, r^3 for each REE is calculated by summing the product of the radius of each cation (REE^{3+} and Ca^{2+}) in the A(2) site and its mole fraction; i.e., $r^3 = \sum C_i r^3_i$ (radii from Shannon, 1976). The cations in the A(2) site were normalized to 2.00 before multiplying by the ionic radii and summing. The unit cell volumes are plotted against r^3 in Fig. 8. There is a decrease in the unit cell volume for allanite-(La) through allanite-(Y), however, it is possible to assign different coordinations for the different ions entering the structure to emphasize a systematic decrease (Fig. 9). La and Ce are reasonably assumed to be in XI coordination based on the crystal structure refinement of natural allanite by Dollase (1971). Nd is assigned IX coordination; Sm is assigned VIII coordination; and Gd, Dy, and Y are assigned VII coordination. Er and Yb are assigned VI coordination (cf. Chapter III); i.e., Er and Yb are in the M(3) site and are not plotted.

Natural epidotes (Carbonin and Molin, 1980) and a natural clinozoisite (Dollase, 1971) with the A(2) sites filled with Ca in X and VIII coordination, respectively, are also

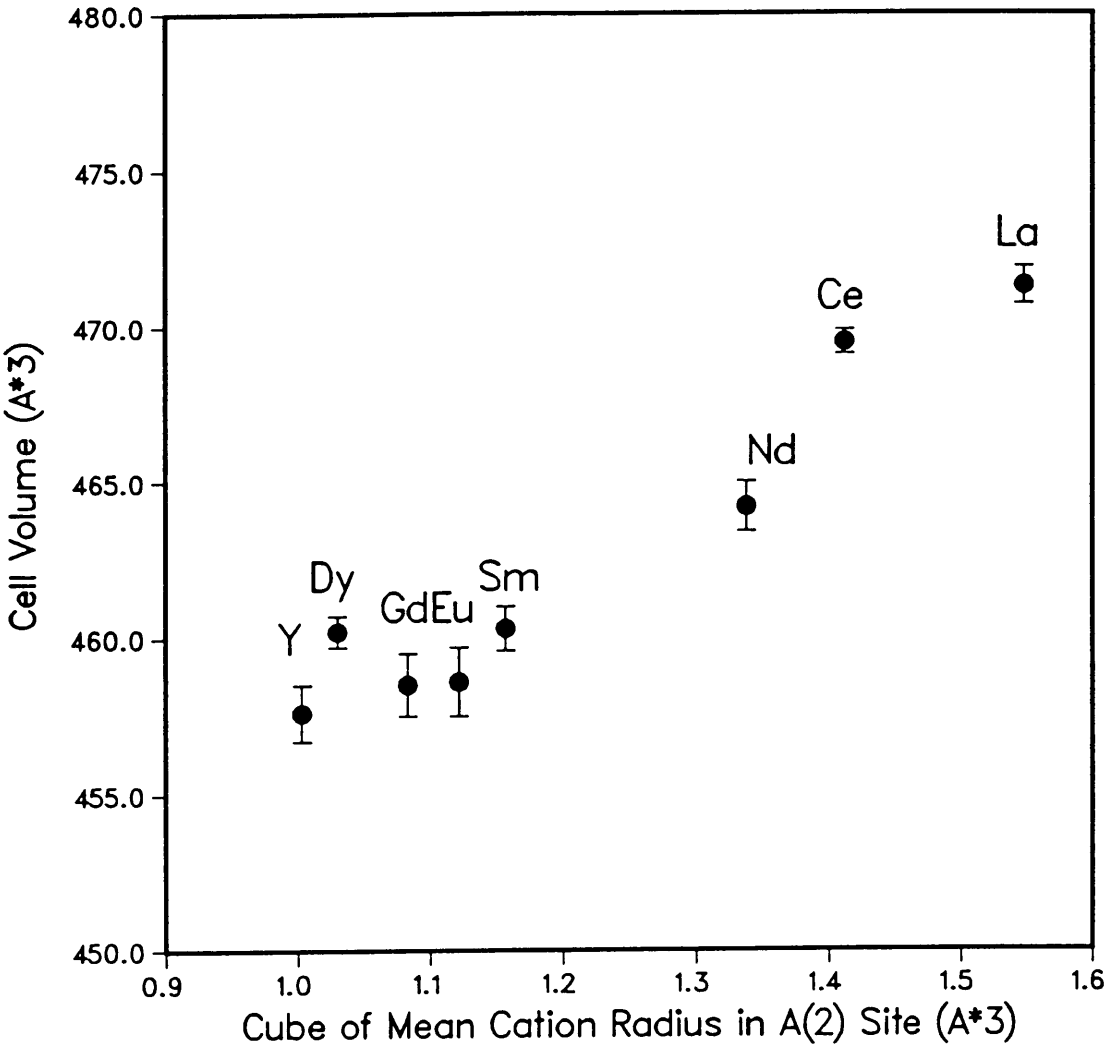

Figure 8. Cell volumes compared to the cube of the mean cation radius in the A(2) site of synthetic allanites (solid dots). All REE are in IX coordination.

Figure 9. Cell volumes compared to the cube of the mean cation radius in the A(2) site of synthetic allanites (solid dots) . Symbols are as follows: X = natural allanite (Cech and Povondra, 1972); O = natural allanite (Dollase, 1971); <> = natural epidotes (Carbonin and Molin, 1980); Δ = natural clinozoisite (Dollase, 1971). The coordination numbers of the REEs in the A(2) site are assigned as follows: La,Ce - XI, Nd - IX, Sm - VIII, Gd, Dy, Y - VII, natural epidote - X, natural clinozoisite - VIII. The Fe^{3+} occupancy for the natural epidotes changes from 0.30 (volume = 454.85 A^3) to 0.86 (volume = 460.20 A^3). Shading encompasses the epidote volumes.

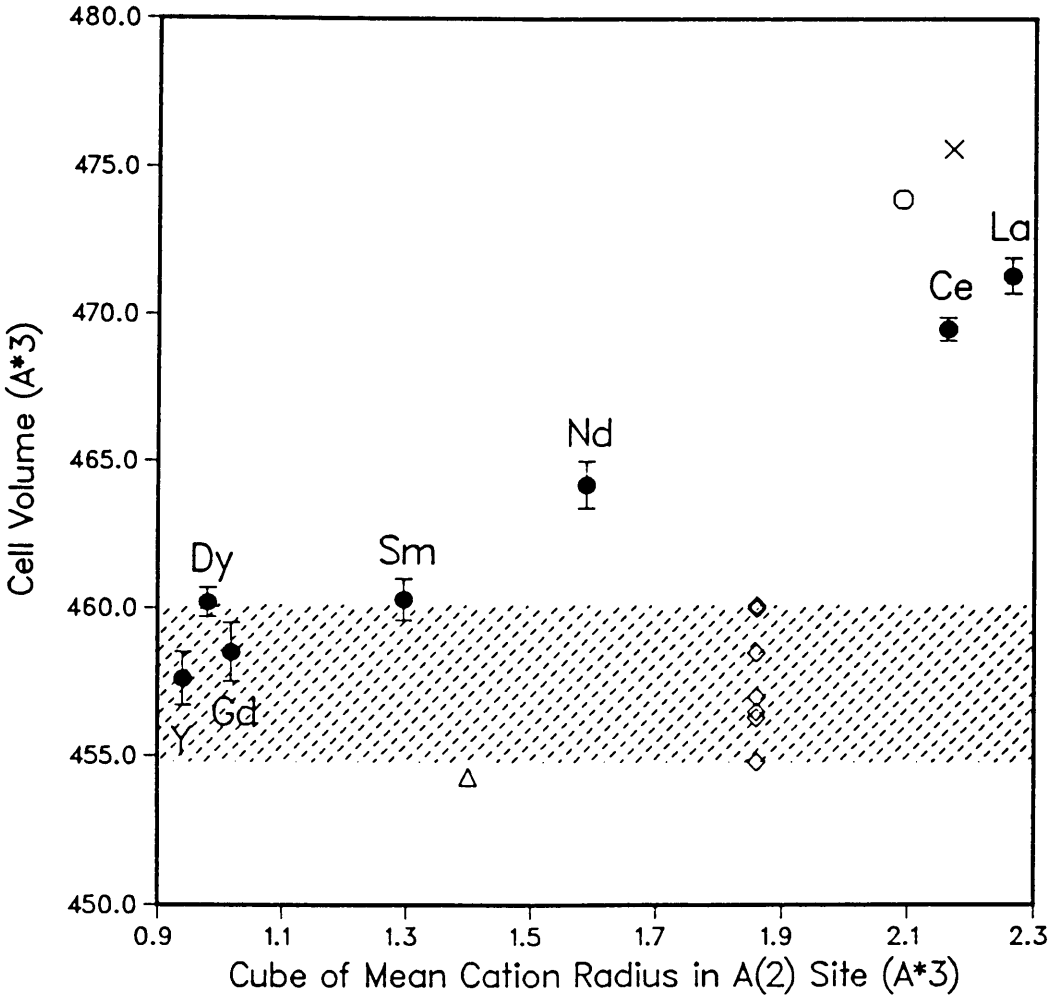
480.0
475.0
470.0
465.0
460.0
455.0
450.0
Cell Volume (A*3)
0.9
1.1
1.3
1.5
1.7
1.9
2.1
2.3
Cube of Mean Cation Radius in A(2) Site (A*3)
La
Ce
Nd
Sm
Dy
Gd
Y

plotted in Fig. 9. The Fe^{3+} occupancy for the epidotes changes from 0.30 (V = 454.85 A^3) to 0.86 (V = 460.20 A^3). The values of most of the epidote cell volumes overlap with the values of the middle rare earth (MREE) allanites. The clinozoisite with Al^{3+} in the M sites has the smallest volume. If the cations in the IX coordinated A(1) site of epidotes were plotted, the sum of the cations in the A(1) site for epidotes would lie at approximately 1.643 A^3, near allanite-(Nd) values.

The epidotes show an increase in volume with increasing Fe^{3+} occupancy in M(3) (data are from Carbonin and Molin, 1980 and Dollase, 1971). The cell volumes of allanite-(La), allanite-(Ce), and allanite-(Nd) are greater than those of the natural epidotes; allanite-(Sm) to allanite-(Y) are within the range of epidote cell volumes. The natural allanites have slightly greater cell volumes than the synthetic allanites most likely due to a small amount of alpha decay damage in their structures.

The allanite cell dimensions are similar to those reported for natural allanites (Fig. 10). All of the cell parameters decrease between La and Gd. After Gd, the **a** cell parameter increases slightly. The **a** cell parameter is most sensitive to substitution at the A site, as the **c** cell parameter is constrained by the SiO_4 and Si_2O_7 tetrahedra that cross-link the octahedral chains. More REE in the A and M sites may account for the slight increase. The **b** cell parameter for the synthetic allanites is greater than those of epidote because Fe^{2+} has substituted for Fe^{3+} in the M(3) site of the octahedral chains that run parallel to **b**. The **a** cell parameter is the least sensitive to substitution in the M site as evidenced by the epidotes plotted in Fig. 10.

Figure 10. Cell parameters of synthetic allanites versus mean cation radius in A(2) site. Natural allanites (X = Cech and Povondra, 1972; O = Dollase, 1971), epidotes (<> = Carbonin and Molin, 1980) and a clinozoisite (Δ = Dollase, 1971) are also plotted.

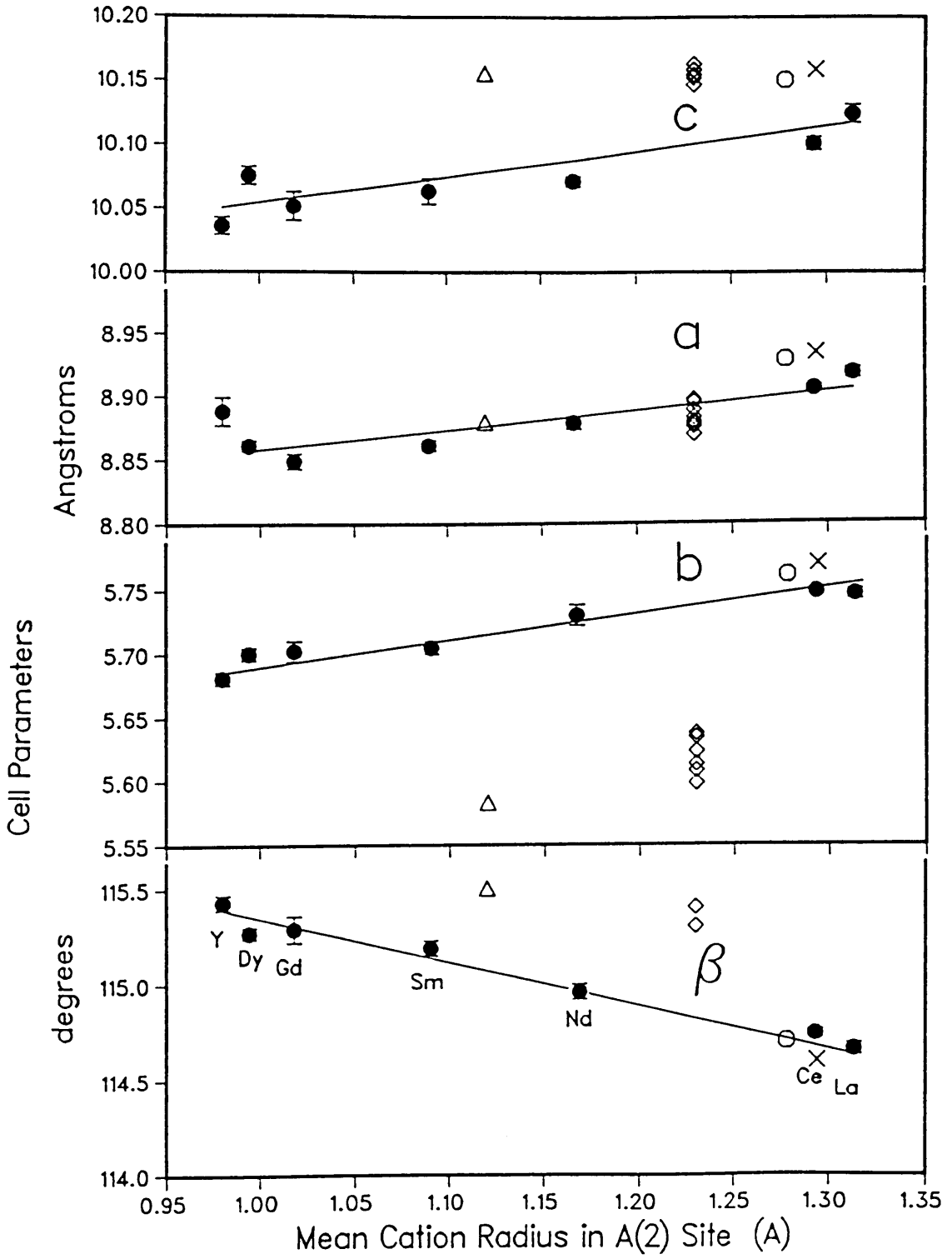
Cell Parameters
Angstroms
degrees
c
a
b
β
Y
Dy
Gd
Sm
Nd
Ce
La
10.20
10.15
10.10
10.05
10.00
8.95
8.90
8.85
8.80
5.75
5.70
5.65
5.60
5.55
115.5
115.0
114.5
114.0
0.95
1.00
1.05
1.10
1.15
1.20
1.25
1.30
1.35
Mean Cation Radius in A(2) Site (A)

Rare Earth Element Patterns In Allanite

The causes of the variations in rare earth element (REE) distributions in minerals have been debated for years. One group of workers (Semenov, 1957, 1958, 1963; Morgan and Wandless, 1980) believes the structure of the mineral plays the predominant role in admitting particular REE ions. In this case the REE ions closest in size to the substitutional site in the mineral will be favored. Thus, minerals with high coordination numbers for their REE sites (X-XII) are considered Ce-selective, those with low coordination number (VI) are Y-selective, and those with intermediate numbers (VII-IX) have the potential for light and heavy REE's present. Other workers (Murata et al., 1953, 1957, 1959) strongly support a paragenetic control to be of major importance in determining the REE distributions. Mineyev (1963) believes the REEs are transported in the form of fluoride, carbonate and phosphate complexes or other ligands, and that the stability difference of the complexes changes with changing conditions. The complex with the lowest stability would condense first, and be taken up in the mineral structure first. A synthesis of both of these ideas was made by Jensen (1973) and Neumann et al. (1966) who point out that although a number of factors, such as pressure, temperature, and composition, play a part in determining which structures crystallize in a given environment, once a structure is forming, the valence and effective size of the various cations competing for a structural position appear to be the all dominant factor in element partitioning.

For the mineral allanite, debate has centered around these two ideas of structural and paragenetic control of REE partitioning. Jensen (1967) studying allanite replacing apatite from the Vishnevye mountains, and Adams (1969), reviewing the distribution of lanthanides in minerals, believe allanite can take up the REEs without appreciable fractionation. This implies the REE composition of allanite could reflect the original composition of the magma from which it crystallized. Brooks et al. (1981) contend the

REE partitioning behavior of allanite is structurally controlled. This implies the presence of allanite could be a significant factor in the evolution of granitic liquids and any attempt to model the evolution of crystallizing magmas. For the Sandy Braes obsidian, Brooks et al. suggest that 0.1 volume percent allanite present decreases the La by a factor of almost two and changes the La/Lu ratio of the residual melt by 45 percent. Allanite can form at the beginning of crystallization sequences (Yurk et al., 1970; Ivanov, 1969; Kupriyanova et al., 1964) or near the final stages of magma solidification (Hildreth, 1979; Sawka et al., 1984; Hickling et al., 1970; Zdorik, 1964). When crystallizing in the late stages, allanite has no effect in partitioning REEs.

Naturally observed compositions. Reported chemical analyses indicate allanite preferentially incorporates the LREEs, La and Ce, and, in some instances, the element, Y (Fleischer, 1985).

Reviewing 387 analyses of natural allanite (appendix C), cerium is present in greater amounts than lanthanum in all but nine analyses, and is equal to lanthanum in one analysis. The allanites that contain more lanthanum than cerium are found in granite, granodiorite, quartz monzonite, and a granulite gneiss (Putalova, 1978; Hugo, 1961; Ghent, 1972; Jesus-Ojeda and Mendoza, 1981). The ratio of La/Ce in the La-dominant allanites range from 1.00 to 1.06 in the igneous rocks to 1.13 to 1.44 in two gneiss samples. More commonly allanite has a La/Ce ratio near 0.57, the average of 139 granites and 29 granodiorites, (Fleischer, 1985). Because so few allanites with La > Ce have been reported, the existence of allanite-(La) is questioned by Fleischer (1985).

The rarity of allanite-(La) in nature is probably due to compositional constraints under which the mineral forms. Cerium is nearly twice as abundant as lanthanum in the Earth's crust (Vlasov, 1966), and the La/Ce ratio in chondrites, 0.372, slightly less than the La/Ce ratio of about 1/2 reported for most allanites. In nature, allanite-(La) may occur

in instances when La is more concentrated than Ce, for example, in extremely fractionated environments such as alkalic pegmatites.

Yttrium substitution in allanite is interesting because geochemically it behaves like a rare earth element, and has an ionic radius between the heavy rare earth elements, Dy and Er. Because of this similarity, the expectation is that it would be present in allanite in approximately the same minor amounts (Fig. 11) as the heavy rare earth elements. However, the literature contains some analyses of allanite, mostly from pegmatites, in which yttrium predominates over the other lanthanides (Semenov and Barinskii, 1958; Neumann and Nilssen, 1962; Protopopov, 1940; Zhirov et al., 1961). Comparing the abundances of La, Ce, Y, Gd, Dy, Er and Yb in chondrites, there is 0.34 ppm La, 0.91 ppm Ce, 2.8 ppm Y, 0.26 ppm Gd, 0.30 ppm Dy, 0.20 ppm Er and 0.22 ppm Yb (Henderson, 1984). The greater availability of yttrium compared to the heavy rare earth elements may account for its greater abundance in allanite compared to the other heavy rare earth elements it geochemically resembles.

A number of workers have looked at the REE compositions in natural allanites, and have determined the partitioning of REEs between allanite and a melt (the glass phase) or between allanite and associated REE minerals.

Brooks et al. (1981) have acquired the rare earth partition data for the obsidian of Sandy Braes, Ireland. There is a marked difference between the rare earth distribution coefficients, the ratio of the concentration of REE in the mineral to that in the glass. Those reported by Brooks et al. were 820 for La and 635 for Ce compared with 8.9 for Yb and 7.7 for Lu. Brooks et al. also show a gradual decrease in the partition coefficients: (La = 820), Ce (635), Nd (463), Sm (205), Gd (130), Tb (71), (Dy and Er were not reported). Experimental work by Green and Pearsons (1983) for partitioning between allanite, titanite, and chevkinite in coexisting intermediate felsic liquids show similar results. In their study,

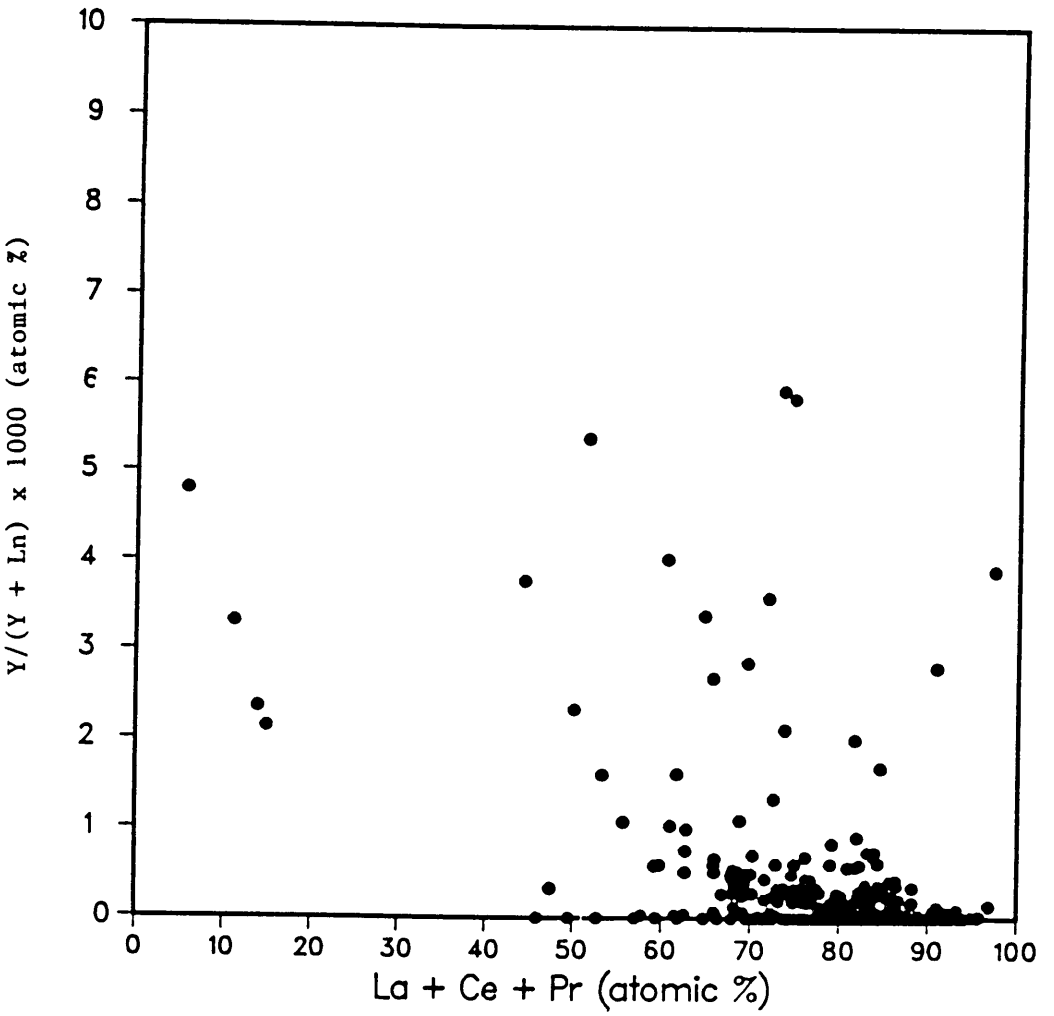

Figure 11. [Y/(Y + Ln)] x 1000(atomic %) versus the light lanthanides La + Ce + Pr (atomic %) for 387 allanites.

the partition coefficient between allanite/liquid, is ~30 to 120 for La and ~0.5 to 6 for Lu. Nash and Congdon (1987) studied a highly evolved fluorine enriched rhyolite and report LREEs are partitioned into fluocerite > allanite ≥ chevkinite, whereas HREEs and MREEs are partitioned more strongly into zircon, titanite and apatite rather than allanite. These studies indicate allanite favors the LREEs rather than the HREEs.

Synthetic compositions possible. The make-up of the run products and the chemical formulas of the synthetic allanites suggest they preferentially incorporate the LREEs rather than the HREEs. Allanite was readily synthesized for all but the allanite-(Y), allanite-(Er) and allanite-(Yb) compositions; however, the yields decreased from 100 volume percent for allanite-(La) to 90 volume percent for allanite-(Dy). The presence of additional phases suggests the allanites are not stoichiometric; electron microprobe analysis confirms this. An increase of Fe^{2+} in the A site of allanite reduced the REE content from 0.84 atom per formula unit for allanite-(Ce) to 0.75 for allanite-(Dy).

The cell parameters of synthetic allanite-(La) are similar to natural and synthetic allanite-(Ce) (Dollase, 1971 and this study).The cell dimensions of allanite-(Y) are close to the cell dimensions of the HREE allanite, allanite-(Dy). The REE content of allanite-(La), 0.93 atom per formula unit, suggests it should have another phase present, La-Al-silicate?, although other phases were not detected. Allanite with equal parts La and Ce (i.e., $CaLa_{.50}Ce_{.50}FeAl_2Si_3O_{12}OH$), synthesized at 700°C and 4 kbar (400 MPa) shows no structural preference for either La or Ce (based on qualitative EDS analysis, Appendix A). The allanite-(Y) yield was approximately 50 to 60 volume percent allanite, with the remaining being pyrosilicate, britholite, anorthite, magnetite and quartz. Frondel (1964) reported that two natural allanite-(Y) samples recrystallized after heating for three days, gave x-ray patterns somewhat different from that of allanite, suggesting this might

represent a new structural variation. Unfortunately, these x-ray patterns were not published so comparison of the d-spacings between the synthetic and natural samples could not be made. The x-ray diffraction peaks of allanite-(Y) are shifted compared to those of allanite-(Ce); however, the cell parameters of allanite-(Y) could be refined using a subset of the 16 diffraction peaks of allanite-(Ce), so a new structure is not suggested. It is possible that with natural allanite-(Y) which always has some La and Ce present, the La and Ce substitute at the A(2) site and the Y substitutes at the A(1) site. In the allanite-(Er) and allanite-(Yb) runs, pyrosilicate, anorthite and magnetite were dominant; epidote-(Er) and -(Yb) were subordinate phases.

The partitioning of REEs between the allanite starting compositions and the allanite in the run products would suggest the preference allanite shows for the LREEs and/or the HREEs. This can be estimated crudely by multiplying the percentage of allanite in the run product (Table 2) by the amount of REE in the allanite (Table 4) and dividing by the amount of REE in the starting composition (always 1 a.f.u. X 100%) This ratio, a "partition coefficient", can be compared to those reported in natural rocks. The partition coefficients for the synthetic allanites are as follows: La (93), Ce (80), Sm (74), Gd (67), Dy (67), Y (48), Yb (24). Although the absolute values are not important, the general trend parallels the results of REE partitioning in natural samples (see Green and Pearson, 1983).

Crystal structural control. The REE substitution in the synthetic allanites is a function of the geometry of the allanite structure. Although the allanites with different REEs were grown under similar pressures, temperatures, and oxidative conditions (close to the NNO buffer because of the Rene 41 pressure vessels), the LREEs preferentially substituted in allanite compared to the HREEs. The LREE ions best approximated the ionic radii of the calcium ions they replaced. The presence of REEs in other phases in the

synthetic allanite run products (Table 2) also appear to be a function of the size of the REE cation, and the coordination of the REE sites in which they occur (Fig. 12). A larger percentage of REE phases other than allanite were present in runs from the HREE allanite starting compositions.

Allanite and epidote are isostructural. The primary difference between them is that ideal allanite has Fe^{2+} in the M(3) site; ideal epidote has Fe^{3+} in the M(3) site. Allanite has 3+ rare earth elements (substituting for Ca^{2+} cations) in the A site for charge balance. A natural epidote could have REEs in the A site if some Fe2+ were present or if charge balance were maintained by some O^{2-} replacing $(OH)^{1-}$. The substitution of Fe^{2+} in the M(3) site of the epidote structure is important, not only because it allows a 3+ ion to substitute in the structure, but also because it expands the structure to accomodate the LREEs. The following is a description of that substitution, and the importance of matching size of the substituting ion to the coordination of the substituted sites in the REE minerals formed in the run products.

Epidote has Ca^{2+} in two X- and IX-coordinated crystallographically distinct sites, A(1) and A(2), respectively. It has been demonstrated for allanite that the REE's replace Ca^{2+} at the larger X-coordinated A(2) site in epidote (Dollase, 1973). This site changes to XI-coordination in allanite to accommodate the REEs, and the accompanying substitution of Fe^{2+} in the structure. The A(1) site remains IX-coordinated in both the epidote and the allanite structure. The X-coordinated site in epidote has an average Ca-O distance of 2.679 A (Dollase,1971) . If the oxygen radius is assumed to be 1.40 A, then the apparent Ca^{2+} (CN = X) radius is 1.279 A. The average ionic radii for trivalent REE ions in X-coordination range from 1.090 A (Lu-extrapolated) to 1.270 A (La). Therefore, the light

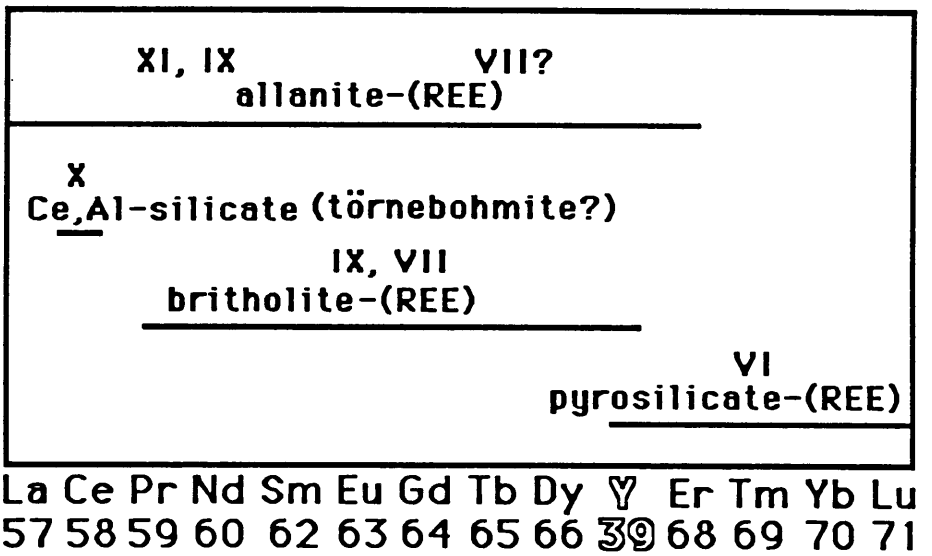

Figure 12. The occurrence of phases in the synthetic run products as a function of the size of the cation and coordination of the REE site. The REE coordination number is written above each mineral. Allanites with even REEs plus La, Eu and Y were synthesized. The percent of allanite in the run products decreased from 100% for allanite-(La) to 70% for allanite-(Dy) compositions.

rare earth ions (La, 1.27 A and Ce, 1.25 A) could reasonably be accommodated within the available X-coordinated site by substitution for calcium ions. The IX-coordinated site in epidote has an average Ca-O distance of 2.593 A (Dollase, 1971), so the effective Ca^{2+} radius (CN = IX) would be 1.19 A. In IX-coordination the effective radii range from 1.032 A (Lu) to 1.216 A (La). This site could conceivably allow for substitution of the smaller REEs, or the X-coordinated polyhedra of the A(2) site could possibly reduce to IX- or even VII-coordination when substitution of the smaller REEs occurs. Note that the site refinement which assigned the REEs in allanite to an XI-coordinated site was done on a natural allanite which was Ce-group selective, and none have been done on an allanite which is Y-group selective.

Tornebohmite has two crystallographically distinct REE sites; both are X coordinated (Shen and Moore, 1982). The average REE-O distances for each site are 2.64 and 2.68 A. Subtracting 1.40 A (radius of oxygen) from these, the apparent REE radii are 1.24 and 1.28 A, consistent with substitution of the larger light REEs (La, Ce) in this mineral. A minor amount of tornebohmite, which has a REE structural site with X coordination, appeared in the allanite-(Ce) run products, but none occurred in the runs with MREE or HREE compositions.

The structure of apatite (Posner et al., 1958; Kay and Young, 1964; Sudarsanan and Young, 1969; Calvo et al., 1975) has two crystallographically distinct sites: Ca^{2+} in IX- and VII-coordination, which can accommodate substitution of the REEs (Henderson,1980). Hydrous britholites, Ca-REE-silicate apatites, have been synthesized for even numbered REEs from La to Lu at 650°C, 2 kbars, and anhydrous britholites at 1200°C in air (Ito, 1968). Natural apatites incorporate the light and middle rare earth elements, especially Sm. Nagasawa (1970) found that apatite incorporated Nd, Sm, Gd and Dy whereas zircon incorporated Er, Yb and Lu. Henderson (1980) and Cullers and

Medaris (1977) note LREEs are preferentially accommodated by apatite relative to titanite. The synthetic REE-apatite, britholite, appeared in the allanite starting compositions that had the middle rare earth elements; it did not appear in the run products of allanite-(La), allanite-(Ce), allanite-(Er) or allanite-(Yb) compositions. Britholite-(Ce) did appear in the decomposition products of allanite-(Ce).

The pyrosilicates, $REE_2Si_2O_7$, grown in a flux between 900 and 1800°C at 1 atm. have numerous polymorphs with the REEs in sites with coordinations that vary from VIII to IX for the light rare earth elements La-Eu, to coordination VI to VIII for the heavy rare earth elements, Eu to Lu (Felsche, 1973). Extending the polymorphic fields determined by Felsche to lower temperatures (e.g., 650°C) relevant to this study, the structures favored for the La to Sm pyrosilicates would be Type A ($P4_122$ or $P4_1$) which has the REEs in IX coordination; for the Eu to Tm pyrosilicates, Type B (P1 or P1) with the REEs in VIII coordination; and for the Yb pyrosilicate, C2/m, C2 or Cm with the REEs in IV coordination. The Er pyrosilicate could have either VIII or VI coordination; not enough data is in this region of Felsche's plot to extrapolate. From examination of x-ray diffraction patterns of the synthetic pyrosilicates, $Y_2Si_2O_7$ (run #133), $Er_2Si_2O_7$ (run #163 and #144 and $Yb_2Si_2O_7$, (run #125), have the thortveitite (or Type C) structure, C2/m, which has the REE in VI coordination (Felsche, 1973). This expands the field of the Type C pyrosilicate on Felsche's plot illustrating the polymorphism of $REE_2Si_2O_7$ compounds. The pyrosilicates occurred in the run products of the HREE allanites, allanite-(Y), allanite-(Er) and allanite-(Yb).

Garnet synthesized at 700°C, 4 kbar and 0.33 Yb starting composition has Yb in VI coordination deduced from its structural formula: $(Ca_{1.84}Fe^{2+}_{1.16})_{3.0}(Al_{1.2}Fe^{2+}_{.24}Yb_{.54})_{1.98}(Si_{2.96}Al_{.04})_{3.0}O_{12}$. In addition, Ponader and

Brown (1986) used x-ray absorption spectroscopy to determine that Yb in quenched albite melt was coordinated by 7.7 oxygens on the average. The IR spectroscopy and ^{57}Fe Mossbauer data (cf. Chapter 3 and 4) also suggest that the epidote-(Yb), found in some runs with Yb starting composition, may have the Yb in VI coordination.

Other accessory minerals associated with allanite and epidote that incorporate REEs are listed in Table 6. The coordination site available for substitution of the REEs in these minerals and the REEs that are preferentially incorporated by them in nature are listed. The minerals with high coordination sites take up the light REEs, and those with low coordination sites incorporate the HREEs.

Influence of oxygen fugacity. Oxygen fugacity indirectly controls the REE substitution in allanite. Although not many reports include the intensive conditions of allanite-bearing assemblages, those that do (Speer, 1987; Hildreth, 1979; Evans and Vance, 1987) suggest a limited range of oxygen fugacity for their formation. Oxygen fugacity determines the Fe^{2+}/Fe^{3+} ratio in minerals; the Fe^{2+}/Fe^{3+} ratio in allanite and epidote controls the REE substitution in them. Natural allanite has more Fe^{2+} in the M(3) site than epidote, so has an expanded structure (especially along the **b** direction) compared to epidote. The expanded structure favors LREE substitution.

Three zoned allanites from the Skye granite (Exley, 1980), two hydrothermal in origin and one metamorphic, have rims enriched in the middle REEs and depleted in the LREEs. Also in every case, the Fe^{3+}/Fe^{2+} ratio increased from the core to the rim. The chemical formulas for the core of one sample, $(Ca_{1.24}REE_{.496}Y_{.01}Mn_{.029}Mg_{.035}Th_{.101})(Fe^{2+}_{.831}Fe^{3+}_{.158})_{.99}Al_{2.02}Si_{3.05}O_{12}(OH)$ and the rim, $(Ca_{1.61}REE_{.05}Y_{.14}Mn_{.09}Mg_{.03}Th_{.004})(Fe^{2+}_{.34}Fe^{3+}_{.39}Al_{.28})_{1.01}Al_{2.0}Si_{3.06}O_{12}(OH)$ illustrate

Table 6. Coordination number of REEs in minerals associated with allanite.

mineral	ideal chemical formula	REE CN	REE pattern	reference
allanite-(Ce)	$Ca(Ce,La,Y)Fe^{2+}Al_2O(Si_2O_7)(SiO_4)(OH)$	IX, XI	LREE	Dollase (1971)
chevkinite	$(Ca,Ce)_2(Fe^{2+},Mg)(Ti,Fe^{3+})_{1.5}Si_2O_{11}$	X	LREE	Ito & Arem (1971)
tornebohmite	$Ce_2AlSi_2O_8(OH)$	X	LREE	Shen & Moore (1982)
monazite	$(Ce,La,Nd,Th)PO_4$	IX	LREE	Beall et al. (1981)
britholite	$(Ca,Ce)_5(SiO_4,PO_4)_3(OH,F)$	IX, VII	MREE	Ito (1968)
apatite	$Ca_5(PO_4)_3(OH,F)$	IX, VII	MREE	Posner et al. (1958)
zircon	$ZrSiO_4$	VIII	LREE HREE	Speer (1982); Hollabaugh & Foit (1984)
titanite*	$CaTiOSiO_4$	VII	LREE	Speer & Gibbs (1976)
pumpellyite	$Ca_2(Fe^{2+},Fe^{3+})Al_2SiO_4Si_2O_6(OH)_4$	VII	HREE	Yoshiasa & Matsumoto (1985)

* The titanite REE content rarely exceeds 5% and can incorporate Y.

that the composition of the rim is close to that of epidote.

Exley notes the lack of a correlation between Al^{3+} and Ce_N/Y_N (N = chondrite normalized) for the allanite data; however the ions substituting in M(3), Fe^{3+} and Fe^{2+}, are the ions that should be considered rather than Al^{3+}. There is a correlation between the ratio of Fe^{3+}/Fe^{2+} and Ce_N/Y_N (Fig. 13) for the igneous allanites he reports. Ce_N/Y_N is always lower and Fe^{3+}/Fe^{2+} higher for the rims of all the core/rim pairs.

Sawka et al. (1984) also report allanite crystals with rims enriched in middle rare earths. They attribute the change in REE concentration in the rims to the increase of the NBO/T ratio (nonbridging oxygens/tetrahedra) in the melt due to an increase in fluorine which depolymerizes tetrahedral networks. Ponader and Brown (1986) suggest a similar effect on the melt due to fluorine in their study of Yb in glass. Complete chemical analyses of allanite were not reported so the Fe^{3+}/Fe^{2+} ratio could not be compared.

Epidotes reported by Nystrom (1984) show LREE enrichment, although the values of the distribution coefficients were low for three of the four epidotes. The large amount of LREE in the one sample would suggest the Fe^{2+}/Fe^{3+} ratio in that sample is high, and the mineral may be closer in composition to allanite than to an epidote. Complete chemical analyses were not reported.

The above examples suggest a REE control that is indirectly related to oxygen fugacity. At a fixed temperature and pressure, if the environment becomes more oxidizing, epidote could form rather than allanite. The change of the Fe^{2+}/Fe^{3+} ratio in an epidote-group mineral, changes the size of the A sites in the structure which then fixes the REE substitution. With oxidizing conditions, the LREEs would no longer prefer the structure of epidote with the smaller A sites. This may explain the apparent immiscibility of allanite and

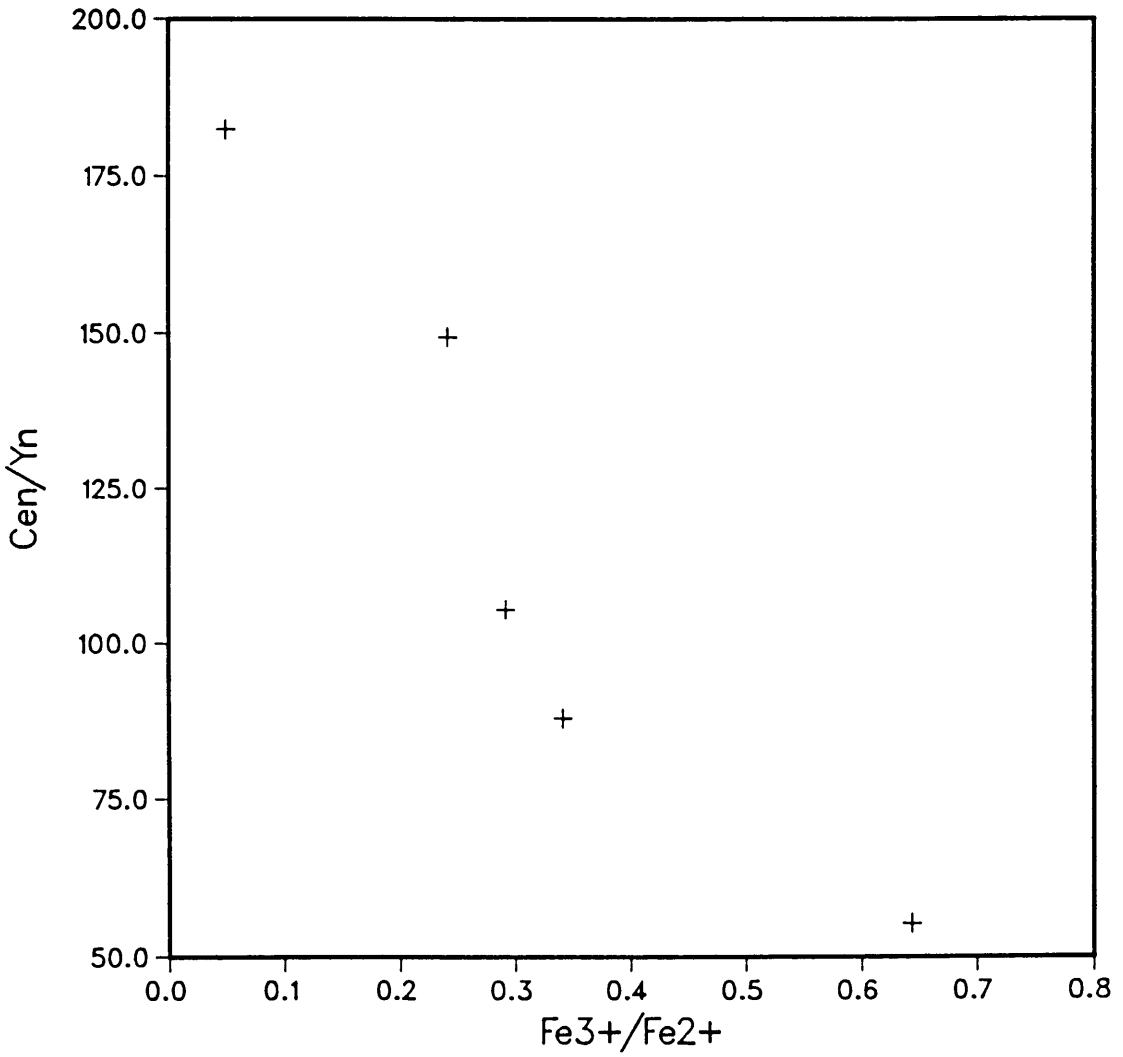

Figure 13. The ratio Fe^{3+}/Fe^{2+} versus Ce_N/Y_N. The Ce_N/Y_N ratio decreases with increasing Fe^{3+}/Fe^{2+} (N = chondrite normalized).

epidote in the occurrences where epidote rims allanite.

Allanite Phase Relations

Allanite-bearing assemblages. Allanite occurs in pegmatites, granites, rhyolites, quartz veins, hornfelses and gneisses (see Appendix D), and less commonly in migmatites (Metcalf, pers. comm.) and eclogites (Franz et al., 1986). The relative concentrations of the lanthanides vary in igneous host rocks, the LREE increasing from granitic pegmatites to alkalic pegmatites (Fleischer, 1985). Other minerals associated with allanite that incorporate REEs are chevkinite, zircon, titanite, britholite, bastnaesite, apatite, monazite and epidote. It can be difficult to determine from the literature, those equilibrium mineral assemblages which include allanite. For example, while allanite is reported with certain minerals from pegmatites, the allanite can occur in the wall zone and the "associated" minerals in the core zone. However, some mineral associations are reasonably interpreted as reported.

Allanite reaction relations. Allanite is commonly reported to alter to bastnaesite, a REE carbonate. More rarely allanite is associated with britholite and/or monazite, in a reaction relationship. In two cases of allanite associated with monazite (Appendix D), the allanite rims monazite in one case, and rims britholite which in turn rims monazite in the other case. The decomposition of allanite in annealing studies of natural metamict samples occurs over a wide temperature range, 850 to 1000°C, and the products in most of these studies include a REE-apatite phase (Kauffman and Dilling, 1950; Orcel, 1953; Khvostova, 1962). In addition to "an apatite-like mineral" [britholite], Mitchell (1966) reports anorthite, magnetite, ±cerianite. Similar results have been obtained by Ueda and Korekawa (1955), Khvostova (1962), and Faria (1964). A decomposition reaction that includes these products can be written: 3 $CaCeAl_2FeSi_3O_{12}(OH)$ =

$Ca(Ce_2Al_2)Si_3O_{13} + 2\ CaAl_2Si_2O_8 + Fe_3O_4 + 2\ SiO_2 + CeO_2 + 1.5\ H_2$.

In nature allanite is reported to rim britholite in a sample from the Vishnevye Mountains (Jensen, 1967; Yes'kova and Ganzeyev, 1964); it rims a britholite-bearing rock in a vein in the Silver Plume granite in Colorado (Goddard and Glass, 1940); and it occurs in the center of an apatite-magnetite vein in India (Rao, 1976). The occurrence of allanite after britholite seems to be rare (see allanite associations, Appendix D), as is the occurrence of britholite itself. Nash (1972) studying the Shonkin Sag laccolith, a sequence of rocks from shonkinite to soda syenite, has shown that britholite rather than apatite occurs if silica activity increases. This appears to have influenced mineral crystallization in the sample from the Vishnevye Mountains where allanite rims britholite which in turn rims monazite. A change in silica activity may also have influenced the crystallization sequence of minerals at Jamestown, Colorado where monazite, britholite and allanite are present.

At Jamestown, Colorado, allanite rims a vein of britholite and other REE minerals (Affholter and Adams, 1987). The britholite from the northern locality, previously reported as cerite (Goddard and Glass, 1940; Hanson and Pearce, 1941; Gay, 1957), has lattice constants of **a** = 9.602(1) and **c** = 7.017(1) A. These values fall between those reported for the synthetically grown silicate apatites, britholite-(Ce) and britholite-(Nd) (Ito, 1968). The structural formula

$$(REE_{2.93}U_{.01}Th_{.01}Fe^{2+}_{.05})_{3.0}(Ca_{1.55}Y_{.19})_{1.74}(Si_{2.88}P_{.16})_{3.04}O_{12.5}F_{1.07}$$

is similar to the silicate apatite reported by Belokoneva et al. (1972) which contains vacancies in the IX-coordinated site. The vein of rare earth minerals containing britholite occurs at an aplite-gneiss contact, the aplite grading into pegmatite. The igneous rocks are part of the Silver Plume granite pluton. The vein contains allanite, britholite, tornebohmite, monazite, fluorite and quartz (Fig. 14). According to Goddard and Glass (1940), the britholite was probably the first mineral to crystallize, and, with fluorite and monazite, may

Figure 14. X-ray diffraction pattern of the "cerite" rock from Jamestown, Colorado. The cerite is actually britholite. Other minerals present are monazite (JCPDS 29-403), fluorite (JCPDS 4-864), tornebohmite (JCPDS 34-160) and quartz (JCPDS card not shown).

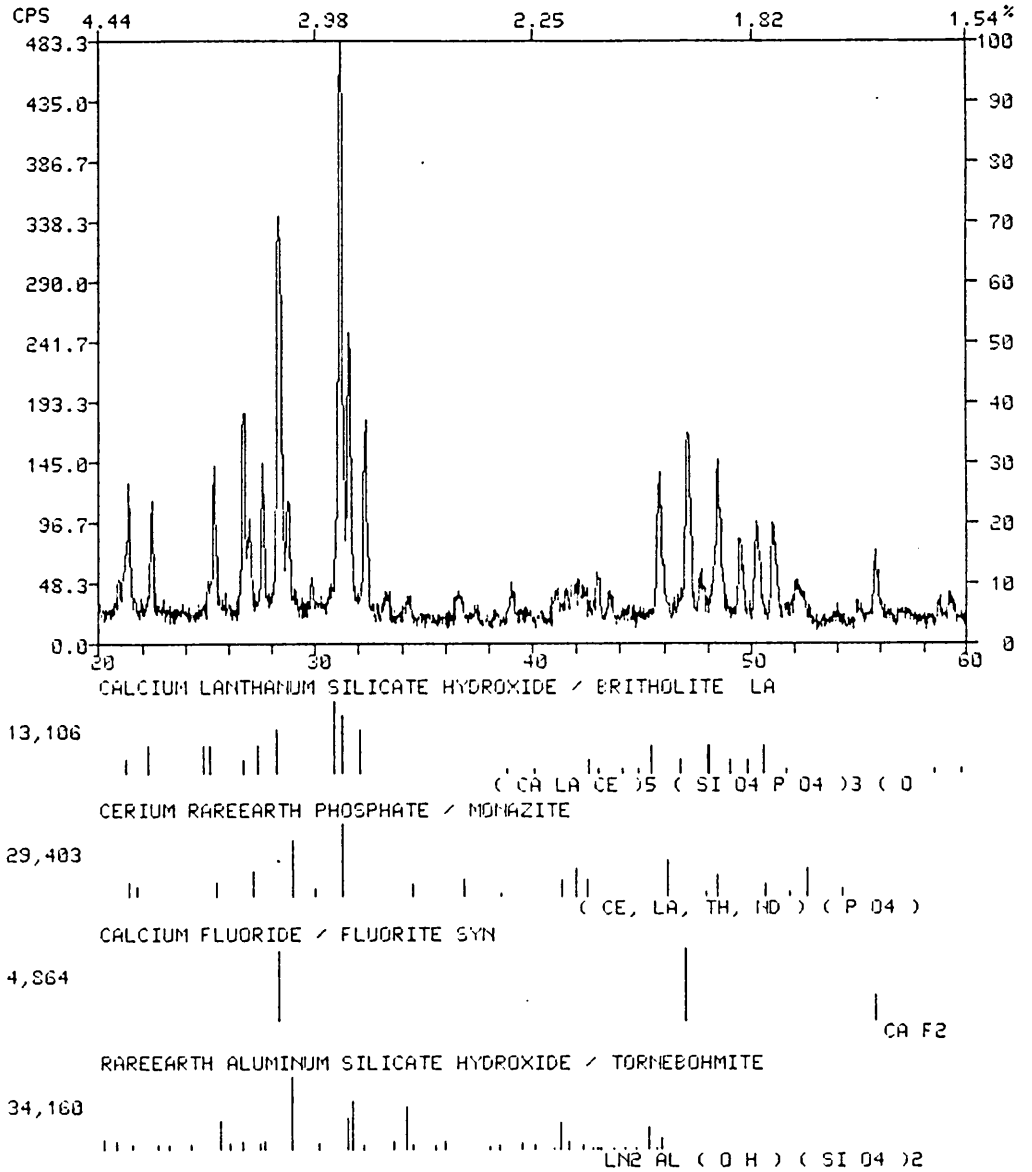
CPS
4.44
2.38
2.25
1.82
1.54 %
483.3
435.0
386.7
338.3
290.0
241.7
193.3
145.0
96.7
48.3
0.0
100
90
80
70
60
50
40
30
20
10
0
20
30
40
50
60
CALCIUM LANTHANUM SILICATE HYDROXIDE / BRITHOLITE LA
13,106
(CA LA CE)5 (SI O4 P O4)3 (O
CERIUM RAREEARTH PHOSPHATE / MONAZITE
29,403
(CE, LA, TH, ND) (P O4)
CALCIUM FLUORIDE / FLUORITE SYN
4,864
CA F2
RAREEARTH ALUMINUM SILICATE HYDROXIDE / TORNEBOHMITE
34,160
LN2 AL (O H) (SI O4)2

have occupied most of the vein . The fluorite occurs in "pods" with the britholite, and the monazite is associated with the britholite and tornebohmite. The britholite and fluorite exhibit metamorphic triple junction contacts. The britholite was replaced by tornebohmite which is veined by monazite. Allanite, the last mineral to form, extensively replaced tornebohmite, residual britholite and aplite bordering the vein. Quartz occurs within the allanite. The allanite grains are larger than those of any of the minerals which they replace, and are zoned red brown in contact with the britholite to green in contact with the aplite. Electron microprobe analyses are listed in Table 7. Although the mineralogic relationships here are complex, it appears as though the allanite was enriched in light rare elements compared to the britholite which it replaced. At a nearby locality near Jamestown, called the "southern locality" (Goddard and Glass, 1940), there is cerite; however the cerite is not rimmed by allanite. New mineral identifications of the cerite samples from Jamestown, loaned by the Harvard Mineralogical Museum, are listed in Table 8.

Rao (1976) studied some apatite-magnetite veins in India containing REE-rich apatite rimmed by allanite. The veins are well-zoned, pegmatitic, and intrude granite. Prismatic crystals of allanite occur as a narrow zone in the central portion of a few of the veins. The allanite occurs in the interspaces between apatite crystals and often encloses and replaces the apatite along weak planes denoting its later paragenetic sequence.

Stability conditions. Pressure and temperature determinations for igneous and metamorphic rocks that contain allanite constrain its stability. A preliminary P-T diagram based on reports of allanite in those rocks, the decomposition of natural allanites, and experiments using synthetic allanite is shown in Fig. 15.

Allanite is a ubiquitous REE primary phase in most of the granitoids of the Liberty Hill pluton (Speer, 1987). According to Speer, the allanite-bearing granitoids were emplaced at 725 ($fO_2 \sim 10^{-15}$, $P_{fluid} \sim 0.5P_{total}$) to 647°C ($fO_2 \sim 10^{-16}$, $P_{fluid} \sim P_{total}$) and 4.5

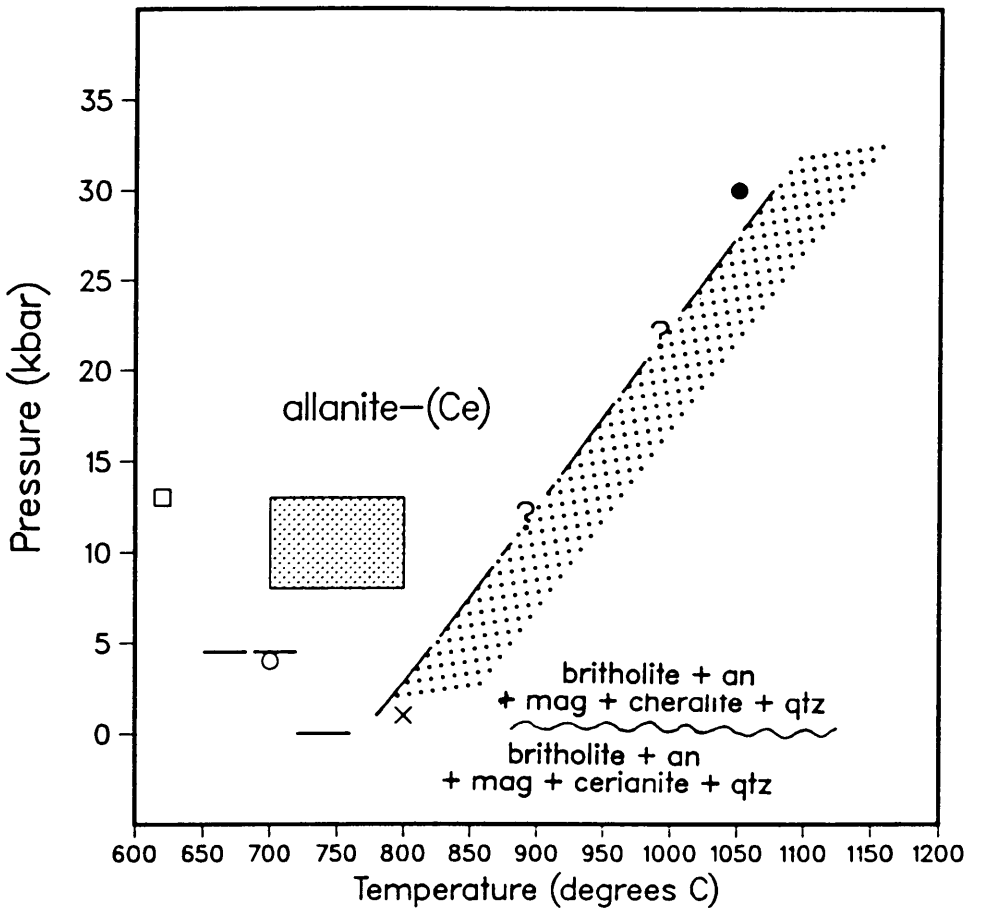

Figure 15. Preliminary P-T diagram for allanite-(Ce) stability. Synthetic: o = allanite (this study), x = decomposition products for $X(H_2O)$ = 0.25 (this study), • = allanite (Green and Pearson, 1984); Natural: __ __ = allanite from the Liberty Hill granitoid (Speer, 1987), _____ = allanite from the Bishop Tuff rhyolite (Hildreth, 1979), shaded box = granitoid (Evans and Vance, 1987), o = allanite from eclogite (Franz et al., 1986)

Table 7. Electron microprobe analyses[1] of selected minerals from Jamestown, Colorado

wt. % oxides	allanite (green)	allanite (red)	britholite*	tornebohmite
SiO_2	31.6	29.9	21.4	23.6
P_2O_5	-	-	1.4	-
Al_2O_3	21.5	11.4	-	11.5
ThO_2	-	-	0.2	-
UO_2	-	-	0.3	-
RE_2O_3	22.4	27.5	58.7	62.5
Y_2O_3	0.4	0.1	2.6	0.3
CaO	9.9	8.0	10.6	0.1
MnO	1.0	1.0	-	-
MgO	0.6	0.7	-	0.2
FeO	11.5	19.8	0.4	0.5
F	-	-	2.5	-
less $O \equiv F$	-	-	1.0	-
Total	98.9	98.4	97.1	98.1

allanite (green)

$(Ca_{.97}RE_{.76}Mn_{.08}Y_{.02}Fe^{2+}_{.17})_2(Al_{2.21}Fe^{2+}_{.57}Fe^{3+}_{.14}Mg_{.08})_3(Si_{2.87}Al_{.13})_3O_{12}OH$

allanite (red)

$(Ca_{.87}RE_{1.01}Mn_{.09}Fe^{2+}_{.05})_{2.02}(Al_{1.29}Fe^{2+}_{.86}Fe^{3+}_{.74}Mg_{.11})_3(Si_{2.95}Al_{.05})_3O_{12}OH$

britholite

$(RE_{2.93}U_{.01}Th_{.01}Fe^{2+}_{.05})_3(Ca_{1.55}Y_{.19})_{1.7}(Si_{2.83}P_{.16})_{3.04}O_{12.5}F_{1.07}$

tornebohmite

$(RE_{1.90}Y_{.02}Ca_{.01}Mg_{.02}Fe^{2+}_{.03})_{1.98}Al_{1.06}(Si_{1.94}Al_{.06})_{2.00}O_8OH$

* Previously misidentified as cerite by Goddard and Glass (1940).
[1] Analyst: G. R. Lumpkin. Synthetic allanite-(Ce) (this study) was used as a standard.

Table 8. Reexamination of "cerite" from Jamestown, Colorado.

sample	locality	identification
cerite HMM[1] #106993	northern outcrops	britholite, allanite, quartz
cerite with allanite HMM #105675	northern outcrops	britholite, allanite
cerite HMM #101633	northern outcrops	britholite, allanite
cerite[2]	northern outcrops	britholite, monazite, fluorite, tornebohmite
cerite with allanite HMM #118261	southern outcrops	allanite, quartz, monazite, bastnaesite, microcline
cerite HMM #106996	southern outcrops	cerite, bastnaesite, mica

[1] Harvard Mineralogical Museum, courtesy of Carl Francis.

[2] Provided by Jack Adams.

kbar. The Bishop Tuff rhyolite contains euhedral allanite in early erupted samples at T = 763 (fO_2 ~10^{-14}) to 720°C (fO_2~10^{-16}) (Hildreth,1979). Although REEs were available, allanite did not crystallize in magmas erupted at conditions much more reducing than the QFM buffer. Evans and Vance (1987) looked at rhyodacite dikes that contained primary epidotes with "allanitic epidote" as cores of most of them. The epidotes crystallized at P = 8 to 13 kbar (80 MPa to 130 MPa), T = 700 to 800°C, and fO_2 ~ 10^{-13}. Perhaps the allanitic cores crystallized at the same P and T but under more reducing conditions. Franz et al. (1986) report an eclogite with the accessory minerals allanite, apatite, zircon and titanite. The allanite occurs as inclusions in garnet or between aggregates of pyroxene where the allanite is rimmed by epidote. The pressure and temperature of eclogite formation was determined to be P = 13 to 17 kbar (130 to 170 MPa) and T = 620°C + 50°C.

High pressure piston-cylinder experimental work by Green and Pearson (1984) with natural rock compositions doped with La, Sm, Ho, and Lu resulted in allanite as a stable phase at 1050°C, 30 kbar (300 MPa). The rock compositions ranged from basalt to rhyolite and oxygen fugacity was between the quartz-fayalite-magnetite and magnetite-wustite buffers (Green, personal communication).

Some preliminary P-T stability experiments with synthetic allanite-(Ce) (this study) were made. The allanite-(Ce) end-member was chosen because it is the most abundant REE found in natural allanites. Previously crystallized allanite-(Ce) was used as starting material. These starting runs had ~95 volume percent allanite, with minor Ce-Al-silicate (törnebohmite?) and quartz. At 800°C and 1 kbar with 25% H_2O to lower the water fugacity, the allanite decomposition products included britholite-(Ce), anorthite, magnetite, a Ce-silicate (cheralite?), minor quartz, and minor Ce-Al-silicate (törnebohmite?). These

decomposition products were then subjected to 700°C and 4 kbar with 100% H_2O. The resulting products were allanite with minor britholite. In the annealing runs at one atmosphere mentioned earlier in this section, cerianite was reported with britholite, magnetite, anorthite and quartz. At the higher pressures of this study, cerianite was not detected, perhaps because the mineral, cheralite was formed by the combination quartz + cerianite = cheralite.

CONCLUSIONS

1) Allanite can readily be synthesized hydrothermally in the P-T range of 450°C, 5.5 kbar to 726°C, 4.0 kbar, but high yields are obtained only for allanite-(LREE) compositions. The synthesis results support the contention that allanite is Ce-selective.

2) Incorporation of REEs in allanite is controlled by the geometry of the structure and indirectly by fO_2. Fe^{2+} in the M(3) site favors LREE substitution. An increase in the amount of Fe^{2+} in the A site corresponds to a decrease in REEs at that site. A change in oxygen fugacity from reducing to more oxidizing conditions is one explanation for allanite with epidote rims seen in nature.

Er and Yb ions are too small to substitute at A(2) in allanite, although a small amount can substitute at the VI-coordinated site in epidote.

3) Complete solid solution between epidote and allanite is possible for the LREEs. The HREEs do not completely replace Ca at the A(2) site. That allanite prefers the LREEs should be considered in any description of REE behavior during the process of magma or igneous rock formation.

4) Synthetic allanite-(Ce) decomposes to britholite, anorthite, magnetite, quartz and a Ce-silicate (cheralite?) at 800°C, 1 kbar, and 0.25 $X(H_2O)$. Natural allanite breaks

down to britholite, anorthite, magnetite, cerianite and quartz at T > 800°C and P = 1 atmosphere. At higher pressure, cerianite may combine with quartz to form cheralite. An example of allanite after britholite occurs at Jamestown, Colorado, where britholite from the "northern locality" was previously misidentified as cerite.

Chapter III

^{57}Fe MÖSSBAUER CHARACTERIZATION OF SITE OCCUPANCIES IN A EFFECT OF Fe^{2+} ON REE SUBSTITUTION

INTRODUCTION

With the ^{57}Fe Mössbauer technique, total Fe determined using the electron microprobe may be resolved into its Fe^{2+} and Fe^{3+} valence states. For a mineral such as allanite, where the Fe^{2+}/Fe^{3+} ratio is variable in nature (giving insight into the fO_2 conditions of formation), ^{57}Fe Mössbauer can be an effective tool. In addition, this technique can qualitatively give the site occupancy of iron among the nonequivalent crystallographic sites.

Site occupancies in the epidote group minerals have been determined by a variety of methods. The site preference of cations in natural epidote group minerals has been demonstrated qualitatively and quantitatively through measurement of indices of refraction (Strens, 1964b), optical absorption spectra (Burns and Strens, 1967), site refinement with x-ray diffraction (Dollase, 1969; Gabe et al., 1973), electron paramagnetic resonance (Ghose et al., 1970), ^{27}Al NMR spectroscopy (Tsang and Ghose, 1974) and Mössbauer spectroscopy (DeCoster et al., 1963; Bancroft et al., 1967; Dollase, 1971; 1973). In epidote, most Fe^{3+} has been assigned to the distorted M(3) site, with a minor amount in M(1). The Fe^{2+} in allanite has been assigned to the M(3) site with minor amounts in another site [A, M(1) or M(2)]. Problems such as complex chemistry and metamictization have prohibited previous investigators from obtaining simple and well resolved Mössbauer spectra of allanite (Dollase, 1973). Two or more species and oxidation states of cations

may be present in the octahedral M-sites (i.e., Fe^{2+}, Fe^{3+}, Mn^{2+}, Mn^{3+}, Al^{3+}) and in the polycoordinated A sites (Ca, REE^{3+}, Fe^{2+}, Mn^{2+}, U, Th, and others). The constituent U and Th promote metamictization of natural allanite, causing spectra to have broad absorption lines that are typical of disordered environments and poor crystallinity.

Herein is reported the cation site occupancy in synthetic REE allanites as revealed by using ^{57}Fe Mössbauer spectroscopy (Affholter and Annersten, 1986). In the materials studied, REE (La, Ce, Sm, Gd, Dy, and Yb) substitute for Ca in the A site, and Al and Fe^{3+} are replaced by Fe^{2+} in the M sites.

DESCRIPTION OF THE CRYSTAL STRUCTURE

The crystal structure of the epidote group minerals with the general formula, $A_2M_3Si_3O_{12}(OH)$, has been described in detail by Dollase (1968, 1971, 1973). The major structural feature is edge-sharing zigzag chains of octahedra, parallel to **b**. These chains are cross-linked to parallel straight chains of octahedra in the (100) plane through corner-sharing SiO_4 and Si_2O_7 tetrahedral groups (Fig. 16) . The large polyhedral A sites are sandwiched between the octahedral layers.

The monoclinic epidotes have two nonequivalent A sites (A1 and A2) and three types of octahedral M sites (M1, M2 and M3). The volume of the M(1) and M(2) is 10% smaller than the M(3) site, based on the volume calculation of the octahedra using the program POLYVOL (Swanson and Peterson, 1981). M-O bond distances increase most dramatically in the M(3) octahedron as the composition is changed from clinozoisite ($Ca_2Al_3Si_3O_{12}(OH)$) to allanite ($CaREE(Fe^{2+},Fe^{3+})Al_2Si_3O_{12}(OH)$). This correlates with the amount of distortion of the M(1), M(2) and M(3) octahedra described by the

comparison of the mean octahedral elongation (Fleet, 1976) to the octahedral angle variance (Robinson et al., 1971) for members of the epidote group (see Fig. 3, Chapter 1). The M(3) octahedron of allanite is more distorted than all other octahedra in members of the epidote group.

With reference to Fig. 16, one might expect the **a** and **c** cell dimensions of allanite to decrease more than the **b** cell dimension as smaller rare earth elements are substituted into the structure. The **c** and **a** cell dimensions, **a** in particular, would be sensitive not only to cation substitution on the M sites, but also to the flexing of the Si_2O_7 tetrahedra and to substitution in the A site. Although substitution occurs at M(3), the **b** cell edge is constrained by chains of M(1) and M(2) edge-sharing octahedra, where substitution is limited.

EXPERIMENTAL METHOD

Seven allanite compositions (REE = La, Ce, La-Ce, Sm, Gd, Dy, and Yb) were synthesized hydrothermally at P=5.5 kbar (550 MPa) and T ranging from 450 to 650°C with an approximate Ni-NiO buffer (i.e., the buffering effect from the Rene 41 pressure vessel) (Affholter et al., 1983). The run products were examined with a petrographic microscope to determine contamination by oxide phases such as magnetite. Magnetite was carefully removed with a hand magnet under acetone. Other impurities that were present (Table 2, Chapter 2) in the Ce run products include a Ce-Al-silicate and quartz (total ~5 volume percent). Quartz, anorthite, and britholite (total ~5 volume percent) occurred in the allanite-(Nd), -(Sm), -(Gd) and -(Dy) runs. In the Yb run, quartz, anorthite, pyrosilicate, and an Fe-Al-silicate - a chlorite group mineral(?), were present (total of all impure phases less than 6 volume percent). The impurity most likely to skew the Mössbauer characterization of synthetic allanite compositions is the Fe-Al silicate. The mean ratio of

Figure 16. Polyhedral drawing of the monoclinic allanite structure. M(1) = dark stipple, M(2) = medium stipple, M(3) = light stipple, tetrahedra (T) are unshaded. (A) Projection down (001), showing edge-sharing between M(1) and M(3) octahedra in the M(1)-M(3) zigzag chain running parallel to **b** and corner-sharing between M(1)-T-M(2). (B) Projection down the **b**-axis showing positions of A sites and cross-linking of octahedral chains by SiO_4 and Si_2O_7 groups. (C) Projection down (100), showing chains of octahedra cross-linked by the SiO_4 groups.

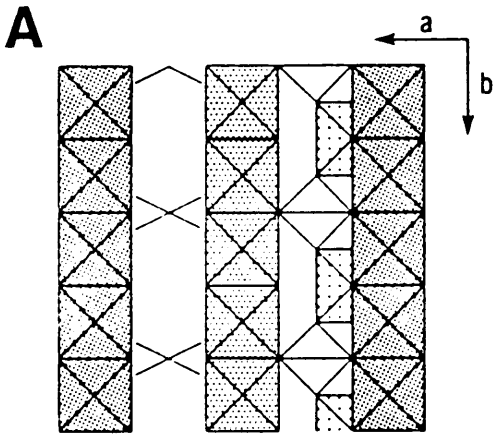
A
a
b

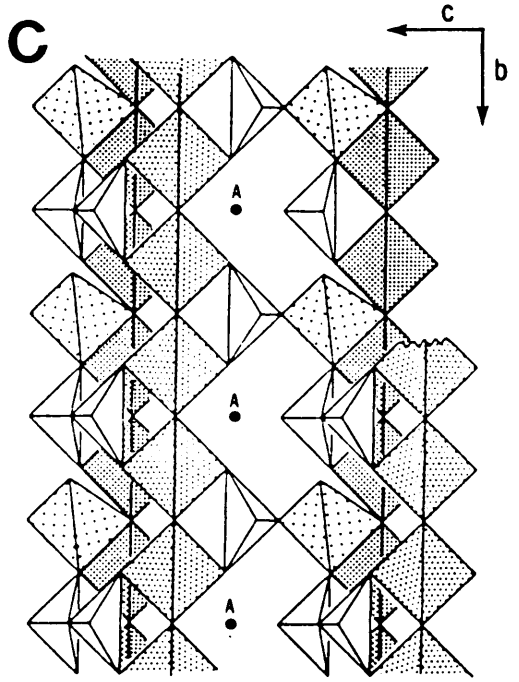
C
c
b
A
A
A

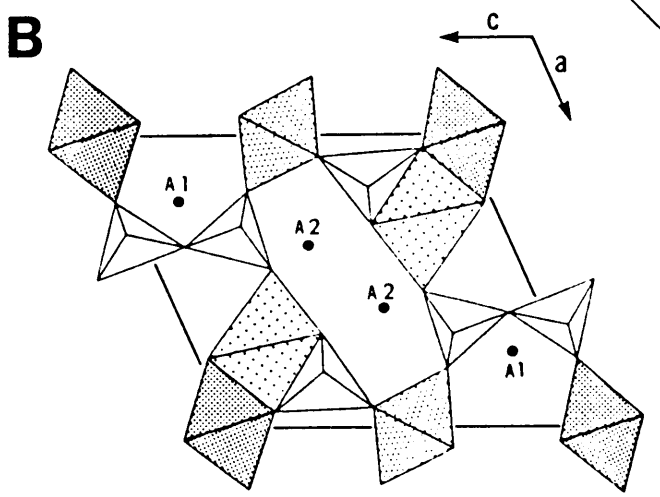
B
c
a
A1
A2
A2
A1

the Fe-Al-silicate, $(Fe^{2+},Al^{3+})_{2-3}(Si,Al)_2O_5(OH)_4$, compared to allanite is low (x = 1:89 volume percent) in the Nd to Dy run products. In the Yb run product, at its maximum abundance it occurred with allanite in a mean ratio of 1:4 volume percent. Electron microprobe analysis indicates that the britholite also contains minor amounts of iron, but the amount is so insignificant (see Chapter 2), that it should have no effect on the results.

Cell parameters and chemical compositions of the synthetic allanites (see Table 4, Chapter 2) were obtained from powder x-ray diffraction data (7 to 17 reflections) using the refinement program of Burnham (1962). The natural epidote is zoned; in contrast, no zoning was observed in the synthetic allanites.

Mössbauer spectra of powder samples were produced by means of an electromechanical Doppler velocity generator, operating at constant acceleration, in conjunction with a Nd 1200 Multichannel Analyzer (512 channels). Absorption spectra were obtained at room temperature with ^{57}Co in Rh used as a source. The spectrometer velocity was calibrated against metallic iron.

The mirror symmetric spectra thus obtained were folded and analyzed through a computer technique using a least-squares fitting program with the assumption that line shape would be Lorentzian. Fitted Mössbauer spectra are shown in Fig. 17 and Appendix E, and Mossbauer parameters and site occupancies of iron are given in Table 9.

RESULTS

Assignment of Site Occupancies

Table 4 (Chapter 2) summarizes the structural formulas for the synthetic allanites as well as the natural allanite and epidote included in this investigation. As indicated by the Mössbauer parameters, iron in the synthetic allanites occurs in both the ferric and ferrous

Figure 17. Fitted ^{57}Fe Mössbauer spectra of epidote group members. (A) Natural epidote, Prince of Wales Island, Alaska. (B) Natural crystalline allanite, Zambia (JCPDS 25-169). (C) Synthetic allanite (Ce). Symbols: _____ Fe^{2+} in the A sites; ..... Fe^{2+} in M sites; - - - Fe^{3+} in M(3).

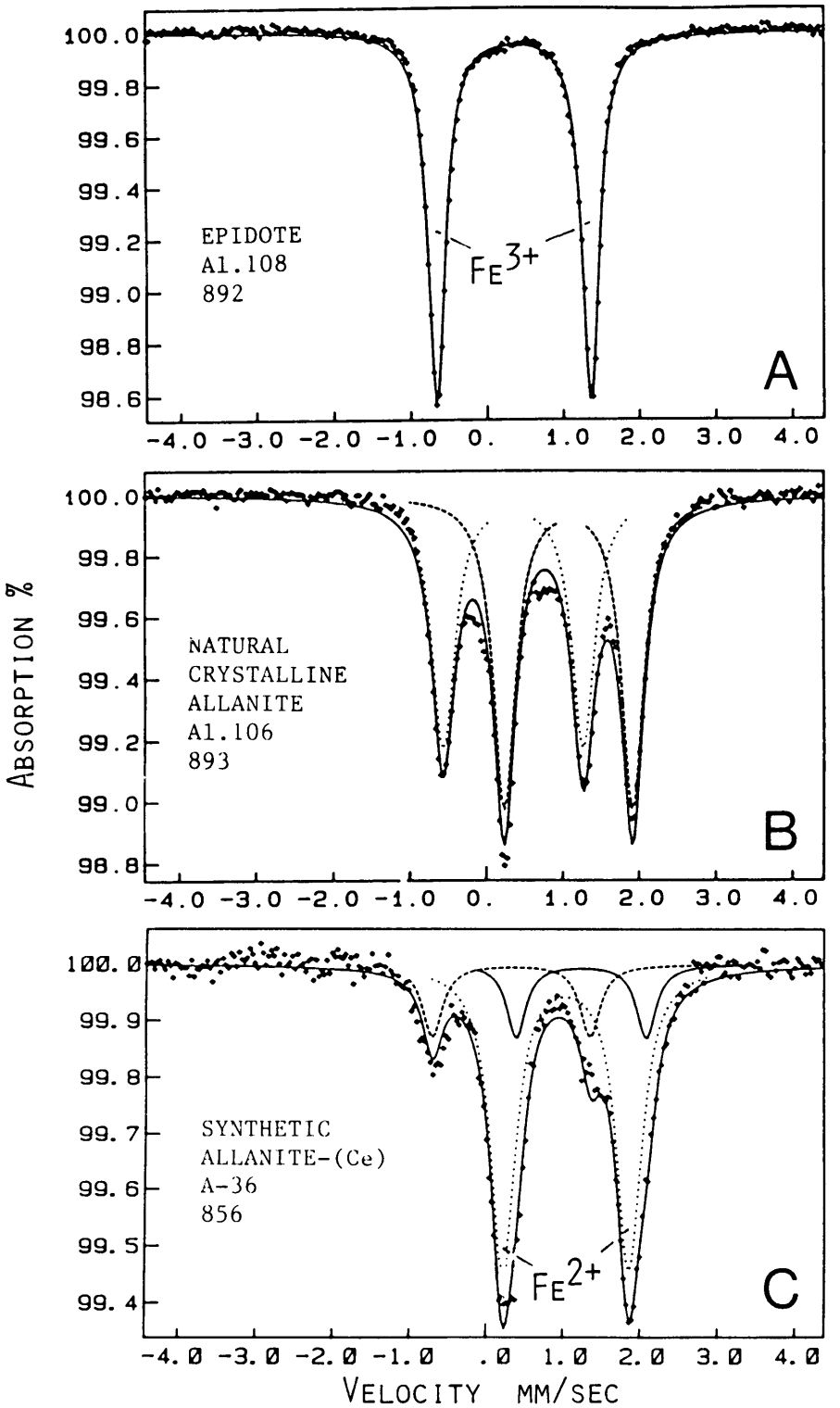
EPIDOTE
A1.108
892
Fe^{3+}
A
NATURAL
CRYSTALLINE
ALLANITE
A1.106
893
B
SYNTHETIC
ALLANITE-(Ce)
A-36
856
Fe^{2+}
C
ABSORPTION %
VELOCITY MM/SEC

TABLE 9. ^{57}Mössbauer parameters for synthetic allanite and a natural allanite and epidote. Absorber temperature 300 K.

REE	Fe^{2+} A site IS	ΔEQ	FWHH	Int	Fe^{2+} M site IS	ΔEQ	FWHH	Int	Fe^{3+} M3 site IS	ΔEQ	FWHH	Int
La	not observed				1.08	1.67	0.29	85.3	0.36	1.98	0.34	14.7
La heated	not observed				1.10	1.63	0.40	12.8	0.36	2.24	0.40	87.2
La H_2-red	not observed				1.08	1.64	0.32	88.0	0.34	1.96	0.32	12.0
La,Ce	1.30	1.97	0.35	6.2	1.06	1.62	0.35	79.4	0.34	2.03	0.35	14.4
Ce	1.24	1.69	0.30	13.5	1.04	1.64	0.39	72.5	0.34	2.06	0.32	14.0
Sm	1.19	1.83	0.35	19.8	1.06	1.53	0.35	64.2	0.38	1.94	0.35	16.0
Gd	1.21	1.88	0.33	21.3	1.06	1.54	0.33	64.4	0.37	2.06	0.33	13.3
Dy	1.23	1.92	0.37	18.7	1.05	1.50	0.37	69.0	0.37	2.07	0.37	12.4
Yb	1.17	2.62	0.32	59.2	1.07	1.61	0.42	22.5	0.34	2.10	0.39	18.3
Allanite	not observed				1.08	1.68	0.32	48.9	0.36	1.86	0.33	41.9
									0.37	0.85	0.53	9.3
Epidote	not observed				not observed				0.36	2.02	0.28	100.0

IS, EQ and FWHH are isomer shift, quadrupole splitting and full width at half height and given in mm/s (±0.02 mm/s). Int is the area under the absorption doublet and given in percent of the total absorption (±2%). IS relative to iron.

states.

Ferric iron. The absorption pattern having the smallest isomer shift (IS = 0.34-0.38 mm/s) is assigned to ferric iron. The extremely large quadrupole splitting (ΔEQ = 1.94 - 2.24 mm/s) of this cation suggests that it is situated in a highly distorted octahedral site. Ferric iron can therefore be assigned to the M(3) site. This is in agreement with earlier suggestions made by Dollase (1973). Relatively large variations in the quadrupole splittings for the different compositions are observed. This indicates considerable change in octahedral distortion which is in agreement with the observed flexibility of the M(3) polyhedra.

In the natural allanite, a second ferric iron pattern is observed (Fig. 17). It shows considerably smaller quadrupole splitting and can therefore be assigned to either the M(1) or M(2) sites.

Ferrous iron. Two ferrous iron patterns are resolved in the synthetic REE allanites, except for allanite-(La). Those patterns with isomer shifts ranging from 1.04 to 1.08 mm/s are characteristic of FeO_6 octahedra (Annersten and Halenius, 1976). Such absorption patterns may be assigned to any of the M-sites; however, in as much as small splittings are indicative of a fairly distorted site, they are most likely to correspond to the M(3) site.

The second ferrous iron pattern is characterized by large isomer shift values (1.17 mm/s for allanite-(Yb) to 1.30 mm/s for allanite-(La,Ce)) approaching the values found for this cation in the large dodecahedra of silicate garnets (Amtauer et al., 1976). Since the isomer shift may be correlated with the size of the coordination polyhedra (Tang-Kai et al., 1980), this pattern is here assigned to either of the large A sites (A1 or A2). The large isomer shifts could also reflect the increasing ionic radii of the REE substituted into the A site in the synthetic allanites. The Yb composition, having the REE with the smallest

radius, contains ferrous iron in the smallest A site polyhedra. Surprisingly, the structural formula of allanite-Yb (Table 4, Chapter 2), as obtained from site assignments and from area ratios of the absorption doublets in the Mössbauer spectra, indicates that the Yb occupies the M site instead of the A(2) site. If this is true, "allanite-(Yb)" should properly be called epidote-Yb. This observation is further supported by the lack of a Yb(A2)-OH stretching band at 3181 cm^{-1} in the infrared spectra of this sample (see Chapter IV).

The oxidation of allanite-(La) in air at 600°C for 24 hours (Fig. 18) produced an oxyallanite with an Fe^{3+}:Fe^{2+} ratio of 6.8 (see Table 9, this Chapter and Table 4, Chapter 2). The disappearance of the OH-band in the infrared spectrum of this sample (see Chapter 4) suggests a deprotonated oxyallanite.

CONCLUSION

Fe^{2+} occupies both an A site and the M(3) site in allanite. The A site could be either A(1) or A(2); however the ionic size of Fe^{2+} makes it more likely to occupy the smaller IX-coordinated A(1) site. The amount of Fe^{2+} substituting at the A site increases as size and amount of REE decrease. As more Fe^{2+} occupies the A(1) site, more Ca^{2+} (and less REE) occupies the A(2) site. The amount of Fe^{2+} in the A site appears to limit the amount of substitution of REE under the conditions of these experiments. Natural allanites follow this trend, with few showing occupation of more than 0.90 REE/12.5 anions (the limit of REE substitution in allanite-(La) for these synthesis experiments).

In natural allanites, other divalent ions take the same role as iron. For example, Mn appears in the allanite from Zambia, which has the following formula $(Ca_{1.06}Mn_{.07}REE_{.89})(Fe^{2+}_{.74}Fe^{3+}_{.16}Mg_{.09})(Al_{1.38}Fe^{3+}_{.62})(Si_{2.91}Al_{.09})_3O_{13}H_{1.07}$. The ratio of

Figure 18. Fitted ^{57}Fe Mössbauer spectra of (A) Synthetic allanite-(La), (B) Oxyallanite-(La) heated 24 hours at 600°C in air and (C) the same oxyallanite sample reduced to allanite-(La). Symbols: ___ Fe^{2+} in the A sites; ..... Fe^{2+} in M sites; ---- Fe^{3+} in M(3).

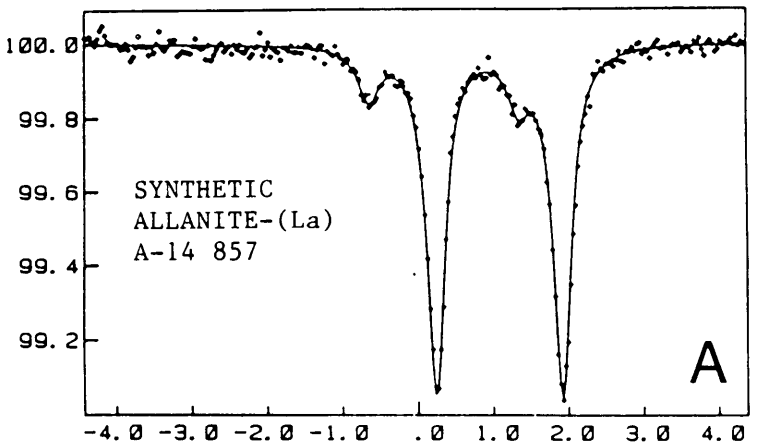
100.0
99.8
99.6
99.4
99.2
SYNTHETIC
ALLANITE-(La)
A-14 857
A
-4.0 -3.0 -2.0 -1.0 .0 1.0 2.0 3.0 4.0

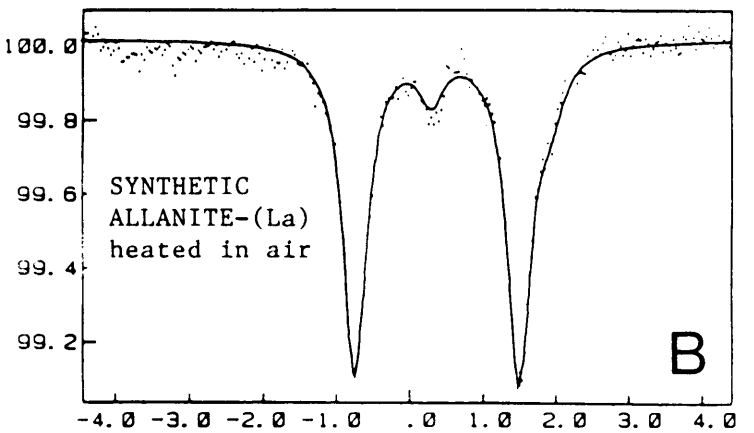
100.0
99.8
99.6
99.4
99.2
SYNTHETIC
ALLANITE-(La)
heated in air
B
-4.0 -3.0 -2.0 -1.0 .0 1.0 2.0 3.0 4.0

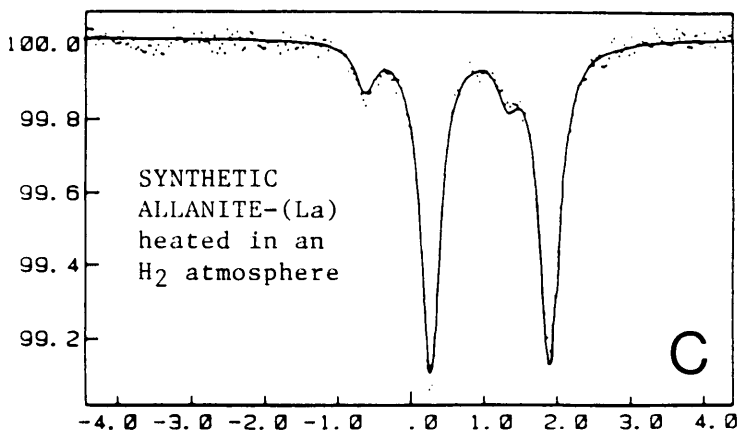
100.0
99.8
99.6
99.4
99.2
SYNTHETIC
ALLANITE-(La)
heated in an
H_2 atmosphere
C
-4.0 -3.0 -2.0 -1.0 .0 1.0 2.0 3.0 4.0

trivalent to divalent ions occupying the M(3) and A(2) sites, $Fe^{3+}/(Fe^{2+} + Mg^{2+} + Mn^{2+} + Ca)$, equals 0.17. This ratio is similar to that found in the synthetic allanites of this study; for example, in allanite-(Ce), $Fe^{3+}/(Fe^{2+} + Ca) = 0.15$ (values of site occupancy are normalized to 2 for the A site and 1 for the M(3) site). The occupancy ratio for the A(2) and M(3) sites in the Zambia allanite is the same as that in the synthetic allanite even though the total Fe^{3+}/Fe^{2+} ratios differ. In the Zambia allanite, total Fe^{3+}/Fe^{2+} is 1.04; in synthetic allanite-(Ce), the ratio is 0.17. Much of the Fe^{3+} in the Zambia allanite is in the M(1) or M(2) sites. This suggests that the amount of REE that can occupy the A(2) site may be restricted in more oxidizing environments as well.

As indicated by the chemical formula of allanite, REE substitution in the epidote group of minerals should, as for iron, occur predominantly by divalent ion substitution. REE substitution can also be expected to occur to a lesser extent by deprotonation processes.

The cell dimension changes due to substitution at the M(3) and the A site predicted by inspection of the structure are indeed borne out by the Mössbauer results. In the synthetic allanite series (allanite-La to allanite-Dy), the major substitution is REE at the A(2) site, so the smallest changes are observed in the **b** cell dimension. When allanite, in which substitution is at M(3) and the A site, is compared to other epidotes in which substitution is at M(3) only, the largest differences are seen in the **b** cell dimension. This is because Fe^{2+} is substituting for Fe^{3+} at M(3). The difference between the effective ionic radii of Fe^{2+} and Fe^{3+}, which substitute at the M(3) site, is larger than the difference between the effective ionic radii of Ce and Ca, which substitute at the A(2) site. The **a** cell dimension changes slightly more than the **c** cell dimension with substitution of REE into the A(2) site.

Chapter IV

INFRARED SPECTRA OF LANTHANIDE ALLANITES

INTRODUCTION

Zoisite and clinozoisite-epidote can be distinguished by the position of the OH stretching vibration for hydroxyl groups in the region 3400-3000 cm^{-1}, and by a distinctive band at 2610 cm^{-1} present only in zoisite spectra (Langer and Raith, 1974). The position of the OH band (3160 cm^{-1}) in zoisite is lower than the OH bands (3326-3365 cm^{-1}) in clinozoisite-epidote which indicates the O-H...O bond is stronger in zoisite.

Of the reported infrared absorption spectra of natural allanite (Cech et al., 1972; Aleksandrova et al., 1966; Moenke, 1974, 1966; Akhmanova et al., 1963), only that reported by Cech et al. covers the spectral range 4000-3000 cm^{-1} where OH stretching vibrations occur. In this region a spectrum shows two peaks: a strong one at 3445 cm^{-1} that they attribute to an OH stretching vibration and a broad peak at 3200 cm^{-1} that they do not identify. Adsorbed molecular water in the liquid form has an HOH bending vibration at 1630 cm^{-1}. In these allanite spectra, the intensity of the HOH bending vibration at 1630 cm ^{1} indicates that a large part (if not all) of corresponding OH vibrations in the 3445 cm^{-1} peak is due to adsorbed water, and thus the OH vibration(s) of hydroxyl groups cannot be unambiguously identified.

In order to identify and compare the OH stretching vibration of the hydroxyl group in allanite with published spectra of the other epidote group minerals, synthetic allanites where REE = La, Ce, Nd, Sm, Gd, Dy, Y, Er, and Yb were analyzed by IR spectroscopy. For comparison, the IR spectra of a natural crystalline allanite, a natural epidote, and a

synthetic zoisite (from D. A. Hewitt) were recorded in the same manner as the synthetic allanite. The synthesis products from the Er and Yb compositions suggest these should be more properly called epidote-(Er) and epidote-(Yb), and will be referred to as such in the following text.

EXPERIMENTAL METHOD

The rare earth element allanites were synthesized hydrothermally at 700 to 725°C and 4 kbar (Affholter et al., 1983) and the zoisite at 650°C and 7 kbar (Hewitt, pers. comm.).

Chemical analysis of the natural epidote from Green Monster Mountain, Prince of Wales Island, Alaska, is given by Myers and Myers (1983) and Leavens and Thomssen (1977), and that of the crystalline allanite from the Luangwa Bridge area, Zambia, by Cech et al. (1972).

From 2 to 11 mg of sample were mixed with 200 mg of KBr and pressed into pellets. The spectra were recorded with a Perkin-Elmer 283 spectrophotometer over the range 4000-200 cm^{-1}. Minor impurities were detected in the synthetic samples from prior examination; see Table 2, Chapter 2. Allanite-(Gd) and allanite-(Dy) contained ~four percent total of britholite, anorthite, magnetite, Fe-Al-silicate and quartz. The epidote-(Er) and -(Yb) contained pyrosilicate, anorthite, magnetite and quartz. The spectra of these impurities do not interfere with that of the allanite in the region 3600-3000 cm^{-1} because all but the Fe-Al-silicate are anhydrous phases. The Fe-Al-silicate could be berthierine, a hydrous phase, but the amount present compared to allanite is small. To eliminate adsorbed molecular water the pressed pellets were dried at 115°C for one week, and the spectra showed no absorption in the region 1600-1750 cm^{-1}, the region of the HOH

deformation vibration in molecular water (Lazarev, 1972; Nakamoto, 1978).

THE OH BOND AND SITE OCCUPANCIES

In the epidote group minerals, $A_2M_3Si_3O_{12}(OH)$, principal substitutions occur at the A(2) amd M(3) sites (Dollase, 1973, 1971, 1969). For synthetic zoisite, both A sites are occupied by Ca and all M sites by Al. For epidote, Fe^{3+} occupies the M(3) site. For allanite, REE^{3+} and Ca occupy A(2), Fe^{2+} occupies an A site, probably A(1), Fe^{2+} and Fe^{3+} occupies M(3), and (Al^{3+},Fe^{3+}) occupy M(1) and M(2); see Chapter III for further details.

The hydrogen forms a bridge between O(10) and O(4), O(10)-H...O(4) (Dollase, 1968; Gabe et al., 1973; Hanisch and Zemann, 1966; Linke, 1970). In turn O(10) is bonded to A(2) and O(4) is bonded to M(3) (Fig. 19). Substitution of ions with different valences in A(2) and M(3) will change the strength of the OH bond because of the change in the charge distribution for A(2)-O(10) and M(3)-O(4). A decrease in the cation charge at the A(2) site (e.g., Ca^{2+} for REE^{3+} or Fe^{2+} for REE^{3+} if the Fe^{2+} is on the A(2) site) will shift the electronic charge density of the O(10) towards the hydrogen. As a consequence, higher frequencies will be observed for the OH stretching vibration. An increase in cation charge at the M(3) site (e.g., Fe^{3+} for Fe^{2+}) will shift the electronic charge density of O(4) towards the cation in M(3). Again, higher OH frequencies will be observed, because this substitution indirectly shortens the OH bond. In addition, if Fe^{2+} already present in the M site is oxidized, an H^+ will be released to compensate for the increased charge on the Fe. In this case no OH stretching frequency would be observed. Although the substitution at the A(2) site will have a more pronounced effect (i.e., greater increase in OH frequency)

than substitution at the M(3) site because O(10) forms the hydroxyl bond and is bonded to A(2), the latter substitution also produces significant change to the OH stretching frequency. For instance, in comparing clinozoisite (with all Al^{3+} and no Fe^{3+}) and epidote (0.89 Fe^{3+} per formula unit) where substitution is at the M(3) site only, the frequency of the OH stretching vibration increases by 36 cm^{-1} (Langer and Raith, 1974).

In order to determine the A and M site occupancies, ^{57}Fe Mossbauer analyses were made on the run products of allanite starting compositions synthesized at 650°C and 5.5 kbar and with REE = La, Ce, Sm, Gd, Dy, and Yb . The results indicate that Fe^{3+} is in the M(3) site and Fe^{2+} is in an A site, probably A(1), and an M site, most probably M(3). The ratio of Fe^{3+}/Fe^{2+} is constant at approximately 0.16 for all but the Yb composition. This composition has appreciably more Fe^{2+} in the A site than the other REE allanites (0.50 atom compared to 0.14 to 0.23); however, the amount of Fe^{3+} in the M(3) site is the same (0.16 atom). Allanite-(La) is the only composition that does not have Fe^{2+} in an A site.

^{57}Fe Mossbauer analysis on the natural epidote suggests that all Fe present is Fe^{3+} in the M(3) site. For natural allanite, Cech et al. (1972) assigned 0.74 and 0.16 Fe^{2+} in the M(3) site and 0.62 Fe^{3+} in the other M sites, based on the calculation of the structural formula. This ferric/ferrous ratio is high compared to that of the synthetic allanites.

The possible substitutions on the A(2) and M(3) sites in allanite are shown in Fig. 19. For simplification, assume that the M(1) and M(2) sites are fully occupied by Al. This is supported by x-ray structural studies of natural allanites (Dollase, 1972). For allanite-(La), only configurations 1 and 2 (Fig. 19) are possible, because no Fe^{2+} was found in the A site. For allanite-(Ce) through allanite-(Dy), all four configurations (1 through 4 in Fig.

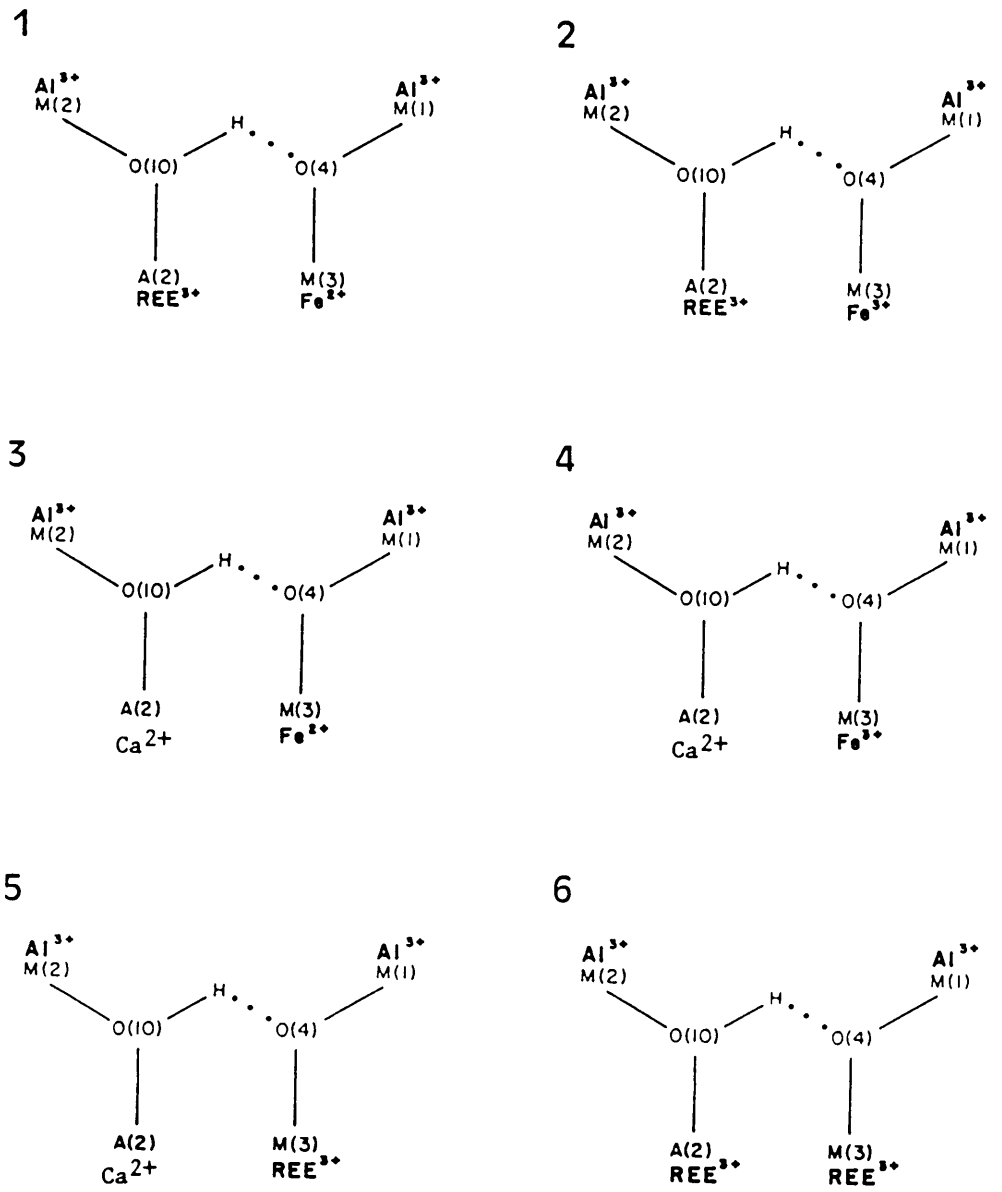

Figure 19. Schematic environments of the O-H...O bond in synthetic allanites for different combinations of cations in the A(2) and M(3) sites.

19) may occur simultaneously in the structure, because Ca^{2+} is found in the A(2) site and Fe^{2+} in the M(3) site. The Yb composition structural formula is improved if some REE substitution occurs at the smaller VI coordinated M sites. The preference of the heavy REE for smaller substitutional sites rather than larger sites has been demonstrated in carbonates by Morgan and Wandless (1980). Configurations 5 and 6 represent the REE substitution at the M site. The longer OH bonds in configurations 1, 2, and 6 are manifested by lower frequencies on the IR spectra and the shorter bonds of configurations 3, 4, and 5 yield higher OH stretching frequencies. Configurations 2 and 6 favor long OH and hydrogen bonds, and probably promote the release of hydrogen.

The infrared spectra for the synthetic allanites (REE = La, Ce, Nd, Sm, Eu, Gd, Dy, Y, Er, and Yb) and a synthetic zoisite, natural epidote and allanite are shown in Fig. 20. Positions of the absorption bands and inflections or shoulders for zoisites, clinozoisites, epidotes and allanites from the literature and the synthetic allanites in this study are compiled in Table 10. The accuracy for the allanite analyses is $\pm$ 2 cm^{-1}. The position of bands appearing as shoulders are estimated. The accuracy for the clinozoisite and epidote spectra are reported in Langer and Raith (1974).

The infrared absorption spectra in the region 3600-3000 cm^{-1} have one or two peaks depending on the allanite composition. The OH stretching vibration for allanite-(La) occurs at 3160 cm^{-1} similar to that assigned to zoisite by Langer and Raith (1974). For the Ce- through Dy- allanites, two peaks occur; one at 3360 cm^{-1} like that in epidote and one at 3150 cm^{-1}. For Er and Yb compositions, there is a strong peak at 3380 cm^{-1} with a weaker peak at 3550 cm^{-1}.

The weak band at 2160 cm^{-1} present in zoisite spectra, but not in epidote spectra

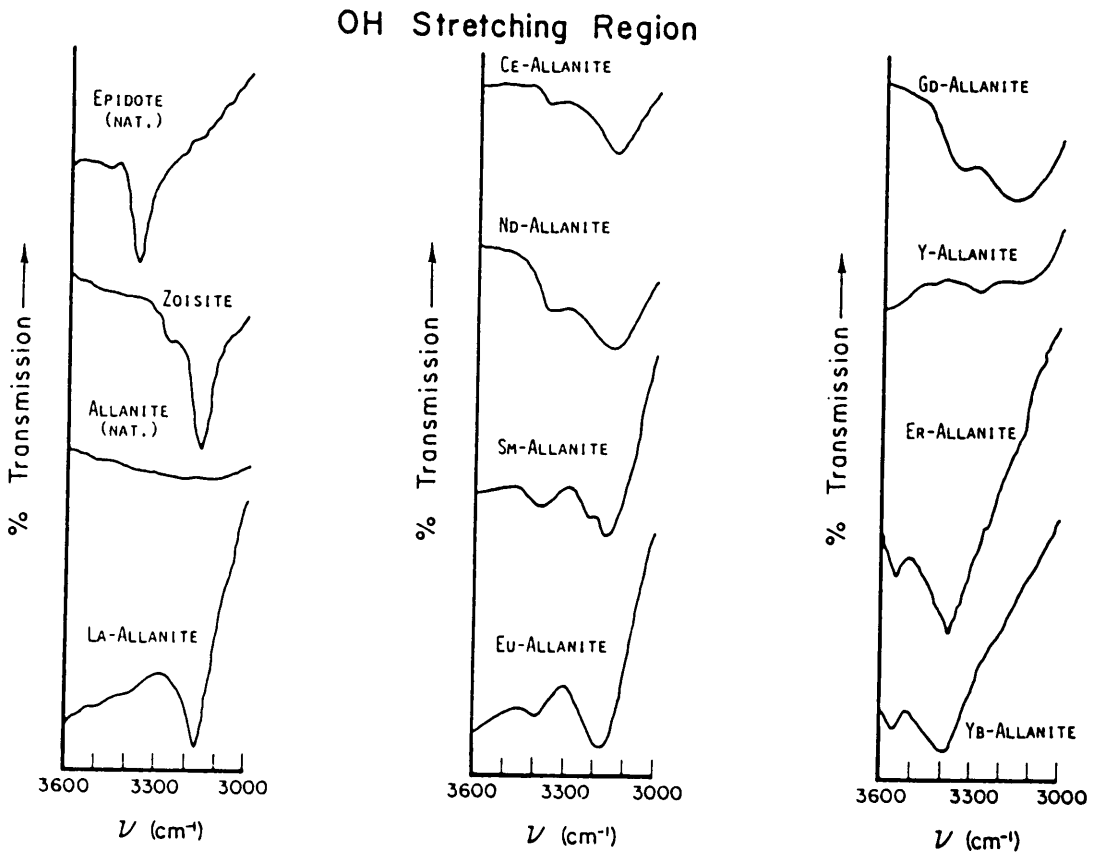

Figure 20. IR absorption spectra for synthetic REE allanites in the region 3000 to 3600 wavenumbers.

Table 10. Band positions (cm^{-1}) in the IR absorption spectra of the epidote group.

band no.	zoisite*			clinozoisite*		epidote*				
	1	2	3	4	5	6	7	8	9	10
(1)	3270	3260	3255	3326	3338	3345	3360	3365	3340	3465
	-	-	-	-	-	-	-	-	-	3379
	-	-	-	1630	1630	1630	1630	1630	-	1634
(2)	3160	3153	3157sh	1143	1126	1120	1110	1108	1102	-
(3)	3065sh	3050wsh	3060wsh	1116	1106	1100	1079	1076	1068	-
(4)	2165	2161	2160	-	-	1090	-	-	-	-
(5)	1158wsh	1160wsh	1158wsh	1047	1043	1039	1037	1035	1025	1043
(6)	1125	1116	1116	980sh	973wsh	977wsh	980wsh	975wsh	-	-
(7)	1064	1043	1040wsh	950	954	952	953	951	947	958
(8)	970sh	975wsh	973sh	906	910wsh	905wsh	910wsh	900wsh	-	-
(9)	950	949	950	895	892	889	889	886	885	890
(10)	928	929	928wsh	869	865sh	865sh	862sh	861	-	(868)
(11)	906	907	901	849	843	843	840	836	-	(842)
(12)	890wsh			-	805	800wsh	802wsh	800wsh	-	(830)
(13)	878	880wsh		741	733	731	723	718	-	(725)
(14)	860	863	863	690sh	695wsh	697wsh	697wsh	697wsh	-	-
(15)	830wsh	834wsh	832wsh	676	670	668sh	673wsh	670wsh	-	-
(16)	777	778	774	650	649	648	649	648	-	655
(17)	755	756	752	603	599	596wsh	590wsh	585wsh		(592)
(18)	717	715	714	575	575	571	-	-		572
(19)	695	697	693	561	558	557	568	563		-
(20)	679	679	677	527	544wsh	541	530wsh	-		526
(21)	655	655	654	-	517	518	519	517		-
(22)	618	619	619	498	495wsh	495wsh	-	-		(472)
(23)	593	595	595	487	477	474	467	460wsh		460
(24)	578	572	572	457	457	457	457	454		-
(25)	562sh	557wsh	556wsh	-	430wsh	430wsh	430wsh	410wsh		408
(26)	524sh	523wsh	522wsh	419	411	408	400	395		-
(27)	512	511	511	393	389	387	385sh	381		
(28)	486	485wsh	481wsh	363	359	359	355	351		

* 1. zoisite, 0.00 mole % Fe^{3+}.
2. zoisite, 0.01 mole % Fe^{3+}.
3. zoisite, 0.10 mole % Fe^{3+}.
4. clinozoisite, 0.00 mole % Fe^{3+}.
5. clinozoisite, 0.29 mole % Fe^{3+}.
6. epidote, 0.44 mole % Fe^{3+}, 5000-250 cm^{-1}
7. epidote, 0.68 mole % Fe^{3+}, Langer and Raith (1974)
8. epidote, 0.89 mole % Fe^{3+}.
9. epidote, 4000-650 cm^{-1}, Strens (1964)
10. epidote, 4000-400 cm^{-1}, Cech et al. (1972)

Table 10. Continued.

allanite*		synthetic REE allanites**								
11	12	La	La	Ce	Nd	Sm	Eu	Gd	Dy	Y
3445	-	3385	3380	3380	3360	3390	3360	3395	3398	3365
3200	-	3168	3167	3150	3140	3140	3153	3180	3190	3220
1638	-	1629	1625	1630	1622	1628	-	1622	1624	1626
-	-	-	-	-	-	-	-	-	-	-
-	-	-	-	-	-	-	-	-	-	-
-	-	-	-	-	-	-	-	-	-	-
1047	1045	1050	1050	1039	1050	1052	1047	1066	1054	1067
-	-	-	-	-	-	992	-	991	986	-
938	950	-	-	-	-	-	-	-	-	-
-	-	925	925	925	923	930	-	934	934	-
890	-	-	-	-	884	890	902	890	880	902
-	-	-	-	-	-	-	-	-	-	-
-	-	-	-	-	-	-	-	-	-	-
-	-	802wsh	800wsh	-	802wsh	-	798	-	800wsh	-
-	-	-	-	-	-	-	774	-	777	-
-	-	701wsh	698wsh	694wsh	701wsh	700wsh	701wsh	703wsh	706wsh	-
-	-	675sh	674sh	670sh	670sh	667sh	-	-	-	-
628	640	635	633	634	644	653	650	650	650	652
-	-	-	579	-	587	600	581	585	-	-
573	586	-	-	573	-	587	-	-	569	-
-	-	-	-	-	-	-	-	-	-	-
-	-	-	-	-	-	-	-	-	-	-
506	510	515	514	507	515	515	513	523	503	499
-	-	-	-	-	-	-	-	-	-	-
-	460	459	460	455	455	455	460	457	-	-
-	-	-	-	-	-	-	-	-	-	-
407	-	-	-	-	-	-	-	-	-	-
-	-	-	-	394	403	407	410	407	398	-
		-	-	-	-	-	-	-	-	-
		333	357	356	355	360	366	350	338	350

*11. allanite, 4000-400 cm^{-1}, Cech et al. (1972)
12. allanite, 1800-400 cm^{-1}, Moenke (1974)

**4000-300 cm^{-1}, this work

sh = shoulder, wsh = weak shoulder

(Langer and Raith, 1974), is present at about 2140 cm^{-1} in the allanite spectra that have a strong peak at the lower 3150 cm^{-1} frequency (i.e., all but Y, Er and Yb compositions). The intensity of the 2140 cm^{-1} peak is proportional to the intensity of the 3160 cm^{-1} peak. The spectra for the Er and Yb compositions are more like epidote than allanite (Fig. 20).

In addition to the region discussed, the synthetic allanites show IR absorptions in the following regions: 3360-3310, 3240-3137, 1093-1045, 936-926, 902-891, 804-798, 700-695, 659-637, 599-572, 529-499, 468-457, 410-391, and 365-346 cm. Many of the bands that are present in the zoisite, clinozoisite, and epidote spectra are absent in the allanite spectra.

"Oxyallanite"

To explore the conversion of allanite to oxyallanite, the synthetic allanite-(La) was heated in air at 600°C for 24 hours, and then in a H atmosphere at 600°C for another 24 hours. The La composition was chosen so there would be no ambiguity in the oxidation state of the A site cation after heating. Heating the allanite-(La) to 1100°C resulted in La_2O_3 as one of the decomposition products, suggesting that the La remains trivalent over this range of temperature.

The OH stretching vibration at 3150 cm^{-1} in the IR spectrum for synthetic allanite-(La) disappeared when the sample was heated in air (Fig. 21), and a new peak appears at 3380 cm^{-1}, suggesting the formation of "oxyallanite" by the reaction $(OH)^- + Fe^{2+} = O^{2-} + Fe^{3+} + 0.5\ H_2$ (Dollase, 1968). The oxidation process was reversed by heating the same sample in a hydrogen atmosphere. By reducing the sample, the peak at 3150 cm^{-1} reappeared and the peak at 3360 cm^{-1} disappeared, the restored IR spectra being nearly

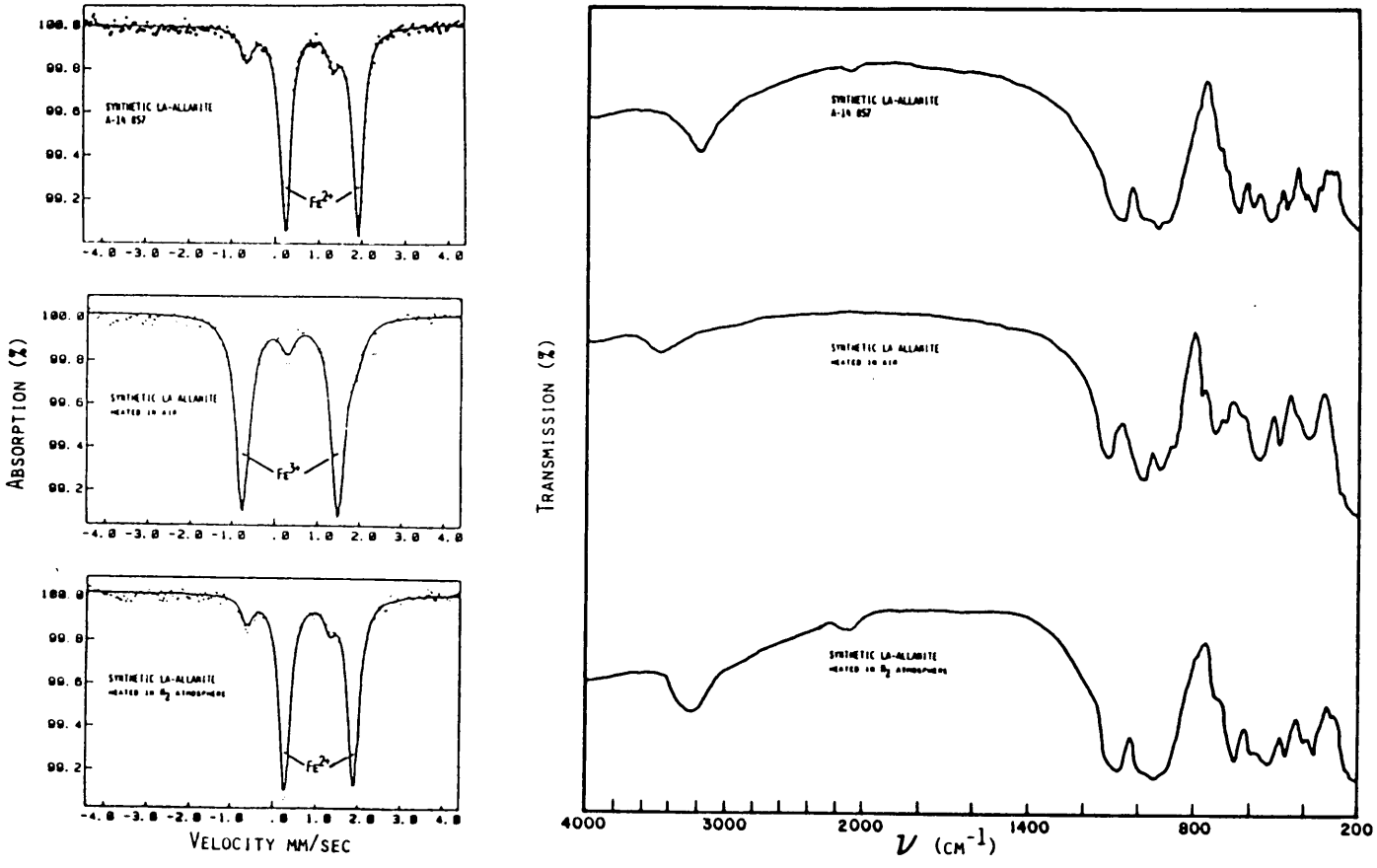

Figure 21. ^{57}Fe Mössbauer and infrared spectra of synthetic untreated (top), oxidized (middle) and reduced (bottom) synthetic allanite-(La).

identical to that of the original untreated sample.

^{57}Fe Mossbauer spectroscopy confirms the oxidation and subsequent reduction of Fe^{2+} in the allanite. Nearly all of the Fe^{2+} was oxidized when heated in air, and the ferric/ferrous ratio in the same allanite-(La) heated in H_2 is nearly identical to the original allanite, Fe^{3+}/Fe^{2+} (untreated) = 0.13 and Fe^{3+}/Fe^{2+} (reduced) = 0.17. Although the oxidation and subsequent reduction of allanite was successful in this experiment, it should be noted, there is no evidence that this process happens under equilibrium conditions.

Natural Allanite

Infrared absorption spectra were measured on a natural allanite studied by Cech et al. (1972). The new spectra lacks the bands at 3400 cm^{-1} and 1630 cm^{-1}, which were on the spectra collected by Cech et al., but has the broad band centered at about 3200 cm^{-1}. This band is due to structural OH in the allanite.

DISCUSSION

There are one or two OH stretching vibrations due to hydroxyl in allanite depending on composition. For natural samples care has not always been taken to remove adsorbed water from the sample, which will contribute an additional OH band that complicates their spectra (see for instance, Cech et al., 1972). Moreover, natural samples with significant accumulation of alpha-decay damage will have a more complicated distribution of hydrous species due to new kinds of hydroxl groups and molecular water in the damaged regions of the crystal (see Aines and Rossman, 1986). Natural allanite without significant alpha-decay damage will be similar to the synthetic allanite.

The position of these diagostic band(s) depends on the valence of the cations in the A(2) and M(3) sites, because this valence affects the strength of the O(10)-H...O(4) bonds that are coordinated to A(2) and M(3). The combination of a trivalent cation in the A(2) site and a divalent cation in the M(3) site, as in ideal allanite, yields a band at a lower frequency in the OH stretching region. A divalent cation substituting on the A(2) site or a trivalent cation substituting on the M(3) site, as in ideal epidote, yields a higher frequency band.

The synthetic allanite-(La) approximates ideal allanite and has a band on the IR spectrum at an expected lower frequency, 3150

cm^{-1}. A band at higher frequency caused by some Fe^{3+} in the M(3) site, does not appear on this spectrum possibly because the amount of sample used in the pellet (2 mg) or the amount of Fe^{3+} (0.15) in the M(3) site for this sample is not sufficient to produce a peak. With the increase in Ca^{2+} in the A(2) site, the allanite-(Ce) to allanite-(Dy) and allanite-(Y) have two peaks in the OH stretching region, one at 3380 cm^{-1} and one at 3150 cm^{-1}. The 3150 cm^{-1} peak disappears for the Er and Yb compositions. For allanite-(Er) and allanite-(Yb), the greater amount of Fe^{2+} and Ca^{2+} in the A site and the possibility of the Er^{3+} or Yb^{3+} residing in the M(3) site, accounts for the higher frequency band.

Oxidation-reduction experiments on allanite-(La) confirm the relationship between Fe^{2+} in the M(3) site and the lower frequency OH stretching vibration. After oxidizing this sample, this peak disappeared, and after reducing the same sample it reappeared. The peak at the higher frequency, 3380 cm^{-1}, suggests total deprotenization did not occur. This peak may result from change in the OH bond strength when Fe^{3+} rather than Fe^{2+} occupies the M(3) site. It is probably not due to REE^{3+} in the M(3) site (the size of the La ion precludes

this). Although it could be due to small amounts of adsorbed water, the associated deformation vibration at 1630 cm^{-1} does not appear on the spectrum. This peak also does not occur on the original and H-treated allanite-(La) spectrum when these samples were kept at 110°C for one week.

The frequency of the OH-stretching vibration observed in allanite is a function of substitution on both the A(2) and M(3) sites unlike the other epidote group minerals (except thulite) where substitution only occurs on M(3). Substitution at A(2) has a strong effect on the position of the OH-stretching frequency. For this reason, the trend of increasing frequency with increasing O(10)-O(4) separation observed for clinozoisite and epidote is not followed by allanite (Fig. 22). Although the position of one of the OH stretching vibrations in allanite is similar to zoisite, and one is similar to epidote, the number and position of the bands at the frequencies below 1100 cm^{-1} are close to epidote. These bands that represent
Si-O-Si and M-O linkages also reflect the monoclinic symmetry that epidote and allanite exhibit. The 2160 cm^{-1} band reported by Langer and Raith (1974) for zoisite and not clinozoisite-epidote group minerals is present for those allanites that have a band at the lower frequency, 3150 cm^{-1}.

The position of the OH stretching vibrations suggest there is a strong hydrogen bond, O(10)-H...O(4) in the LREE allanites in agreement with hydrogenation experiments with natural allanites by Dollase (1973). The OH bond strength for the LREE allanites is comparable to that found in zoisite, and that of the HREE allanites is like that in epidote. The higher thermal stability observed for allanite as compared to epidote is consistent with the stronger OH bond measured in the LREE allanites. The stability of these similar structures must be determined by their weakest bonds.

Figure 22. O(10)...O(4) interatomic distances and OH stretching frequencies compared with the environment of the O-H...O bond in the epidote group minerals.

Zoisite (Dollase, 1968)

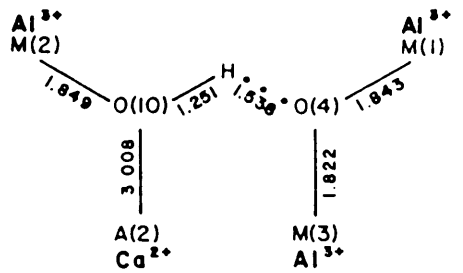

O(10)-O(4) = 2.749 A

ν = 3157 cm^{-1}

Epidote (Gabe, 1973)*

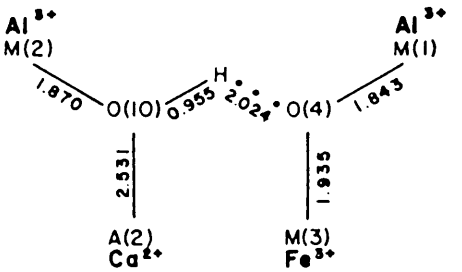

O(10)-O(4) = 2.933 A

ν = 3364 cm^{-1}

Clinozoisite (Dollase, 1968)**

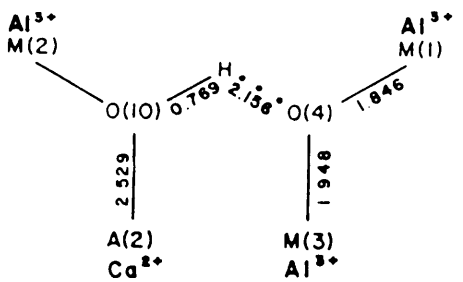

O(10)-O(4) = 2.892 A

ν = 3327 cm^{-1}

Allanite (Dollase, 1973)

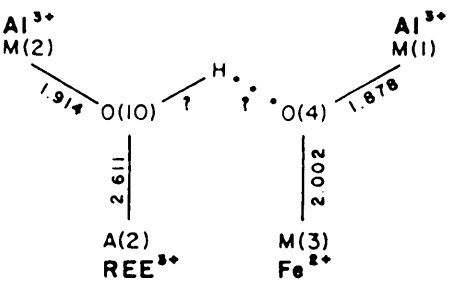

O(10)-O(4) = 2.917 A

ν = 3150 cm^{-1}

*This Study

REFERENCES

Adams, J. W. (1969) Distribution of lanthanides in minerals. U.S. Geological Survey Professional Paper, 650-C, 38-44.

Affholter, K. A. and Adams, J. W. (1987) Thermal breakdown of allanite to britholite. Geological Society of America Abstracts with Program, 19, 567.

Affholter, K. A. and Annersten, H. (1986) Mossbauer characterization of site occupancies in synthetic allanite, CaREEFeAl2Si3O12(OH). The 14th General Meeting of the International Mineralogical Association, Abstracts with Program, p. 41.

Affholter, K. A., Hewitt, D. A., and Wones, D. R. (1983) Synthesis of rare earth element allanites. Geological Society of America Abstracts with Program, 15, 511.

Aines, R. D. and Rossman, G. R. (1986) Relationships between radiation damage and trace water in zircon, quartz, and topaz. American Mineralogist, 71, 1186-1193.

Akhamanova, M. V., Karyakin, A. V., and Yukhnevich, G. V. (1963) Determination of hydroxyl groups in silicate minerals by infrared spectrophotometry. Geochemistry, 8, 596-600.

Aleksandrova, I. T., Ginsburg, A. I., Kupriyanova, I. I., and Sidorenko, G. A. (1966) Rare earth silicates. Geologiya Mestorozh. redk. Elem. vses. Nauch-Issled. Inst. Mineral'n Syr'ya., 26.

Amtauer, G., Annersten, H., and Hafner, S. S. (1976) The Mossbauer spectra of silicate garnets. Zeitschrift fur Kristallographie, 143, 14-55.

Anastasiou, P. and Langer, K. (1977) Synthesis and physical properties of piemontite $Ca_2Al_3Mn^{3+}(Si_2O_7/SiO_4/O/OH)$. Contributions to Mineralogy and Petrology, 60, 225-245.

Annersten, H. and Halenius, U. (1976) Ion distribution in pink muscovite, a discussion. American Mineralogist, 61, 1045-1050.

Bancroft, G. M., Maddock, A. G., and Burns, R. G. (1967) Application of the Mossbauer effect to silicate mineralogy: I. Iron silicates of known crystal structure. Geochimica et Cosmochimica Acta, 31, 2219-2246.

Beall, G. W., Boatner, L. A., Mullica, D. F. and Milligan, W. O. (1981) The structure of cerium orthophosphate, a synthetic analogue of monazite. Journal of Inorganic Nuclear Chemistry, 43, 101-105.

Belokoneva, E. L., Petrova, T. L., Simonov, M. A., and Belov, N. V. (1972) Crystal structure of synthetic TR analogs of apatite $Dy_{4.67}[GeO_4]_3O$ and $Ce_{4.67}[SiO_4]_3O$. Soviet Physics- Crystallograph.y, 17, 429-431.

Belov, N. V. and Rumanova, I. M. (1953) The crystal structure of epidote. Doklady Akademi Nauk SSSR, 89, 853-856.

Dollase, W. A. (1973) Mossbauer spectra and iron distribution in the epidote group minerals. Zeitschrift fur Kristallographie, 138, 41-63.

Dollase, W. A. (1971) Refinement of the crystal structures of epidote, allanite, and hancockite. American Mineralogist, 56, 447-464.

Dollase, W. A. (1969) Crystal structure and cation ordering of piemontite. American Mineralogist, 54, 710-717.

Dollase, W. A. (1968) Refinement and comparison of the structures of zoisite and clinozoisite. American Mineralogist, 53, 1882-1898.

Enami, M. and Banno, S. (1977) Compositional range of alpha and beta zoisites. Journal of the Geological Society of Japan, 83, 737-739.

Evans, B. W. and Vance, J. A. (1987) Epidote phenocrysts in dacitic dikes, Boulder County, Colorado. Contributions to Mineralogy and Petrology, 96, 178 - 185.

Ewing, R. C., Chakoumakos, B. C., Murakami, T. and Lumpkin, G. R. (1987) The metamict state. Materials Research Society Bulletin, 12, 58-66.

Exley, R. A. (1980) Microprobe studies of REE-rich accessory minerals: Implications for Skye granite petrogenesis and REE mobility in hydrothermal systems. Earth and Planetary Science Letters, 48, 97-110.

Felsche, J. (1973) The Crystal Chemistry of the Rare-Earth Silicates. Structure and Bonding, Vol. 13, Springer-Verlag, New York, p. 99-197.

Fleet, M. E. (1976) Distortion parameters for coordination polyhedra. Mineralogical Magazine, 40, 531-533.

Fleischer, M. (1987) Glossary of Mineral Species. Mineralogical Record, Inc., Tucson, AZ, 227 p.

Fleischer, M. (1985) A summary of the variations in relative abundance of the lanthanides and yttrium in allanites and epidotes. Bulletin of the Geological Society of Finland, 57, 15 - 155.

Franz, G., Thomas, S. and Smith, D. C. (1986) High-pressure phengite decomposition in the Weissenstein eclogite, Munchberger Gneiss Massif, Germany. Contributions to Mineralogy and Petrology, 92, 71 - 85.

Frondel, J. W. (1964) Variation of some rare earths in allanite. The American Mineralogist, 49, 1159-1177.

Gabe, E. J., Portheine, J. C., and Whitlow, S. H. (1973) A reinvestigation of the epidote structure: Confirmation of the iron location. American Mineralogist, 58, 218-223.

Gay, P. (1957) An x-ray investigation of some rare-earth silicates: cerite, lessingite, beckelite, britholite and stillwellite. Mineralogical Magazine, 31, 455-468.

Bence, A. E. and Albee, A. L. (1968) Empirical correction factors for the electron microanalysis of silicates and oxides. Journal of Geology, 76, 382-403.

Black, P. M. (1970) A note on the occurrence of allanite in hornfelses at Paritu, Coromandel County. New Zealand Journal of Geology and Geophysics, 13, 343-345.

Bloss, F. D. (1985) Labelling refractive index curves for mineral series. American Mineralogist, 70, 428-432.

Bloss, F. D. (1981) The Spindle Stage: Principles and Practice. Cambridge University Press, Cambridge, England, 340 p.

Bocquet, J. (1975) Sur une allanite filonienne, a Bramans en Maurienne (Alpes occidentales, Savoie). Bulletin Societe Francaise de Mineralogie et de Cristallographie, 98, 171-174.

Brixner, L. H. and Abramson, E. (1965) On the lumininescent properties of the rare earth vanadates. Journal of the Electrochemical Society, 112, 70-74.

Brooks, C. K., Henderson, P. and Ronsbo, J. G. (1981) Rare-earth partition between allanite and glass in the obsidian of Sandy Braes, Northern Ireland. Mineralogical Magazine, 44, 157-160.

Burnham, C. W. (1962) Lattice constant refinement. Annual Report of the Director of the Geophysical Laboratory, Carnegie Institution of Washington Yearbook, 61, 132-135.

Burns, R. G. and Strens, R. G. J. (1967) Structural interpretation of polarized absorption spectra of the Al-Fe-Mn-Cr epidotes. Mineralogical Magazine, 36, 204-226.

Calvo, C., Faggiani, R., Krishnamachari, N. (1975) The crystal structure of $Sr_{9.402}Na_{0.209}(PO_4)_6B_{0.99602}$ - a deviant apatite. Acta Crystallographica, B31, 188-192.

Carbonin, S. and Molin, G. (1980) Crystal chemical considerations on eight metamorphic epidotes. Neues Jahrbuch fur Mineralogie Abhandlungen, 139, 205-215.

Cech, F. and Povondra, P. (1972) New data on metamict allanite from Domaninek, Czechoslovakia. Acta Universitatis Carolinae-Geologica, 3, 151-160.

Cech, F., Vrana, S, and Povondra, P. (1972) A non-metamict allanite from Zambia. Neues Jahrbuch fur Mineralogie Abhandlungen, 116, 208-223.

Cullers, R. L. and Medaris G., Jr. (1977) Rare earth elements in carbonatites and cogenetic igneous rocks: examples from Seabrook Lake and Callander Bay, Ontario. Contributions to Mineralogy and Petrography, 65, 143-153.

DeCoster, M., Pollak, H., and Amelinckx, S. (1963) A study of Mossbauer absorption in iron silicates. Physica Status Solidi, 3, 283-288.

Deer, W. A., Howie, R. A., and Zussman, J. (1966) An Introduction to the Rock Forming Minerals. John Wiley and Sons, New York.

Ghent, E. D. (1972) Electron microprobe study of allanite from Mt. Falconer quartz monzonite pluton, lower Taylor Valley, South Victoria Land, Antarctica. Canadian Mineralogist, 11, 526-530.

Ghose, S. and Tsang, T. (1970) Ordering of V^{2+}, Mn^{2+}, and Fe^{3+} ions in zoisite, $Ca_2Al_3Si_3O_{12}(OH)$. Science, 171, 374-376.

Gibbs, G. V. (1982) Molecules as models for bonding in silicates. American Mineralogist, 67, 421-450.

Goddard, E. N. and Glass, J. J. (1940) Deposits of radioactive cerite near Jamestown, Colorado. American Mineralogist, 25, 381-404.

Green, T. H. and Pearson, N. J. (1984) Stability of REE acceptor minerals at high pressures and temperatures. In Geoscience in the Development of Natural Resources, Abstract No. 12, 197-199. Geological Society of Australia.

Green, T. H. and Pearson, N. J. (1983) REE partitioning between sphene, allanite and chevkinite and coexisting intermediate - felsic liquids at high P, T. Lithosphere dynamics and evolution of the continental crust [abstract]: Canberra, Geological Society of Australia, 157.

Hanisch, K. and Zemann, J. (1966) Messung des Ultrarot-Pleochroismus von Mineralen. IV. Der pleochroismus der OH-streckfrequenz in epidot. Neues Jahrbuch fur Mineralogie, Monatschefte, 19-23.

Hanson, R. A. and Pearce, D. W. (1941) Colorado cerite. American Mineralogist, 26, 110-120.

Haskin, L. A. and Haskin, M. A. (1968) Rare-earth elements in the Skaergaard intrusion. Geochimica et Cosmochimica Acta, 32, 433-447.

Hawthorne, F. C. (1987) A general structural classification for oxy-salt minerals. Geological Association of Canada - Mineralogical Association of Canada, Abstracts with Program, 10, 30.

Headley, T. J., Ewing, R. C., and Haaker, R. F. (1982) TEM study of the metamict state. IMA Meeting, Varna, Bulgaria, Proceedings.

Henderson, P. (1984) General geochemical properties and abundances of the rare earth elements. In Rare Earth Element Geochemistry (Ed., P. Henderson, Elsevier, New York), Chapter 1, 1-32.

Henderson, P. (1980) Rare earth element partition between sphene, apatite and other coexisting minerals of the Kangerdlugssuaq Intrusion, E. Greenland. Contributions to Mineralogy and Petrology, 72, 81-85.

Hickling, N. C., Phair, G., Moore, R., and Rose, H. J., Jr. (1970) Boulder Creek Batholith, Colorado, Part I: Allanite and its bearing upon age patterns. Geological Society

of America Bulletin, 81, 1973-1994.

Hildreth, W. (1979) The Bishop Tuff: Evidence for the origin of compositional zonation in silicic magma chambers. Geological Society of America Special Paper, 180, 43-75.

Hollabaugh, C. L. and Foit, F. F. Jr. (1984) The crystal structure of an Al-rich titanite from Grisons, Switzerland. American Mineralogist, 61, 238-247.

Holmqvist, A. (1975) Low 2-V allanite and Mg-bearing allanite from the Kallmorberg mine, Norberg, Sweden. Geologiska Foreningens i Stockholm Forhandlingar, 97, 162-166.

Hugo, P. J. (1961) The allanite deposits of Vrede, Gordonia district, Cape Province. Republic of South Africa Department of Mines, Geological Survey Bulletin, 37, 1-65.

Ito, J. (1968) Silicate apatites and oxyapatites. American Mineralogist, 53, 890-907.

Ito, J. and Arem, J. E. (1971) Chevkinite and perrierite: Synthesis, crystal growth and polymorphism. American Mineralogist, 56, 307-319.

Ito, T. (1950) The structure of epidote ($HCa_2(Al,Fe)Al_2Si_3O_{13}$). In x-ray studies on polymorphism. Maruzen Co., Tokyo, Chapter 5, 309-320.

Ito, T., Morimoto, N. and Sadanaga, R. (1954) On the structure of epidote. Acta Crystallographica, 7, 53-59.

Ivanov, V. S. (1969) Formation of allanite in granitic rocks of the western and eastern Iultinsk intrusions, Central Chukotka. Petrol. Izverzh. Metamorfich. Porod, 1969, 169-176 [abstr. Ref. Zhurnal, Geol., 1970, No. 1V247].

Izett, G. A. (1981) Volcanic ash beds: Recorders of upper Cenozoic silicic pyroclastic volcanism in the Western United States. Journal of Geophysical Research, 86, 10200-10222.

Izett, G. A. and Wilcox, R. E. (1968) Perrierite, chevkinite and allanite in upper Cenozoic ash beds in the western United States. American Mineralogist, 53, 1558-1567.

Jahns, R. H. (1982) Internal evolution of granitic pegmatites. In P. Cerny, Ed., Short Course in Granitic Pegmatites in Science and Industry, Mineralogical Association of Canada, Short Course Notes 8, 293-328.

Jensen, B. B. (1967) Distribution patterns of rare earth elements in cerium rich minerals. Norsk Geologisk Tidsskrift, 47, 9-19.

Jensen, B. B. (1973) Patterns of trace element partitioning. Geochimica et Cosmochimica Acta, 37, 2227-2242.

Jesus Ojeda, M. and Mendoza, A. (1981) Distribution of rare earths in zircons, fluorites, apatites, garnets, and allanites from Peru. Bol. Soc. Quim. Peru 1981, 179-192.

Kauffman, A. J. and Dilling, E. D. (1950) Differential thermal curves of certain hydrous and anhydrous minerals, with a description of the apparatus used. Economic Geology, 45, 222-244.

Kay, M. I. and Young, R. A. (1964) Crystal structure of hydroxyapatite. Nature (London), 204, 1050-1052.

Khvostova, V. A. (1962) Mineralogy of orthite. Akademii Nauk SSSR, Institute Mineralog. Geokhim., Kristallokhim. Redkikh Elementov, trudy, no. 11, 118 p. [in Russian].

Kokkinakis, A. (1980) Orthit in magmatischen Gesteinen des Symvolongebiges und des Kavala-Gebietes (Nordgriechenland). Neues Jahrbuch fur Mineralogie, Abhandlungen, 138, 31-38.

Kostov, I. and Panaiotov (1967) Rare earths in epidote and allanite. Compte Rendue Academie Bulgaria Sciences, 20, 1057-1059.

Kretz, R. (1983) Symbols for rock-forming minerals. American Mineralogist, 68, 277-279.

Kupriyanova, I. I., Volkova, M. I., and Goroshchenko, Z. I. (1964) Rare earth minerals in one molybdenite deposit in the European U.S.S.R. Trudy Mineralog. Muzeya Akademi Nauk SSSR, 15, 123-133.

Langer, K. and Raith, M. (1974) Infrared spectra of Al-Fe(III) epidotes and zoisites, $Ca_2(Al_{1-p}Fe^{3+})Al_2O(OH)(Si_2O_7)(SiO_4)$. American Mineralogist, 59, 1249-1258.

Lazarev, A. N. (1972) Vibrational Spectra and Structure of Silicates. Consultants Bureau.

Leavens, P. B. and Thomssen, R. W. (1977) Famous mineral localities; Prince of Wales Island, Alaska. Mineralogical Record, 8, 4-12.

Lee, D. E. and Bastron, H. (1967) Fractionation of rare-earth elements in allanite and monazite as related to geology of the Mt. Wheeler mine area, Nevada. Geochimica et Cosmochimica Acta, 31, 339-356.

Levinson, A. A. (1966) A system of nomenclature for rare-earth minerals. American Mineralogist, 51, 152-158.

Liebau, F. (1960) Classification of silicates. In P.H. Ribbe, Ed., Orthosilicates, M. S. A. Short Course Reviews in Mineralogy, 5, 1-23.

Linke, W. (1970) Messung des Ultrarot-Pleochroismus von Mineralen. X. Der Pleochroismus der OH-Streckfrequenz in Zoisit. Tschermaks Mineralogische und Petrographische Mitteilungen, 14, 61-63.

Liou, J. G. (1973) Synthesis and stability relations of epidote, $Ca_2Al_2FeSi_3O_{12}(OH)$. Journal of Petrology, 14, 381-413.

Mackinnon, I. D. R., Lumpkin, G. R. and Van Deusen, S. B. (1986) Thin-film analyses of silicate standards at 200 kV: the effect of temperature on element loss. In A. D. Romig, Jr. and W. F. Chambers, Eds., Microbeam Analysis - 1986, San Francisco Press, San Francisco, 451-454.

Merrin, S. (1962) Experimental Investigation of Epidote Paragenesis. Ph.D. thesis, Pennsylvania State University.

Meyer, G. H. (1966) New data on zoisite and epidote. American Journal of Science, 264, 364-385.

Mineyev, D. A. (1963) Geochemical differentiation of the rare earths: Geochimiya 1963, 12, 1082-1100 [transl. Geochemistry 1963, 12, 1129-1149].

Mitchell, R. S. (1966) Virginia metamict minerals: Allanite. Southeastern Geology, 7, 183-195.

Moenke, H. H. W. (1974) Silica, the three dimensional silicates, borosilicates and beryllium silicates. In V. C. Farmer, Ed., The Infrared Spectra of Minerals, Mineralogical Society Monograph 4, Mineralogical Society of London, London, 365-382.

Moenke, H. H. W. (1966) Mineral-Spektren, II. Akademie-Verlag, Berlin.

Morgan, J. W. and Wandless, G. A. (1980) Rare earth element distribution in some hydrothermal minerals: Evidence for crystallographic control. Geochimica et Cosmochimica Acta, 44, 973-980.

Murata, K. J., Rose, H. J., Jr., and Carron, M. K. (1953) Systematic variation of rare earths in monazite. Geochimica et Cosmochimica Acta, 4, 292-300.

Murata, K. J., Dutra, C. V., DaCosta, M. T. and Branco, J. J. R. (1959) Composition of monazite from pegmatites of eastern Minas Gerais, Brazil. Geochimica et Cosmochimica Acta, 16, 1-14.

Murata, K. J., Rose, H. J., Jr., Carron, M. K. and Glass, J. J. (1957) Systematic variation of rare-earths in cerium-earth minerals. Geochimica et Cosmochimica Acta, 11, 141-161.

Myers, L. and Myers, M. (1983) Green Monster Mountain and its exquisite epidote crystals. Australian Gem and Treasure Hunter Yearbook, 76, 37-42.

Nagasawa, H. (1970) Rare earth concentrations in zircons and apatites and their host dacites and granites. Earth and Planetary Science Letters, 9, 357 - 364.

Nakamoto, K. (1978) Infrared and Raman Spectra of Inorganic Compounds. John Wiley and Sons, New York.

Nash, W. P. (1972) Apatite chemistry and phosphorus fugacity in a differentiated igneous intrusion. American Mineralogist, 57, 877-886.

Nash, W. P. and Congdon, R. (1987) Accessory minerals in high fluorine rhyolite:

Composition and partition coefficients. Geological Society of America Abstracts with Program, 19, 1513.

Neumann, H., and Nilssen, B. (1962) Lombaardite, a rare-earth silicate, identical with, or very closely related to, allanite. Norsk Geologisk Tidsskrift, 42, 277-286.

Neumann, H., Jensen, B. B. and Brunfelt, A. O. (1966) Distribution patterns of rare earth elements in minerals. Norsk Geologisk Tidsskrift, 46, 141-179.

Nystrom, J. O. (1984) Rare earth element mobility in vesicular lava during low-grade metamorphism. Contributions to Mineralogy and Petrology, 88, 328-331.

Orcel, M. J. (1953) Analyse thermique differentielle de quelques mineraux metamictes. Academie de Science [Paris] Comptes Rendus, 236, 1052-1054.

Pellas, P. (1962) Essai de determination de l'age geologique a partir des distances reticulaires et des proprietes optique des allanites radioactives (II). Bulletin de la Societe francaise, Mineralogie et Cristallographie, 85, 213-233.

Philips, W. R. and Griffen, D. T. (1981) Optical Mineralogy: The Nonopaque Minerals. W. H. Freeman and Co., San Francisco.

Ponader, and Brown, G. E., Jr. (1986) X-ray absorption study of ytterbium in quenched aluminosilicate melts. The 14 General Meeting of the International Mineralogical Association, Abstracts with Program, p. 202.

Posner, A. S., Perloff, A., Dioro, A. F. (1958) Refinement of the hydroxyapatite structure. Acta Crystallographica, 11, 308-309.

Povarennykh, A. S. (1972) Crystal Chemical Classification of Minerals. (Transl. by J. E. S. Bradley), Vol. 1, Plenum Press, New York.

Protopopov, V. N. (1940) X-ray spectroscopic study of yttro-orthite, orthite, monazite, and cyrtolites of northern Karelie. Mat. Tsentral Nauch. Issled. Geol. Razvod. Inst., Geokhim. 5, 30-54 (in Russian).

Prunier, A. R., Jr. (1978) Calculation of Temperature-Oxygen Fugacity Tables for H_2-CO_2 Gas Mixtures at One Atmosphere Total Pressure, and An Investigation of the Zoisite-Clinozoisite Transition. M. S. Thesis, Virginia Polytechnic Institute and State University, 124 p.

Pudovkina, Z. V. and Pyatenko, Yu. A. (1963) The crystalline structure of non-metamict orthite. Doklady Akademiia Nauk SSSR, 153, 146-149.

Putalova, R. V. (1978) Accessory minerals of granitic intrusives of the Chingiz meganticlinorium. Izdat. Nauka Kazakh S. S. R., Alma-Ata 1978, 150 p.

Rao, A. T. (1976) Study of the apatite-magnetite veins near Kasipatnam, Visakhapatnam District, Andhra Pradesh, India. Tschermaks Mineralogische und Petrographische Mitteilungen, 23, 87-103.

Rapp, G. J., Jr. (1960) Some Physico-Chemical Properties of the Zoisite-Epidote Group. Ph. D. Thesis, Pennsylvania State University.

Remy, P. H., Dambly, M., Pollak, H., Ledocte, P., and Bruyneel, W. (1969) Study of phase changes in allanite by Mossbauer spectroscopy. Peaceful Uses Atomic Energy Afr., Proceedings Symposia (pub. 1970), 405-409.

Robinson, K., Gibbs, G. V., and Ribbe, P. H. (1971) Quadratic elongation: A quantitative measure of distortion in coordination polyhedra. Science, 172, 567-570.

Rumanova, I. M. and Nikolaeva, T. V. (1959) Crystal structure of orthite. Kristallografiya, 4, 829-835 (trans. Soviet Physics - Crystallography, 4, 789-795, 1959).

Sawka, W. N. and Chappell, B. W. (1986) The distribution of radioactive heat production in I- and S-type granites and residual source regions: implications to high heat flow areas in the Lachlan Fold Belt, Australia. Australian Journal of Earth Sciences, 33, 107-118.

Sawka, W. N., Chappell, B. W., and Norrish, K. (1984) Light rare-earth-element zoning in sphene and allanite during granitoid fractionation. Geology, 12, 131-134.

Schreiber, H. D., Lauer, H. V., Jr. and Thanyasiri, T. (1985) The redox state of cerium in basaltic magmas: an experimental study of iron-cerium interactions in silicate melts. Geochimica et Cosmochimica Acta, 44, 1599-1612.

Schreiber, H. D. and Balazs, B. (1980) An electromotive force series for redox couples in a borosilicate melt: The basis for electron exchange interactions of the redox couples. Journal of Non-Crystalline Solids, 71, 59-67.

Semenov, E. I. (1963) Mineralogy of the Rare Earths. Izdat. Akad. Nauk S. S. S. R., Moscow, 410 p.

Semenov, E. I. (1958) Relationship between composition of rare earths and composition and structure of minerals. Geokhimiya, 1958, 5, 452-461 [transl. Geochemistry, 1957, 5, 574-586].

Semenov, E. I. (1957) Isomorphism and camouflage of rare earths. Geokhimiya, 1958, 7, 626-637 [transl. Geochemistry 1957, 7, 735-748].

Semenov, E. I. and Barinskii, R. L. (1958) Characteristics of the composition of rare earths in minerals. Geokhimiya, 1958, 314-333; translation in Geochemistry International, 1958, 398-419.

Shannon, R. D. (1976) Revised effective ionic radii and systematic studies of interatomic distances in halides and chalcogenides. Acta Crystallographica, A32, 751-767.

Shen, J. and Moore, P. B. (1982) Tornebohmite, $RE_2Al(OH)[SiO_4]_2$: crystal structure and geneology of RE(III)Si(IV) = Ca(II)P(V) isomorphisms. American Mineralogist, 67, 1021 1028.

Smith, D. K. and Zolensky, M. E. (1983) A FORTRAN IV program for calculating x-ray powder diffraction patterns - Version 10. Department of Geological Sciences, The Pennsylvania State University.

Smith, W. L., Franck, M. L. and Sherwood, A. M. (1957) Uranium and thorium in the accessory allanite of igneous rocks. American Mineralogist, 42, 367-378.

Sneeringer, M. A. and Watson, E. B. (1985) Milk cartons and ash cans; two unconventional welding techniques. American Mineralogist, 70, 200-201.

Solberg, T. N. (1981) Graphical procedures for the refinement of electron microprobe analysis of fine-grained particles. Mircobeam Analysis- 1981, 160-162.

Speer, J. A. (1982) Zircon. In P.H. Ribbe, Orthosilicates, Second Edition, Mineralogical Society of America Reviews in Mineralogy, Vol. 5, 67-106.

Speer, J. A. and Gibbs, G. V. (1976) The crystal structure of synthetic titanite, $CaTiOSiO_4$, and the domain textures of natural titanites. American Mineralogist, 61, 238-247.

Speer, J. A. and Solberg, T. N. (1982) Rare-earth pyrosilicates ($REE_2Si_2O_7$) as potential electron microprobe standards. Mircobeam Analysis- 1982, 445-446.

Strens, R. G. J. (1964a) Synthesis and properties of piemontite. Nature, 201, 175-176.

Strens, R. G. J. (1964b) Epidotes of the Borrowdale volcanic rocks of central Borrowdale. Mineralogical Magazine, 33, 868-896.

Strens, R. G. J. (1963) Some relationships between the members of the epidote group. Nature, 198, 80-81.

Strunz, H. (1986) On the classification of the silicates. The 14th General Meeting of the International Mineralogical Association, Abstracts with Program, p. 240.

Strunz, H. (1966) Mineralogische Tabellen, 4th Edition. Akademische Verlagsgesellschaft, Leipzig.

Sudarsanan, K. and Young, R. A. (1969) Significant precision in crystal structural details: Holly Springs hydroxyapatite. Acta Crystallographica, B25, 1534-1543.

Swanson, D. K. and Peterson, R. C. (1981) Polyhedral volume calculations. Canadian Mineralogist, 18, 153-156.

Tang-Kai, A., Annersten, H., and Ericsson, T. (1980) Molecular Orbital ($MSX\partial$) calculations of s-electron densities of tetrahedrally coordinated ferric iron: Comparison with experimental isomer shift. Physics and Chemistry of Minerals, 5, 343-349.

Tempel, H. G. (1938) Influence of rare earths and some other components on physical and optical properties of the minerals of the epidote group. Chemie der Erde, 11, 525.

Tsang, T. and Ghose, S. (1974) Nuclear magnetic resonance of ^{27}Al in epidote, $Ca_2Al_2(Fe,Al)Si_3O_{12}(OH)$. Journal of Chemical Physics, 61, 414-417.

Tuttle, O. F. (1949) Two pressure vessels for silicate-water studies. Geological Society of America Bulletin, 60, 1727-1729.

Ueda, T. (1955) The crystal structure of allanite $OH(CaCe)_2(Fe^{3+}, Fe^{2+})Al_2OSi_2O_7SiO_4$. Memoirs of the College of Science, University of Kyoto, Series B, 22, 145-163.

Ueda, T. and Korekawa, M. (1955) Studies on the stability of radioactive minerals at high temperature. College of Science Memoirs, University of Kyoto, Series B, 22, 165-176.

Vlasov, K. A. (1966) Mineralogy of Rare Elements Volume I, Geochemistry and Mineralogy of Rare Elements and Genetic Types of Their Deposits. Translated from Russian; published by the Israel Program for Scientific Translations, 945 pp.

Volborth, A. (1962) Allanite pegmatites, red rock, Nevada compared with allanite pegmatites in Southern Nevada and California. Economic Geology, 57, 209-216.

Wahlstrom, E. E. (1955) Petrographic Mineralogy. John Wiley and Sons, New York, 410 p.

Wilcox, R. E. (1983) Refractive index determination using the central focus masking technique with dispersion colors. American Mineralogist, 68, 1226-1236.

Wolff, T. von (1941) Methodisches zur quantitativen Gesteins- und Mineral-Untersuchung mit Hilfe der Phasenanalyse. Tschermaks Mineralogische und Petrographische Mitteilungen, 54, 1-122.

Yes'kova, Ye. M. and Ganzeyev, A. A. (1964) Rare earth elements in accessory minerals of the Vishnevye mountains. Geochemistry, 6, 1152-1163.

Yoshiasa, A. and Matsumoto, T. (1985) Crystal structure refinement and crystal chemistry of pumpellyite. American Mineralogist, 70, 1011-1019.

Yurk, Y. Y., Marchenko, E. Ya. and Chashka, A. I. (1970) Accessory allanite of Precambrian granites and pegmatites of the Azov Sea area. Dopov. Akad. Nauk Ukr. RSR, Ser. B, 32, 225-227.

Zdorik, B., Kupriyanova, I. I. and Kumskova, N. M. (1964) Crystalline allanite in some Siberian metasomatic rocks. Trudy Mineralog. Muzeya, Akademi Nauk SSSR, 15, 208-214.

Zhirov, K. K., Bandurkin, G. A., and Lavront'ov, Yu. G. (1961) The geochemistry of rare earth elements in pegmatites of northern Karelii. Geokhimiya, 1961, 895-1004; translated in Geochemistry International, 1961, 1107-1118.

Zimmerle, W. (1971) Akzessorischer Allanit im Rattlesnake-Granit (San Diego County, Sudkalifornien) und seine allgemeine petrogenetische stellung. Neues Jarhbuch fur Mineralogie, Abhandlungen, 114, 281-300.

Zoltai, T. (1960) Classification of silicates and other minerals with tetrahedral structures. American Mineralogist, 45, 960-973.

APPENDIX A

SELECTED ANALYTICAL ELECTRON MICROSCOPE EDS SPECTRA OF SYNTHETIC ALLANITES, OTHER RUN PRODUCTS AND AN EPIDOTE

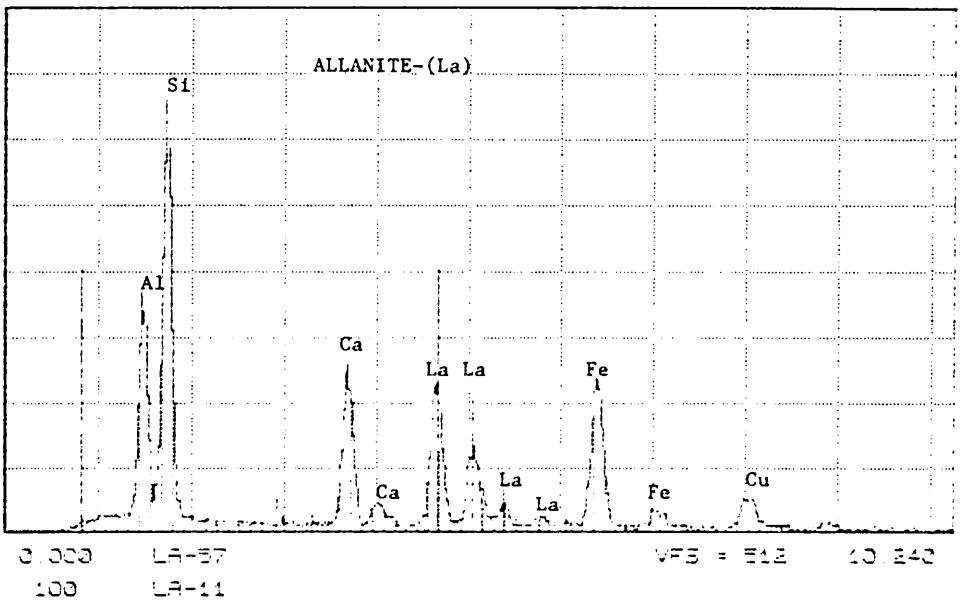
ALLANITE-(La)
Si
Al
Ca
La La
Fe
Ca
La
La
Fe
Cu
0.000
100
LA-57
LA-11
VFS = 512
10.240

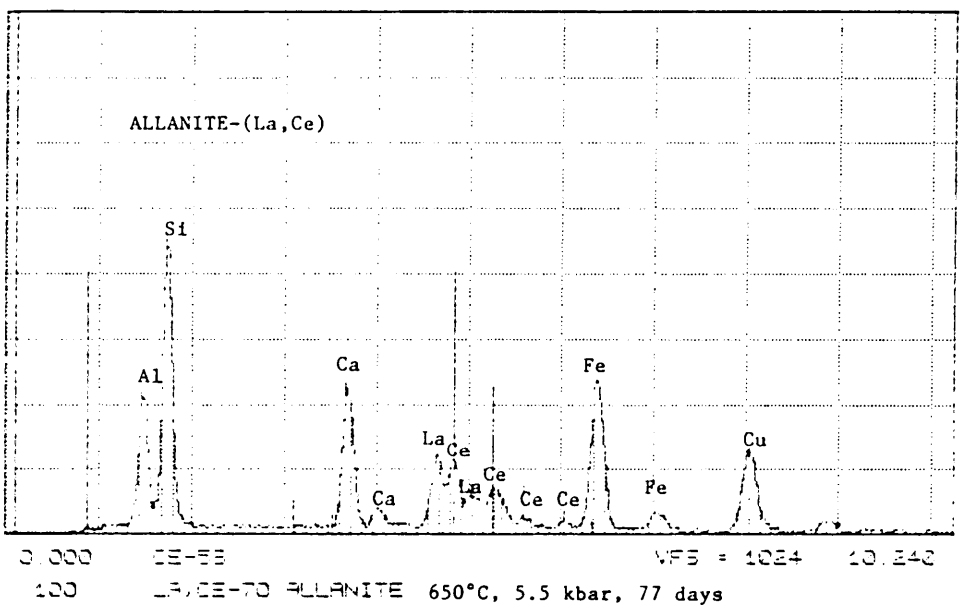
ALLANITE-(La,Ce)
Si
Al
Ca
Fe
La
Ce
Ce
Cu
Ca
La
Ce Ce
Fe
0.000
100
CE-53
LA,CE-70 ALLANITE 650°C, 5.5 kbar, 77 days
VFS = 1024
10.240

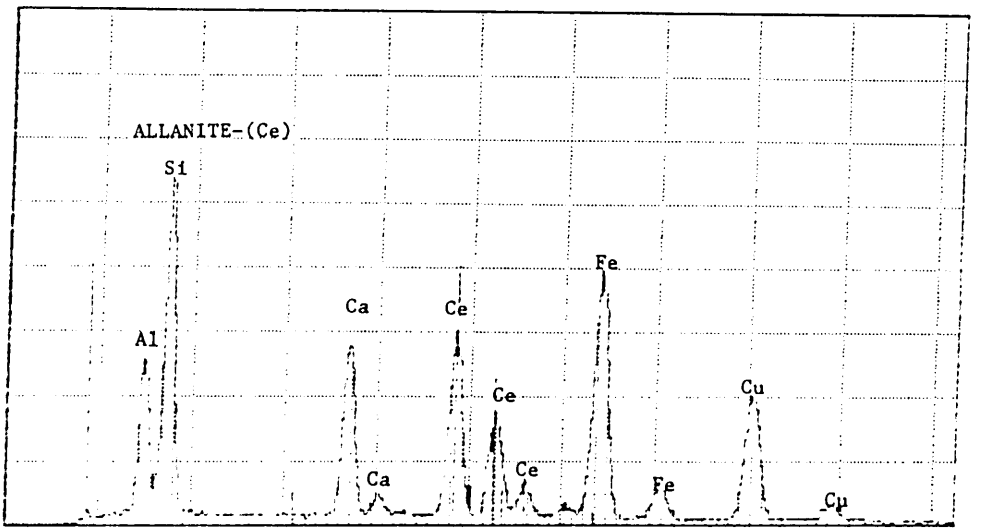
ALLANITE-(Ce)
Si
Al
Ca
Ce
Fe
Cu
Ca
Ce
Ce
Fe
Cu
725°C, 4 kbar

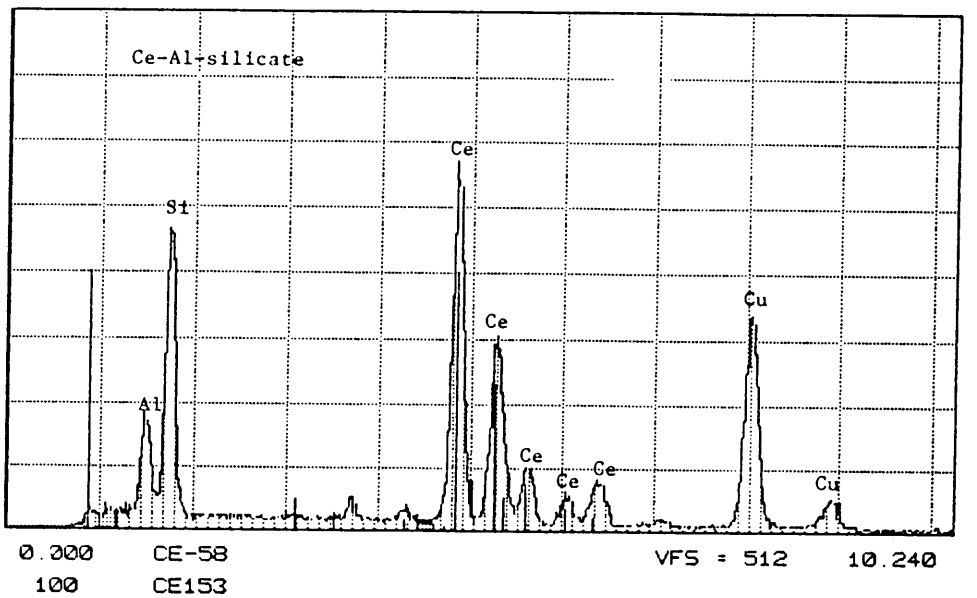
Ce-Al-silicate
Ce
Si
Ce
Cu
Al
Ce
Ce
Ce
Cu
0.000
CE-58
VFS = 512
10.240
100
CE153

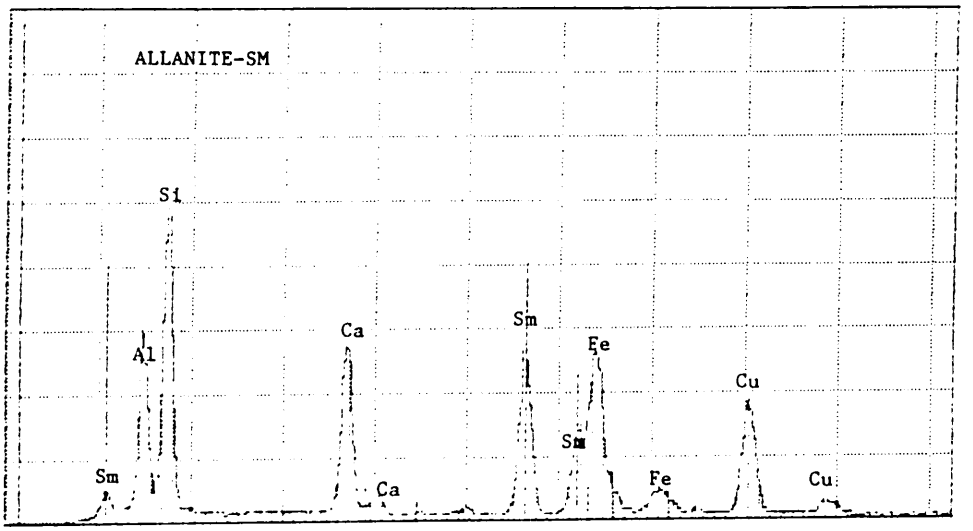
ALLANITE-SM
Si
Al
Ca
Sm
Fe
Cu
Sm
Ca
Sm
Fe
Cu
0.000 EM-62 VFS = 1024 10.240
100 EM 127 ALLANITE 723°C, 4 kbar

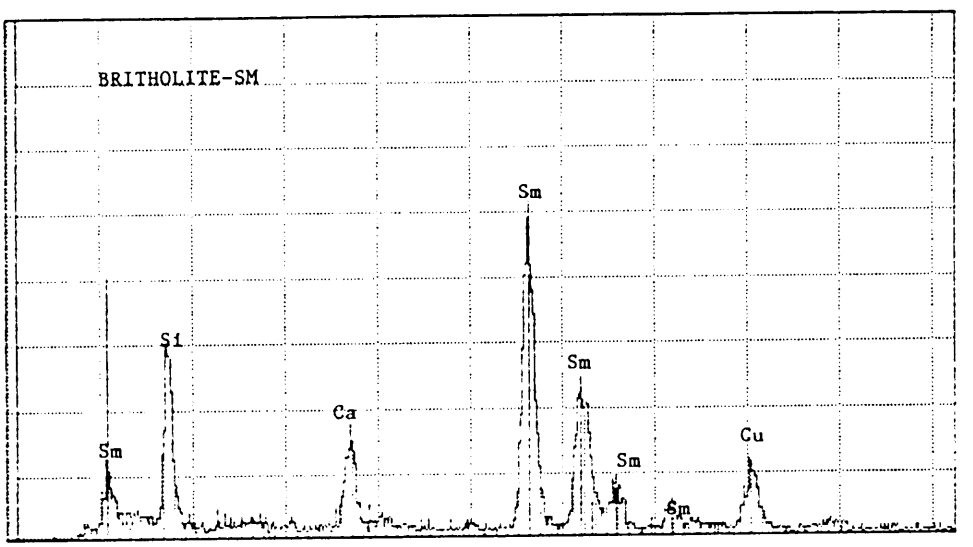
BRITHOLITE-SM
Sm
Si
Ca
Sm
Sm
Sm
Cu
Sm
0.000 EM-62 VFS = 128 10.240
100 EM-164 ALLANITE 700°C, 4 kbar, 6 days

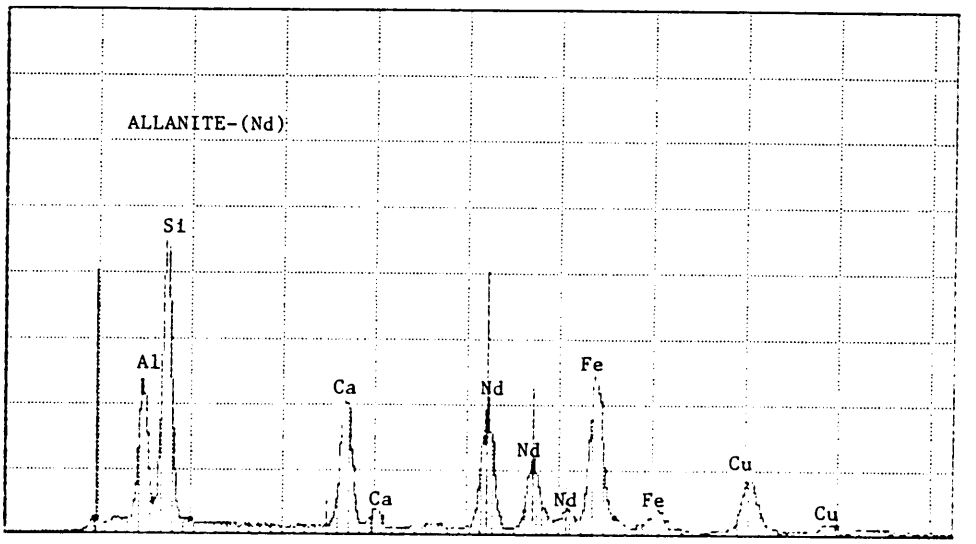

0 000 ND-60 VFE = 1034 10.240
30 ND-140 ALLANITE 723°C, 4 kbar

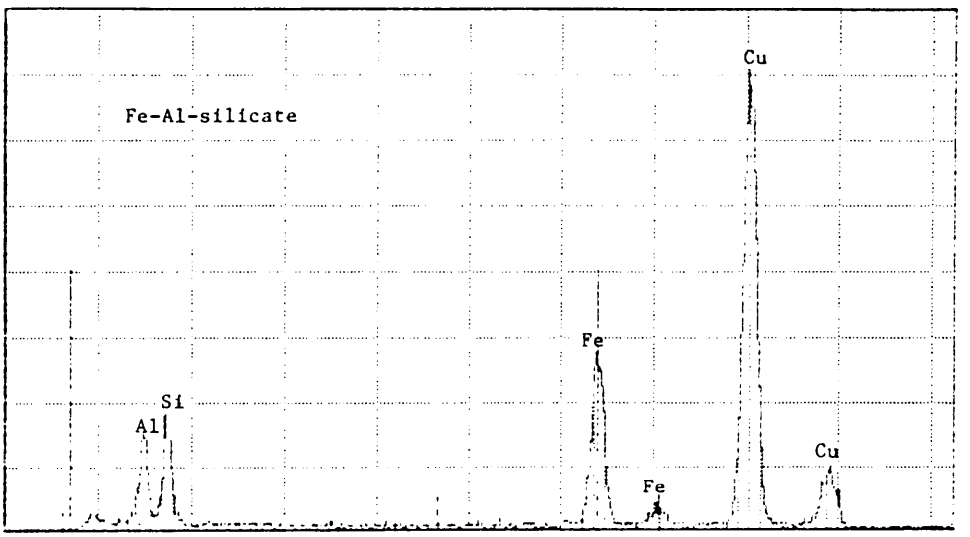

0.000 FE-35 VFE = 256 10.240
100 ND-31 ALLANITE 560°C, 5.5 kbar, 4 days

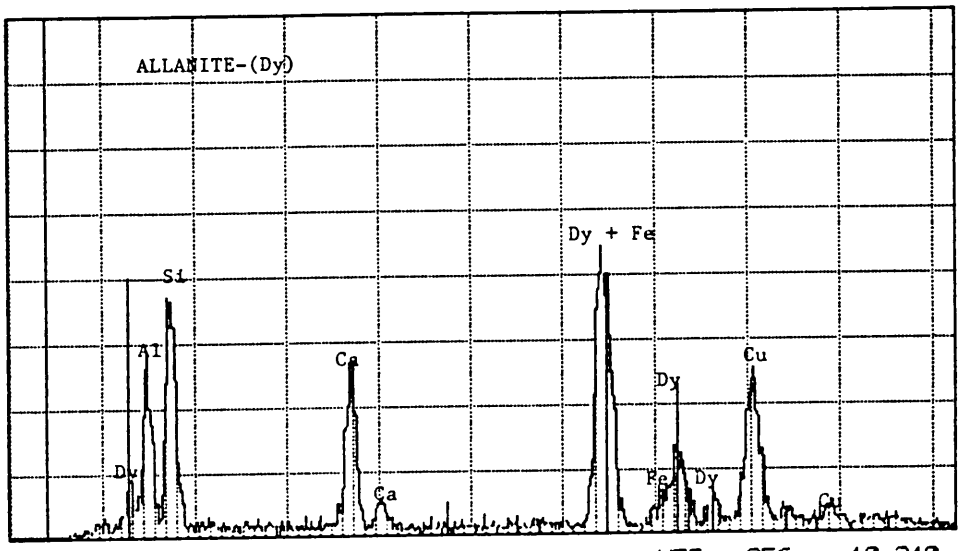
ALLANITE-(Dy)
Si
Al
Dy
Ca
Ca
Dy + Fe
Fe
Dy
Dy
Cu
Cu
0.000
DY-66
VFS = 256
10.240
100
DY130 ALLANITE OXIDE MIX 723°C, 4 kbar, 11 days

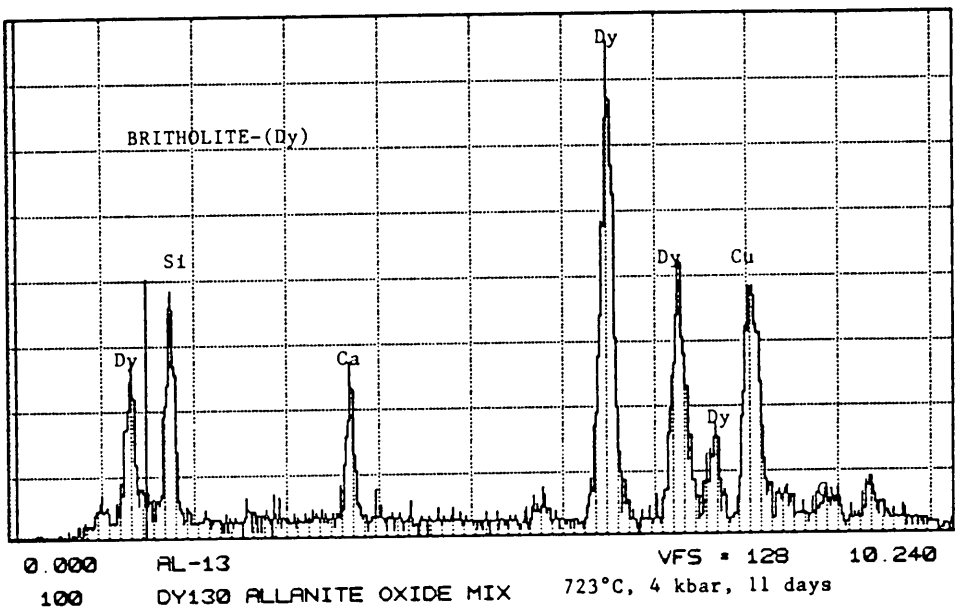
BRITHOLITE-(Dy)
Dy
Si
Dy
Ca
Dy
Dy
Cu
Cu
0.000
AL-13
VFS = 128
10.240
100
DY130 ALLANITE OXIDE MIX
723°C, 4 kbar, 11 days

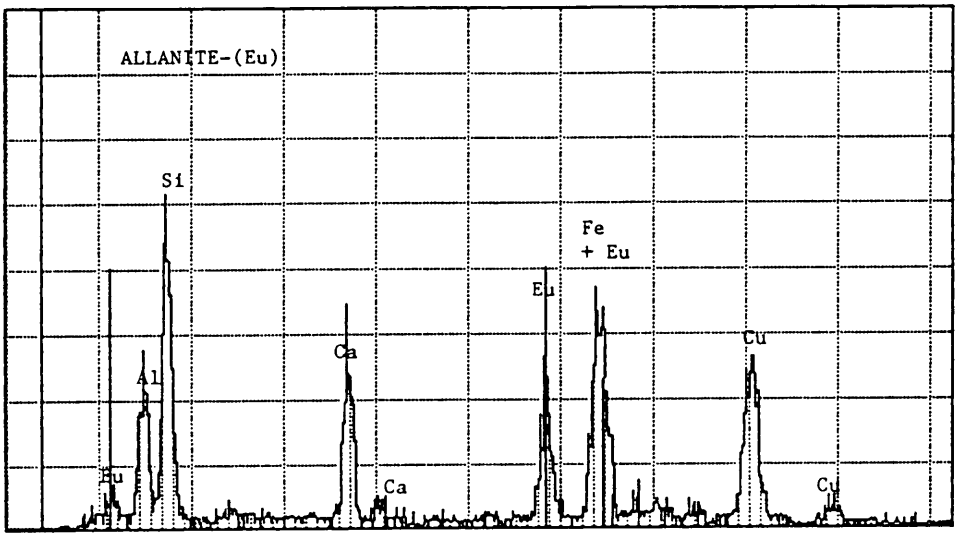
ALLANITE-(Eu)
Si
Fe
+ Eu
Eu
Ca
Al
Cu
Eu
Ca
Cu
0.000
EU-63
VFS = 128
10.240
100
EU135 ALLANITE OXIDE MIX
726°C, 4 kbar,11 days

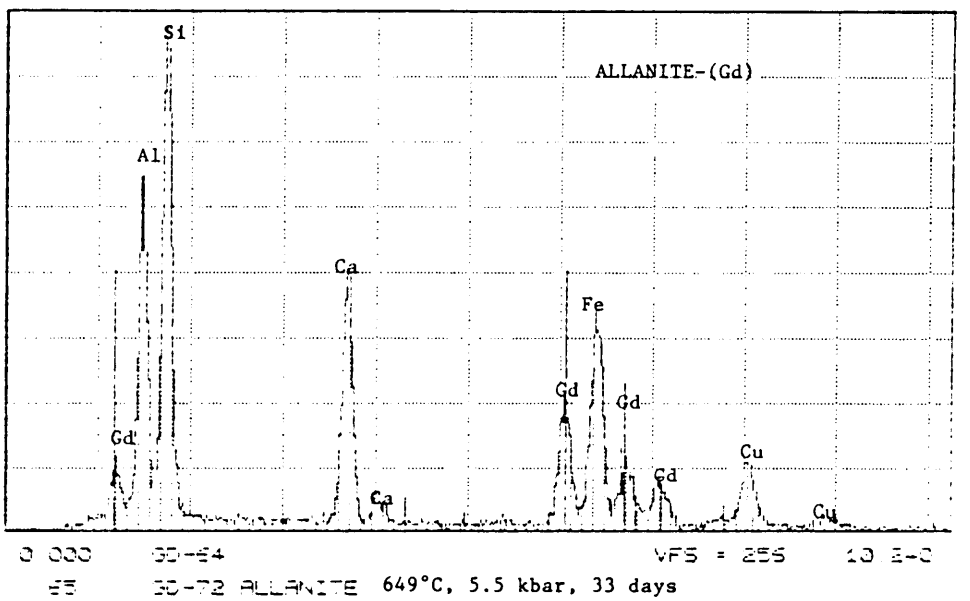
Si
ALLANITE-(Gd)
Al
Ca
Fe
Gd
Gd
Gd
Cu
Gd
Ca
Cu
0.000
GD-64
VFS = 255
10.240
55
GD-72 ALLANITE
649°C, 5.5 kbar, 33 days

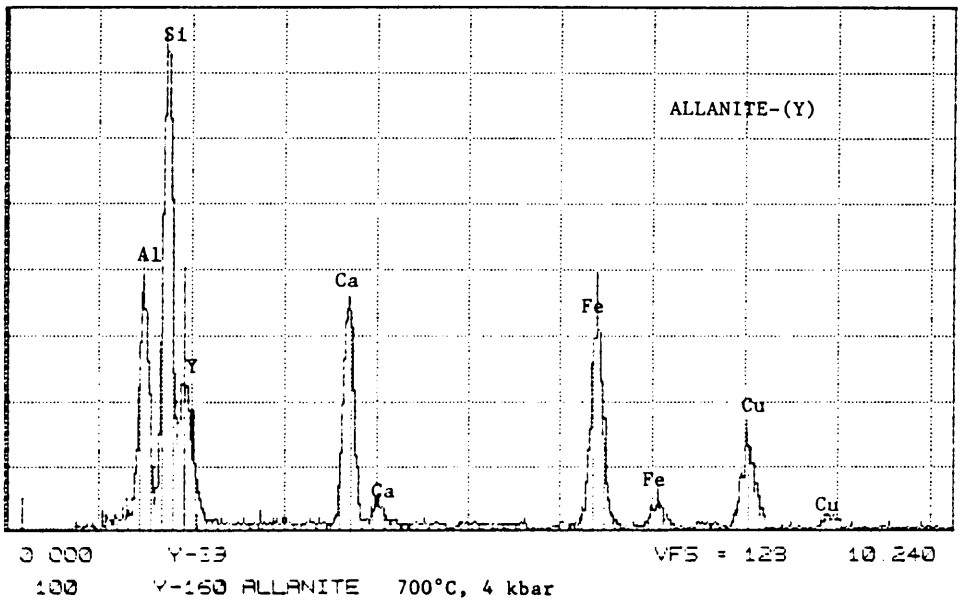
Si
ALLANITE-(Y)
Al
Ca
Fe
Y
Cu
Ca
Fe
Cu
0.000
Y-39
VFS = 128
10.240
100
Y-160 ALLANITE
700°C, 4 kbar

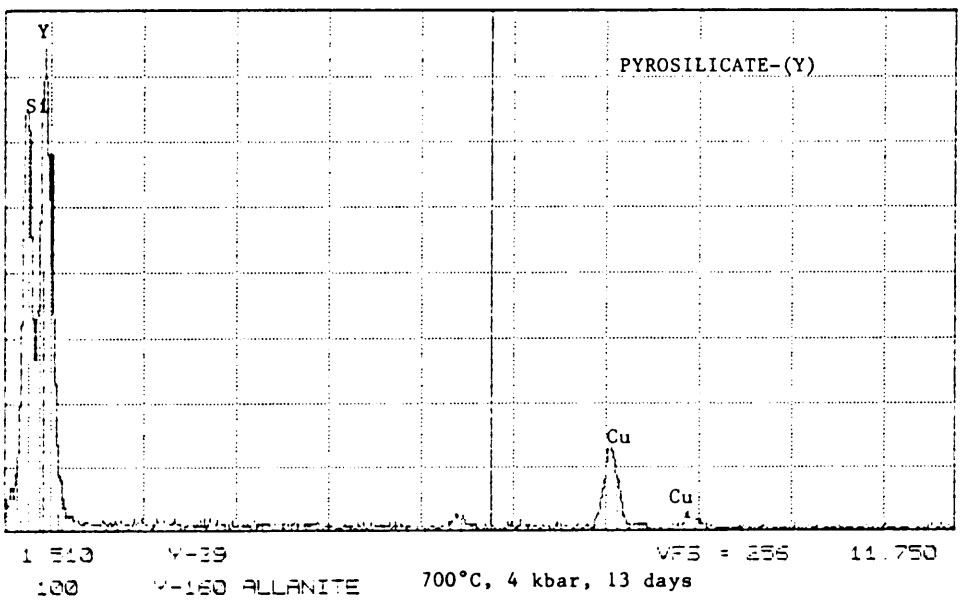
Y
PYROSILICATE-(Y)
Si
Cu
Cu
1.510
Y-39
VFS = 256
11.750
100
Y-160 ALLANITE
700°C, 4 kbar, 13 days

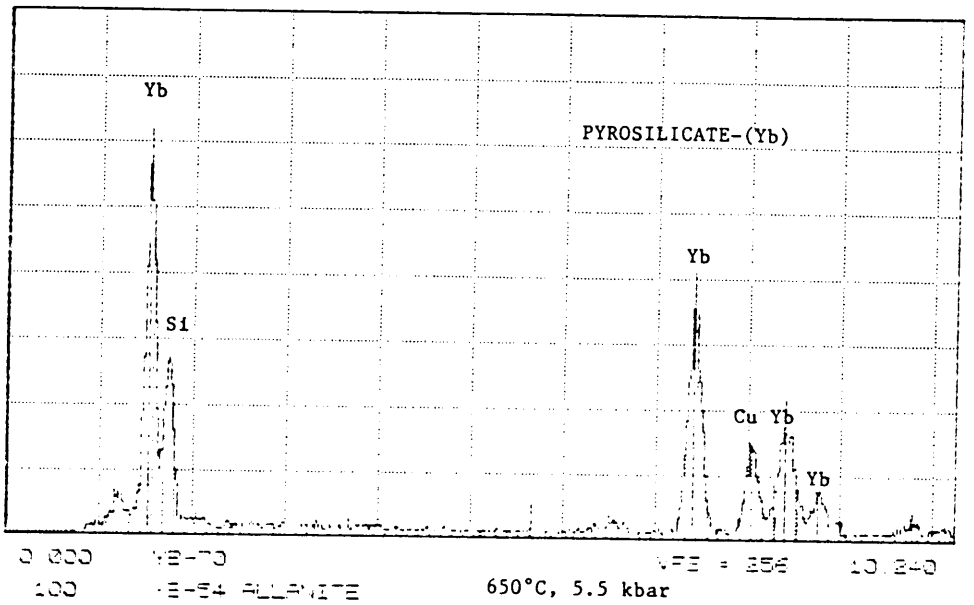
Yb
PYROSILICATE-(Yb)
Yb
Si
Cu Yb
Yb
650°C, 5.5 kbar

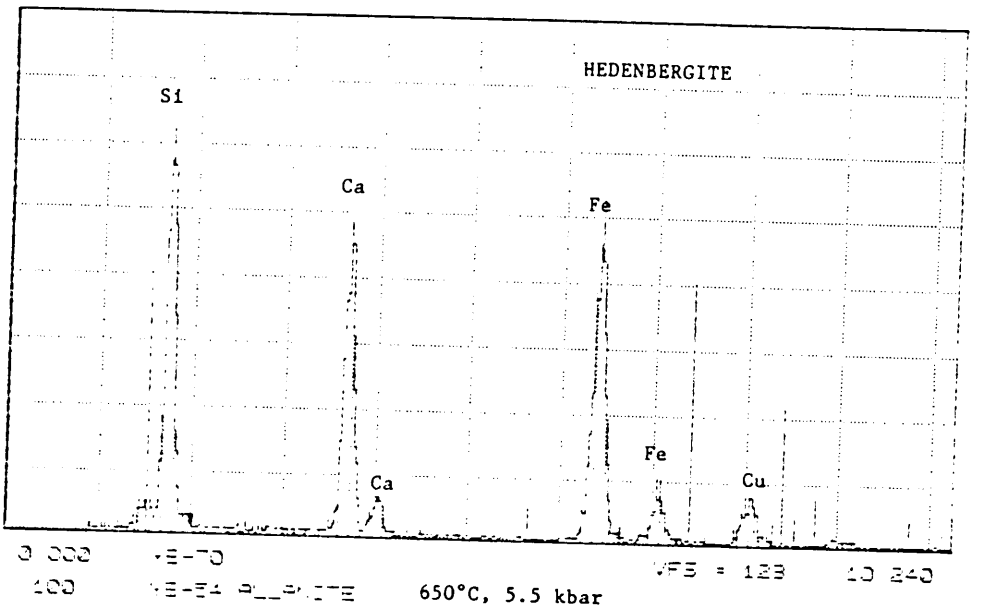
HEDENBERGITE
Si
Ca
Fe
Fe
Ca
Cu
650°C, 5.5 kbar

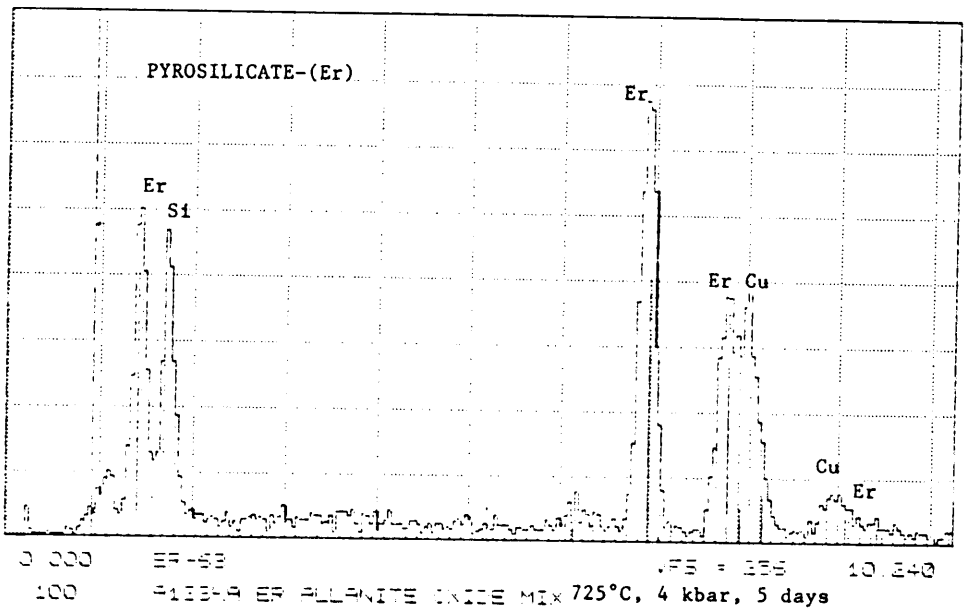
PYROSILICATE-(Er)
Er
Si
Er
Er Cu
Cu
Er
0.000
ER-63
FE = 335
10.240
100
725°C, 4 kbar, 5 days

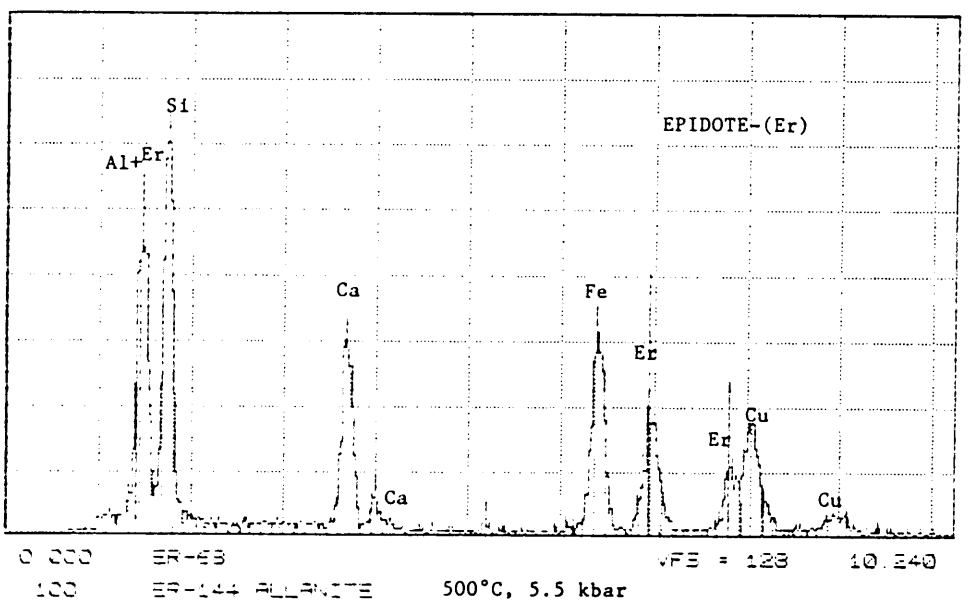
Si
Al+Er
EPIDOTE-(Er)
Ca
Fe
Er
Cu
Er
Ca
Cu
0.000
ER-63
FE = 128
10.240
100
500°C, 5.5 kbar

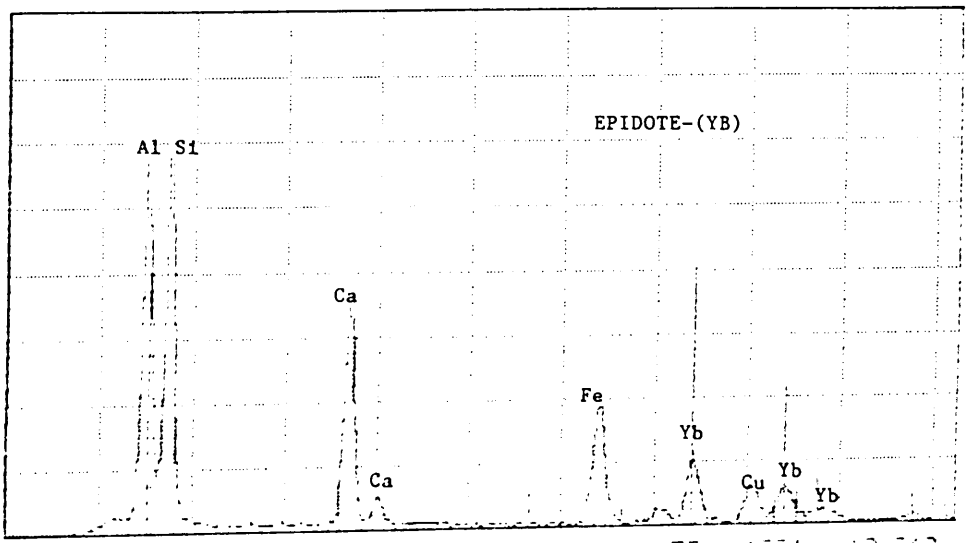

560°C, 5.5 kbar

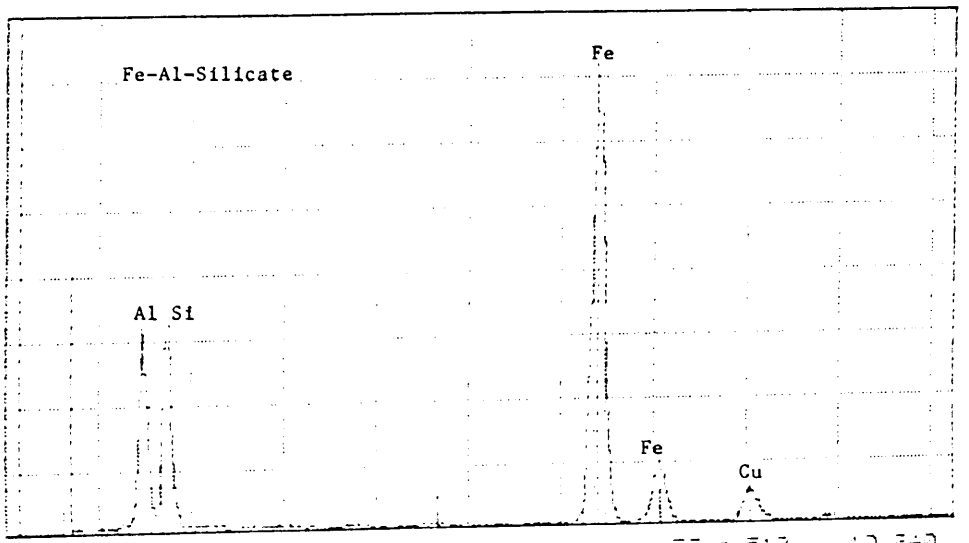

560°C, 5.5 kbar

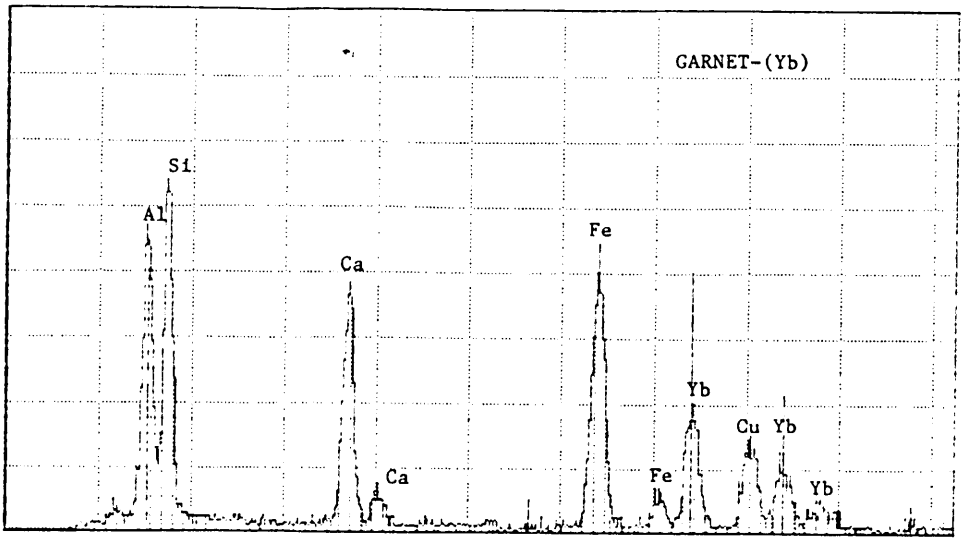
GARNET-(Yb)
Si
Al
Ca
Ca
Fe
Fe
Yb
Cu
Yb
Yb
0.000
YB-70
VFS = 123
10.240
103
YB-132 35 YB ALLANITE 703°C, 4 kbar, 13 days

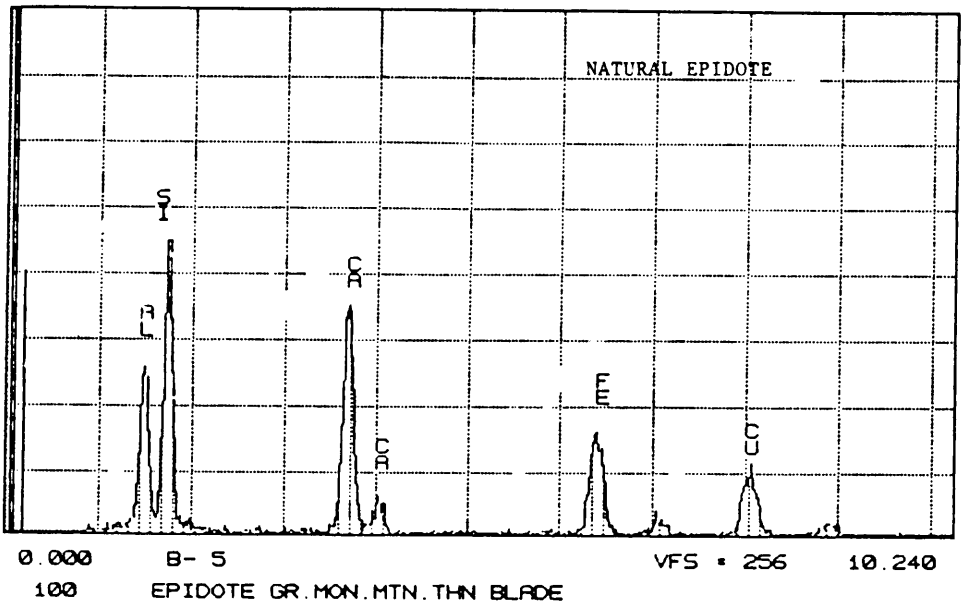
NATURAL EPIDOTE
SI
AL
CA
CA
FE
CU
0.000
B- 5
VFS = 256
10.240
100
EPIDOTE GR.MON.MTN.THN BLADE

APPENDIX B

INDEXED X-RAY POWDER DIFFRACTION PATTERNS OF SYNTHETIC ALLANITES

La allanite,

observed and calculated interplanar spacings, d, based on input parameters to cycle 1

h	k	l	corrected theta(obs)	corrected d(obs)	d(calc)	residuals of d (obs-calc)	residuals of d (obs-calc)/sigma	residuals of q (obs-calc)	residuals of q (obs-calc)/sigma
-2	1	1	12.650	3.52024	3.52152	-0.00127	-0.00008	0.00006	0.00008
2	0	1	13.740	3.24573	3.24226	0.00347	0.00026	-0.00020	-0.00026
-1	1	3	15.354	2.91142	2.90774	0.00368	0.00035	-0.00030	-0.00035
0	1	3	16.559	2.70486	2.70541	-0.00055	-0.00006	0.00006	0.00006
-3	1	1	17.114	2.61979	2.62073	-0.00094	-0.00011	0.00010	0.00011
2	0	2	17.545	2.55725	2.55687	0.00037	0.00005	-0.00004	-0.00005
-3	1	3	18.696	2.40500	2.40454	0.00045	0.00006	-0.00007	-0.00006
-2	2	2	19.357	2.32581	2.32773	-0.00192	-0.00029	0.00030	0.00029
-2	1	4	19.672	2.29006	2.28993	0.00013	0.00002	-0.00002	-0.00002
-4	0	1	20.729	2.17799	2.17839	-0.00039	-0.00007	0.00008	0.00007
-2	2	3	21.260	2.12607	2.12599	0.00008	0.00002	-0.00002	-0.00002
0	2	3	21.586	2.09551	2.09662	-0.00111	-0.00021	0.00024	0.00021
2	0	3	21.914	2.06556	2.06536	0.00020	0.00004	-0.00005	-0.00004
-3	1	5	24.760	1.84069	1.84166	-0.00097	-0.00024	0.00031	0.00024
-4	2	4	28.139	1.63464	1.63347	0.00117	0.00038	-0.00054	-0.00038
4	1	2	29.649	1.55837	1.56022	-0.00185	-0.00068	0.00098	0.00068
4	2	2	33.068	1.41288	1.41187	0.00101	0.00046	-0.00071	-0.00046

direct lattice constants after least-squares cycle 1

parameter	old	change	new	error
a (ang.)	8.91600	0.00001	8.91601	0.00411
b (ang.)	5.74600	0.00005	5.74605	0.00496
c (ang.)	10.12300	0.00046	10.12346	0.00700
alpha (deg.)	90.00000		90.00000	
beta (deg.)	114.66000	0.00842	114.66841	0.03397
gamma (deg.)	90.00000		90.00000	
unit cell volume (cubic ang.)	471.3169	-0.0056	471.3112	0.6212

direct lattice constant variance-covariance matrix

	a(ang.)	b(ang.)	c(ang.)	alpha(rad.)	beta(rad.)	gamma(rad.)
a	0.169180e-04	-0.198844e-05	0.238445e-05	0.510289e-13	-0.106104e-05	0.510289e-13
b		0.246421e-04	-0.656770e-05	0.443671e-13	-0.922520e-06	0.443671e-13
c			0.490210e-04	0.116413e-12	-0.242056e-05	0.116413e-12
alpha				0.813240e-21	-0.169096e-13	0.813240e-21
beta					0.351599e-06	-0.169096e-13
gamma						0.813240e-21

Ce allanite, 137

observed and calculated interplanar spacings, d, based on input parameters to cycle 1

h	k	l	corrected theta(obs)	corrected d(obs)	d(calc)	residuals of d (obs-calc)	residuals of d (obs-calc)/sigma	residuals of q (obs-calc)	residuals of q (obs-calc)/sigma
-2	1	1	12.652	3.51970	3.51928	0.00042	0.00003	-0.00002	-0.00003
2	0	1	13.789	3.23431	3.23408	0.00022	0.00002	-0.00001	-0.00002
-1	1	3	15.383	2.90606	2.90308	0.00298	0.00028	-0.00024	-0.00028
0	1	3	16.582	2.70129	2.69964	0.00166	0.00018	-0.00017	-0.00018
-3	1	1	17.129	2.61742	2.61793	-0.00051	-0.00006	0.00006	0.00006
2	0	2	17.603	2.54909	2.54970	-0.00061	-0.00008	0.00007	0.00008
-3	1	3	18.702	2.40426	2.40228	0.00197	0.00028	-0.00028	-0.00028
-2	2	2	19.357	2.32586	2.32740	-0.00154	-0.00023	0.00024	0.00023
-2	1	4	19.701	2.28677	2.28638	0.00039	0.00006	-0.00007	-0.00006
-4	0	1	20.764	2.17453	2.17496	-0.00042	-0.00007	0.00008	0.00007
-2	2	3	21.274	2.12478	2.12496	-0.00017	-0.00003	0.00004	0.00003
0	2	3	21.609	2.09334	2.09429	-0.00095	-0.00018	0.00021	0.00018
2	0	3	21.999	2.05802	2.05932	-0.00130	-0.00026	0.00030	0.00025
-3	1	5	24.795	1.83826	1.83891	-0.00065	-0.00016	0.00021	0.00016
-4	2	4	28.183	1.63229	1.63233	-0.00004	-0.00001	0.00002	0.00001
4	1	2	29.705	1.55572	1.55663	-0.00090	-0.00033	0.00048	0.00033
4	2	2	33.136	1.41029	1.40932	0.00097	0.00045	-0.00070	-0.00045

direct lattice constants after least-squares cycle 1

parameter	old	change	new	error
a (ang.)	8.90440	0.00004	8.90444	0.00309
b (ang.)	5.74850	0.00006	5.74856	0.00375
c (ang.)	10.10050	0.00012	10.10062	0.00526
alpha (deg.)	90.00000		90.00000	
beta (deg.)	114.73999	0.00719	114.74718	0.02557
gamma (deg.)	90.00000		90.00000	
unit cell volume (cubic ang.)	469.5602	-0.0147	469.5454	0.4674

direct lattice constant variance-covariance matrix

	a(ang.)	b(ang.)	c(ang.)	alpha(rad.)	beta(rad.)	gamma(rad.)
a	0.957148e-05	-0.112143e-05	0.137785e-05	0.289841e-13	-0.602267e-06	0.289841e-13
b		0.140933e-04	-0.371024e-05	0.252994e-13	-0.525703e-06	0.252994e-13
c			0.276292e-04	0.659551e-13	-0.137050e-05	0.659551e-13
alpha				0.461162e-21	-0.958260e-14	0.461162e-21
beta					0.199119e-06	-0.958260e-14
gamma						0.461162e-21

Nd allanite, 81 + 140

observed and calculated interplanar spacings, d, based on input parameters to cycle 1

h	k	l	corrected theta(obs)	corrected d(obs)	d(calc)	residuals of d (obs-calc)	residuals of d (obs-calc)/sigma	residuals of q (obs-calc)	residuals of q (obs-calc)/sigma
-2	1	1	12.696	3.50770	3.50885	-0.00115	-0.00007	0.00005	0.00007
2	0	1	13.867	3.21647	3.21271	0.00376	0.00029	-0.00023	-0.00029
-1	1	3	15.433	2.89696	2.89281	0.00416	0.00040	-0.00034	-0.00040
0	1	3	16.668	2.68767	2.68567	0.00201	0.00022	-0.00021	-0.00022
-3	1	1	17.194	2.60797	2.60871	-0.00074	-0.00009	0.00008	0.00009
2	0	2	17.711	2.53410	2.53178	0.00232	0.00029	-0.00029	-0.00029
-3	1	3	18.746	2.39881	2.39792	0.00090	0.00013	-0.00013	-0.00013
-2	1	4	19.719	2.28482	2.28021	0.00461	0.00072	-0.00078	-0.00073
-4	0	1	20.854	2.16552	2.16624	-0.00072	-0.00013	0.00014	0.00013
-2	2	3	21.326	2.11980	2.11932	0.00048	0.00009	-0.00010	-0.00009
0	2	3	21.725	2.08270	2.08501	-0.00231	-0.00044	0.00051	0.00044
2	0	3	22.171	2.04281	2.04477	-0.00197	-0.00039	0.00046	0.00039
-3	1	5	24.875	1.83268	1.83481	-0.00212	-0.00054	0.00069	0.00054
-4	2	4	28.267	1.62784	1.62893	-0.00109	-0.00036	0.00050	0.00036
4	1	2	29.859	1.54841	1.54671	0.00170	0.00063	-0.00092	-0.00063
4	2	2	33.339	1.40271	1.40112	0.00159	0.00074	-0.00115	-0.00075

direct lattice constants after least-squares cycle 1

parameter	old	change	new	error
a (ang.)	8.87890	0.00003	8.87893	0.00563
b (ang.)	5.72950	0.00002	5.72952	0.00807
c (ang.)	10.06650	0.00008	10.06658	0.00972
alpha (deg.)	90.00000		90.00000	
beta (deg.)	115.03001	-0.05679	114.97322	0.04646
gamma (deg.)	90.00000		90.00000	
unit cell volume (cubic ang.)	464.0062	0.2220	464.2281	0.8788

direct lattice constant variance-covariance matrix

	a(ang.)	b(ang.)	c(ang.)	alpha(rad.)	beta(rad.)	gamma(rad.)
a	0.316531e-04	-0.554227e-05	0.564577e-05	0.958829e-13	-0.198629e-05	0.958829e-13
b		0.651646e-04	-0.205542e-04	0.901447e-13	-0.186742e-05	0.901447e-13
c			0.945438e-04	0.215637e-12	-0.446708e-05	0.215637e-12
alpha				0.153203e-20	-0.317371e-13	0.153203e-20
beta					0.657458e-06	-0.317371e-13
gamma						0.153203e-20

Sm allanite, 127

observed and calculated interplanar spacings, d, based on input parameters to cycle 1

h	k	l	corrected theta(obs)	corrected d(obs)	d(calc)	residuals of d (obs-calc)	residuals of d (obs-calc)/sigma	residuals of q (obs-calc)	residuals of q (obs-calc)/sigma
-2	1	1	12.715	3.50268	3.49906	0.00362	0.00023	-0.00017	-0.00023
0	1	3	16.711	2.68111	2.67968	0.00143	0.00016	-0.00015	-0.00016
-3	1	3	18.758	2.39727	2.39519	0.00208	0.00029	-0.00030	-0.00029
-2	2	2	19.461	2.31391	2.31423	-0.00032	-0.00005	0.00005	0.00005
-2	1	4	19.782	2.27783	2.27847	-0.00063	-0.00010	0.00011	0.00010
-4	0	1	20.906	2.16047	2.16041	0.00006	0.00001	-0.00001	-0.00001
-2	2	3	21.355	2.11701	2.11430	0.00271	0.00050	-0.00057	-0.00050
0	2	3	21.781	2.07760	2.07865	-0.00104	-0.00020	0.00023	0.00020
-4	2	4	28.323	1.62486	1.62615	-0.00129	-0.00043	0.00060	0.00043
4	1	2	30.009	1.54141	1.54111	0.00030	0.00011	-0.00016	-0.00011
4	2	2	33.532	1.39557	1.39587	-0.00030	-0.00014	0.00022	0.00014

direct lattice constants after least-squares cycle 1

parameter	old	change	new	error
a (ang.)	8.86160	0.00006	8.86166	0.00498
b (ang.)	5.70490	0.00003	5.70493	0.00578
c (ang.)	10.06310	0.00015	10.06324	0.01036
alpha (deg.)	90.00000		90.00000	
beta (deg.)	115.19001	0.00124	115.19125	0.04221
gamma (deg.)	90.00000		90.00000	
unit cell volume (cubic ang.)	460.3552	0.0078	460.3630	0.7258

direct lattice constant variance-covariance matrix

	a(ang.)	b(ang.)	c(ang.)	alpha(rad.)	beta(rad.)	gamma(rad.)
a	0.247611e-04	-0.220256e-05	0.815804e-05	0.962381e-13	-0.199232e-05	0.962381e-13
b		0.333677e-04	-0.249181e-04	0.525722e-13	-0.108835e-05	0.525722e-13
c			0.107431e-03	0.178482e-12	-0.369493e-05	0.178482e-12
alpha				0.126622e-20	-0.262133e-13	0.126622e-20
beta					0.542669e-06	-0.262133e-13
gamma						0.126622e-20

Eu allanite, 135 + 136

observed and calculated interplanar spacings, d, based on input parameters to cycle 1

h	k	l	corrected theta(obs)	corrected d(obs)	d(calc)	residuals of d (obs-calc)	residuals of d (obs-calc)/sigma	residuals of q (obs-calc)	residuals of q (obs-calc)/sigma
-2	1	1	12.701	3.50634	3.50152	0.00481	0.00031	-0.00022	-0.00031
2	0	1	13.974	3.19233	3.19673	-0.00440	-0.00034	0.00027	0.00034
-3	1	1	17.232	2.60232	2.60080	0.00152	0.00018	-0.00017	-0.00018
2	0	2	17.829	2.51787	2.51664	0.00123	0.00016	-0.00015	-0.00016
-2	2	2	19.420	2.31855	2.31993	-0.00138	-0.00021	0.00022	0.00021
-4	0	1	20.913	2.15973	2.15651	0.00322	0.00057	-0.00064	-0.00057
-2	2	3	21.343	2.11819	2.11383	0.00436	0.00080	-0.00092	-0.00081
0	2	3	21.764	2.07919	2.07933	-0.00014	-0.00003	0.00003	0.00003
2	0	3	22.258	2.03527	2.03097	0.00430	0.00087	-0.00102	-0.00087
-3	1	5	25.105	1.81700	1.81877	-0.00177	-0.00046	0.00059	0.00045
-4	2	4	28.392	1.62129	1.62177	-0.00048	-0.00016	0.00022	0.00016
4	1	2	30.071	1.53851	1.53997	-0.00146	-0.00055	0.00080	0.00055
4	2	2	33.526	1.39579	1.39696	-0.00118	-0.00056	0.00086	0.00056

direct lattice constants after least-squares cycle 1

parameter	old	change	new	error
a (ang.)	8.83190	0.00007	8.83197	0.00779
b (ang.)	5.74960	0.00007	5.74967	0.00948
c (ang.)	9.95930	0.00003	9.95933	0.01478
alpha (deg.)	90.00000		90.00000	
beta (deg.)	114.89999	0.00887	114.90887	0.06889
gamma (deg.)	90.00000		90.00000	
unit cell volume (cubic ang.)	458.7212	-0.0220	458.6992	1.1894

direct lattice constant variance-covariance matrix

	a(ang.)	b(ang.)	c(ang.)	alpha(rad.)	beta(rad.)	gamma(rad.)
a	0.606193e-04	-0.264789e-05	-0.732290e-05	0.194799e-12	-0.404262e-05	0.194799e-12
b		0.898212e-04	-0.258073e-04	0.200358e-12	-0.415800e-05	0.200358e-12
c			0.218468e-03	0.408170e-12	-0.847067e-05	0.408170e-12
alpha				0.335695e-20	-0.696661e-13	0.335695e-20
beta					0.144577e-05	-0.696661e-13
gamma						0.335695e-20

Gd allanite, 161

observed and calculated interplanar spacings, d, based on input parameters to cycle 1

h	k	l	corrected theta(obs)	corrected d(obs)	d(calc)	residuals of d (obs-calc)	residuals of d (obs-calc)/sigma	residuals of q (obs-calc)	residuals of q (obs-calc)/sigma
-2	1	1	12.710	3.50390	3.49536	0.00854	0.00055	-0.00040	-0.00055
2	0	1	13.972	3.19277	3.20189	-0.00912	-0.00071	0.00056	0.00071
0	1	3	16.731	2.67784	2.67891	-0.00107	-0.00012	0.00011	0.00012
-3	1	1	17.244	2.60049	2.59893	0.00156	0.00019	-0.00018	-0.00019
2	0	2	17.835	2.51705	2.52409	-0.00704	-0.00090	0.00088	0.00090
-2	2	2	19.477	2.31209	2.31190	0.00018	0.00003	-0.00003	-0.00003
-4	0	1	20.924	2.15864	2.15856	0.00008	0.00001	-0.00002	-0.00001
-2	2	3	21.367	2.11592	2.11197	0.00395	0.00073	-0.00084	-0.00073
0	2	3	21.802	2.07570	2.07785	-0.00215	-0.00041	0.00048	0.00041
2	0	3	22.273	2.03397	2.03908	-0.00511	-0.00103	0.00121	0.00102
-4	2	4	28.359	1.62302	1.62376	-0.00073	-0.00024	0.00034	0.00024
4	1	2	30.118	1.53635	1.54134	-0.00499	-0.00188	0.00274	0.00188
4	2	2	33.610	1.39271	1.39591	-0.00321	-0.00153	0.00236	0.00152

direct lattice constants after least-squares cycle 1

parameter	old	change	new	error
a (ang.)	8.84970	0.00020	8.84990	0.00694
b (ang.)	5.70190	0.00014	5.70204	0.00855
c (ang.)	10.05100	0.00022	10.05122	0.01150
alpha (deg.)	90.00000		90.00000	
beta (deg.)	115.07000	0.22126	115.29126	0.07171
gamma (deg.)	90.00000		90.00000	
unit cell volume (cubic ang.)	459.3938	-0.8015	458.5923	1.0345

direct lattice constant variance-covariance matrix

	a(ang.)	b(ang.)	c(ang.)	alpha(rad.)	beta(rad.)	gamma(rad.)
a	0.481573e-04	0.176331e-04	-0.195678e-04	0.275596e-12	-0.572494e-05	0.275596e-12
b		0.731110e-04	-0.400416e-04	0.321233e-12	-0.667295e-05	0.321233e-12
c			0.132253e-03	-0.649711e-14	0.134964e-06	-0.649711e-14
alpha				0.363036e-20	-0.754132e-13	0.363036e-20
beta					0.156655e-05	-0.754132e-13
gamma						0.363036e-20

Dy allanite, 166

observed and calculated interplanar spacings, d, based on input parameters to cycle 1

h	k	l	corrected theta(obs)	corrected d(obs)	d(calc)	residuals of d (obs-calc)	residuals of d (obs-calc)/sigma	residuals of q (obs-calc)	residuals of q (obs-calc)/sigma
-2	1	1	12.715	3.50268	3.49816	0.00452	0.00029	-0.00021	-0.00029
2	0	1	13.950	3.19782	3.19898	-0.00116	-0.00009	0.00007	0.00009
0	1	3	16.708	2.68142	2.68036	0.00106	0.00012	-0.00011	-0.00012
-3	1	1	17.239	2.60129	2.60041	0.00088	0.00011	-0.00010	-0.00011
2	0	2	17.803	2.52143	2.52181	-0.00038	-0.00005	0.00005	0.00005
-3	1	3	18.755	2.39770	2.39666	0.00104	0.00015	-0.00015	-0.00015
-2	2	2	19.457	2.31437	2.31378	0.00059	0.00009	-0.00010	-0.00009
-4	0	1	20.911	2.15998	2.15960	0.00038	0.00007	-0.00008	-0.00007
-2	2	3	21.357	2.11682	2.11460	0.00222	0.00041	-0.00047	-0.00041
0	2	3	21.780	2.07769	2.07832	-0.00063	-0.00012	0.00014	0.00012
2	0	3	22.230	2.03770	2.03758	0.00012	0.00002	-0.00003	-0.00002
-4	2	4	28.314	1.62536	1.62674	-0.00138	-0.00046	0.00064	0.00046
4	1	2	30.025	1.54064	1.54002	0.00062	0.00023	-0.00034	-0.00023
4	2	2	33.572	1.39410	1.39487	-0.00077	-0.00037	0.00057	0.00037

direct lattice constants after least-squares cycle 1

parameter	old	change	new	error
a (ang.)	8.86180	0.00011	8.86191	0.00425
b (ang.)	5.70050	0.00011	5.70061	0.00508
c (ang.)	10.07520	0.00019	10.07539	0.00734
alpha (deg.)	90.00000		90.00000	
beta (deg.)	115.27000	0.00497	115.27498	0.03812
gamma (deg.)	90.00000		90.00000	
unit cell volume (cubic ang.)	460.2608	0.0044	460.2652	0.5970

direct lattice constant variance-covariance matrix

	a(ang.)	b(ang.)	c(ang.)	alpha(rad.)	beta(rad.)	gamma(rad.)
a	0.180262e-04	0.455396e-05	-0.702445e-05	0.847798e-13	-0.175403e-05	0.847798e-13
b		0.257840e-04	-0.147100e-04	0.886261e-13	-0.183361e-05	0.886261e-13
c			0.538351e-04	0.148944e-13	-0.308154e-06	0.148944e-13
alpha				0.103395e-20	-0.213917e-13	0.103395e-20
beta					0.442578e-06	-0.213917e-13
gamma						0.103395e-20

Er allanite 144

observed and calculated interplanar spacings, d, based on input parameters to cycle 1

h	k	l	corrected theta(obs)	corrected d(obs)	d(calc)	residuals of d (obs-calc)	residuals of d (obs-calc)/sigma	residuals of q (obs-calc)	residuals of q (obs-calc)/sigma
-2	1	1	12.745	3.49430	3.49274	0.00156	0.00010	-0.00007	-0.00010
-1	1	3	15.476	2.88911	2.88780	0.00131	0.00013	-0.00011	-0.00013
-3	1	1	17.289	2.59393	2.59416	-0.00023	-0.00003	0.00003	0.00003
-3	1	3	18.736	2.40005	2.40141	-0.00136	-0.00019	0.00020	0.00019
-2	2	2	19.482	2.31146	2.31061	0.00085	0.00013	-0.00014	-0.00013
-4	0	1	20.983	2.15285	2.15319	-0.00034	-0.00006	0.00007	0.00006
-2	2	3	21.375	2.11512	2.11321	0.00191	0.00035	-0.00040	-0.00035
0	2	3	21.895	2.06736	2.06994	-0.00258	-0.00050	0.00058	0.00050
2	0	3	22.414	2.02187	2.02135	0.00052	0.00011	-0.00012	-0.00011

direct lattice constants after least-squares cycle 1

parameter	old	change	new	error
a (ang.)	8.85890	0.00017	8.85907	0.00945
b (ang.)	5.67930	0.00006	5.67936	0.00648
c (ang.)	10.08130	0.00020	10.08150	0.00994
alpha (deg.)	90.00000		90.00000	
beta (deg.)	115.87001	0.01038	115.88039	0.07234
gamma (deg.)	90.00000		90.00000	
unit cell volume (cubic ang.)	456.3840	-0.0178	456.3662	1.2182

direct lattice constant variance-covariance matrix

	a(ang.)	b(ang.)	c(ang.)	alpha(rad.)	beta(rad.)	gamma(rad.)
a	0.893158e-04	0.242601e-04	0.243811e-04	0.489437e-12	-0.100761e-04	0.489437e-12
b		0.419338e-04	-0.143763e-04	0.225034e-12	-0.463279e-05	0.225034e-12
c			0.987544e-04	0.220608e-12	-0.454167e-05	0.220608e-12
alpha				0.376072e-20	-0.774221e-13	0.376072e-20
beta					0.159389e-05	-0.774221e-13
gamma						0.376072e-20

Y allanite 123

observed and calculated interplanar spacings, d, based on input parameters to cycle 1

h	k	l	corrected theta(obs)	corrected d(obs)	d(calc)	residuals of d (obs-calc)	residuals of d (obs-calc)/sigma	residuals of q (obs-calc)	residuals of q (obs-calc)/sigma
-1	1	3	15.514	2.88221	2.87900	0.00321	0.00031	-0.00027	-0.00031
-3	1	3	18.762	2.39678	2.39749	-0.00071	-0.00010	0.00010	0.00010
-2	2	2	19.493	2.31032	2.30946	0.00086	0.00013	-0.00014	-0.00013
-2	1	4	19.824	2.27320	2.27394	-0.00074	-0.00012	0.00013	0.00012
0	2	3	21.883	2.06839	2.06948	-0.00109	-0.00021	0.00025	0.00021
2	0	3	22.307	2.03103	2.03089	0.00014	0.00003	-0.00003	-0.00003
-4	2	4	28.296	1.62631	1.62619	0.00012	0.00004	-0.00006	-0.00004

direct lattice constants after least-squares cycle 1

parameter	old	change	new	error
a (ang.)	8.88850	0.00005	8.88855	0.01115
b (ang.)	5.68100	0.00005	5.68105	0.00524
c (ang.)	10.03610	0.00002	10.03612	0.00783
alpha (deg.)	90.00000		90.00000	
beta (deg.)	115.43001	0.00083	115.43084	0.04508
gamma (deg.)	90.00000		90.00000	
unit cell volume (cubic ang.)	457.6770	0.0043	457.6812	0.9468

direct lattice constant variance-covariance matrix

	a(ang.)	b(ang.)	c(ang.)	alpha(rad.)	beta(rad.)	gamma(rad.)
a	0.124400e-03	0.309863e-05	0.190661e-05	0.267580e-12	-0.552845e-05	0.267580e-12
b		0.274963e-04	-0.586587e-05	0.778137e-13	-0.160770e-05	0.778137e-13
c			0.613454e-04	0.145054e-12	-0.299695e-05	0.145054e-12
alpha				0.145031e-20	-0.299648e-13	0.145031e-20
beta					0.619100e-06	-0.299648e-13
gamma						0.145031e-20

PARAMETER SHIFTS, LEAST-SQUARES CYCLE 5

PARAMETER	OLD	CHANGE	NEW	ERROR
A *	0.123670	-0.000014	0.123656	0.000052
B *	0.174146	-0.000018	0.174128	0.000098
C *	0.108837	-0.000014	0.108823	0.000050
ALPHA *	90.00008		90.00008	
BETA *	65.19490	0.00063	65.19551	0.02654
GAMMA *	90.00008		90.00008	
CR TERM 1 (TYPE 1)	0.000227	0.000078	0.000305	0.000168
CR TERM 2 (TYPE 4)	0.000000		0.000000	

0ESTIMATED STANDARD ERROR OF UNIT WEIGHT OBSERVATION OF Q, BASED ON REFINEMENT OF 5 PARAMETERS
SQRT(SUM(W*(OBS-CALC)**2)/M-N) = 0.00050
1SYNTHETIC CE ALLANITE------- RUN 153

DIRECT LATTICE CONSTANTS AFTER LEAST-SQUARES CYCLE 5

PARAMETER	OLD	CHANGE	NEW	ERROR
A (ANG.)	8.90788	0.00099	8.90887	0.00473
B (ANG.)	5.74230	0.00061	5.74291	0.00322
C (ANG.)	10.12190	0.00126	10.12316	0.00541
ALPHA (DEG.)	89.99997		89.99997	
BETA (DEG.)	114.80508	-0.00061	114.80447	0.02654
GAMMA (DEG.)	89.99997		89.99997	
0 UNIT CELL VOLUME (CUBIC ANG.)	469.9846	0.1628	470.1475	0.6159

0

DIRECT LATTICE CONSTANT VARIANCE-COVARIANCE MATRIX

	A(ANG.)	B(ANG.)	C(ANG.)	ALPHA(RAD.)	BETA(RAD.)	GAMMA(RAD.)
A	0.223910E-04	0.197256E-05	0.148782E-04	-0.512217E-12	-0.147958E-05	-0.512217E-12
B		0.103892E-04	0.248677E-05	-0.496231E-13	-0.143340E-06	-0.496231E-13
C			0.292271E-04	-0.450638E-12	-0.130170E-05	-0.450638E-12
ALPHA				0.257062E-19	0.742542E-13	0.257062E-19
BETA					0.214489E-06	0.742542E-13
GAMMA						0.257062E-19

0

DIRECT LATTICE CONSTANT CORRELATION MATRIX

	A	B	C	ALPHA	BETA	GAMMA
A	1.000000	0.129331	0.581594	-0.675148	-0.675147	-0.675148
B		1.000000	0.142709	-0.096023	-0.096023	-0.096023
C			1.000000	-0.519894	-0.519894	-0.519894
ALPHA				1.000000	1.000000	1.000000
BETA					1.000000	1.000000
GAMMA						1.000000

1SYNTHETIC CE ALLANITE------- RUN 153

OBSERVED AND CALCULATED INTERPLANAR SPACINGS, D, BASED ON REFINED PARAMETERS AFTER CYCLE 5

0

H	K	L	CORRECTED THETA(OBS)	CORRECTED D(OBS)	D(CALC)	RESIDUALS OF D (OBS-CALC)	RESIDUALS OF D (OBS-CALC)/SIGMA	RESIDUALS OF Q (OBS-CALC)	RESIDUALS OF Q (OBS-CALC)/SIGMA	
0	0	1	4.797	9.21923	9.18924	0.02999	0.00027	-0.00008	-0.00027	*
1	0	0	5.461	8.10020	8.08698	0.01322	0.00016	-0.00005	-0.00016	*
-1	0	1	5.512	8.02569	7.94491	0.08079	0.00098	-0.00032	-0.00098	*
1	0	1	8.692	5.10122	5.10152	-0.00031	-0.00001	0.00000	0.00001	
-1	0	2	8.872	4.99823	4.99507	0.00316	0.00010	-0.00005	-0.00010	
0	1	1	9.093	4.87797	4.87006	0.00791	0.00026	-0.00014	-0.00026	*
1	1	0	9.466	4.68717	4.68236	0.00481	0.00017	-0.00009	-0.00017	
0	0	2	9.608	4.61879	4.59462	0.02417	0.00089	-0.00049	-0.00089	*
1	1	1	11.669	3.81160	3.81401	-0.00241	-0.00013	0.00009	0.00013	
-1	1	2	11.800	3.76968	3.76891	0.00078	0.00004	-0.00003	-0.00004	
0	1	2	12.408	3.58778	3.58771	0.00007	0.00000	-0.00000	-0.00000	
-2	1	1	12.647	3.52104	3.51920	0.00184	0.00012	-0.00008	-0.00012	
2	1	0	13.481	3.30673	3.30620	0.00053	0.00004	-0.00003	-0.00004	
-2	1	2	13.624	3.27284	3.26703	0.00581	0.00043	-0.00033	-0.00043	*
2	0	1	13.783	3.23563	3.23446	0.00117	0.00009	-0.00007	-0.00009	
1	1	2	15.192	2.94181	2.94166	0.00015	0.00001	-0.00001	-0.00001	
-1	1	3	15.373	2.90799	2.90716	0.00083	0.00008	-0.00007	-0.00008	
0	2	0	15.566	2.87280	2.87145	0.00135	0.00013	-0.00011	-0.00013	
2	1	1	15.864	2.82009	2.81822	0.00187	0.00019	-0.00017	-0.00019	
0	2	1	16.190	2.76481	2.74076	0.02404	0.00253	-0.00231	-0.00256	*
0	1	3	16.571	2.70300	2.70268	0.00032	0.00003	-0.00003	-0.00003	
-3	0	3	16.932	2.64692	2.64830	-0.00139	-0.00016	0.00015	0.00016	
-3	1	1	17.122	2.61841	2.61795	0.00045	0.00005	-0.00005	-0.00005	
2	0	2	17.599	2.54965	2.55076	-0.00111	-0.00014	0.00013	0.00014	
-2	0	4	17.980	2.49734	2.49753	-0.00019	-0.00002	0.00002	0.00002	
3	1	0	18.409	2.44107	2.44021	0.00086	0.00012	-0.00012	-0.00012	
-3	1	3	18.691	2.40553	2.40491	0.00062	0.00009	-0.00009	-0.00009	
-2	2	2	19.345	2.32722	2.32714	0.00007	0.00001	-0.00001	-0.00001	
-1	1	4	19.530	2.30600	2.29460	0.01141	0.00176	-0.00187	-0.00177	*
-2	1	4	19.699	2.28700	2.29032	-0.00332	-0.00052	0.00055	0.00052	
-4	0	2	20.235	2.22890	2.22665	0.00225	0.00037	-0.00041	-0.00037	
1	2	2	20.525	2.19874	2.20047	-0.00173	-0.00030	0.00033	0.00029	
-1	2	3	20.614	2.18960	2.18592	0.00368	0.00063	-0.00070	-0.00063	
-4	0	1	20.758	2.17507	2.17530	-0.00022	-0.00004	0.00004	0.00004	
2	2	1	21.050	2.14629	2.14735	-0.00106	-0.00019	0.00021	0.00019	
0	1	4	21.203	2.13145	2.13298	-0.00153	-0.00028	0.00032	0.00028	
-2	2	3	21.261	2.12591	2.12582	0.00009	0.00002	-0.00002	-0.00002	
0	2	3	21.600	2.09414	2.09490	-0.00076	-0.00014	0.00016	0.00014	
2	0	3	21.987	2.05905	2.06070	-0.00165	-0.00032	0.00038	0.00032	
-3	2	2	22.085	2.05035	2.04755	0.00280	0.00056	-0.00065	-0.00056	
-2	0	5	22.411	2.02208	2.02313	-0.00104	-0.00021	0.00025	0.00021	
-4	0	4	22.848	1.98539	1.98623	-0.00083	-0.00018	0.00021	0.00018	
-3	2	3	23.360	1.94419	1.94675	-0.00255	-0.00057	0.00069	0.00057	
2	2	2	23.864	1.90550	1.90701	-0.00150	-0.00035	0.00043	0.00035	
1	2	3	23.945	1.89939	1.89994	-0.00055	-0.00013	0.00016	0.00013	
-2	2	4	24.161	1.88342	1.88445	-0.00103	-0.00025	0.00031	0.00025	
1	3	0	24.425	1.86431	1.86282	0.00149	0.00036	-0.00046	-0.00036	
-3	1	5	24.725	1.84306	1.84228	0.00078	0.00019	-0.00025	-0.00019	
0	2	4	25.485	1.79165	1.79385	-0.00221	-0.00059	0.00077	0.00059	
-4	0	5	25.596	1.78443	1.78203	0.00240	0.00064	-0.00085	-0.00065	

1SYNTHETIC CE ALLANITE------- RUN 153

OBSERVED AND CALCULATED INTERPLANAR SPACINGS, D, BASED ON REFINED PARAMETERS AFTER CYCLE 5

H	K	L	CORRECTED THETA(OBS)	CORRECTED D(OBS)	D(CALC)	RESIDUALS OF D (OBS-CALC)	RESIDUALS OF D (OBS-CALC)/SIGMA	RESIDUALS OF Q (OBS-CALC)	RESIDUALS OF Q (OBS-CALC)/SIGMA
-5	0	2	25.696	1.77792	1.77687	0.00105	0.00028	-0.00037	-0.00028
-4	2	2	26.011	1.75784	1.75960	-0.00176	-0.00049	0.00065	0.00049
4	1	1	26.397	1.73397	1.73559	-0.00162	-0.00046	0.00062	0.00046
-1	3	3	27.543	1.66711	1.66462	0.00248	0.00078	-0.00107	-0.00078
4	2	0	27.801	1.65285	1.65310	-0.00025	-0.00008	0.00011	0.00008
-4	2	4	28.101	1.63664	1.63351	0.00313	0.00102	-0.00143	-0.00102
-3	2	5	28.676	1.60655	1.61039	-0.00385	-0.00131	0.00185	0.00130
1	1	5	29.093	1.58546	1.58486	0.00060	0.00021	-0.00030	-0.00021
4	1	2	29.655	1.55806	1.55668	0.00138	0.00050	-0.00073	-0.00050
-5	2	4	31.803	1.46281	1.46299	-0.00018	-0.00008	0.00011	0.00008
-6	0	4	31.850	1.46086	1.46025	0.00061	0.00026	-0.00039	-0.00026
-2	2	6	32.069	1.45196	1.45358	-0.00163	-0.00070	0.00106	0.00070
-6	1	3	32.461	1.43632	1.43720	-0.00088	-0.00039	0.00059	0.00039
1	2	5	32.606	1.43061	1.42990	0.00071	0.00032	-0.00048	-0.00032
2	1	5	33.077	1.41252	1.41358	-0.00105	-0.00049	0.00075	0.00049
4	2	2	33.153	1.40963	1.40911	0.00052	0.00024	-0.00037	-0.00024
1	1	6	34.415	1.36398	1.36123	0.00275	0.00138	-0.00218	-0.00139
-6	2	2	36.101	1.30837	1.30898	-0.00060	-0.00034	0.00054	0.00034
-4	3	5	36.265	1.30326	1.30434	-0.00108	-0.00061	0.00097	0.00061
-5	3	1	37.103	1.27792	1.27980	-0.00189	-0.00112	0.00180	0.00111
-5	3	4	37.247	1.27369	1.27121	0.00247	0.00148	-0.00240	-0.00148

1SYNTHETIC CE ALLANITE------- RUN 153

DISCREPANCY FACTORS BASED ON REFINED PARAMETERS AFTER CYCLE 5

NUMBER OF OBSERVATIONS (M) = 63
NUMBER OF VARIED PARAMETERS (N) = 5

FACTORS FOR D
SUM (W*(OBS-CALC)**2) = 0.14334E-04
SQRT(SUM(W*(OBS-CALC)**2)/M-N) = 0.49712E-03

FACTORS FOR Q
SUM (W*(OBS-CALC)**2) = 0.14310E-04
SQRT(SUM(W*(OBS-CALC)**2)/M-N) = 0.49671E-03

APPENDIX C

LANTHANIDE, YTTRIUM, URANIUM AND THORIUM ANALYSES OF NATURAL ALLANITES FROM THE LITERATURE

Appendix C. Lanthanide, Yttrium, Uranium, and Thorium Analyses of Natural Allanite

	1	2	3	4	5	6	7	8	9	10
Atomic %										
La	26.6	28.9	23.1	13.2	18.6	21.9	21.2	24.3	29.8	27.3
Ce	53.3	53.3	54.0	33.3	42.4	47.1	53.5	53.8	52.4	53.9
Pr	4.6	4.1	4.7	4.9	4.5	4.9	4.4	5.0	3.2	4.5
Nd	14.2	12.8	16.9	18.8	18.0	17.8	17.9	14.6	12.2	12.3
Sm	1.3	0.9	1.3	5.9	4.7	3.5	1.5	1.5	1.5	1.4
Eu	-	-	-	-	-	-	-	-	-	-
Gd	-	-	-	11.0	5.2	2.9	1.5	0.8	0.9	0.6
Tb	-	-	-	-	-	-	-	-	-	-
Dy	-	-	-	6.8	3.5	1.5	-	-	-	-
Ho	-	-	-	-	-	-	-	-	-	-
Er	-	-	-	4.3	3.0	0.4	-	-	-	-
Tm	-	-	-	-	-	-	-	-	-	-
Yb	-	-	-	1.8	-	-	-	-	-	-
Lu	-	-	-	-	-	-	-	-	-	-
Y/(Y+Ln)x100	-	-	-	53.9	27.0	6.1	0.3	1.0	2.2	2.4
La+Ce+Pr	84.5	86.3	81.8	51.4	65.6	74.9	79.1	83.1	85.4	85.7
ΣLa-Nd	98.7	99.1	98.7	70.2	83.6	92.7	97.0	97.7	97.6	98.0
ΣSm-Ho	1.3	0.9	1.3	23.7	13.4	7.9	3.0	2.3	2.4	2.0
ΣEr-Lu	-	-	-	6.1	3.0	0.4	-	-	-	-
RE_2O_3	-	-	-	12.25	14.64	21.86	15.07	23.73	18.58	23.71
La/Nd	1.87	2.26	1.37	0.70	1.03	1.23	1.19	1.66	2.44	2.21
ThO_2,wt %	0.60	0.48	1.51	-	-	0.64	4.88	0.80	0.08	0.33
U_3O_8,wt %	-	-	-	-	-	-	-	-	-	-
Method	EMPA	EMPA	EMPA	EMPA	EMPA	EMPA	EMPA	EMPA	EMPA	EMPA

(1-3) Bennett et al. (1984), hornblende-biotite granite. Afu complex, Nigeria, (2, core, 3 rim of same sample); (4-10) Exley (1980), Skye, Scotland, (4,6,10) epigranite, (5) arkose, (7) mica schist, (8) gneiss, (9) allivolite (complete analysis given).

Appendix C. Continued.

	11	12	13	14	15	16	17	18	19	20
Atomic %										
La	27.9	28.7	30.8	33.0	63.6	18.1	31.9	16.8	33.7	18.2
Ce	54.1	53.3	53.3	52.2	8.6	37.1	46.2	58.9	63.1	38.4
Pr	4.4	4.7	4.1	3.7	25.0	7.3	5.1	5.7	-	6.1
Nd	11.7	12.2	10.8	10.0	2.8	33.3	15.0	16.8	0.3	28.1
Sm	1.3	0.9	0.6	0.7	-	3.2	1.4	1.1	0.9	4.7
Eu	-	-	-	-	-	0.1	0.3	0.5	-	-
Gd	0.6	0.2	0.4	0.4	-	0.7	0.1	0.2	1.7	3.1
Tb	-	-	-	-	-	-	-	-	-	-
Dy	-	-	-	-	-	0.2	-	-	0.3	1.4
Ho	-	-	-	-	-	-	-	-	-	-
Er	-	-	-	-	-	-	-	-	-	-
Tm	-	-	-	-	-	-	-	-	-	-
Yb	-	-	-	-	-	-	-	-	-	-
Lu	-	-	-	-	-	-	-	-	-	-
Y/(Y+Ln)x100	3.6	2.1	1.8	0.3	39.1	0.4	0.6	0.6	1.4	10.0
La+Ce+Pr	86.4	86.7	88.2	88.9	97.2	62.5	83.2	81.4	96.8	62.7
ΣLa-Nd	98.1	98.9	99.0	98.9	100.0	95.8	98.2	98.2	97.1	90.8
ΣSm-Ho	1.9	1.1	1.0	1.1	-	4.2	1.8	1.8	2.9	9.2
ΣEr-Lu	-	-	-	-	-	-	-	-	-	-
RE_2O_3	24.23	12.34	26.07	21.95	12.46	-	-	-	-	28.4
La/Nd	2.38	2.34	2.86	3.31	22.6	0.54	2.12	1.00	110.6	0.65
ThO_2,wt %	0.03	0.01	0.04	1.80	0.06	-	-	-	-	-
U_3O_8,wt %	-	-	-	-	-	-	-	-	-	-
Method	EMPA	EMPA	EMPA	EMPA	EMPA	OS	OS	OS	-	XRF

(11-15) Exley (1980), Skye, Scotland, (11) quartz-feldspar porphyry, (12) granophyre, (13) epigranite, (15) arkose, (14) gneiss, Austria;(16-18) Gable (1980), Boulder Creek Batholith, Colorado, (16-17) hornblende diorite, (18) granodiorite, (19) Ivashchenko et al. (1980), metamict, granite, E. Baltic Shield; (2) Adams and Sharp (1972), White Cloud pegmatite, Colorado.

Appendix C. Continued.

	21	22	23	24	25	26	27	28	29	30
Atomic %										
La	31.0	22.8	29.5	34.6	6.8	26.3	16.1	19.4	26.2	28.9
Ce	45.2	37.8	47.1	47.8	75.8	41.5	63.9	55.8	54.0	35.8
Pr	10.2	10.3	1.1	3.7	4.3	8.4	1.6	4.8	6.4	7.1
Nd	10.9	25.0	16.8	10.3	10.0	17.8	12.5	15.2	11.5	20.9
Sm	1.0	1.9	2.3	1.2	0.7	4.7	4.5	1.7	1.6	3.3
Eu	-	-	-	-	-	1.3	-	-	-	0.3
Gd			2.3	1.7	1.9			1.1	0.3	1.9
Tb	1.4	1.7	-	-	-	-	1.4	-	-	-
Dy	-	-	0.2	0.2	-	-	-	1.5	-	1.2
Ho	0.1	0.2	0.1	-	-	-	-	-	-	
Er	-	0.1	-	-	-	-	-	0.5	-	0.3
Tm	-	-	0.2	0.2	0.2	-	-	-	-	-
Yb	0.1	0.1	0.1	0.2	0.3	-	-	-	-	0.3
Lu	0.1	0.1	-	-	-	-	-	-	-	-
Y/(Y+Ln)x100	0.3	0.2	1.0	1.2	0.5	-	20.1	1.1	-	36.0
La+Ce+Pr	86.4	70.9	78.0	86.1	86.9	76.2	81.6	80.0	86.6	71.8
ΣLa-Nd	97.3	95.9	94.8	96.4	96.9	94.0	94.1	95.2	98.1	92.7
ΣSm-Ho	2.5	3.8	4.9	3.1	2.6	6.0	5.9	4.3	1.9	6.7
ΣEr-Lu	0.2	0.3	0.3	0.5	0.5	-	-	0.5	-	0.6
RE_2O_3	21.6	18.8	20.92	11.77*	15.18*	22.47	7.3*	16.92*	29.7	38.3
La/Nd	2.95	0.81	1.78	3.37	0.68	1.48	1.29	1.27	2.28	1.38
ThO_2,wt %	-	-	-	-	-	-	-	-	-	-
U_3O_8,wt %	-	-	-	-	-	-	-	-	-	-
Method	XRF	XRF	XRF	XFR	XRF	MS	XRF	XRF	XRF	XRF

(21-23). Aleksiev and Ivanov (1970), Srodna Gora Mts, Bulgaria; (21)amphibole-biotite granite; (22) biotite granite; (25) microcline-albite pegmatite; (24-25) Aleksiev, Khisina, and Pavlora (1969), Plana Pluton, Bulgaria; granodiorite (26) Bocquet (1975). allanite-albite-hematite vein in schist, E. Alps, Savoy, France. (27-30) Azimov and Khemrabaev (1965), Aktau intrusive, W. Uzbekistan. (27) granite, (28) granite-aplite, (29-30) pegmatite.

* % REE.

Appendix C. Continued.

	31	32	33	34	35	36	37	38	39	40
Atomic %										
La	23.9	32.5	33.4	14.6	21.4	31.6	27.8	22.3	15.0	24.1
Ce	46.9	43.2	43.9	40.4	49.7	50.9	54.0	53.7	41.5	48.9
Pr	5.1	5.8	5.7	4.2	5.1	3.9	2.9	3.9	4.4	3.8
Nd	17.1	15.6	13.6	23.1	16.4	10.1	8.9	13.5	24.0	15.4
Sm	3.1	1.3	1.9	5.5	1.8	0.7	0.5	0.7	5.7	3.0
Eu	0.3	**a**	**a**	**a**	**a**	**a**	**a**	**a**	0.5	-
Gd	1.8	1.0**a**	1.3**a**	3.8**a**	1.4**a**	0.8**a**	0.9**a**	1.7**a**	3.5	1.9
Tb	0.3	-	-	3.6	0.3	-	-	-	0.6	0.4
Dy	0.9	0.6	0.2	2.1	2.0	-	1.7	1.3	2.2	0.9
Ho	0.1	-	-	0.6	-	-	-	-	0.6	-
Er	0.3	-	-	0.9	1.1	2.0	1.3	1.3	0.9	0.6
Tm	-	-	-	0.2	0.3	-	-	-	0.2	0.4
Yb	0.2	-	-	0.2	0.5	-	2.0	1.6	0.9	0.3
Lu	-	-	-	0.8	-	-	-	-	-	0.3
Y/(Y+Ln)x100	3.5	1.5	1.9	5.9	2.7	-	-	-	10.4	-
La+Ce+Pr	75.9	81.5	83.0	59.2	76.2	86.4	84.7	79.9	60.9	76.8
ΣLa-Nd	93.0	97.1	96.6	82.3	92.6	96.5	93.6	93.4	84.9	92.2
ΣSm-Ho	6.5	2.9	3.4	15.6	5.5	1.5	3.1	3.7	13.1	6.8
ΣEr-Lu	0.5	-	-	2.1	1.9	2.0	3.3	2.9	2.0	1.0
RE_2O_3	17.44	18.26	20.81	22.44	23.62	16.7	18.0	18.5	24.49	-
La/Nd	1.39	2.07	2.46	0.63	1.31	3.15	3.12	1.66	0.63	1.56
ThO_2,wt %	-	-	-	-	-	-	-	-	-	-
U_3O_8,wt %	-	-	-	-	-	-	-	-	-	-
Method	XRF	CH	CH	CH	CH	CH	CH	CH	CH	CH

(31) Batieva (1976), alkali granite, Kola Peninsula, USSR, (32-38) Belkov (1979), Kola Peninsula; (32) granodiorite, (33) tonalite; (39-36) alkalic granite; (37-38) porphyritic granite-granodiorite; (39-40) Belolipetskii and Elina (1967), alkalic granites.

a Eu+Gd calculated as Gd.

Appendix C. Continued.

	41	42	43	44	45	46	47	48	49	50
Atomic %										
La	26.6	28.9	23.1	17.2	20.3	18.9	20.4	20.1	20.3	31.4
Ce	53.3	53.3	54.0	47.6	50.0	47.3	49.1	47.7	48.6	43.0
Pr	4.6	4.1	4.7	3.1	3.4	3.1	3.5	3.8	3.4	4.5
Nd	14.2	12.8	16.9	22.1	15.5	20.9	17.2	18.6	18.4	13.0
Sm	1.3	0.9	1.3	2.6	2.6	3.0	3.8	3.5	3.1	3.5
Eu	-	-	-	-	-	-	-	-	-	-
Gd	-	-	-	7.4	9.2	6.8	6.0	6.3	6.2	2.1
Tb	-	-	-	-	-	-	-	-	-	-
Dy	-	-	-	-	-	-	-	-	-	-
Ho	-	-	-	-	-	-	-	-	-	-
Er	-	-	-	-	-	-	-	-	-	2.2
Tm	-	-	-	-	-	-	-	-	-	0.2
Yb	-	-	-	-	-	-	-	-	-	0.1
Lu	-	-	-	-	-	-	-	-	-	-
Y/(Y+Ln)x100	-	-	-	4.8	3.4	4.0	3.3	2.1	2.4	6.1
La+Ce+Pr	84.5	86.3	81.8	67.9	73.7	69.3	73.0	71.6	72.3	78.9
ΣLa-Nd	98.7	99.1	98.7	90.0	89.2	90.2	90.2	90.2	90.7	91.9
ΣSm-Ho	1.3	0.9	1.3	10.0	11.8	9.8	9.8	9.8	9.3	5.6
ΣEr-Lu	-	-	-	-	-	-	-	-	-	2.5
RE_2O_3	20.00	26.28	28.18	16.79	16.80	19.33	22.39	26.09	25.23	14.19
La/Nd	1.87	2.26	1.37	0.78	1.31	0.91	1.18	1.08	1.10	2.41
ThO_2,wt %	0.60	0.48	1.51	0.51	0.11	0.33	-	-	-	0.09
U_3O_8,wt %	-	-	-	-	-	-	-	-	-	-
Method	EMPA	EMPA	EMPA	EMPA	EMPA	EMPA	EMPA	EMPA	EMPA	OS

(41-43) Bennett et al. (1984), hornblende-biotite granite, Afu complex, Nigeria (42-443) some sample, (42) core, (43) rim; (44-49) Campbell and Ethier (1984), footwall, Sullivan ore body, British Columbia; (44-46) metamict, (47-48) fresh, (50) Cech and Povondra (1972), metamict, pegmatite, Domaninek, Czechoslovakia.

Appendix C. Continued.

	51	52	53	54	55	56	57	58	59	60
Atomic %										
La	29.3	20.9	22.2	26.1	26.0	23.6	26.0	23.4	28.0	25.6
Ce	51.8	54.7	57.1	54.6	54.9	58.8	56.5	59.3	55.2	60.2
Pr	4.0	-	-	-	-	-	-	-	-	-
Nd	12.2	15.6	14.9	15.0	14.4	14.2	12.5	13.0	14.1	11.8
Sm	2.3	2.1	1.9	1.4	1.8	1.1	1.4	1.2	1.1	0.8
Eu	0.2	0.1	0.2	0.1	0.2	0.2	0.1	0.2	0.1	0.1
Gd	0.2	5.3	3.4	2.4	2.3	2.0	3.0	1.5	1.4	1.4
Tb	-	0.2	0.1	-	0.1	-	0.1	-	-	-
Dy	-	0.7	0.2	0.2	0.2	0.1	0.2	1.1	0.1	0.1
Ho	-	-	-	-	-	-	-	-	-	-
Er	0.1	-	-	-	-	-	-	-	-	-
Tm	-	-	-	-	-	-	-	-	-	-
Yb	-	0.3	0.1	0.1	0.1	0.1	0.1	0.4	-	-
Lu	-	-	-	-	-	-	-	-	-	-
Y/(Y+Ln)x100	0.3	-	-	-	-	-	-	-	-	-
La+Ce+Pr	85.1	75.6	79.3	80.7	80.9	82.4	82.5	82.7	83.2	85.8
ΣLa-Nd	97.3	91.2	94.2	95.7	95.3	96.6	95.0	95.7	97.3	97.6
ΣSm-Ho	2.6	8.5	5.7	4.2	4.6	3.3	4.9	3.9	2.7	2.4
ΣEr-Lu	0.1	0.3	0.1	0.1	0.1	0.1	0.1	0.4	-	-
RE_2O_3	24.86	14.1*	18.4*	10.9*	14.5*	17.9*	11.6*	21.0*	18.2*	16.6*
La/Nd	2.40	1.34	1.49	1.74	1.81	1.66	2.08	1.79	1.98	2.18
ThO_2,wt %	-	-	-	-	-	-	-	-	-	-
U_3O_8,wt %	-	-	-	-	-	-	-	-	-	-
Method	OS	INAA	INAA	INAA	INAA	INAA	INAA	INAA	INAA	INAA

(51) Cech et al. (1972), gneiss (?), Zambia; (52-60) Cerneva et al (1983), granites, S. Bulgaria; (52, 54, 57, granite, Rila Massif, (53,55,60) granite, Sredna Gora, (56 , 58, 59) granite, Pirin.
* % REE.

Appendix C. Continued.

	61	62	63	64	65	66	67	68	69	70
Atomic %										
La	27.8	28.3	29.5	25.4	24.2	28.8	28.6	25.3	30.9	12.3
Ce	58.1	58.4	58.7	54.1	54.9	50.8	46.5	44.2	53.4	41.6
Pr	-	-	-	4.4	-	-	4.0	5.5	-	7.7
Nd	10.9	10.2	10.0	13.6	18.0	17.6	13.0	21.0	14.2	24.6
Sm	1.6	1.8	0.7	1.8	2.9	2.5	3.1	2.3	1.3	8.4
Eu	-	0.1	0.1	-	-	-	0.5	-	-	-
Gd	1.6	1.2	0.9	0.7	-	-	2.7	1.7	-	5.4
Tb	-	-	-	-	-	0.2	-	-	-	c
Dy	-	-	0.1	-	-	-	0.8	-	0.2	c
Ho	-	-	-	-	-	-	0.2	-	-	-
Er	-	-	-	-	-	-	0.4	-	-	-
Tm	-	-	-	-	-	-	0.1	-	-	-
Yb	-	-	-	-	-	0.1	0.1	-	-	-
Lu	-	-	-	-	-	-	-	-	-	-
Y/(Y+Ln)x100	-	-	-	-	-	-	8.4	-	0.6	16.2c
La+Ce+Pr	85.9	86.7	88.2	83.9	79.1	79.6	79.1	75.0	84.3	61.6
ΣLa-Nd	96.8	96.9	98.2	97.5	97.1	97.2	92.1	96.0	98.5	86.2
ΣSm-Ho	3.2	3.1	1.8	2.5	2.9	2.7	7.3	4.0	1.5	13.8
ΣEr-Lu	-	-	-	-	-	0.1	0.6	-	-	-
RE_2O_3	15.1*	19.9*	20.6*	20.54	-	-	20.78	25.00	-	24.40
La/Nd	2.55	2.78	2.93	1.86	1.35	1.64	2.20	1.20	2.18	0.50
ThO_2,wt %	-	-	-	0.30	-	-	-	-	-	-
U_3O_8,wt %	-	-	-	-	-	-	-	-	-	-
Method	INAA	INAA	INAA	CH	EMPA	INAA	-	-	INAA	CH

(61-63) Cerneva et al. (1983), granites, S. Bulgaria, (61) Rila Massif, (62) Sredna Gora; (63) Pirin Massif; (64) Chistyakova and Kazakova (1968), Quartz-crystal pegmatite, Kazokhstan; (65) Demanage and Elsass (1973), Stratiform Cu deposit, Morocco; (66) Fourcade and Allegre (1981), granite-gneiss. Querigut complex, France; (67) Ganzeeve (1972) rare-earth-beryl metasomatite; (68) Gorasimovskii (1964), Zeolite-calcite vein, N. Baikel; (69) Hildrith (1979), Bishop tuff, Calif., (70) Ivanov et al. (1981), quartz veins, Chukotka, USSR.

c Tb+Dy+Y calculated as Y.

Appendix C. Continued.

	71	72	73	74	75	76	77	78	79	80
Atomic %										
La	17.0	18.0	20.4	25.3	18.8	18.3	18.2	23.2	10.1	36.9
Ce	48.7	48.8	48.9	45.2	49.5	48.3	50.1	46.0	37.0	47.9
Pr	5.8	5.3	5.1	4.4	5.4	5.4	6.0	6.0	6.1	8.2
Nd	16.8	15.6	16.3	23.3	16.4	17.0	19.5	20.5	25.0	6.7
Sm	3.5	3.4	2.7	1.1	3.0	3.1	2.8	2.4	9.9	0.3
Eu	0.3	0.4	0.3	0.3	-	0.5	0.3	0.1	-	-
Gd	1.8	1.9	1.4	0.5	1.7	1.7	1.8	1.3	11.5	-
Tb	0.4	0.3	0.3	-	0.3	0.3	0.2	0.1	-	-
Dy	2.6	2.9	1.2	0.2	1.2	2.2	0.9	0.4	0.4	-
Ho	0.1	0.3	-	-	-	0.2	0.1	-	-	-
Er	1.3	1.8	1.3	-	1.3	1.5	0.2	0.1	-	-
Tm	-	-	-	-	-	-	-	-	-	-
Yb	1.6	1.4	2.1	-	1.9	1.7	0.1	-	-	-
Lu	-	-	-	-	-	-	-	-	-	-
Y/(Y+Ln)x100	-	-	-	-	-	-	-	-	16.8	0.6
La+Ce+Pr	71.5	72.1	74.4	74.9	73.7	72.0	74.3	75.2	53.2	93.0
ΣLa-Nd	88.3	87.7	90.7	98.2	90.1	89.0	93.8	95.7	78.2	99.7
ΣSm-Ho	8.8	9.1	5.9	1.8	6.7	7.8	5.9	4.2	21.8	0.3
ΣEr-Lu	2.9	3.2	3.4	-	3.2	3.2	0.3	0.1	-	-
RE_2O_3	-	-	-	-	-	-	-	-	10.18	19.96
La/Nd	1.01	1.15	1.25	1.09	1.15	1.08	0.93	1.13	0.51	5.53
ThO_2,wt %	-	-	-	-	-	-	-	-	0.72	1.54
U_3O_8,wt %	-	-	-	-	-	-	-	-	-	-
Method	-	-	-	-	-	-	-	-	-	-

(71-78) Fishman et al. (1968), (71-73) meta-granites, Neroisk. Petok Massif, near Polar Urals, (74) metagranite, Man-Khambo, N. Urals, (75) quartz-fluorite vein in metagranite, (76-78) pegmatites, source of Bol'she Patok R., Polar Urals; (79-80) Ivanov et al. (1974), pegmatites; (79) Pre-Paleozoic; (80) Paleozoic.

Appendix C. Continued.

	81	82	83	84	85	86	87	88	89	90
Atomic %										
La	36.4	24.8	33.7	33.2	32.6	29.7	45.2	35.0	27.7	25.7
Ce	41.4	46.5	40.1	46.9	46.2	49.7	42.7	49.5	50.9	53.9
Pr	7.0	6.9	5.8	6.5	5.5	6.1	-	4.3	6.3	4.8
Nd	8.1	8.9	8.5	6.4	9.4	7.8	6.7	4.2	11.6	12.5
Sm	1.7	1.6	1.6	1.6	1.3	1.2	1.5	1.6	1.7	2.0
Eu	-	-	-	-	-	-	-	-	-	-
Gd	4.7	5.5	4.9	4.7	4.4	5.0	3.9	4.7	1.3	0.6
Tb	-	-	-	-	-	-	-	-	-	-
Dy	-	-	-	-	-	-	-	-	0.8	-
Ho	-	-	-	-	-	-	-	-	-	-
Er	0.7	0.8	0.4	0.7	0.6	0.5	-	0.7	0.2	0.2
Tm	-	-	-	-	-	-	-	-	-	0.1
Yb	-	-	-	-	-	-	-	-	0.3	0.2
Lu	-	-	-	-	-	-	-	-	0.2	-
Y/(Y+Ln)x100	-	-	-	-	-	-	-	-	7.4	3.6
La+Ce+Pr	84.8	83.2	84.6	86.6	84.3	85.5	87.9	88.8	83.9	84.4
ΣLa-Nd	92.9	92.1	93.1	93.0	93.7	93.3	94.6	93.0	95.5	96.9
ΣSm-Ho	6.4	7.1	6.5	6.3	5.7	6.2	5.4	6.3	3.8	2.6
ΣEr-Lu	0.7	0.1	0.4	0.7	0.6	0.5	-	0.7	0.7	0.5
RE_2O_3	23.9	23.2	24.1	23.2	14.6	16.4	18.8	-	18.4	16.4
La/Nd	4.51	2.79	3.93	5.23	3.47	3.81	6.67	8.25	2.39	2.07
ThO_2,wt %	0.7	0.5	0.4	0.3	0.3	0.4	0.3	0.8	-	-
U_3O_8,wt %	-	-	-	-	-	-	-	-	-	-

(81-88) Ghent (1972), Mt. Falconer quartz monzonite pluton, Antarctica; (81-84) fresh, (85-88) altered; (89) Koptyaev (1969), metamorphosed conglomerate. Urals, USSR, altered.

Method	EMPA	EMPA	EMPA	EMPA	EMPA	EMPA	EMPA	EMPA	XRF	XRF

Appendix C. Continued.

	91	92	93	94	95	96	97	98	99	100
Atomic %										
La	16.8	17.8	20.4	18.3	23.2	18.8	29.4	29.6	28.2	45.1
Ce	48.0	48.2	48.9	50.6	46.1	49.4	54.1	54.9	54.0	44.1
Pr	5.8	5.3	5.1	6.0	6.0	5.5	-	-	-	-
Nd	17.9	16.6	16.3	18.7	20.4	16.3	14.6	15.5	16.4	10.8
Sm	3.7	3.4	2.7	2.9	2.4	3.0	1.9	-	1.4	-
Eu	0.4	0.3	0.3	0.1	-	0.5	-	-	-	-
Gd	1.7	1.8	1.4	1.8	1.3	1.7	-	-	-	-
Tb	0.4	0.3	0.3	0.2	0.1	0.3	-	-	-	-
Dy	2.6	2.9	1.2	0.9	0.4	1.2	-	-	-	-
Ho	0.1	0.3	-	0.1	-	-	-	-	-	-
Er	1.3	1.7	1.3	0.3	0.1	1.3	-	-	-	-
Tm	-	-	-	-	-	-	-	-	-	-
Yb	1.6	1.4	2.1	0.1	-	2.0	-	-	-	-
Lu	-	-	-	-	-	-	-	-	-	-
Y/(Y+Ln)x100	-	-	-	3.3	-	-	1.6	16.9	6.0	0.1
La+Ce+Pr	70.6	71.3	74.4	74.9	75.3	73.7	83.5	84.5	82.2	89.2
ΣLa-Nd	88.5	87.9	90.7	93.6	95.7	90.0	98.1	15.5	98.6	100.0
ΣSm-Ho	8.6	9.0	7.2	6.0	4.2	8.0	1.8	-	1.4	-
ΣEr-Lu	2.9	3.1	2.1	0.4	0.1	2.0	-	-	-	-
RE_2O_3	-	-	-	15.3	19.0	-	21.05	13.41	23.16	21.79
La/Nd	0.94	1.07	1.25	0.98	1.14	1.15	2.02	1.91	1.72	4.18
ThO_2,wt %	-	-	-	-	-	-	-	0.43	-	-
U_3O_8,wt %	-	-	-	-	-	-	-	-	-	-
Method	XRF	XRF	XRF	XRF	XRF	XRF	EMPA	EMPA	EMPA	OS

(91-96) Goldin (1966), near Polar Urals, U.S.S.R., (91-93) granites, (94-95) pegmatite, (96) quartz-fluorite veinlet; (97-99) Harding et al. (1982), St. Kilda, Scotland, (97-98) granite vein, (97) red-brown core, (98) pale green rim, (99) gabbro pegmatite; (100) Jesus-Ojeda and Mendoza A. (1981), Cerro Camacho, Peru.

Appendix C. Continued.

	101	102	103	104	105	106	107	108	109	110
Atomic %										
La	15.7	20.6	24.5	33.5	33.5	36.9	29.2	33.8	32.8	33.7
Ce	48.7	48.3	46.0	45.9	46.8	46.4	38.0	41.9	40.0	44.6
Pr	5.4	6.5	5.1	3.6	3.4	7.4	13.4	5.2	10.3	3.0
Nd	19.1	17.0	16.0	14.8	13.8	7.4	17.8	16.8	14.5	17.8
Sm	4.0	2.9	3.0	0.9	1.3	0.4	0.6	1.3	1.3	0.9
Eu	-	0.2	0.2	-	-	-	-	-	-	-
Gd	2.0	1.3	2.1	0.9	0.8	0.7	0.6	0.7	1.1	-
Tb	0.4	0.2	0.2	-	-	-	-	-	-	-
Dy	3.5	1.2	1.5	0.4	0.4	0.8	0.4	0.3	-	-
Ho	-	-	-	-	-	-	-	-	-	-
Er	0.4	0.8	0.2	-	-	-	-	-	-	-
Tm	-	-	-	-	-	-	-	-	-	-
Yb	0.8	0.6	1.2	-	-	-	-	-	-	-
Lu	-	-	-	-	-	-	-	-	-	-
Y/(Y+Ln)x100	-	-	-	1.1	0.8	0.8	1.4	5.7	3.0	-
La+Ce+Pr	69.8	75.4	75.6	83.0	83.7	90.7	80.6	80.9	83.1	81.3
ΣLa-Nd	88.9	92.8	91.6	97.8	97.5	98.1	98.4	97.7	97.6	99.1
ΣSm-Ho	9.9	5.8	7.0	2.2	2.5	1.9	1.6	2.3	2.4	0.9
ΣEr-Lu	1.2	1.4	1.4	-	-	-	-	-	-	-
RE_2O_3	-	-	-	21.50	21.35	16.03	16.85	17.50	18.00	26.30
La/Nd	0.82	1.18	1.53	2.26	2.43	4.99	1.64	2.00	2.26	1.89
ThO_2,wt %	-	-	-	1.11	1.07	1.04	0.71	1.34	-	-
U_3O_8,wt %	-	-	-	-	-	-	-	-	-	-
Method	XRF	XRF	XRF	-	-	-	-	-	-	XRF

(101-103) Ipat'eva and Leskova (1977), Okhotsk-Chukotsk volcanic field, U.S.S.R., (101) aplite, (102-103) biotite granite; (104-109) Ivanov et al. (1979), Cis-Baikal, U.S.S.R., (104-106) Paleozoic pegmatites, (107-109) Precambrian pegmatites; (110) Kapustin (1966), carbonatite, Vuerijavi, Karelia, U.S.S.R.

Appendix C. Continued.

	111	112	113	114	115	116	117	118	119	120
Atomic %										
La	8.4	20.8	13.4	18.7	26.9	29.2	28.3	29.0	27.6	26.0
Ce	57.0	49.5	63.4	48.0	50.4	47.2	47.1	44.3	46.9	51.4
Pr	4.1	4.6	3.1	6.4	4.0	4.8	6.1	6.4	5.9	5.6
Nd	25.2	18.9	14.8	16.7	16.1	10.7	15.4	14.4	15.8	13.9
Sm	1.9	2.5	1.9	5.1	1.5	4.0	1.5	2.4	1.8	1.4
Eu	-	0.9	0.9	-	-	-	-	-	-	-
Gd	1.8	2.8	2.2	2.2	0.8	1.5	0.7	2.1	1.7	1.0
Tb	0.3	-	-	-	-	-	-	0.1	-	-
Dy	0.9	-	0.3	1.5	-	1.4	0.5	0.7	-	0.4
Ho	-	-	-	-	-	-	-	0.2	-	0.1
Er	0.4	-	-	1.1	0.1	1.0	0.1	0.2	0.1	-
Tm	-	-	-	-	-	-	-	-	-	-
Yb	-	-	-	0.3	0.1	0.2	0.2	0.1	0.1	0.1
Lu	-	-	-	-	0.1	-	-	0.1	0.1	0.1
Y/(Y+Ln)x100	-	-	-	1.9	1.5	1.3	1.5	2.7	1.5	1.8
La+Ce+Pr	69.5	74.9	79.9	73.1	81.3	81.2	81.5	79.7	80.4	83.0
ΣLa-Nd	94.7	93.8	94.7	89.8	97.4	91.9	96.9	94.1	96.2	96.9
ΣSm-Ho	5.3	6.2	5.3	8.8	2.3	6.9	2.8	5.5	3.5	2.9
ΣEr-Lu	-	-	-	1.4	0.3	1.2	0.3	0.4	0.3	0.2
RE_2O_3	-	-	-	-	-	-	-	-	-	-
La/Nd	0.33	1.10	0.91	1.12	1.67	2.72	1.83	2.02	1.74	1.87
ThO_2,wt %	-	-	-	-	-	-	-	-	-	-
U_3O_8,wt %	-	-	-	-	-	-	-	-	-	-
Method	-	-	-	-	-	-	-	-	-	-

(111-113) Kalita (1969), pegmatites, eastern Baltic Shield, (114-20) quoted by Lezarenko et al. (1981), Ukraine, USSR; (114-115) pegmatite. Staro-ignetiera; (116-117) hornblende-biotite granites; (116) Dimitrievka, (117) Novgorod; (118-120) biotite granites, (118) Kohski Radovy; (119) Sadoviz, (120) Lidina.

Appendix C. Continued.

	121	122	123	124	125	126	127	128	129	130
Atomic %										
La	20.6	26.8	27.3	28.6	28.5	29.9	25.0	19.0	29.1	33.0
Ce	48.9	47.5	43.9	46.4	47.5	47.6	45.0	45.3	54.1	48.7
Pr	5.9	5.4	5.7	5.9	6.1	3.2	4.9	4.8	3.4	4.5
Nd	16.2	12.1	14.2	15.2	13.5	14.9	24.2	20.5	12.0	12.5
Sm	4.0	4.5	4.8	1.8	1.8	2.6	0.7	4.1	0.5	0.8
Eu	-	-	-	-	-	0.1	-	0.5	0.1	0.2
Gd	1.8	1.4	1.5	1.8	1.7	1.5	0.2	3.7	0.3	0.3
Tb	-	-	-	-	-	-	-	0.3	-	-
Dy	1.4	1.2	1.4	-	0.5	-	-	1.0	0.3	-
Ho	-	-	-	-	-	-	-	0.2	-	-
Er	1.0	1.0	1.0	0.1	0.2	0.2	-	0.4	0.1	-
Tm	-	-	-	-	-	-	-	-	-	-
Yb	0.2	0.1	0.2	0.1	0.1	-	-	0.2	0.1	-
Lu	-	-	-	0.1	0.1	-	-	-	-	-
Y/(Y+Ln)x100	2.0	1.9	1.8	1.5	2.2	1.0	-	>0.7	-	0.15
La+Ce+Pr	75.4	79.7	76.9	80.9	82.1	80.7	74.9	69.1	86.6	86.2
ΣLa-Nd	91.6	91.8	91.1	96.1	95.6	95.6	89.1	89.6	98..6	98.7
ΣSm-Ho	7.2	7.1	7.7	3.6	4.0	4.2	0.9	9.8	1.2	1.3
ΣEr-Lu	1.2	1.1	1.2	0.3	0.4	0.2	-	0.6	0.2	-
RE_2O_3	-	-	-	-	-	-	-	13.03	-	19.20
La/Nd	1.27	2.08	1.93	1.88	2.10	2.01	1.03	0.93	2.42	2.64
ThO_2,wt %	-	-	-	-	-	-	-	-	-	-
U_3O_8,wt %	-	-	-	-	-	-	-	-	-	-
Method	-	-	-	-	- -	-	-	MS	XRF	At Abs

(121-127) quoted by Lazarenko et al. (1981), Ukraine, USSR (121) pegmatite. Staro ignatiova; (122) pegmatite in granosyenite, Kalchik; (123) migmatized granite. Kichikse; (124) veinlet in migmatite. Dakhan; (125-127) biotite granites, Azor region; (128) Mason (1975), gneiss, Godthab region, W. Greenland; (128) Mikhailov and Mineev (1970), av. of 14 from diopside metasomatites, Aldan, USSR; (130) Pepunen and Lindsjo (1972), in skarn, lead deposit, Korsnas, Finland.

Appendix C. Continued.

	131	132	133	134	135	136	137	138	139	140
Atomic %										
La	19.6	18.6	23.8	4.0	16.7	17.4	27.9	42.2	38.5	45.6
Ce	48.7	55.2	23.6	9.8	27.6	43.0	27.7	41.9	38.2	45.2
Pr	1.9	7.3	-	-	-	-	-	-	-	-
Nd	28.5	17.9	13.8	9.6	5.4	8.4	27.0	12.2	22.4	2.2
Sm	0.9	0.7	4.4	-	5.1	8.0	7.8	-	-	0.4
Eu	-	-	-	-	-	-	-	-	-	-
Gd	0.9	0.3	12.8	1.8	3.4	3.8	7.5	2.3	0.7	0.4
Tb	-	-	1.3	-	-	-	-	-	-	-
Dy	-	-	4.2	8.5	23.8	7.4	-	-	-	-
Ho	-	-	0.4	0.2	-	-	0.2	-	-	-
Er	-	-	12.1	24.6	4.6	5.0	1.2	-	-	3.9
Tm	-	-	0.8	0.4	-	-	-	-	-	-
Yb	-	-	2.0	39.7	13.4	7.0	0.7	1.4	0.2	2.3
Lu	-	-	0.8	1.4	-	-	-	-	-	-
Y/(Y+Ln)x100	7.1	-	3.3	23.6	37.8	40.3	10.8	3.0	4.3	28.2
La+Ce+Pr	70.2	81.1	47.4	13.8	44.3	60.4	55.6	84.1	76.7	90.8
ΣLa-Nd	98.7	99.0	61.2	23.4	49.7	68.8	82.6	96.3	99.1	93.0
ΣSm-Ho	1.3	1.0	23.1	10.5	32.3	19.2	15.5	2.3	0.7	0.8
ΣEr-Lu	-	-	15.7	66.1	28.0	12.0	1.8	1.4	0.2	6.2
RE_2O_3	10.85*	-	-	-	-	-	-	-	-	-
La/Nd	0.69	1.04	1.72	0.41	3.11	2.07	1.03	3.45	1.72	20.7
ThO_2,wt %	-	-	-	-	-	-	-	-	-	-
U_3O_8,wt %	-	-	-	-	-	-	-	-	-	-
Method	OS	OS	OH	OH	OH	OH	OH	OH	OH	OH

(131-132) Nadezhdina (1968). Tungus and Botuobii Rivers, Siberia; (131) diorite pegmatite; (132) granophyre; (133-140) Putalova (1978). Chingiz anticlinorium, Kazakhstan, (133-138) granites; (139) granodiorite; (140) riebeckite-quartz syenite.

* % REE.

Appendix C. Continued.

	141	142	143	144	145	146	147	148	149	150
Atomic %										
La	15.1	22.7	20.9	23.3	35.3	32.0	33.5	37.8	25.9	16.4
Ce	58.2	52.4	44.4	54.2	48.5	51.9	51.8	49.0	39.5	37.4
Pr	5.1	5.2	6.7	5.1	3.5	5.1	4.5	4.1	9.4	5.6
Nd	17.2	15.1	20.0	15.6	8.5	10.0	9.2	9.1	22.2	19.9
Sm	2.4	2.2	4.6	1.4	0.8	1.0	1.0	-	2.0	6.6
Eu	**a**	**a**	-	-	0.6	-	-	-	-	-
Gd	1.4**a**	1.1**a**	2.0	0.4	0.7	-	-	-	1.0	6.3
Tb	-	-	-	-	-	-	-	-	-	1.0
Dy	0.6	1.3	0.7	-	1.4	-	-	-	-	3.1
Ho	-	-	0.1	-	-	-	-	-	-	0.4
Er	-	-	0.4	-	-	-	-	-	-	1.5
Tm	-	-	0.1	-	-	-	-	-	-	0.4
Yb	-	-	0.1	-	0.7	-	-	-	-	0.8
Lu	-	-	-	-	-	-	-	-	-	0.6
Y/(Y+Ln)x100	-	2.0	-	-	-	-	-	-	1.8	-
La+Ce+Pr	78.4	80.3	72.0	82.6	87.3	89.0	89.8	90.9	74.8	59.4
ΣLa-Nd	95.6	95.4	92.0	98.2	95.8	99.0	99.0	9.1	97.0	79.3
ΣSm-Ho	4.4	4.6	7.4	1.8	3.5	1.0	1.0	-	3.0	17.4
ΣEr-Lu	-	-	0.6	-	0.7	-	-	-	-	3.3
RE_2O_3	-	-	21.35	20.17	24.55	24.59	24.83	18.0	16.99	36.9
La/Nd	0.88	1.50	1.05	1.49	4.17	3.19	3.63	4.12	1.17	0.83
ThO_2,wt %	-	-	-	-	-	-	-	-	1.61	-
U_3O_8,wt %	-	-	-	-	-	-	-	-	-	-
Method	CH	CH	-	-	-	-	-	-	CH	EP

(141-149) Orsa (1965), Dnioper basin, USSR; (141-142) pegmatite granite. Vol'nyanka River (also in Orsa et al, 1967); (143-148) Semenov et al. (1978), carbonates, Tamil Nadu, India; (149) Serdyachenko and Pap (1969), crystalline rocks, Byelorusse; (149) Shmakin and Shiryaeva (1970, 1971), muscovite pegmatite, E. Siberia.

a Eu + Gd calculated as Gd.

Appendix C. Continued.

	151	152	153	154	155	156	157	158	159	160
Atomic %										
La	22.6	25.5	23.8	32.3	22.9	21.2	36.0	28.8	23.7	25.8
Ce	42.7	49.0	49.4	49.7	48.4	48.3	39.6	37.9	49.6	50.4
Pr	7.2	5.4	4.8	5.1	5.7	6.8	5.7	5.7	4.4	5.3
Nd	19.9	16.2	13.5	11.5	18.3	20.4	16.5	24.9	19.3	15.7
Sm	1.9	2.6	2.8	6.4	3.4	0.6	1.2	1.7	1.4	0.9
Eu	**a**	**a**	0.2	-	0.1	-	-	-	-	-
Gd	5.7	0.5	0.9	0.5	0.8	2.3	0.8	0.9	0.7	1.1
Tb	**c**	0.2	0.2	-	-	**b**	0.2	0.4	0.5	0.7
Dy	**c**	0.6	2.0	-	0.3	0.4	-	0.5	0.4	-
Ho	-	-	0.3	-	-	-	-	-	-	-
Er	-	-	0.9	-	-	-	-	-	-	-
Tm	-	-	0.1	-	-	-	-	-	-	-
Yb	-	-	1.0	-	0.1	-	-	-	-	-
Lu	-	-	0.1	-	-	-	-	-	-	-
Y/(Y+Ln)x100	13.4**c**	-	-	-	-	1.7**b**	-	-	-	-
La+Ce+Pr	72.5	79.9	78.0	87.1	77.0	76.3	81.3	71.6	77.7	81.5
ΣLa-Nd	92.4	96.1	91.5	98.6	95.3	96.7	97.8	96.5	97.0	97.3
ΣSm-Ho	7.6	3.9	6.4	6.9	4.6	3.3	2.2	3.5	3.0	2.7
ΣEr-Lu	-	-	2.1	-	0.1	-	-	-	-	-
RE_2O_3	15.10	-	-	21.52	15.36	18.13	13.97	15.73	15.70	15.73
La/Nd	1.14	1.57	1.77	2.82	1.25	1.04	2.18	1.16	1.23	1.65
ThO_2,wt %	1.25	-	-	1.07	0.80	2.42	2.28	0.49	1.64	1.59
U_3O_8,wt %	-	-	-	-	-	-	-	-	-	-
Method	CH	CH	XRF	XRF	CH	CH	CH	CH	CH	CH

(151-160) Ploshko and Knyezeva (1965), Urushten complex, N. Caucasas, USSR; (151-152) granitoids; (153) granite; (154) ignimbrite; (150) gneiss; (156) rock host not given; (157) albitized schist; (159) carbonate-sulfate veinlets; (160) carbonatized amphibolite.

a Eu+Gd calculated as Gd; **a** Tb+Y calculated as Y; **a** Tb+Dy+Y calculated as Y.

Appendix C. Continued.

	161	162	163	164	165	166	167	168	169	170
Atomic %										
La	37.3	36.1	38.4	38.2	39.2	37.0	33.9	36.2	37.6	40.5
Ce	50.5	52.1	52.1	52.4	50.3	52.0	53.5	51.4	51.6	47.8
Pr	3.8	3.9	2.0	2.6	3.4	3.3	3.6	3.4	3.0	3.2
Nd	7.9	7.6	7.4	5.8	6.6	7.1	8.3	8.0	7.0	8.0
Sm	0.4	0.2	0.1	0.6	0.4	0.4	0.5	0.6	0.5	0.3
Eu	-	-	-	-	-	-	-	-	-	-
Gd	0.1	0.1	-	0.4	0.1	0.2	0.2	0.4	0.3	0.2
Tb	-	-	-	-	-	-	-	-	-	-
Dy	-	-	-	-	-	-	-	-	-	-
Ho	-	-	-	-	-	-	-	-	-	-
Er	-	-	-	-	-	-	-	-	-	-
Tm	-	-	-	-	-	-	-	-	-	-
Yb	-	-	-	-	-	-	-	-	-	-
Lu	-	-	-	-	-	-	-	-	-	-
Y/(Y+Ln)x100	0.7	0.15	-	0.9	0.4	0.6	1.2	0.4	0.15	0.15
La+Ce+Pr	91.6	92.1	92.5	93.2	92.9	92.3	91.0	91.0	92.2	91.5
ΣLa-Nd	99.5	99.7	99.9	99.0	99.5	99.4	99.3	99.0	99.2	99.5
ΣSm-Ho	0.5	0.3	0.1	1.0	0.5	0.6	0.7	1.0	0.8	0.5
ΣEr-Lu	-	-	-	-	-	-	-	-	-	-
RE_2O_3	21.46	21.61	22.42	24.60	23.54	22.70	23.53	22.53	19.91	23.75
La/Nd	4.72	4.24	5.18	6.60	5.97	5.18	4.11	4.51	5.35	5.06
ThO_2,wt %	0.51	0.35	0.55	0.50	0.36	-	0.77	0.20	0.56	0.25
U_3O_8,wt %	-	-	-	-	-	-	-	-	-	-
Method	CH	CH	CH	CH	CH	CH	CH	CH	CH	CH

(161-170) Popova et al (1980), Il'men Mts, Urals, USSR (161-165) pegmatite in gneiss; (166-167) pegmatites in syenite; (168) pegmatite in fenite; (169) biotite syenite; (170) migmatite.

Appendix C. Continued.

	171	172	173	174	175	176	177	178	179	180
Atomic %										
La	34.7	37.1	32.7	38.6	38.5	28.3	32.5	34.9	21.0	39.3
Ce	52.2	50.7	55.5	51.4	51.1	54.1	35.9	48.8	48.9	50.5
Pr	3.3	3.7	3.2	2.7	3.5	4.5	6.4	4.4	5.4	2.6
Nd	9.4	7.8	7.8	7.0	7.0	11.9	21.2	10.0	16.7	7.4
Sm	0.3	0.5	0.6	0.2	0.2	0.9	2.5	0.7	3.3	0.2
Eu	-	-	-	-	-	-	-	-	-	-
Gd	0.1	0.2	0.2	0.1	0.1	0.3	1.5	1.2	2.5	-
Tb	-	-	-	-	-	-	-	-	-	-
Dy	-	-	-	-	-	-	-	-	1.5	-
Ho	-	-	-	-	-	-	-	-	-	-
Er	-	-	-	-	-	-	-	-	0.7	-
Tm	-	-	-	-	-	-	-	-	-	-
Yb	-	-	-	-	-	-	-	-	-	-
Lu	-	-	-	-	-	-	-	-	-	-
Y/(Y+Ln)x100	0.15	0.1	0.3	0.15	0.15	0.5	1.9	1.6	2.8	-
La+Ce+Pr	90.2	91.5	91.4	92.7	92.7	86.9	74.8	88.1	75.3	92.4
ΣLa-Nd	99.6	99.3	99.2	99.7	99.7	98.8	96.0	98.1	92.0	99.8
ΣSm-Ho	0.4	0.7	0.8	0.3	0.3	1.2	4.0	1.9	7.3	0.2
ΣEr-Lu	-	-	-	-	-	-	-	-	0.7	-
RE_2O_3	19.30	20.73	22.08	22.52	22.50	22.47	21.87	19.75	22	-
La/Nd	3.70	4.76	4.18	5.51	5.49	2.39	1.53	3.50	1.26	5.30
ThO_2,wt %	0.50	0.60	0.56	0.51	1.07	-	-	-	-	-
U_3O_8,wt %	-	-	-	-	-	-	-	-	-	-
Method	CH	CH	CH	CH	CH	CH	CH	CH	CH	-

(171-179) Popova et al. (1986), Il'men Mts., Urals, USSR; (171-172) feldspar veins in fenites; (173-175) feldspar veins in pegmatites; (176) migmatite; (177-178) border zone of pegmatite; (179) corundum-feldspar pegmatite, (180) Semanov and Khomyakov (1981), alkalic rocks, Vishnevye Mountains, Urals.

Appendix C. Continued.

	181	182	183	184	185	186	187	188	189	190
Atomic %										
La	13.5	9.8	9.0	19.1	26.2	9.1	22.2	23.0	26.8	12.9
Ce	47.4	58.5	69.2	53.6	51.0	56.9	49.2	52.7	53.7	49.8
Pr	7.1	4.0	4.9	7.4	6.5	10.2	4.7	7.2	5.3	6.8
Nd	27.1	15.3	9.2	15.0	14.5	19.8	23.9	15.0	13.5	25.8
Sm	4.9	3.9	4.3	2.8	1.2	2.1	-	-	-	4.7
Eu	-	-	-	-	-	-	-	-	-	-
Gd	-	4.0	1.2	0.8	0.4	0.9	-	-	-	-
Tb	-	1.1	0.6	0.4	-	0.5	-	-	-	-
Dy	-	3.4	1.6	0.9	0.2	0.5	-	2.1	0.7	-
Ho	-	-	-	-	-	-	-	-	-	-
Er	-	-	-	-	-	-	-	-	-	-
Tm	-	-	-	-	-	-	-	-	-	-
Yb	-	-	-	-	-	-	-	-	-	-
Lu	-	-	-	-	-	-	-	-	-	-
Y/(Y+Ln)x100	5.4	10.4	7.4	2.5	7.0	2.8	6.9	3.7	0.3	5.0
La+Ce+Pr	68.0	72.3	83.1	80.1	83.7	76.2	76.1	82.9	85.8	69.5
ΣLa-Nd	95.1	87.6	92.3	95.1	98.2	96.0	100.0	97.9	99.3	95.3
ΣSm-Ho	4.9	12.4	7.7	4.9	1.8	4.0	-	2.1	0.7	4.7
ΣEr-Lu	-	-	-	-	-	-	-	-	-	-
RE_2O_3	-	27.34	19.22	28.69	25.15	26.20	26.72	24.7	37.4	22.9
La/Nd	0.50	0.64	0.97	1.27	1.82	0.46	0.93	1.53	1.99	0.50
ThO_2,wt %	4.4	-	-	-	-	-	4.6	4.4	2.4	1.0
U_3O_8,wt %	-	-	-	-	-	-	-	-	-	-
Method	XRF	XRF	XRF	XRF	XRF	XRF	XRF	XRF	XRF	XRF

(181-189) Rub et al (1965a), N.E. USSR, (181-185) granites, (181) Mejok , (182 183) Levo-Omsunchan , (184) Vilichin , (185) Nevekii , (186) granodiorite, Valkaneish ; Chakotka; (187) nevadite; (188) perlite; (189) liparite; (190) Rub et al (1965b) N.E. USSR, granite Majok .

Appendix C. Continued.

	191	192	193	194	195	196	197	198	199	200
Atomic %										
La	18.1	21.9	29.3	33.2	33.5	33.5	40.2	36.7	36.2	34.4
Ce	28.7	37.8	38.1	43.7	45.9	46.8	31.7	46.5	50.1	52.4
Pr	14.8	8.1	13.2	4.9	3.6	3.4	12.4	7.4	5.0	4.8
Nd	21.6	23.7	17.9	16.0	14.8	13.8	7.5	7.5	7.9	7.7
Sm	6.0	4.4	0.5	1.2	0.9	1.3	2.2	0.4	0.6	0.5
Eu	-	-	-	-	-	-	-	-	-	-
Gd	8.7	3.5	0.6	0.7	0.9	0.8	5.2	0.7	0.2	0.2
Tb	-	-	-	-	-	-	-	-	-	-
Dy	1.1	0.6	0.4	0.3	0.4	0.4	0.8	0.8	-	-
Ho	-	-	-	-	-	-	-	-	-	-
Er	-	-	-	-	-	-	-	-	-	-
Tm	-	-	-	-	-	-	-	-	-	-
Yb	-	-	-	-	-	-	-	-	-	-
Lu	-	-	-	-	-	-	-	-	-	-
Y/(Y+Ln)x100	5.2	4.8	0.8	2.0	1.1	0.8	6.2	0.8	0.4	0.4
La+Ce+Pr	62.6	67.8	80.6	81.8	83.0	83.7	84.3	90.6	91.3	91.6
ΣLa-Nd	84.2	91.5	98.5	97.8	97.8	97.5	91.8	98.1	99.2	99.3
ΣSm-Ho	15.8	8.5	1.5	2.2	2.2	2.5	8.2	1.9	0.8	0.7
ΣEr-Lu	-	-	-	-	-	-	-	-	-	-
RE_2O_3	14.32a	13.99a	16.85	17.50	21.50	21.35	14.19a	17.07	20.81a	21.00a
La/Nd	0.84	0.92	1.63	2.07	2.26	2.43	5.39	4.91	4.59	4.49
ThO_2,wt %	a	a	0.71	1.39	1.11	1.02	a	1.04	a	a
U_3O_8,wt %	-	-	-	-	-	-	-	-	-	-
Method	CH	CH	CH	CH	CH	CH	CH	CH	CH	CH

(191-200) Shiryaeva and Shmakin (1982), pegmatites, Baikal region, Siberia.
a includes ThO_2.

Appendix C. Continued.

	201	202	203	204	205	206	207	208	209	210
Atomic %										
La	34.3	35.8	33.8	43.2	21.8	21.1	25.2	22.5	24.5	21.0
Ce	51.3	52.1	52.9	45.8	40.3	39.4	37.8	40.4	40.0	38.3
Pr	4.9	3.7	5.2	4.1	6.1	7.7	5.6	6.1	5.7	13.6
Nd	8.7	7.7	7.6	6.3	23.2	26.3	24.3	24.0	23.7	20.2
Sm	0.6	0.5	0.3	0.5	3.2	2.0	3.0	3.8	3.4	3.2
Eu	-	-	-	-	-	-	-	-	-	-
Gd	0.2	0.2	0.2	0.1	4.5	2.7	2.9	2.8	2.7	2.9
Tb	-	-	-	-	-	-	-	-	-	-
Dy	-	-	-	-	0.6	0.5	0.8	0.4	-	0.5
Ho	-	-	-	-	0.1	0.1	0.1	-	-	0.1
Er	-	-	-	-	0.2	0.2	0.3	-	-	0.2
Tm	-	-	-	-	-	-	-	-	-	-
Yb	-	-	-	-	-	-	-	-	-	-
Lu	-	-	-	-	-	-	-	-	-	-
Y/(Y+Ln)x100	0.5	0.3	0.2	0.3	3.7	3.5	5.2	2.8	2.8	2.2
La+Ce+Pr	90.5	91.6	91.9	93.1	68.2	68.2	68.6	69.0	70.2	72.9
ΣLa-Nd	99.2	99.3	99.5	99.4	91.4	94.5	92.9	93.0	93.9	93.1
ΣSm-Ho	0.8	0.7	0.5	0.6	8.4	5.3	6.8	6.6	6.1	6.7
ΣEr-Lu	-	-	-	-	0.2	0.2	0.3	0.4	-	0.2
RE_2O_3	18.5	20.49	19.42	20.00a	15.21	15.50	17.28	17.08	16.73	16.51
La/Nd	3.95	4.64	4.45	6.91	0.94	0.80	1.04	0.94	1.04	1.04
ThO_2,wt %	1.36	1.71	1.68	a	1.39	2.90	1.52	1.72	1.17	1.69
U_3O_8,wt %	-	-	-	-	-	-	-	-	-	-
Method	CH	CH	CH	CH	CH	CH	CH	CH	CH	CH

(201-204) Shiryaeva and Shmakin (1982), pegmatites, Baikal region, Siberia; (205 210) Shmakin and Shiryaeva (1970, 1971), muscovite pegmatites, eastern Siberia.

Appendix C. Continued.

	211	212	213	214	215	216	217	218	219	220
Atomic %										
La	23.9	24.0	28.6	30.5	28.7	30.1	33.9	33.9	25.7	29.2
Ce	49.2	38.4	40.2	41.7	44.6	46.5	44.8	46.1	49.4	49.6
Pr	4.2	4.4	4.1	4.0	3.7	4.8	3.9	4.0	7.4	6.6
Nd	11.9	20.9	22.5	18.5	17.6	14.0	14.8	13.5	15.2	12.9
Sm	6.7	4.8	2.6	2.7	2.4	2.5	1.6	1.6	2.3	1.7
Eu	0.2	0.2	0.1	0.2	0.3	0.1	0.1	0.1	-	-
Gd	0.8	4.2	1.4	1.6	2.0	1.5	0.7	0.6	-	-
Tb	-	-	-	-	-	-	-	-	-	-
Dy	0.8	1.2	0.2	0.4	0.3	0.2	0.1	0.1	-	-
Ho	-	0.2	-	0.1	0.1	-	-	-	-	-
Er	0.3	0.6	0.2	0.2	0.2	0.2	0.1	0.1	-	-
Tm	-	-	-	-	-	-	-	-	-	-
Yb	1.7	0.5	0.1	0.1	0.1	0.1	-	-	-	-
Lu	0.3	0.6	-	-	-	-	-	-	-	-
Y/(Y+Ln)x100	-	2.7	0.3	4.4	3.2	0.4	0.2	0.2	-	-
La+Ce+Pr	77.3	66.8	72.9	76.2	77.0	81.4	82.6	84.0	82.5	85.4
ΣLa-Nd	89.2	87.7	95.4	94.7	94.6	95.4	97.4	97.5	97.7	98.3
ΣSm-Ho	8.5	10.6	4.3	5.0	5.1	4.3	2.5	2.4	2.3	1.7
ΣEr-Lu	2.3	1.7	0.3	0.3	0.3	0.3	0.1	0.1	-	-
RE_2O_3	21.40	20.83	8.53	13.31	10.61	18.63	17.91	14.59	-	-
La/Nd	2.01	1.15	2.29	1.65	1.63	2.15	2.29	2.51	1.69	2.27
ThO_2,wt %	-	4.20	0.51	1.30	0.96	1.40	2.30	1.70	-	-
U_3O_8,wt %	-	-	-	-	-	-	-	-	-	-
Method	-	-	-	-	-	-	-	-	XRF	XRF

(211) Tikhonenkova and Kazokova (1964), contact of alkalic rocks, Lovozero , Kola Peninsula, USSR; (212-218) Tskhelishvili (1980), granitic rocks, Daryal , Georgian SSR; (219-220) Znamenskii et al. (1967), eastern Sayen; (219) granodiorite, (220) quartz diorite.

Appendix C. Continued.

	221	222	223	224	225	226	227	228	229	230
Atomic %										
La	20.2	21.8	22.1	22.4	29.7	22.3	27.8	26.6	32.3	18.7
Ce	45.3	50.8	51.4	51.2	52.4	53.7	53.8	56.0	51.9	43.0
Pr	3.7	2.9	2.9	2.9	2.2	3.9	3.1	2.3	4.0	6.2
Nd	13.7	19.2	17.1	18.3	13.2	13.5	8.9	13.8	10.3	27.7
Sm	13.1	2.1	3.0	2.3	0.8	0.7	0.5	0.8	0.7	4.4
Eu	0.4	0.6	0.3	0.3	-	-	-	a	a	-
Gd	1.8	2.0	2.5	1.9	1.5	1.7	0.4	0.5a	0.8a	-
Tb	-	-	-	-	-	-	-	c	c	-
Dy	0.3	0.1	0.2	0.3	-	1.3	1.7	c	c	-
Ho	0.3	0.3	0.3	0.3	0.2	-	-	-	-	-
Er	-	-	-	-	-	1.3	1.3	-	-	-
Tm	-	-	-	-	-	-	-	-	-	-
Yb	1.2	0.2	0.2	0.1	-	1.6	2.0	-	-	-
Lu	-	-	-	-	-	-	-	-	-	-
Y/(Y+Ln)x100	2.6	3.4	3.0	2.6	2.6	-	-	3.3c	3.4c	-
La+Ce+Pr	69.2	75.5	76.4	76.5	84.3	79.9	84.7	84.9	88.2	67.9
ΣLa-Nd	82.9	94.7	93.5	94.8	97.5	93.4	93.6	98.7	98.5	95.6
ΣSm-Ho	15.9	5.1	6.3	5.1	2.3	3.7	3.1	1.3	1.5	4.4
ΣEr-Lu	1.2	0.2	0.2	0.1	0.2	2.9	3.3	-	-	-
RE_2O_3	6.62*	13.54*	9.40*	13.54*	15.2	21.5	21.0	20.7	18.1	-
La/Nd	1.47	1.14	1.29	1.23	2.25	1.66	3.12	1.93	3.15	0.68
ThO_2,wt %	-	-	-	-	-	-	-	-	-	-
U_3O_8,wt %	-	-	-	-	-	-	-	-	-	-
Method	XRF	XRF	XRF	XRF	XRF	XRF	XRF	CH	CH	XRF

(221-225) Tsvetkova-Golera, and Karadzhova (1968), granites, Rila , Bulgaria; (226-229) Vinogradov and Elina (1968), granites, NW Kola Peninsula, USSR; (230) Znamenskii et al. (1967), biotite granite, Tikhoi River, E. Sayan.
* % REE.

Appendix C. Continued.

	231	232	233	234	235	236	237	238	239	240
Atomic %										
La	40.5	35.2	28.4	37.7	31.4	32.5	31.3	34.0	34.0	25.3
Ce	51.0	60.3	62.8	58.0	45.7	47.4	52.1	48.0	45.4	36.4
Pr	3.4	-	-	-	2.7	6.5	4.1	5.9	5.6	12.9
Nd	5.1	4.5	9.8	4.3	18.6	11.5	11.5	12.1	11.3	15.7
Sm	-	-	-	-	0.7	1.1	0.8	-	3.7	6.6
Eu	-	-	-	-	0.1	-	-	-	-	0.2
Gd	-	-	-	-	0.6	1.0	-	-	-	1.4
Tb	-	-	-	-	-	-	-	-	-	-
Dy	-	-	-	-	0.2	-	0.1	-	-	1.1
Ho	-	-	-	-	-	-	-	-	-	0.3
Er	-	-	-	-	-	-	-	-	-	-
Tm	-	-	-	-	-	-	-	-	-	0.1
Yb	-	-	-	-	-	-	0.1	-	-	0.02
Lu	-	-	-	-	-	-	-	-	-	-
Y/(Y+Ln)x100	0.1	0.1	0.2	0.2	-	1.2	0.4	-	-	4.9
La+Ce+Pr	94.9	95.5	91.2	95.7	79.8	86.4	87.5	87.9	85.0	74.6
ΣLa-Nd	100.0	100.0	100.0	100.0	98.4	97.9	99.0	100.	96.3	90.3
ΣSm-Ho	-	-	-	-	1.6	2.1	0.9	-	3.7	9.6
ΣEr-Lu	-	-	-	-	-	-	0.1	-	-	0.1
RE_2O_3	25.39	24.83	28.18	23.00	-	-	-	-	-	15.5
La/Nd	7.86	7.91	3.22	8.90	1.69	2.82	2.72	2.80	3.00	1.61
ThO_2,wt %	-	-	-	-	-	-	-	-	-	-
U_3O_8,wt %	-	-	-	-	-	-	-	-	-	-
Method	XRF	XRF	XRF	XRF	XRF	CHR	CHR	XS	XS	OS

(231-234) Vorontsov (1972), eastern Sayan, Siberia, (231-232) leucocratic granites, (233-234) alaskites; (235) Semenov (1969), Ilimausseq, Greenland; (236 237) Ploshko and Bogdanova (1963), ignimbrites, Kozlinka River, Northern Caucasus; (238-240) Kosterin et al. (1961), Caledonian diorites, Zaliskii Alatau, northern Kirghizia.

Appendix C. Continued.

	241	242	243	244	245	246	247	248	249	250
Atomic %										
La	29.3	32.0	27.7	32.0	28.8	28.5	28.1	29.4	29.2	25.9
Ce	40.4	39.2	42.6	40.6	44.7	43.2	40.7	38.8	40.6	33.8
Pr	8.1	7.5	7.3	6.2	5.9	7.2	8.0	9.2	9.2	6.1
Nd	17.4	16.8	16.3	17.2	15.3	16.9	17.1	15.3	15.6	17.2
Sm	3.2	2.8	4.3	2.5	3.9	2.7	4.1	4.8	3.5	8.1
Eu	0.1	0.1	0.2	0.1	0.2	0.2	0.2	0.2	0.1	0.1
Gd	0.9	1.0	0.9	0.9	0.7	0.7	1.1	1.4	1.2	2.8
Tb	-	-	-	-	-	-	-	-	-	-
Dy	0.5	0.5	0.5	0.4	0.4	0.4	0.5	0.6	0.5	1.7
Ho	0.1	0.1	0.2	0.1	0.1	0.2	0.1	0.2	0.1	0.3
Er	-	-	-	-	-	-	-	-	-	-
Tm	-	-	-	-	-	-	0.03	0.04	-	0.1
Yb	0.02	0.02	0.02	0.02	0.03	0.02	0.1	0.1	0.03	0.2
Lu	-	-	-	-	-	-	-	-	-	-
Y/(Y+Ln)x100	1.3	0.9	1.1	0.9	1.1	1.1	2.9	3.3	1.8	6.0
La+Ce+Pr	77.8	78.7	77.6	78.8	79.4	78.9	76.8	77.4	79.0	65.8
ΣLa-Nd	95.2	95.5	93.9	96.0	94.7	95.8	93.9	92.7	94.6	86.7
ΣSm-Ho	4.8	4.5	6.1	4.0	5.3	4.2	6.0	7.2	5.4	13.0
ΣEr-Lu	-	-	-	-	-	-	0.1	0.1	-	0.3
RE_2O_3	23.8	21.0	21.7	23.3	24.7	20.2	23.0	20.3	19.8	24.6
La/Nd	1.68	1.90	1.69	1.86	1.88	1.68	1.64	1.92	1.87	1.50
Method	OS	OS	OS	OS	OS	OS	OS	OS	OS	OS

(241-250) Lee and Bastron (unpublished), quartz monzonite, Mt. Wheeler area, Nevada.

Appendix C. Continued.

	251	252	253	254	255	256	257	258	259	260
Atomic %										
La	27.5	26.1	36.7	33.9	35.4	28.9	25.9	28.9	27.8	24.5
Ce	35.1	35.6	54.2	48.5	47.8	36.8	49.8	47.7	47.5	45.9
Pr	7.4	7.2	3.1	6.5	5.6	8.1	5.1	4.2	4.9	5.3
Nd	19.3	20.9	5.9	11.1	11.2	16.0	19.2	15.6	16.4	20.4
Sm	6.5	6.3	0.1	-	-	2.9	-	2.2	2.1	2.7
Eu	0.2	0.1	-	-	-	-	-	-	-	-
Gd	2.5	2.2	-	-	-	5.6	-	1.4	1.3	1.2
Tb	-	-	-	-	-	-	-	-	-	-
Dy	1.2	1.3	-	-	-	0.7	-	-	-	-
Ho	0.2	0.2	-	-	-	-	-	-	-	-
Er	-	-	-	-	-	0.7	-	-	-	-
Tm	0.04	-	-	-	-	-	-	-	-	-
Yb	0.1	0.1	-	-	-	0.3	-	-	-	-
Lu	-	-	-	-	-	-	-	-	-	-
Y/(Y+Ln)x100	5.0	4.3	-	-	-	-	-	-	-	-
La+Ce+Pr	70.0	68.9	94.0	88.9	88.8	73.8	80.8	80.8	80.2	75.7
ΣLa-Nd	89.3	89.8	99.9	100.	100.	89.8	100.	96.4	96.6	96.1
ΣSm-Ho	10.6	10.1	0.1	-	-	9.9	-	3.6	3.4	3.9
ΣEr-Lu	0.1	0.1	-	-	-	0.3	-	-	-	-
RE_2O_3	25.3	24.1	-	-	-	-	-	-	-	-
La/Nd	1.42	1.24	6.22	3.05	3.16	1.80	1.34	1.85	1.69	1.20
Method	OS	OS	XS	XS	XS	XS	XS	XS	XS	XS

(251-252) Lee and Bastron (unpublished), quartz monzonite, Mt. Wheeler area, Nevada; (253) Meliksetyan (1960), monzonite, Megrim pluton, Armenia; (254-255) Kosterin et al. (1961), Caledonian granodiorites, Zaliskii Alatau, northern Kirghizia; (256) Sahama and Vahatalo (1941), granite, Juva, Finland; (257-259) Vainshtein et al. (1956b), granites, (257) Hirschberg, Poland, (258) Mitrofanovka, Ukraine, (259) Sob River, Ukraine, (260) Babany Sta., Ukraine.

Appendix C. Continued.

	261	262	263	264	265	266	267	268	269	270
Atomic %										
La	32.2	30.1	33.5	25.9	24.5	22.0	20.7	23.6	24.9	23.8
Ce	49.0	50.4	49.0	45.9	49.8	51.4	46.3	44.7	47.9	53.9
Pr	4.2	4.4	4.0	5.4	3.8	5.9	6.9	7.8	5.8	6.0
Nd	14.6	15.1	13.5	20.0	11.3	14.7	21.1	20.7	15.9	14.0
Sm	-	-	-	1.8	2.6	2.9	2.6	2.0	2.5	0.9
Eu	-	-	-	-	0.3	0.2	0.3	0.1	-	0.1
Gd	-	-	-	1.0	1.0	0.7	1.1	0.7	1.7	0.6
Tb	-	-	-	-	0.2	0.1	0.2	-	-	-
Dy	-	-	-	-	3.0	0.9	0.4	0.3	1.3	0.1
Ho	-	-	-	-	0.4	0.2	-	-	-	-
Er	-	-	-	-	1.0	0.7	0.3	-	-	0.1
Tm	-	-	-	-	0.2	-	-	-	-	-
Yb	-	-	-	-	1.7	0.3	0.1	0.1	-	0.5
Lu	-	-	-	-	0.2	-	-	-	-	-
Y/(Y+Ln)x100	-	-	-	-	-	-	3.1	-	1.6	-
La+Ce+Pr	85.4	84.9	86.5	77.2	78.1	79.3	73.9	76.1	78.6	83.7
ΣLa-Nd	100.	100.	100.	97.2	89.4	94.0	95.0	96.8	94.5	97.7
ΣSm-Ho	-	-	-	2.8	7.5	5.0	4.6	3.1	5.5	1.7
ΣEr-Lu	-	-	-	-	3.1	1.0	0.4	0.1	-	0.6
RE_2O_3	-	-	-	-	-	-	-	-	-	-
La/Nd	2.20	1.99	2.48	1.29	2.16	1.49	0.98	1.14	1.56	1.70
Method	XS	XS	XS	XS	XS	XS	XS	CHR	CHR	XS

(260-264) Vainshtein et al. (1956b), granites, (260) Uman, Ukraine, (261) Pervomaisk, Ukraine, (262) apical portion of pluton, Saltyche Mogila, Ukraine, (263) rapakivi, Shpola, Ukraine; (265) Lyakhovich and Barinskii (1961), granite, El'dzhurtin massif, northern Caucasus; (266) Lyakhovich (1962), granite, El'dzhurtin massif, northern Caucasus; (267) Khvostova (1962b), granite, Magisko, northern Caucasus; (268-269) Ploshko and Boghanova (1963), (268) granitic rock, Blyb River, Magisko Range, northern Caucasus, (269) gravel of granitic rock, Kuban River, northern Caucasus; (270) Semenov and Barinskii (1958), granite, Kuramin Ridge.

Appendix C. Continued.

	271	272	273	274	275	276	277	278	279	280
Atomic %										
La	25.3	23.8	32.1	38.8	23.3	32.2	25.0	31.1	26.9	24.1
Ce	49.3	53.1	50.0	44.9	44.3	54.0	51.0	53.3	50.3	56.3
Pr	6.0	6.0	4.1	3.6	7.0	3.6	4.3	-	4.5	5.1
Nd	17.7	15.4	12.8	12.2	22.6	9.7	17.3	15.6	16.6	14.5
Sm	1.1	0.8	1.0	0.5	2.0	0.3	2.4	-	1.7	-
Eu	-	0.1	-	-	-	-	-	-	-	-
Gd	0.5	0.5	-	-	0.6	0.1	-	-	-	-
Tb	0.1	0.1	-	-	0.1	-	-	-	-	-
Dy	-	0.2	-	-	-	0.1	-	-	-	-
Ho	-	-	-	-	-	-	-	-	-	-
Er	-	-	-	-	-	-	-	-	-	-
Tm	-	-	-	-	-	-	-	-	-	-
Yb	-	-	-	-	-	-	-	-	-	-
Lu	-	-	-	-	-	-	-	-	-	-
Y/(Y+Ln)x100	-	-	-	-	-	-	-	-	-	-
La+Ce+Pr	80.6	82.9	86.2	87.3	74.6	89.8	80.3	84.4	81.7	85.5
ΣLa-Nd	98.3	98.3	99.0	99.5	97.2	99.5	97.6	100.	98.3	100.
ΣSm-Ho	1.7	1.7	1.0	0.5	2.8	0.5	2.4	-	1.7	-
ΣEr-Lu	0.6	-	-	-	-	-	-	-	-	-
RE_2O_3	-	-	-	-	-	-	-	-	-	-
La/Nd	1.42	1.54	2.50	3.18	1.03	3.31	1.44	1.99	1.62	1.66
Method	XS	XS	XS	XS	XS	XS	XS	XS	XS	XS

(271) Lyakhovich (1962), granite, eastern Transbaikal; (272) Khvostova (1962b), granite, western Tuva; (273-274) Pavlenko et al. (1959), biotite granite, (273) Ilektyah massif, eastern Tuva; (274) Erzinsk massif, eastern Tuva; (275-276) Khvostova (1962b), granite, (275) Taimyr, (276) alteration product of allanite, Taimyr; (277-280) Kosterin et al. (1961), (277-278) Caledonian porphyritic hornblende granite, (279-280) Variscan alaskites.

Appendix C. Continued.

	281	282	283	284	285	286	287	288	289	290
Atomic %										
La	30.2	31.5	25.5	28.2	24.3	14.0	19.1	18.1	7.3	10.6
Ce	53.8	45.1	54.2	49.1	50.3	51.0	41.5	51.0	47.4	51.9
Pr	5.9	8.1	4.8	5.1	5.3	3.1	5.3	5.2	5.0	3.4
Nd	10.1	15.3	14.7	15.6	17.6	19.8	22.3	22.7	28.3	21.3
Sm	-	-	0.6	1.3	1.5	8.5	7.5	2.1	7.8	3.7
Eu	-	-	0.1	0.2	0.1	-	-	-	-	-
Gd	-	-	0.3	0.3	0.5	3.6	4.3	0.9	4.2	9.1
Tb	-	-	-	-	-	-	-	-	-	-
Dy	-	-	-	0.2	0.3	-	-	-	-	-
Ho	-	-	-	-	-	-	-	-	-	-
Er	-	-	-	-	-	-	-	-	-	-
Tm	-	-	-	-	-	-	-	-	-	-
Yb	-	-	-	-	-	-	-	-	-	-
Lu	-	-	-	-	-	-	-	-	-	-
Y/(Y+Ln)x100	-	-	-	-	-	4.2	6.7	2.7	6.0	5.2
La+Ce+Pr	89.9	84.7	84.3	82.4	79.9	68.1	65.9	74.3	59.7	65.9
ΣLa-Nd	100.	100.	99.0	98.0	97.5	87.9	88.2	97.0	88.0	87.2
ΣSm-Ho	-	-	1.0	2.0	2.5	12.1	11.8	3.0	12.0	12.8
ΣEr-Lu	-	-	-	-	-	-	-	-	-	-
RE_2O_3	-	23.	-	19.3	12.3	-	-	-	-	-
La/Nd	2.99	2.05	1.72	1.80	1.38	0.70	0.85	0.79	0.25	0.49
Method	XS	XS	XS	XS	XS	OS	OS	OS	OS	OS

(281) Kosterin et al. (1961), gneissic alaskite, (282)Borovskii and Gerasimovskii (1945), granite, Babi-Dzhid River, northern Kirghizia; (283) Khvostova and Bykova (1961), alaskitic granite, Emel'dzhak deposit, southern Yakutia; (284-285) Lyakhovich (1962), granite, (284) Tatubinsk massif, Far East, (285) Ol'ginsk massif, Far East; (286) McCarty (1935) Amherst County, Virginia; (287-288) Murata et al. (1957), (287) granite pegmatite, Crabtree Creek, North Carolina, (288) aplite-pegmatite zone, Jamestown, Colorado; (289-290) McCarty (1935), (289) Colorado, (290) Hittero, Norway.

Appendix C. Continued.

	291	292	293	294	295	296	297	298	299	300
Atomic %										
La	17.4	16.6	12.2	14.9	-	23.6	21.9	22.9	13.4	13.4
Ce	38.4	34.5	30.6	44.4	6.7	37.6	43.8	45.7	33.4	36.5
Pr	6.0	5.9	6.7	5.3	4.3	7.5	5.6	5.4	5.9	8.1
Nd	24.8	25.6	30.6	24.5	35.2	19.4	20.8	20.8	26.7	20.9
Sm	7.9	9.0	11.0	6.2	24.4	5.6	5.4	5.2	11.0	7.7
Eu	-	-	-	-	-	-	-	-	-	0.3
Gd	5.5	8.4	8.9	3.6	16.0	4.8	2.5	-	9.6	4.6
Tb	-	-	-	-	1.9	-	-	-	-	0.7
Dy	-	-	-	1.1	7.9	1.0	-	-	-	6.3
Ho	-	-	-	-	-	-	-	-	-	0.5
Er	-	-	-	-	1.5	0.5	-	-	-	0.7
Tm	-	-	-	-	-	-	-	-	-	-
Yb	-	-	-	-	2.1	-	-	-	-	0.3
Lu	-	-	-	-	-	-	-	-	-	-
Y/(Y+Ln)x100	-	-	-	34.0	33.2	11.0	-	-	-	-
La+Ce+Pr	61.8	57.0	49.5	64.6	11.0	68.7	71.3	74.0	52.7	58.0
ΣLa-Nd	86.6	82.6	80.1	89.1	46.2	88.1	92.1	94.8	79.4	78.9
ΣSm-Ho	13.4	17.4	19.9	10.9	50.2	11.4	7.9	5.2	20.6	20.1
ΣEr-Lu	-	-	-	-	3.6	0.5	-	-	-	1.0
RE_2O_3	-	-	-	-	22.2	-	-	-	-	-
La/Nd	0.70	0.64	0.39	0.60	-	1.21	1.05	1.10	0.50	0.64
Method	XS	XS	XS	XS	XS	XS	XS	XS	XS	XS

(291-293) Vainshtein et al. (1956b), pegmatite, (291) Hittero, Norway, (292) Ytterby, Sweden, (293) Fahlun, Sweden; (294) Quensel and Alufelst (1945), "muromontite" = Be-allanite from pegmatite, Skuleboda, Sweden; (295) Neumann and Nilssen (1962) lombaardite from pegmatite, Askagen, Sweden; (296) Sahama and Vahatalo (1939), pegmatite, Impilahti, Finland; (297-299) Vainshtein et al. (1956b), pegmatite (297) Impilahti, Finland, (298-299) Vaarala, Finland; (300) Kalita (1959), pegmatite, northwestern Karelia.

Appendix C. Continued.

	301	302	303	304	305	306	307	308	309	310
Atomic %										
La	18.4	7.1	20.1	30.8	19.4	12.8	14.8	1.5	2.2	2.0
Ce	48.4	18.4	45.7	15.3	48.4	27.4	32.1	2.4	10.8	3.3
Pr	7.4	4.2	6.4	9.4	7.6	5.4	6.6	0.2	1.1	0.3
Nd	17.5	9.6	16.6	22.0	17.5	13.8	17.5	0.4	7.4	0.6
Sm	3.8	9.3	5.5	5.5	3.2	7.8	7.3	1.2	7.1	1.6
Eu	0.6	2.6	1.1	1.3	0.8	0.9	0.4	0.2	-	0.3
Gd	1.8	14.1	2.6	2.6	1.6	10.6	9.5	15.5	29.1	20.5
Tb	-	3.8	-	1.3	-	1.8	1.9	2.8	3.9	3.6
Dy	2.1	13.7	2.0	5.1	1.5	10.3	5.7	27.1	28.3	3.6
Ho	-	1.2	-	0.6	-	1.7	1.2	6.5	3.7	8.5
Er	-	7.2	-	2.5	-	3.4	1.5	16.7	3.7	22.0
Tm	-	1.2	-	1.2	-	1.3	0.2	2.6	-	3.5
Yb	-	7.0	-	1.8	-	2.0	1.0	19.0	2.7	25.1
Lu	-	0.6	-	0.6	-	0.8	0.3	3.9	-	5.1
Y/(Y+Ln)x100	1.9	24.8	-	-	-	21.3	39.3	64.1	50.6	48.0
La+Ce+Pr	74.2	29.7	72.2	55.5	75.4	45.6	53.5	4.1	14.1	5.6
ΣLa-Nd	91.7	39.3	88.8	77.5	92.9	59.4	71.0	4.5	21.5	6.2
ΣSm-Ho	8.3	44.7	11.2	16.4	7.1	33.1	26.0	53.3	72.1	38.1
ΣEr-Lu	-	16.0	-	6.1	-	7.5	3.0	42.2	6.4	55.7
RE_2O_3	-	-	-	-	-	-	-	10.3	-	-
La/Nd	1.05	0.40	1.21	1.40	1.10	0.92	0.84	3.10	0.29	3.33
Method	XS	XS	XS	XS	XS	XS	XS	XS	XS	XS

(301-306) Zhirov et al. (1961), granite pegmatites, northern Karelia, (301-302) Topornaya, (302) altered, (303) Kindomys, (304) Olenchik, (305) Mama, (306) Kamennaya Taibola; (307-308) Semenov and Barinskii (1958), pegmatite, (307) Kamennaya Taibola, northern Karelia, (308) Sinyaya Pala, northern Karelia; (309) Protopopov (1940), yttroallanite from Sinyaya Pala; (310) Khvostova (1962b), pegmatite, Sinyaya Pala.

Appendix C. Continued.

	311	312	313	314	315	316	317	318	319	320
Atomic %										
La	4.7	16.6	18.6	23.2	20.2	13.5	4.6	27.3	19.6	14.4
Ce	7.8	44.2	38.4	43.2	41.7	36.0	80.5	55.6	39.8	38.8
Pr	2.3	7.2	5.6	5.3	7.3	8.2	3.2	6.9	6.5	8.3
Nd	4.6	17.4	15.0	21.1	21.4	21.1	9.2	5.8	20.9	23.9
Sm	7.3	5.0	5.8	4.9	5.1	7.7	1.5	0.2	6.0	6.7
Eu	2.2	0.6	1.4	-	0.2	0.3	-	2.4	0.1	0.1
Gd	21.8	2.4	4.6	2.3	2.6	4.7	0.7	0.4	4.6	5.3
Tb	4.2	0.3	0.9	-	0.3	0.7	0.1	0.9	0.5	0.6
Dy	24.6	2.6	4.5	-	0.9	6.3	0.2	0.2	1.5	1.3
Ho	2.7	0.3	0.4	-	0.1	0.5	-	0.3	0.1	0.1
Er	7.4	1.1	2.6	-	0.3	0.7	-	-	0.3	0.3
Tm	1.3	0.4	0.9	-	-	-	-	-	-	-
Yb	6.5	1.6	0.9	-	0.1	0.3	-	-	0.1	0.2
Lu	2.6	0.3	0.4	-	-	-	-	-	-	-
Y/(Y+Ln)x100	21.4	2.8	7.6	-	4.4	0.3	-	-	0.7	0.3
La+Ce+Pr	14.8	68.0	62.6	71.7	69.0	57.7	88.3	89.8	65.9	61.5
ΣLa-Nd	19.4	85.4	77.6	92.8	90.4	78.8	97.5	95.6	86.8	85.4
ΣSm-Ho	62.8	11.2	17.6	7.2	9.2	20.2	2.5	4.4	12.8	14.1
ΣEr-Lu	17.8	3.4	4.8	-	0.4	1.0	-	-	0.4	0.5
RE_2O_3	-	-	-	-	-	-	-	-	-	-
La/Nd	1.02	0.95	1.24	1.09	0.93	0.63	0.50	4.70	0.93	0.60
Method	XS	XS	XS	XS	XS	XS	XS	XS	XS	XS

(311-313) Zhirov et al. (1961), pegmatites, northern Karelia, (311) Sinyaya Pala, (312-313) Tedino, (313) altered; (314) Vainshtein et al. (1956a), pegmatite, Tedino; (315-320) Khvostova (1962b), pegmatite, (315) "hydro-allanite" (altered), Tedino, (316-317) Alakurtti, Karelia, (316) also in kalita (1961), (317) altered, (318) Kury-Vaara, Karelia, (319-320) Chernaya Salma, Karelia, (320) "hydroallanite".

Appendix C. Continued.

	321	322	323	324	325	326	327	328	329	330
Atomic %										
La	12.3	12.6	16.4	21.8	20.5	8.3	22.8	31.2	24.9	20.4
Ce	32.4	29.2	41.4	40.2	38.3	56.6	53.1	57.5	47.1	55.6
Pr	5.3	4.1	8.5	6.1	5.9	4.1	5.9	3.0	5.7	4.7
Nd	17.2	16.3	20.4	16.1	18.3	25.6	15.1	7.9	19.1	13.5
Sm	11.1	9.1	6.7	7.8	8.5	1.9	1.2	0.3	1.9	2.1
Eu	0.7	1.3	0.3	0.4	0.4	-	-	-	0.1	0.4
Gd	10.4	8.2	3.5	4.2	4.0	1.9	0.5	0.1	0.7	1.0
Tb	1.6	1.9	-	0.7	0.9	0.3	-	-	0.1	-
Dy	5.3	7.9	2.8	2.0	1.7	0.9	0.4	-	0.4	1.0
Ho	1.1	1.2	-	0.4	0.4	-	0.1	-	-	-
Er	1.8	2.4	-	-	0.7	0.4	0.3	-	-	0.4
Tm	0.3	1.2	-	-	-	-	-	-	-	-
Yb	0.4	4.0	-	0.3	0.4	-	0.5	-	-	0.9
Lu	0.1	0.6	-	-	-	-	0.1	-	-	-
Y/(Y+Ln)x100	23.4	-	-	1.3	-	2.5	5.8	-	2.9	-
La+Ce+Pr	50.0	45.9	66.3	68.1	64.7	69.0	81.8	91.7	77.7	80.7
ΣLa-Nd	67.2	62.2	86.7	84.2	83.0	94.6	96.9	99.6	96.8	94.2
ΣSm-Ho	30.2	29.6	13.3	15.5	15.9	5.0	2.5	0.4	3.2	4.5
ΣEr-Lu	2.6	8.2	-	0.3	1.1	0.4	0.6	-	-	1.3
RE_2O_3	-	-	-	-	-	-	-	-	-	-
La/Nd	0.71	0.77	0.80	1.35	1.12	0.32	1.50	3.94	1.30	1.51
Method	XS	XS	XS	XS	XS	XS	XS	XS	XS	XS

(321) Khvostova (1962b), pegmatite, Panfilova Vareka, Karelia; (322-323) Zhirov et al. (1961), pegmatites, northern Karelia, (322) Panfilova Vareka, (323) Kaita Tundra; (324) Khvostova (1962b), pegmatite, Kaita Tundra, Karelia; (325) Kalita (1961), pegmatite, Kaita Tundra, Karelia; (326) Protopopov (1940), Kheto-Lambino, Karelia; (327, 329) Semenov and Barinskii (1958), (327) alkali granite pegmatite, Keivy, Kola Peninsula, (329) pegmatite, Kalai-Makhmud River, Turkestan Range; (328) Meliksetyan (1960), feldspar-amphibole pegmatite, Megrin pluton, Armenia; (330) Khvostova (1962b), pegmatite, Chu-Iliisk Mt., southern Kazakhsten.

Appendix C. Continued.

	331	332	333	334	335	336	337	338	339	340
Atomic %										
La	15.4	28.4	22.0	32.2	37.2	23.8	21.4	23.1	6.5	29.2
Ce	45.0	52.4	43.7	54.1	52.2	41.4	52.8	43.9	53.4	53.1
Pr	5.9	4.8	5.9	3.6	2.3	5.2	7.7	5.5	9.6	-
Nd	19.9	12.8	22.3	9.7	8.0	20.7	11.7	23.1	12.3	17.7
Sm	4.8	0.5	3.0	0.3	0.1	4.8	6.4	4.4	7.8	-
Eu	0.4	-	0.2	-	-	-	-	-	-	-
Gd	2.9	0.1	1.8	-	0.2	4.1	-	-	10.4	-
Tb	0.4	0.5	0.8	-	-	-	-	-	-	-
Dy	3.1	0.1	0.1	-	-	-	-	-	-	-
Ho	0.4	0.3	0.2	-	-	-	-	-	-	-
Er	0.7	-	-	-	-	-	-	-	-	-
Tm	-	0.1	-	-	-	-	-	-	-	-
Yb	1.1	-	-	-	-	-	-	-	-	-
Lu	-	-	-	-	-	-	-	-	-	-
Y/(Y+Ln)x100	-	1.0	4.4	-	-	-	9.1**a**	-	28.7	-
La+Ce+Pr	66.3	85.6	71.6	90.0	91.7	70.4	81.9	72.5	69.5	82.3
ΣLa-Nd	86.2	98.4	93.9	99.7	99.7	91.1	93.6	95.6	81.8	100.
ΣSm-Ho	12.0	1.5	6.1	0.3	0.3	8.9	6.4	4.4	18.2	-
ΣEr-Lu	1.8	0.1	-	-	-	-	-	-	-	-
RE_2O_3	-	20.2	-	-	-	-	-	-	-	-
La/Nd	0.77	2.21	0.98	3.32	4.65	1.14	1.82	1.00	0.52	1.64
Method	XS	XS	XS	XS	XS	XS	NA	XS	XS	OS

(331) Khvostova (1962b), pegmatite, Tuva; (332-334) Khvostova and Bykova (1961), pegmatites, southern Yakutia, (332) Leglier, (333) Ammunachi deposit, (334) Emel'dzhak deposit; (335) Khovstova (1962b), "hydroallanite", Federov, Yakutia; (336) Vainshtein et al. (1956b), pegmatite, Haichen, China; (337) Fujii (1962), Songjin, Korea; (338) Vainshtein et al. (1956b), pegmatite, Madagascar; (339) McCarty (1935), locality unknown; (340) Pavlenko et al. (1959), pegmatitic feldspar-magnetite-quartz dike, Dugdin massif, eastern Tuva.

Appendix C. Continued.

	341	342	343	344	345	346	347	348	349	350
Atomic %										
La	30.9	34.7	40.8	21.9	26.3	33.2	36.0	39.8	29.4	32.2
Ce	49.4	49.8	48.0	48.0	43.1	46.6	49.8	45.5	47.8	52.9
Pr	4.3	3.9	3.2	7.1	4.3	3.9	3.1	3.3	4.8	3.7
Nd	15.4	11.6	8.0	16.5	12.0	13.5	11.1	11.4	15.9	10.7
Sm	-	-	-	2.8	2.5	1.4	-	-	2.1	0.5
Eu	-	-	-	0.3	-	-	-	-	-	-
Gd	-	-	-	1.4	3.8	1.4	-	-	-	-
Tb	-	-	-	-	-	-	-	-	-	-
Dy	-	-	-	2.0	4.5	-	-	-	-	-
Ho	-	-	-	-	-	-	-	-	-	-
Er	-	-	-	-	1.8	-	-	-	-	-
Tm	-	-	-	-	-	-	-	-	-	-
Yb	-	-	-	-	-	-	-	-	-	-
Lu	-	-	-	-	-	-	-	-	-	-
Y/(Y+Ln)x100	-	-	-	-	21.2	-	-	-	-	-
La+Ce+Pr	84.6	88.4	92.0	77.0	73.7	83.7	88.9	88.6	82.0	88.8
ΣLa-Nd	100.	100.	100.	93.5	85.7	97.2	100.	100.	97.9	99.5
ΣSm-Ho	-	-	-	6.5	10.8	2.8	-	-	2.1	0.5
ΣEr-Lu	-	-	-	-	3.5	-	-	-	-	-
RE_2O_3	-	-	-	-	-	-	-	-	-	-
La/Nd	2.00	2.99	5.10	1.32	2.19	2.45	3.24	3.49	1.84	3.00
Method	XS	XS	XS	XS	XS	XS	XS	XS	XS	XS

(341-343) Vainshtein et al. (1956b), (341) feldspar vein, Lake Bygden, Norway, (342) hydrothermal vein, Avigeit, Greenland, (343) hydrothermal vein, Radenthal, Germany; (344) Zhirov et al. (1961), quartz-carbonate vein in pegmatite, northern Karelia; (345) Pavlenko et al. (1959), contact metasomatic orthoclase albitite, Dugdin massif, eastern Tuva; (346-349) Vainshtein et al. (1956b), (346) contact hydothermal deposit, Sludyanka, Transbaikal, (347-348) contact-metasomatic amphibole skarns, Bastnaes, Sweden, (348) altered crust of (347), (349) grossular-vesuvianite skarn, New Jersey; (350) Khvostova and Bykova (1961), diopside-scapolite vein, Federov, southern Yakutia.

Appendix C. Continued.

	351	352	353	354	355	356	357	358	359	360
Atomic %										
La	34.2	29.7	29.8	50.5	35.0	46.2	24.9	22.5	29.0	35.8
Ce	57.0	47.4	45.4	35.1	47.2	41.0	58.1	47.6	37.2	39.4
Pr	2.3	4.7	4.8	-	-	-	3.6	5.8	6.0	5.8
Nd	6.4	16.1	16.5	11.8	15.5	9.9	13.1	17.9	25.0	16.4
Sm	0.1	2.1	2.3	-	-	-	0.3	3.3	1.7	1.2
Eu	-	-	-	-	-	-	-	-	-	-
Gd	-	-	1.2	-	-	-	-	-	-	0.9
Tb	-	-	-	-	-	-	-	-	-	-
Dy	-	-	-	1.5	-	0.9	-	0.5	0.4	0.5
Ho	-	-	-	1.1	2.3	2.0	-	-	-	-
Er	-	-	-	-	-	-	-	-	-	-
Tm	-	-	-	-	-	-	-	-	-	-
Yb	-	-	-	-	-	-	-	-	-	-
Lu	-	-	-	-	-	-	-	-	-	-
Y/(Y+Ln)x100	-	-	-	4.1	3.0	0.4	-	1.8	0.7	0.6
La+Ce+Pr	93.5	81.8	80.0	85.6	82.2	87.2	86.6	75.9	72.2	81.0
ΣLa-Nd	99.9	97.9	96.5	97.4	97.7	97.1	99.7	93.8	97.2	97.4
ΣSm-Ho	0.1	2.1	3.5	2.6	2.3	2.9	0.3	6.2	2.8	2.6
ΣEr-Lu	-	-	-	-	-	-	-	-	-	-
RE_2O_3	-	-	-	13.3	16.4	14.1	-	-	-	-
La/Nd	5.34	1.84	1.80	4.27	2.25	4.66	1.90	1.26	1.16	2.18
Method	XS	XS	XS	XS	XS	XS	XS	CHR	CHR	CHR

(351) Khvostova and Bykova (1961), Federov, southern Yakutia, (351) phlogopite-diopside rock; (352-353) Vainshtein et al. (1956b), pegmatitic veinlets in gneiss, locality not given; (354-356) Hugo (1961), granulite-gneiss, Vrede, Cape Province, Union of South Africa; (357) Semenov and Barinskii (1958), para-gneiss, southern Yakutia; (358-360) Ploshko and Bogdanova (1963), Urushten complex, northern Caucasus, (358) plagiogranite gneiss, Greater Laba River, (359-360) Lesser Laba River, (359) albitized crystalline schists, (360) albite.

Appendix C. Continued.

	361	362	363	364	365	366	367	368	369	370
Atomic %										
La	21.6	23.7	26.1	25.2	23.0	26.3	26.1	43.3	24.2	23.0
Ce	49.2	49.8	50.7	43.9	46.2	43.1	43.5	47.3	46.5	48.6
Pr	7.1	4.6	5.5	6.3	7.1	6.2	6.0	-	8.4	4.4
Nd	20.7	19.3	15.8	21.8	23.7	21.4	21.6	9.4	20.9	12.3
Sm	0.6	1.5	0.9	2.8	-	3.0	2.8	-	-	6.9
Eu	-	-	-	-	-	-	-	-	-	-
Gd	0.8	1.1	0.5	-	-	-	-	-	-	0.9
Tb	-	-	-	-	-	-	-	-	-	-
Dy	-	-	0.5	-	-	-	-	-	-	0.9
Ho	-	-	-	-	-	-	-	-	-	-
Er	-	-	-	-	-	-	-	-	-	0.4
Tm	-	-	-	-	-	-	-	-	-	-
Yb	-	-	-	-	-	-	-	-	-	2.0
Lu	-	-	-	-	-	-	-	-	-	0.4
Y/(Y+Ln)x100	0.3	1.2	0.3	-	-	-	-	-	-	-
La+Ce+Pr	77.9	78.1	82.3	75.4	76.3	75.6	75.6	90.6	79.1	76.0
ΣLa-Nd	98.6	97.4	98.1	97.2	100.	97.0	97.2	100.	100.	88.3
ΣSm-Ho	1.4	2.6	1.9	2.8	-	3.0	2.8	-	-	8.9
ΣEr-Lu	-	-	-	-	-	-	-	-	-	2.8
RE_2O_3	-	-	-	-	-	-	-	-	-	20.85
La/Nd	1.04	1.22	1.65	1.15	0.97	1.22	1.20	4.60	1.15	1.86
Method	CHR	CHR	CHR	XS	XS	XS	XS	XS	XS	XS

(361-363) Ploshko and Bugdanova (1963), Lesser Laba River, Urushten complex, nothern Caucasus, (361) allanite-apatite "nests", (362) sulfate-carbonate vein, (363) carbonatized amphibolites; (364-368) Kosterin et al. (1961), Zaliskii Alatau, northern Kirghizia, (364-367) Variscan syenites, (368) Caledonian hybrid syenite; (369) Borovskii and Gerasimovskii (1945), nepheline syenite, Lovozero massif, Kola Peninsula; (370) Tikhonenkov and Tikhonenkova (1962), oligoclasites of contact zone, Lovozero massif, Kola Peninsula.

Appendix C. Continued.

	371	372	373	374	375	376	377	378	379	380
Atomic %										
La	35.4	32.2	31.3	30.7	22.3	36.2	34.3	37.3	32.3	41.3
Ce	49.3	52.9	51.6	49.1	47.3	53.0	52.3	50.3	50.0	45.0
Pr	3.5	3.6	5.0	5.4	6.8	2.6	3.4	3.2	4.3	3.4
Nd	8.9	10.7	9.6	9.2	19.6	7.9	9.6	9.0	12.7	9.4
Sm	0.5	0.2	0.7	1.2	2.6	0.1	0.2	-	0.4	0.9
Eu	0.1	-	-	-	0.1	-	-	0.2	-	-
Gd	0.4	0.1	0.4	1.2	0.9	0.2	0.2	-	0.2	-
Tb	-	-	-	-	-	-	-	-	-	-
Dy	1.2	0.1	0.9	1.2	0.2	-	-	-	0.1	-
Ho	0.2	-	0.2	0.4	-	-	-	-	-	-
Er	0.4	0.1	0.3	0.7	-	-	-	-	-	-
Tm	-	-	-	-	-	-	-	-	-	-
Yb	-	0.1	-	0.7	0.1	-	-	-	-	-
Lu	-	-	-	-	-	-	-	-	-	-
Y/(Y+Ln)x100	-	-	-	-	-	-	-	-	-	-
La+Ce+Pr	88.2	88.7	87.9	85.2	76.4	91.8	90.0	90.8	86.6	89.7
ΣLa-Nd	97.1	99.4	97.5	94.4	96.0	99.7	99.6	99.8	99.3	99.1
ΣSm-Ho	2.5	0.5	2.2	4.2	3.9	0.3	0.4	0.2	0.7	0.9
ΣEr-Lu	0.4	0.1	0.3	1.4	0.1	-	-	-	-	-
RE_2O_3	-	-	-	-	-	-	-	-	-	-
La/Nd	3.97	3.01	3.26	3.33	1.14	4.58	3.57	4.14	2.54	4.39
Method	XS	XS	XS	XS	XS	XS	XS	XS	XS	XS

(371-372) Zhabin and Svyazhin (1962), zoned aggregates in alkalic rocks, Vishnevye Mts., Urals; (373-379) Khvostova (1962b), Vishnevye Mtns., Urals, (373-375) pegmatites, (376-378) alkalic pegmatites, (379) fenitized gneiss; (380) Zhabin et al. (1960), Vishnevye Mtns., Urals.

Appendix C. Continued.

	381	382	383	384	385	386	387
Atomic %							
La	41.1	28.3	31.2	31.5	20.3	30.1	39.0
Ce	44.9	51.1	51.6	51.1	41.3	52.1	49.4
Pr	3.4	4.6	3.5	2.7	3.2	4.3	4.2
Nd	9.6	14.7	12.1	6.9	8.4	13.0	7.4
Sm	1.0	0.5	0.8	1.5	4.5	0.3	-
Eu	-	-	0.1	0.2	0.6	-	-
Gd	-	0.2	0.4	0.5	2.4	0.2	-
Tb	-	-	-	0.1	0.5	-	-
Dy	-	0.2	0.2	2.0	5.9	-	-
Ho	-	-	-	0.3	1.1	-	-
Er	-	0.4	0.1	1.9	7.1	-	-
Tm	-	-	-	0.3	0.7	-	-
Yb	-	-	-	0.9	3.4	-	-
Lu	-	-	-	0.1	0.6	-	-
Y/(Y+Ln)x100	-	-	4.2	-	-	0.5	-
La+Ce+Pr	89.4	84.0	86.3	85.3	64.8	86.5	92.6
ΣLa-Nd	99.0	98.7	98.4	92.2	73.2	99.5	100.
ΣSm-Ho	1.0	0.9	1.5	4.6	15.0	0.5	-
ΣEr-Lu	-	0.4	0.1	3.2	11.8	-	-
RE_2O_3	-	-	-	-	-	-	-
La/Nd	4.28	1.92	2.57	4.57	2.41	2.31	5.27
Method	XS	XS	XS	XS	XS	XS	XS

(381) Vainshtein et al. (1956b), hydrothermal veins, Uskov Sprink, Il'men Mtns., Urals; (382-385) Khvostova (1962b), Il'men Mtns., Urals, (382-383) pegmatites, (384-385) alteration products of allanite; (386) Murata et al. (1957), carbonatite, Mountain Pass district, California; (387) Heinrich and Levinson (1961), carbonatite, Ravalli County, Montana.

REFERENCES

Adams, J. W., and Sharp, W. N. (1972) Thalenite and allanite derived from yttrofluorite in the White Cloud pegmatite, South Platte area, Colorado. U.S. Geological Survey Professional Paper 800-C, C63-C69.

Aleksiev, E., and Ivanov, I. M. (1970) Rare-earth elements in the Sredna Gora granitic rocks and the pegmatites connected with them in the region of Koprivshtitsa and Strelcha. Bulgar Akad. Nauk, Izvest. Ged-Inst., Ser. Geokhim., Mineral, Petrog., 19, 5-15 (Bulgarian with Engl. summary).

Aleksiev, E., Khisina, T., and Pavlova, M. (1969) Geochemistry of rare earths in the Plana pluton. Bulgar. Akad. Nauk, Izvest. Geol. Inst., Ser. Geokhim., Mineral., Petrog., 18, 47-59 (Bulgarian with Engl. summary).

Azimov, P. T., and Khamrabaev, I. Kh. (1965) Distribution of rare-earth elements in rocks and minerals of the Aktan intrusive. Uzbek Geol. Zhurnal 1965, 5, 28-36 (in Russian).

Batieva, I. D. (1976) Petrology of alkalic granitoids of the Kola Penisula. Akad. Nauk S.S.S.R., Kol'sk Filial. Geol. Inst., "Nauka," Leningrad, 1-223 (in Russian).

Bel'kov, I. V. (1979) Accessory minerals of the granitoids of the Kola Peninsula. Akad. Nauk S.S.S.R. Kol'sk Filial, Geol. Inst., "Nauka," Leningrad, 1-184 (in Russian).

Belolipetskii, A. P., and Elina, N. A. (1967) Composition of rare earths in accessory minerals in veins of alkalic granites. Mat. Mineral Kol'sk Poluostr., 5, 124-128 (in Russian).

Bennett, J. N., Turner, D. C., Ike, E. C., and Bowden, P. (1984) The geology of some northern Nigerian anorogenic ring complexes. Overseas Geol. and Mineral Resources 61, 1-66.

Bocquet, J. (1975) Sur une Allanite Filonienne, a Bramans en Maureienne (Alpes Occidentales Savoie) [allanite from a vein at Bramans in the Maurienne, Western Alps, Savoie, France]. Bulletin de la Societe france Mineralogie et Cristallographie, 98, 171-174.

Campbell, F. A. and Ethier, V. G. (1984) Composition of allanite in the footwall of the Sullivan Orebody, British Columbia. Canadian Mineralogist, 22, 507-511.

Borovskii, I. B., and Gerasimovskii, V. I. (1945) Rare earths in minerals. Comptes Rendue Academie Science U.S.S.R. 49, 353-356.

Cech, F., and Povondra, P. (1972) New data on metamict allanite from Domaninek, Czechoslovakia. Acta Univ. Carolinae, Geologie 1972, 3, 151-160.

Cech, F., Varna, S., and Povondra, P. (1972) A nonmetamict allanite from Zambia. Neues Jahrb. Mineral., Abhandl. 116, 208-223.

Cerneva, Z., Daieva, L., and Aleksiev, E. (1983) Rare-earth elements in orthites, apatites,

and sphenes from granitoids in South Bulgaria. Geol. Balcanica 13, 5, 63-74 (Engl.).

Chistyakova, M. B., and Kazakova, M. E. (1968) Rare-earth minerals from crystal-bearing cavities in granitic pegmatites, Kazakhsten. Trudy Mineralog. Muzeya Akad. Nauk S.S.S.R. 18, 245-249 (in Russian).

Demanage, M., and Elsass, P. (1973) Presence of allanite in a cupriferous stratiform deposit in Tolate n'Ouamare, Morocco. Compt. Rend. Acad. Sci. (Paris), Ser. D, 277, 19, 1969-1972 (French), Chemical Abstracts 80, (2), 62058 (1974).

Es'kova, E. M., and Gauzeeva, A. A. (1964) Rare-earth elements in accessory minerals, Vishnerge Mts. Geokhimiya 1964, 1267-1279 (translation in Geochemistry International 1964, 1152-1163).

Exley, R. A. (1980) Microprobe studies of REE-rich accessory minerals: implications for Skye granite petrogenesis and REE mobility in hydrothermal systems. Earth Planet Sci. Lett. 48, 97-110.

Fishman, M. V., Yushkin, N. P., Goldin, B. A., and Kalinin, E. P. (1968) Mineralogy, typomorphism, and genesis of accessory minerals of igneous rocks of the northern Urals and Timan. Akad. Nauk S.S.S.R., Komi Filial, Inst. Geol. "Nauka," Leningrad, 1-250 (in Russian).

Fourcade, S., and Allegre, C. J. (1981) Trace element behavior in granite genesis: a case study. The calc-alkaline plutonic association from the Querigut complex (Pyrenees, France). Contrib. Mineral. Petrol, 76, 177-195.

Frondel, J. W. (1964) Variation of some rare earths in allanite. American Mineralogist, 49, 1159-1177.

Fujii, I. (1961) Distribution of rare-earth elements in rare-earth minerals from Japan, Korea, and northeastern China. Journal Mineralogy Society of Japan, 5, 167-180 (Japanese) (Min. Abstracts, 16, 50, 1963).

Gable, D. J. (1980) The Boulder Creek batholith, Front Range, Colorado. U.S. Geoloical Professional Paper, 1107, 1-88.

Ganzeeva, L. V. (1972) Mineralogical composition of rare-earth-beryl alkali metasomatites. Redk. Elenent., Syr'e Ekon., 7, 112-124 (in Russian).

Ghent, E. D. (1972) Electron microprobe study of allanite from the Mt. Falconer quartz monzonite pluton, lower Taylor Valley, South Victoria Land, Antarctica. Canadian Mineralogist, 11, 526-530.

Goldin, B. A. (1966) Allanite from the near-Polar Urals. Petrog. Mineral. Near. Polar Urals and Timan, 73-80 (in Russian).

Gorasimovskii, V. I. (1964) An unusual association of zeolites and bastnaesite. Vestnik Moskov University, IV, Geol. 1964, 6, 43-49 (in Russian).

Gromet, L. P., and Silver, L. T. (1983) Rare-earth element distributions among minerals

in a granodiorite and their petrogenetic implications. Geochimica et Cosmochimica Acta, 47, 925-939.

Harding, R. R., Merriman, R. J., and Nancarrow, P. H. A. (1982) A note on the occurrence of chevkinite, allanite, and zirkelite on St. Kilda, Scotland. Mineralogical Magazine, 46, 445-448.

Hildreth, W. (1979) The Bishop tuff: evidence for the origin of compositional zonation in silicia magma chambers. Geological Society of America, Special Paper, 180, 43-75.

Hugo, P. J. (1961) The allanite deposits on Vrede, Gordonia district, Cape Province. Republic of South Africa Department of Mines, Geological Survey Bulletin, 37, 1-65.

Ipat'era, I. S., and Leskora, N. V. (1977) Composition of allanites from Late Mesozoic granitic rocks of northeastern U.S.S.R. Minor. Endogen. Obroz. Yakutii 1897, 116-122 (in Russian).

Ivanov, A. N., Shiryaeva, V. A., and Shmakin, B. M. (1974) Allanite as a mineral indicator of the depth of pegmatite formation. Ezheg. Inst. Geokhim., Sib. Ofdel. Akad. Nauk S.S.S. R. 1974, 111-115 (publ. 1976) (in Russian).

Ivanov, A. N., Shiryaeva, V. A., and Shmekia, B.M. (1979) Again on the composition of allanite from pegmatites of western Cio-Baikel. Geokhim., Endogen. Protsesseu, Sib. Inst. Geokhim Irkutsk, 1977, 178-182 (in Russian).

Ivanov, O. P., Vorob'er, Yu. K., Efremenko, L. Ya., and Knyazeva, P. M. (1981) Acicular allanite from veins of the Yultinskii deposit. Zap. Vses Mineralog. Obsh., 110, 361-365 (in Russian).

Ivashchenko, V. I., Vasil'eva, E. S., Zlovidov, I. N., and Ruokolainen, N. A. (1983). Occurrence of a rare variety of metamict allanite in granitic rocks of the eastern part of the Baltic Shield. Magmat. Metallogen. Dokembr. Obraz. Karelil 1983, 64-67 (Russian), Chemical Abstracts 101, 24, 214165 (1984).

Jesus-Ojeda, M., and Mendoza, A. (1981) Distribution of rare earths in zircons, fluorites, apatites, garnets, and allanite from Peru. Bol. Soc. Quim. Peru 1981, 179-192 (in Spanish).

Kalita, A. P. (1959) Distribution of rare earths in the pegmatite minerals of northwestern and southwestern Karelia. Geokhimiya 1959, 140-144; translation in Geochemistry International 1959, 171-177.

Kalita, A. P. (1961) Rare-earth pegmatites of Alakurti and the Ladoga region. Inst. Mineral. Geokhim., Kristallokhim Redk. Elementor (Imgre), 1-118 (in Russian).

Kalita, A. P. (1969) Features of the distribution of lanthanides and yttrium in rare-earth granitic pegmatites of the eastern part of the Baltic Shield, in "Features of the distribution of rare elements in pegmatites," Inst. Mineralogy, Geochemistry, and Crystal Chemistry of Rare Elements, Izdat. "Nauka," Moscow, 79-100 (in Russian).

Kapustin, Yu. L. (1966) Geochemistry of rare-earth elements in carbonatites. Geokhimiya

1966, 1311-1321 (in Russian), translation in Geochemistry International 3, 6, 1054-1066 (1966).

Khvostova, V. A. (1962a) Mineralogy of allanite. Trudy Inst. Mineral., Geokhim., Kristallolchim. Redk. Elementov. 11, 3-118 (in Russian).

Khvostova, V. A. (1962b) Distribution of rare-earth elements in acessory minerals of the South Yakution pegmatites. Trudy Inst. Mineral. Geokhim., Kristallokhim. Redk. Elementov 8, 147-155 (in Russian).

Khvostova, V. A. (1969) Some data on the distribution of rare elements in metamorphased conglomerates of the Ural. Geokhimiya 1969, 3, 328-334 (in Russian).

Khvostova, V. A., and Bykova, A. V. (1961). Accessory allanite from southern Yabrutra. Trudy Inst. Mineral., Geokhim., Kristallokhim. Redk. Elementov, 7, 130-137 (in Russian).

Koptyaev, A. F. (1969) Geochemistry of rare-earth elements in old conglomerates. Geokhimiya 1969, 894-897 (in Russian).

Kosterin, A. V., Kizyura, V. E., and Zuev, V. N. (1961) The ratios of rare-earth elements in allanites of some igneous rocks of northern Kirghizia. Geokhimiya 1961, 454-456; translation in Geochemistry International 1961, 481-484.

Lazarenko, E. K., and others (1981) Mineralogy of the Azov region, Kiev, "Nauke Dumka," 1-430 (in Russian).

Lee, D. E., and Bastron, H. (1967). Fractionation of rare-earth elements in allanite and monazite as related to geology of the Mt. Wheeler area, Nevada. Geochimica et Cosmochimica Acta, 31, 339-356.

Lyakhovich, V. V. (1962) Rare-earth elements in accessory minerals of granitic rocks. Geokhimiya 1962, 37-52; translation in Geochemistry International 1962, 39-55.

Lyakhovich, V. V. , and Barinskii, R. L. (1961) Features of the composition of rare earths in the accessory minerals of granitic rocks. Geokhimiya 1961, 467-479; translation in Geochemistry International 1961, 495-509.

Mason, B. (1975) Mineralogy and geochemistry of two Amitaoq gneisses from the Godthab region, West Greenland. Gronlands Geol. Unders gelsc Rapport, 71, 1-11 (Eng.).

McCarty, C. N. (1935) The quantitative estimation of some of the rare-earth ores by means of their arc spectra. University of Illinois Ph.D. thesis, 1-8.

Meliksetyan, B. M. (1960) Accessory allanite from the Megrin pluton. Izvest. Akad. Nauk Armyan S.S.R., 3, 3-12 (in Russian).

Mikhailov, D. A., and Mineev, d. A. (1970) Distribution of lanthanides in accessory minerals of diopsidic metasomatites of Aldon. In the volume, Regional metamorphism and metamorphogenetic ore formation, Izdat. "Nauka," Leningrad, 222-232 (in Russian).

Murata, K. J., Rose, H. J., Jr., Carron, M. K., and Glass, J. J. (1957) Systematic variation of rare-earths in cerium-earth minerals. Geochimica et Cosmochimica Acta 11, 141-161.

Nadezhdina, E. D. (1968) Some features of the accessory rare-earth mineralization in traps of the region of the source of the Tungus and Greater Botuobii Rivers (Siberian platform). In the volume, "Accessory minerals of igneous rocks," Izdat. "Nauka," Moscow, 1968, 257-265 (in Russian).

Neumann, H., and Nilssen, B. (1962) Lombaardite, a rare-earth silicate, identical with, or very closely related to, allanite. Norsk Geologisk Tidsskrift, 42, 277-286.

Orsa, V. I. (1965) Allanite from red pegmatitic granite of the Volryanka River basin (middle reaches of the Dneiper basin). Akad. Nauk Ukrain S.S.R., Ukrain Ofdel. Vees. Mineral. Obshich. 154-162 (in Russian).

Orsa, V. I., Eliscera, G. D., and Kazantseva, A. I. (1967) Rare-earth assemblages in the acessory minerals of the ancient crystalline rocks of the Middle Dnepr region. Geokhimiya 1967, 243-247; translation in Geochemistry International 1967, 170-173.

Papunen, H., and Lindsjo, O. (1972) Apatite, monazite, and allanite; three rare-earth minerals from Korsnas, Finland. Bulletin of the Geological Society of Finland 44, 123-129.

Pavlenko, A. S., Vairshtein, E. E., and Turanskaya, N. V. (1959) Certain regularities in the behabvior of rare-earths and yttrium in magmatic and post-magmatic processes. Geokhimia 1951, 291-309; translation in Geochemistry International 1959, 357-380.

Ploshko, V. V., and Bogdanova, V. I., (1963) Minerals of the epidote group in rocks of the Urushten magmatic complex, northern Caucasus. Trudy Mineralog. Muzeya Akad. Nauk S.S.S.R., 14, 122-139 (in Russian).

Ploshko, V. V., and Knyezeva, D. N. (1965) Rare-earths, yttrium, and thorium in post-magmatic process of acidic intrusions of the Urushten complex, northern Caucasus. Accessory Mineral Elements as Criteria of Cogenetic Metallogenesis, Izdef, "Naaka," Moscow, 146-152 (in Russian).

Popova, V. I., Bazhenova, L. F., and Polyakov, V. O. (1980) Orthite of Ilimen Mountain. Mineralog. Zhurnal. 2, 3, 73-82 (in Russian).

Protopopov, V. N. (1940) X-ray spectroscopic study of yttro-orthite, orthite, monazite, and cyrtolites of northern Karelie. Mat. Tsentral Nauch. Issled. Geol. Razvod. Inst., Geokhim. 5, 30-54 (in Russian).

Putalova, R. V. (1978) Accessory minerals of granitic intrusions of the Chingiz meganticlinorium. Izdat. "Nauka," Kazakh S.S.R., 1-150 (in Russian).

Quensel, P., and Alvfelst, O. (1945). Beryllium orthite (muromontite) from the Shulebode feldspar. Arkiv Kemi, Mineral., Geol. 18, 22, 1-17 (Swedish with English summary).

Rub, M. G., Ashikhmina, N. A., and Magidovich, T. S. (1965a) Accessory minerals as indicators of comagmaticity and metallogenic specialization of effusive, subvolcanic, and intrusive formations (northeastern U.S.S.R.). Izdat "Nauka," Moscow, 1965, 7-38 (in Russian).

Rub, M. G., Makeev, B. V., and Serezhnikov, A. I. (1965b) Rare-earth minerals of acid lavas as one of the indications of metallogenic specialization of magmatic complexes. Akad. Nauk S.S.S.R., Izvest., Ser. geol. 1965, 7, 21-37 (in Russian).

Sahama, T. G., and Vahatalo, V. (1939) The rare earth content of wiikite. Bull. Comm. Geol. Finlande 125, 97-109.

Sahama, T. G., and Vahatalo, V. (1941) X-ray spectrographic study of the rare earths in some Finnish eruptive rocks and minerals. Bull. Comm. Geol. Finlande, 126, 50-83.

Semenov, E. I. (1963) Mineralogy of the rare earths. Izdat. Akad. Nauk. S.S.S.R., 1-412 (in Russian).

Semenov, E. I. (1969) Mineralogy of the alkalic massif of Ilimausaaq, Greenland. Inst. Mineral., Geokhim., Kristallochim Redk. Elementov, Izdat. "Nauka," 1-164 (in Russian).

Semenov, E. I., and Barinskii, R. L. (1958) Characteristics of the composition of rare earths in minerals. Geokhimiya 1958, 314-333; translation in Geochemistry International1958, 398-419.

Semenov, E. I., and Khomyakov, A. P., (1981) Magnetic susceptibility of rare-earth minerals. Diagn. Diaagn. Svoistra Mineral., 1981, 88-83 (in Russian).

Semenov, E. I., Upendrah, R., and Subramahien, V. (1978) Rare-earth minerals of carbonatites, Tamil, Nadu, India. Jour. Geol. Soc. India, 19, 550-557.

Serdyuchenko, D. P., and Pap, A. M. (1969) Features of the composition and origin of allanite and titanite from crystalline rocks of the Byclorusse Precambrian. Doklady Akad. Nauk S.S.S.R., 185, 166-169 (in Russian).

Shiryaeva, V. A., and Shmakin, B. H. (1982) Composition of allanite from rare-earth pegmatites of the Baikel region. In the volume, Geocheimistry of rare-earth elements in endogenic processes, Izdat. "Nauka," Sibir. Otdel., 165-177 (in Russian).

Shmakin, B. M., and Shiryaeva, V. A. (1970) The composition of rare-earth minerals in muscovite pegmatites of eastern Siberia. Geokhimiya 1970, 1263-1268 (in Russian).

Shmakin, B. M., and Shiryaeva, V. A. (1971) Allanite and monazite of muscovite pegmatites of eastern Siberia. Zapiski Vses. Mineralog. Obsh., 100, 274-281 (in Russian).

Siivola, J. (1975) The lanthanoid content of some minerals from the Pyoronmaa pegmatite, Kangasala, Finland. Bulletin of the Geological Society of Finland, 276, 1-17.

Tikhonenkov, I. P., and Tikhonenkova, R. P. (1962) The mineralogy of the contact zones of the Lovozero massif. Trudy Inst. Mineral. Geokhim., Kristallokhim Redk. Elementov, 9, 3-35 (in Russian).

Tikhonenkova, R. P., and Kazakova, M. E. (1964) Allanite from metasomatites of a massif of nepheline syenites. Miner. Genet. Osobennost Sheheloch. Massiv 1964, 45-48 (in Russian).

Tskhelishvili, Ya. S. (1980) Accessory allanite from granitic rocks of Dar'yal massif. Soobsh. Akad. Nauk Gruz S.S.R., 99, 2, 397-400 (in Russian).

Tsvetkova-Goleva, V., and Karadzhova, B. (1968) Allanite from the Rila granites. Bulgar. Akad. Nauk, Izvest. Geol. Inst. Ser. Geokhim., Mineral., Petrog., 17, 111-121 (Bulgarian with English summary).

Vainshtein, E. E., Tugarinov, A. I., and Turanskaya, N. V. (1956b) Regularities in the distribution of rare earths in certain minerals. Geokhimiya 1956, 36-56, translation in Geochemistry International 1956, 159-178.

Vinogradov, A. N., and Elina, N. A. (1968) Distribution of rare earths in granitic rocks of the northwest part of the Kola Peninsula. Mat. Mineral Kol'sk Poluostr., 6, 80-92 (in Russian).

Vorontsov, A. E. (1972) Lower Paleozoic granitoids of the Bugul'min intrusive complex and their principal geochemical features (central part of eastern Sayen) In the volume, Geochemistry of rare elements in magmatic complexes of eastern Siberia, 216-296 (in Russian).

Zdorik, T. B., Kupriyanaova, I. I., and Kumskova, N. M. (1964) Crystalline allanite from some Siberian metasomatic rocks, Trudy Mineral. Muzeya Akad. Nauk S.S.S.R., 15, 208-214 (in Russian).

Zhabin, A. G., and Svyazhin, N. V. (1962) Concentrically zoned aggregates of rare-earth minerals from the alkalic complex of Vishnevye Mountains. Trudy Inst. Mineral., Geokhim., Kristallakhim Redk. Elementov, 9, 55-66 (in Russian).

Zhirov, K. K., Bandurkin, G. A., and Lavront'ov, Yu. G. (1961) The geochemistry of rare-earth elements in pegmatites of northern Karelii. Geokhimiya 1961, 895-1004; translation in Geochemistry International 1961, 1107-1118.

Znamenskii, E. B., Rekholainen, G. I., Popolitov, R. I., and Flerova, K. V. (1967) Geochemistry of rare earths in Proterozoic granitic rocks of eastern Sayan. Geol. Geofiz. 1967, 2, 137-140 (in Russian).

APPENDIX D

NATURAL ALLANITE ASSOCIATIONS

Appendix D. Natural Allanite Associations

Location	Host Rock	Associations*	Reference**
Irish Flats NE quad Meade County Kansas	ash-fall tuff	Chv, Qtz, Sa, Olg, Mag, Zrn	Izett and Wilcox (1968)
W. side Pueblo Mesa Arriba County New Mexico	ash-fall tuff	Chv, Qtz, Sa, Pl, Fa, Mag, Zrn, Brz	Izett and Wilcox (1968)
Kremmling quad Grand County Colorado	ash-fall tuff	Qtz, Sa, Olg, Bt, Hbl, Mag, Ilm, Ttn, Zrn, Ap	Izett and Wilcox (1968)
Tweed Shield volcano New South Wales	vitrophyric rhyolite	Qtz, Sa, Olg, Ilm, Zrn, Fe-Hyp	Duggan (1976)
Sandy Braes Northern Ireland	obsidian	Qtz, altered Fa, Bt, Zrn, Sa, Olg	Brooks et al. (1981)
Nutarmint, Avigeit West Greenland	granite	Fld, Hbl, Zrn	Frondel (1964)
McMurray Meadows pluton Sierra Nevada Batholith California	granite	Ttn	Sawka et al. (1984)
Alkalic complex Vishnevyye Mountains USSR	granite	Bri, Bas, Mnz	Yes'kova et al. (1964)
Hercynian granite Vosges France	subalkaline potassic granite	Pl, Qtz, Hbl, Ttn Ap, Zrn, Tho	Pagel (1982)
Mount Wheeler Mine area Nevada	granodiorite (CaO > 4.0%); Qtz monzanite (CaO < 0.7%)	Ap, Ttn, Zrn, Ep, Mag Mnz, Ilm, Grt	Lee and Bastron (1967)
Kenora-Vermillion Bay area Northwestern Ontario	syenite, gneiss; granodiorite	Ep, Bt, Hbl, Ttn, Mag; Bt	Morin (1977)
Huddersfield Twp. Pontiac County Quebec, Canada	pegmatite	Phl, Ap	Frondel (1964)

Appendix D. Natural Allanite Associations, continued.

Glen Bay Gabbro St. Kilda Scotland	pegmatite	Fe-Aug, Amp, Chl, Mag, Ilm, Qtz, Olg, Or, Bt, Ep, Ttn, Ap, Zrn, Zrk	Harding et al. (1982)
Dickens Twp. Nipissing Dist. Ontario, Canada	pegmatite	Fld, Mc, Qtz	Frondel (1964)
La Marche Mine Gateneau County Quebec, Canada	pegmatite	Ttn, Cal, Fld, Ap,Mi, Bt, Mo	Frondel (1964)
Lyndoch Twp. Renfrew County Ontario, Canada	pegmatite	Qtz, Fld	Frondel (1964)
Twin Valley Mine Pontiac County Quebec, Canada	pegmatite	Ap, Fl, Phl	Frondel (1964)
Argenteuil County Quebec, Canada	pegmatite	Ilm, Mnz	Frondel (1964)
Woburn, Massachusetts	pegmatite in gneiss	Fld, Ep	Frondel (1964)
Kingman Feldspar Mine Mohave County Arizona	pegmatite in granite, gneiss	Bt, Ms, Grt	
Mineral X Claim Mohave County Arizona	pegmatite in biotite schist	Frg, Zrn, Fl, Ep, Thl	
Hillside Group and Quartz Mountain Mohave County Arizona	pegmatite in gneiss	Eux, Ply, Mnz	
Signal District Mohave County Arizona	pegmatite in gneiss	Sam, Eux	
White Picacho District Maricopa and Yavapai Co. Arizona	pegmatite in schist, gneiss,	Mnz, Mic, Pyr, Bt, Ms, Fl, Euc, Brl, Eux, Mag, Xen	

Appendix D. Natural Allanite Associations, continued.

Buckeye Maricopa County Arizona	pegmatite in gneiss	Eux, Mag, Xen	
Pacoima Canyon Los Angeles County California	pegmatite in norite; mmd norite	Qtz, Bt, Olg, Zrn, Ap, Brl, Pth; Hbl, Bt, Olg, Zrn, Grt, Ttn, Ilm, carbonate	
Pomona Tile Quarry San Bernadino County California	pegmatite in Hbl/Bt schist	Ep, Bt, Ilm, Hem, Mag, Ttn, Mnz, Eux, Cyr	
Alger Creek San Bernadino County California	pegmatite in granite- gneiss	Bt, Mag, Zrn, U-Tho	
New York Mountains Moore, California	pegmatite in schists,	Mc, Qtz, Bt, Ms, Ab, Tur, Chl	Volborth (1962)
Quartz Creek Area Gunnison County Colorado	pegmatite in granite, monzanite, Hbl-gneiss	Mnz, Ms, Pl, Bt, Lpd Mc, Pyr, Nb-Ta-U mineral	
Burroughs Mine Jefferson County Colorado	pegmatite in Bt-gneiss	Bt, Tur, Grt, Xen, Brl, Mnz, Eux, Col, Tan, Gad?	
South Platte Area Jefferson County Colorado	pegmatite in granite	Bt, Qtz,Pl, Fl, Flc, Y-Fl, Gad, Frg, Cyr, Tho, Sam	
Crystal No. 8 Chaffee County Colorado	pegmatite in granite	Qtz, Mc, Pl, Grt, Bt, Eux	
Clora May Mine Chaffee County Colorado	pegmatite	Bt, Grt, Eux, bismuth minerals	
Guffey Area Park County Colorado	pegmatite in granite Bt-gneiss	Bt, Mag, Mnz, Eux U-Tho	
Teller Mine Park County Colorado	pegmatite in granite	Gad, Fl, Xen, Sam?, Eux?, Tho	

Appendix D. Natural Allanite Associations, continued.

Cotopaxi Area Fremont County Colorado	pegmatite in granite	Bt, Mag, Grt, Fl, Hbl, Dov, Kns, Xen, Sam, Eux, Cyr, Urn	
Black Cloud Teller County Colorado	pegmatite in granite	Bt, Gad, Mnz, Y-Tan, Sam, Frg, Tho	
Big Jureano Creek Lemhi County Colorado	pegmatite in gneiss	Bt	
Mineral Hill District Lemhi County Colorado	pegmatite in gneiss, amphibolite	Mnz	
Boulder Creek batholith Colorado	Qtz monzonite, granodiorite	Bt, Ep, Qtz, Fld, Zrn	Hickling et al. (1970)
Silver Plume granite Colorado	granite	Bri*, Mnz	Goddard and Glass (1940)
Standpipe Hill Quarry Sagadahoc County Maine	pegmatite in Qtz-mi schist	Bt, Grt, Mag, Pl, Ms, Hem, Brl, Sam, Mnz, Aut, Mc	
Rollstone Hill (McCauliff Quarries) Worcester County Massachusetts	pegmatite in granite	Bt, Grt, Ap, Ttn, Fl, Ms, Tur, Spd, Brl, Py, Mo, Ccp, Col, Cst, Pol Aut, Urn, phosphate minerals	
Blueberry Mountain Middlesex County Massachusetts	pegmatite in granodiorite	Bt, Hbl, Mag, Ttn, Zrn, Tur, Grt, Pl, Py, Ccp, Mo, Sp, Cyr, Tho	
Cape Ann Area Essex County Massachusetts	pegmatite in granite, syenite	Cal, Fa, Fl, Hbl, Py, Po, Gn,Sp, Mo, Y-Cer, Tan, Frg, Gad, Tho, cyrt, Lep, Dan, Fe-oxides	
Janney Pegmatites Silver Bow County Montana	pegmatite in granite	Bt, Ep, Tur, Grt, Py	
Deer Lodge Claims Storey County Nevada	pegmatite in Bt-granite	Chv	

Appendix D. Natural Allanite Associations, continued.

Gold Butte Pegmatite District Clark County Nevada	pegmatite in granite	Qtz, Ab, Ms, Bt, Chl, Zrn, Pth, Mag, oxides	Volborth (1962)
Cranberry Lake Charlotte Mine Sussex County New Jersey	pegmatite in granite, gneiss, pyroxenite, amphibolite	Zrn, Ap, Hbl, Mag, Fl,Py, Frg, Spn, Tho, U-Tho, Urn	
Gold Hill Area Hildalgo County New Mexico	pegmatite in granite	Bt, Grt, Mag, Fl, Ms, Brl, Sam, Eux	
McLear Pegmatite St. Lawrence New York	pegmatite in marble	Bt-Phl, Diop, Act-Tr, Tal, Ttn, Cal, Ap, Mag, Hem, Lm, Srp, Urn, Mo	
Talcville St. Lawrence County New York	pegmatite in marble	Py, Mo, Urn	
Benson Mines St. Lawrence County New York	pegmatite in granite, gneiss	Mag, Trb	
Batchellerville Saratoga County New York	pegmatite in gneiss, amphibolite	Bt, Ap, Grt, Fl, Tur, Ms, Brl, Cer, Urn	
Crown Point Spar Co. Essex County New York	pegmatite in amphibolite	Bt, Grt, Hbl, Tur	
Spar Bed Hill Quarry Essex County New York	pegmatite in charnockitic gneiss	Bt, Hbl, Tur, Pl, Mag, Toz, Po, Spd, Mnz, Cyr, Frg, Tho, Urn, Uph, other accessory minerals	
Corinth Feldspar Co. Saratoga County New York	pegmatite in Bt-Hbl gneiss, syenite gneiss	Bt, Grt, Zrn, Uph, U-mineral	

Appendix D. Natural Allanite Associations, continued.

Phillips Mine- Camp Smith Putnam County New York	pegmatite in Hbl-gneiss, diorite	Mag, Po, Py, Hbl, Urn
Cattel Estate Putnam County New York	pegmatite granite,	Py, Hbl, Urn
Champin North Carolina	pegmatite	Ms, Grt
Trolley Bent North Carolina	pegmatite	Ms, Bt, Grt, Ap
Tantrough North Carolina	pegmatite	Ms, Bt, Grt, Ap
Francis Ogle North Carolina	pegmatite	Ms, Grt
Grassy Knob North Carolina	pegmatite	Ms, Bt, Grt
Elkins North Carolina	pegmatite	Ms, Bt, Grt
Fox North Carolina	pegmatite	Bt, Tur, Grt
Abernathy North Carolina	pegmatite	Ms, Grt, Ap
Little Bear Creek North Carolina	pegmatite	Ms, Grt
Jeff Cut North Carolina	pegmatite	Ms, Bt, Grt
Lick Ridge North Carolina	pegmatite	Ms, Grt, Ap
Branch North Carolina	pegmatite	Ms, Grt
Slippery Elm North Carolina	pegmatite	Ms, Grt

Appendix D. Natural Allanite Associations, continued.

Powdermill Roughs Mine North Carolina	pegmatite in gneiss	Ms, Grt, Ap Bt, T, ser
Meadow North Carolina	pegmatite	Ms, Bt, Grt
Table : Natural allanite, cont		
Lincoln Rock North Carolina	pegmatite	Ms, Grt
Salley Knob North Carolina	pegmatite in gneiss	Grt, Ms, mult. oxides Thu, Sam
Ray Mica Mine Yancy County North Carolina	pegmatite in mica gneiss	Bt, Grt, Ap, Tur, Ms, Mnz, Col-Tan, Cyr, sec. U minerals
Deake Mine Mitchell County North Carolina	pegmatite in granite, Bt-Hbl gneiss	Bt, Ap, Ms, Col-Tan, sec. U minerals
Pink Mitchell County North Carolina	pegmatite in granite	Grt, Ms, Col-Tan, mult. oxides
Pine Mountain Mitchell County North Carolina	pegmatite in granite, Bt-Hbl gneiss	Grt, Ms, sec. U minerals
McKinney Mine Mitchell County North Carolina	pegmatite in mica gneiss	Grt, Ap, Ms, Col-Tan, Urn, Brl, Ep, Py, Thu, Sam, Trb, Aut, Cv
Johnson North Carolina	pegmatite	Ms, Grt, Ap
Franklyn North Carolina	pegmatite	Ms, Grt, Ap
Doublehead North Carolina	pegmatite	Ms, Bt, Grt
Knight Mine Rockingham County North Carolina	pegmatite in Bt-Qtz schist	Ms, Grt, Urn, Aut

Appendix D. Natural Allanite Associations, continued.

Black Mine North Carolina	pegmatite	Ms, Bt, Ap
Butler Mine North Carolina	pegmatite in mi gneiss	Ms, Grt
Charles Rock Mine North Carolina	pegmatite in Hbl gneiss	Ms, Bt, Grt, ser
Tom Carpenter (Old Hennessey Mine) North Carolina	pegmatite in mi gneiss	Ms, Bt, Vrm
Charles Robinson Mine North Carolina	pegmatite in mi gneiss	Brl, Grt, Ap, Ms
Black Dixie Mine North Carolina	pegmatite in mi gneiss	Ms, Bt, Grt, Ep, Ser, Vrm
Speck Mine North Carolina	pegmatite in mi gneiss	Bt, Ms, Grt, Ep, Vrm
Spider Mine North Carolina	pegmatite in Bt gneiss	Ep, Grt, Ms
Charlie Young Mine North Carolina	pegmatite in mi gneiss	Ep, Grt, Ms, Thu, Vrm
Charons Garden Oklahoma	pegmatite in granite	Zrn
Hale Spring Pegmatite Oklahoma	pegmatite	Zrn, Agt, Rbk
Clear Creek Burnet County Texas	pegmatite in gneiss	Frg, Gad, Sam, Urn, Cyr, Bt, Mag, Fl, Grt, Bas, Zrn, Py, Pyl, Ytt
Rode Ranch Llano County Texas	pegmatite in granite	Bt, Mag, Grt, Bas, Frg, Gad, Be-hydroxide
Snow Mountain Bennington County Vermont	pegmatite in greenstone	Mag

Appendix D. Natural Allanite Associations, continued.

Rutherford Mine Amelia County Virginia	pegmatite in Bt-gneiss, Hbl gneiss	Bt, Ms, Mnz, Pl, Grt, Toz, Fl, Brl, Mic, Frg, Cst, Col-Tan	
Morefield Mine Amelia County Virginia	pegmatite Bt-Hbl schist	Bt, Ms, Pl, Mnz, Fl, Tur, Brl, Mic, Cst, Col	
Champion Amelia County Virginia	pegmatite in mi-schist, Hbl schist	Grt, Tur, Mnz, Zrn, Gn, Py, Ccp, Ms, mic, Pyr, Cal, Brl, Col-Tan, Apy, Scd	
Peterson Grant County Washington	pegmatite in Bt-granite	Bt, Chl, Urn, Eux, Cyr, Brn	
Platt Pegmatite Carbon County Wyoming	pegmatite	Bt, Ms, Grt, Tur, Pl, Mnz, Eux	
Ytterby Sweden	pegmatite	Bt, Gad, Frg, Cyr, Xen, Ytc	
MacDonald Feldspar Mine Ontario, Canada	pegmatite	Ab, Mc, Qtz	
Sui-chung District China	pegmatite	Bt, Ab, Zrn, Sam, Eux, Frg, Bet, Thg	
Iveland Sweden	pegmatite	Bt, Ttn, Mnz, Xen, Sam, Urn, Mc, Gad, Frg, Cyr, Ytt	
Footwall of Sullivan lead-zinc ore body British Colombia Canada	Qtz vein	Tur, Qtz, Cal	Campbell and Ethier (1984)
Bramans Western Alps Savoy France	vein in schist, ss	Ab, Hem	Bocquet (1975)
Malaya Laba River Peredovoy Range Northern Caucasus	vein between granite and actinolite rock	Ap, Zrn, REE-phosphate	Ploshko (1958)

Appendix D. Natural Allanite Associations, continued.

Magnet Cove Arkansas	Ap-Py vein	Ap, Py	Murata et al. (1957)
Kallmorberg Mine Norberg Sweden	amph-skarn; talc gouge	Tr-Act; Tal, Act, Phl, Qtz, Mag	Holmqvist (1975)
Essexville New York	magnetite deposit	Fld	Frondel (1964)
Footwall of Sullivan lead-zinc ore body British Colombia Canada	Qtz vein	Tur, Qtz, Cal	Campbell and Ethier (1984)
Luangwa Bridge area Zambia	gneiss; aggregate	Ttn, Qtz, Mnz, Ap Ilm, Bas, Aes-Pri	Cech et al. (1972)
Paritu Coromandel County New Zealand	hornfelses	Qtz, Fld, Bt, Olg, Ap, Tur, Py	Black (1970)

Appendix D. Natural Allanite Associations, continued.

---

* mineral abbreviations as follows:

Ab	albite	Aes	aeschynite	Agt	aegirine-augite
Amp	amphibole	Ap	apatite	Apy	arsenopyrite
Aug	augite	Aut	autunite	Bas	bastnasite
Bet	betafite	Bri	britholite	Brl	beryl
Brn	brannerite	Brz	bronzite	Bt	biotite
Cal	calcite	Ccp	chalcopyrite	Chl	chlorite
Chv	chevkinite	Col	columbite	Cv	covellitye
Cst	cassiterite	Cyr	cyrtolite	Dan	danalite
Dov	doverite	Ep	epidote	Euc	euclase
Eux	euxenite	Fa	fayalite	Fl	fluorite
Flc	fluocerite	Fld	feldspar	Frg	fergusonite
Gad	gadolinite	Gn	galena	Grt	garnet
Hbl	hornblende	Hem	hematite	Hyp	hypersthene
Ilm	Ilmenite	Kns	Kainosite	Lep	lepidomelane
Lm	limonite	Lpd	lepidolite	Mag	magnetite
Mc	microcline	Mi	mica	Mic	microlite
Mnz	monazite	Mo	molybdenite	Ms	muscovite
Olg	oligoclase	Phl	phlogopite	Pl	plagioclase
Ply	polycrase	Po	pyrrhotite	Pol	pollucite
Pri	priorite	Pth	perthite	Py	pyrite
Pyl	pyrolusite	Qtz	quartz	Rbk	riebeckite
Sa	sanidine	Sam	samarskite	Scd	scorodite
Sp	sphalerite	Spd	spodumene	Spn	spencite
Srp	serpentine	Tan	tantalite	Thg	thorogummite
Thl	thalenite	Tho	thorite	Thu	thulite
Tlc	talc	Toz	topaz	Tr	tremolite
Trb	torbenite	Ttn	titanite	Tur	tourmaline
Uph	uranophane	Urn	uraninite	Vrm	vermiculite
Xen	xenotime	Ytc	yttrocrasite	Ytt	yttrotantalite
Zrn	zircon	Zrk	zirkelite		

**unless otherwise noted, the reference is Adams (1967).

Appendix D. Natural Allanite Associations, continued.

Adams, J. W., Arengi, J. T. and Parrish, I. S. (1980) Uranium- and Thorium-Bearing Pegmatites of the United States. Derry, Michener and Booth, Inc. Golden, Colorado, 313 pages.

Black, P. M. (1970) A note on the occurrence of allanite in hornfelses at Paritu, Coromandel County. New Zealand Journal of Geology and Geophysics, 13, 343-345.

Brooks, C. K., Henderson, P. and Ronsbo, J. G. (1981) Rare-earth partition between allanite and glass in the obsidian of Sandy Braes, Northern Ireland. Mineralogical Magazine, 44, 157-160.

Campbell, F. A. and Ethier, V. G. (1984) Composition of allanite in the footwall of the Sullivan Orebody, British Columbia. Canadian Mineralogist, 22, 507-511.

Cech, F., Vrana, S. and Povondra, P. (1972) A nonmetamict allanite from Zambia. Neues Jb. Miner. Abh., 116, 208-223.

Duggan, M. B. (1976) Primary allanite in vitrophyric rhyolites from the Tweed Shield Volcano, northeastern New South Wales. Mineralogical Magazine, 40, 652-653.

Frondel, J.W. (1964) Variation of some rare earths in allanite. American Mineralogist, 49, 1159-1177.

Goddard, E. N. and Glass, J. J. (1940) Deposits of radioactive cerite near Jamestown, Colorado. American Mineralogist, 25, 381-404.

Griswold, G. B. (1959) Mineral deposits of Lincoln County, New Mexico. New Mexico Bureua of Mines and Mineral Resources, 67, 117 p.

Harding, R. R., Merriman, R.J. and Nancarrow, P.H.A. (1982) A note on the occurrence of chevkinite, allanite, and zirkelite on St. Kilda, Scotland. Mineralogical Magazine, 46, 445-448.

Hickling, N. L., Phair, G., Moore, R. and Rose, H. J., Jr. (1970) Boulder Creek Batholith, Colorado. Part I. Allanite and its bearing upon age patterns. Geological Society of America Bulletin, 81, 1973-1994.

Holmqvist, A. (1975) Low 2-V allanite and Mg-bearing allanite from the Kallmorberg mine, Norberg, Sweden. Geologiska Foreningens i Stockholm Forhandlingar, 97, 162-166.

Izett, G. A. and Wilcox, R. E. (1968) Perrierite, chevkinite, and allanite in upper Cenozoic ash beds in the western United States. American Mineralogist, 53, 1558-1567.

Lee, D. E. and Bastron, H. (1967) Fractionation of rare-earth elements in allanite and monazite as related to geology of the Mt. Wheeler Mine area, Nevada. Geochimica et Cosmochimica Acta, 31, 339-356.

Morin, J. A. (1977) Allanite in granitic rocks of the Kenora-Vermilion Bay area, Northwestern Ontario. Canadian Mineralogist, 15, 297-302.

Murata, K. J., Rose, H. J., Jr., Carron, M. K., and Glass, J. J. (1957) Systematic variation of rare-earth elements in cerium-earth minerals. Geochimica et Cosmochimica Acta, 11, 141-161.

Appendix D. Natural Allanite Associations, continued.

Pagel, M. (1982) The mineralogy and geochemistry of uranium, thorium, and rare-earth elements in two radioactive granites of the Vosges, France. Mineralogical Magazine, 46, 149-161.

Ploshko, V. V. (1958) Accessory ortholite from actinolite rocks of the Malaya Laba River. Izvestiya Akad. Nauk SSSR., Ser. Geol, 96-100.

Rao, A. T. (1976) Study of the Apatite-Magnetite veins near Kasipatnam, Visakhapatnam District, Andrha Pradesh, India. Tschermaks Mineral. Petrogr. Mitt., 23, 87-103.

Sawka, W. N., Chappell, B. W. and Norrish, K. (1984) Light-rare-earth-element zoning in sphene and allanite during granitoid fractionation. Geology, 12, 131-134.

Volborth, A. (1962) Allanite pegmatites, Red Rock, Nevada compared with allanite pegmatites in Southern Nevada and California. Economic Geology, 57, 209-216.

Yes'kova, Ye. M. and Ganzeyev, A. A. (1964) Rare earth elements in accessory minerals of the Vishnev Mountains. Geochemistry, 6, 1152-1163.

APPENDIX E

^{57}Fe MÖSSBAUER DATA AND SPECTRA FOR SYNTHETIC ALLANITES, NATURAL ALLANITES AND AN EPIDOTE

For each spectrum, the x-axis is velocity in mm/sec and the y-axis is percent absorption. The curve fits are ____ for Fe^{2+} in the A sites, ... for Fe^{2+} in the M sites, and ---- for Fe^{3+} in the M sites. Table E1 summarizes the spectral data for the natural samples.

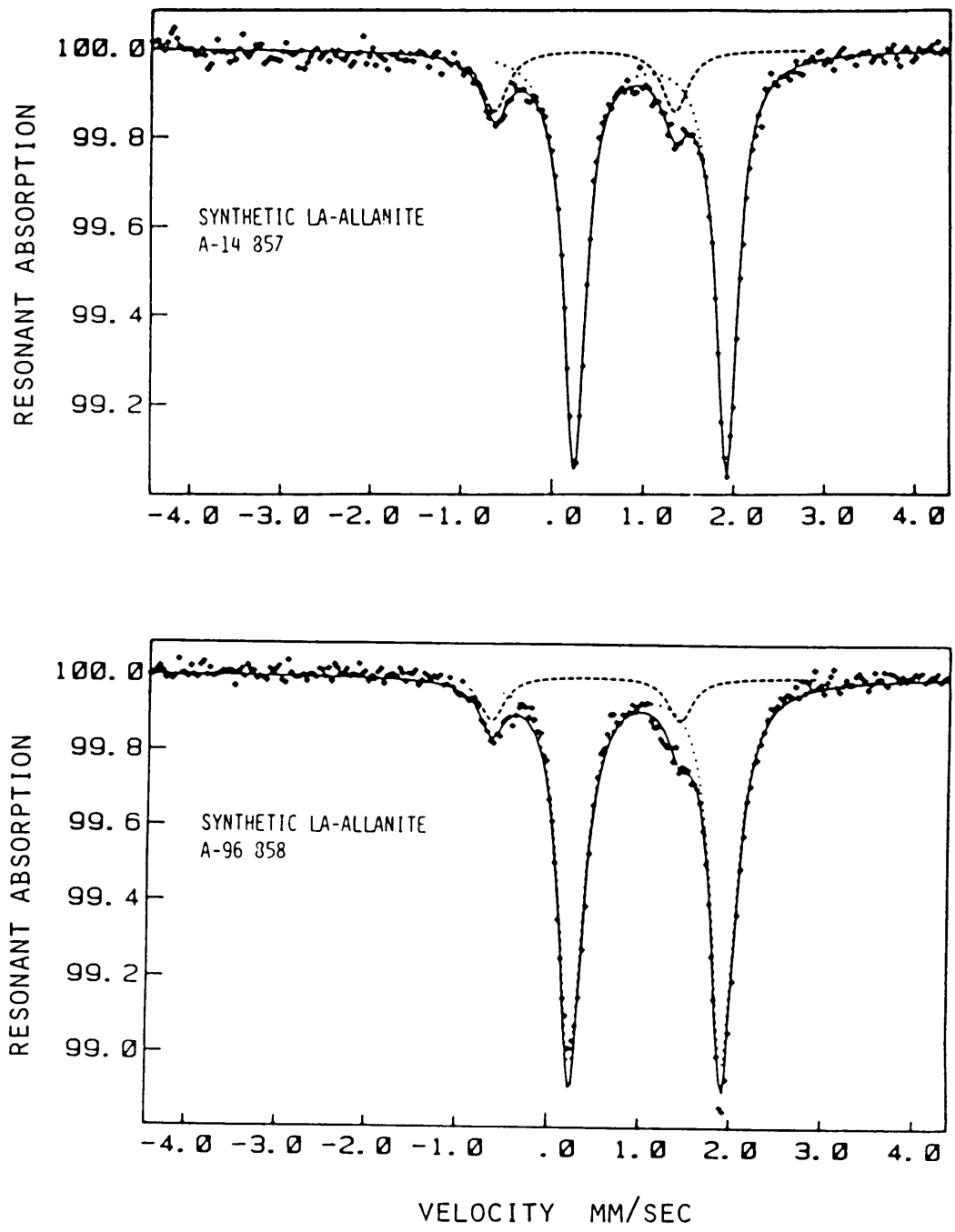
100.0
99.8
99.6
99.4
99.2
99.0
RESONANT ABSORPTION
SYNTHETIC LA-ALLANITE
A-14 857
SYNTHETIC LA-ALLANITE
A-96 858
-4.0 -3.0 -2.0 -1.0 .0 1.0 2.0 3.0 4.0
VELOCITY MM/SEC

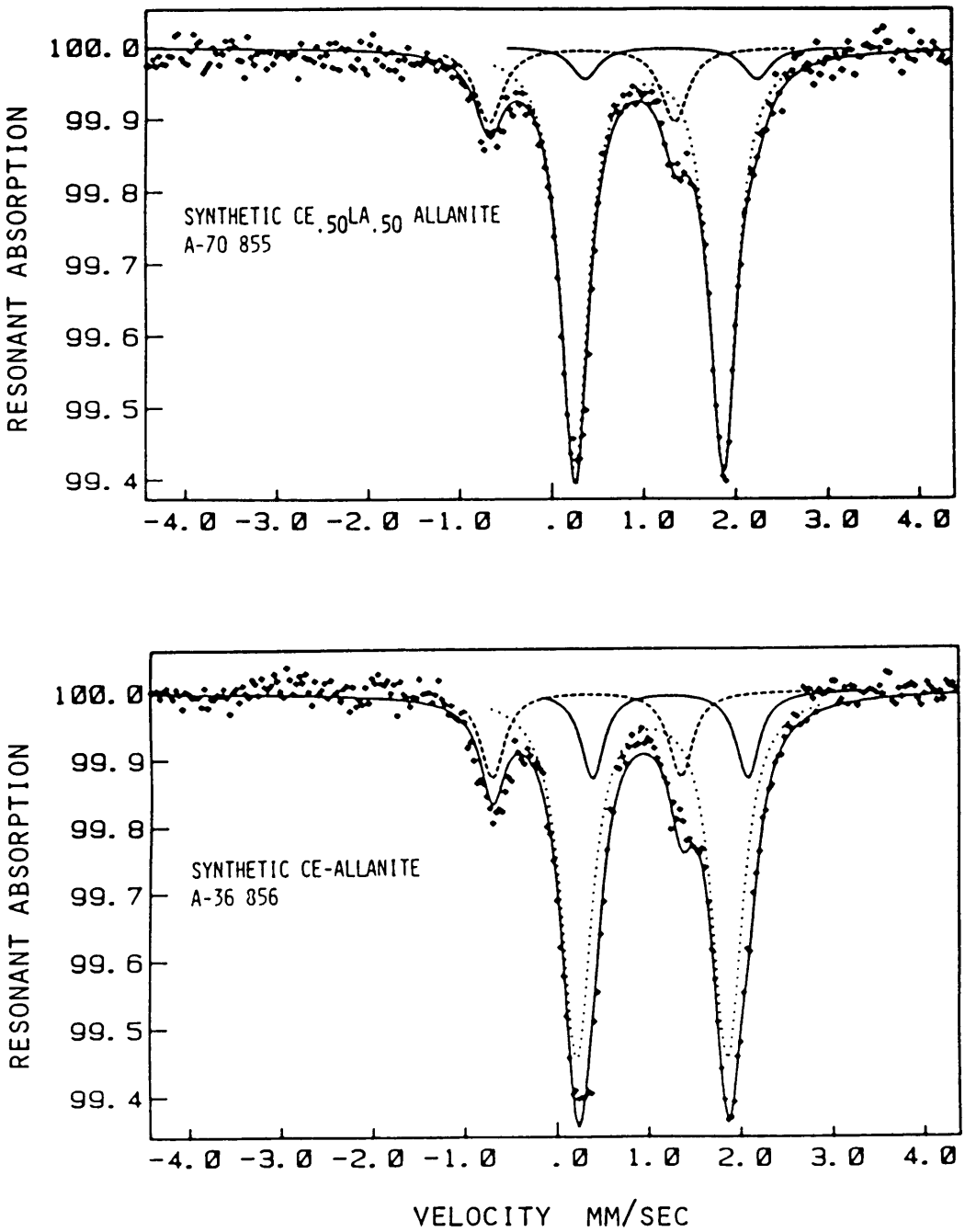
RESONANT ABSORPTION
100.0
99.9
99.8
99.7
99.6
99.5
99.4
SYNTHETIC CE.50LA.50 ALLANITE
A-70 855
-4.0 -3.0 -2.0 -1.0 .0 1.0 2.0 3.0 4.0
RESONANT ABSORPTION
100.0
99.9
99.8
99.7
99.6
99.5
99.4
SYNTHETIC CE-ALLANITE
A-36 856
-4.0 -3.0 -2.0 -1.0 .0 1.0 2.0 3.0 4.0
VELOCITY MM/SEC

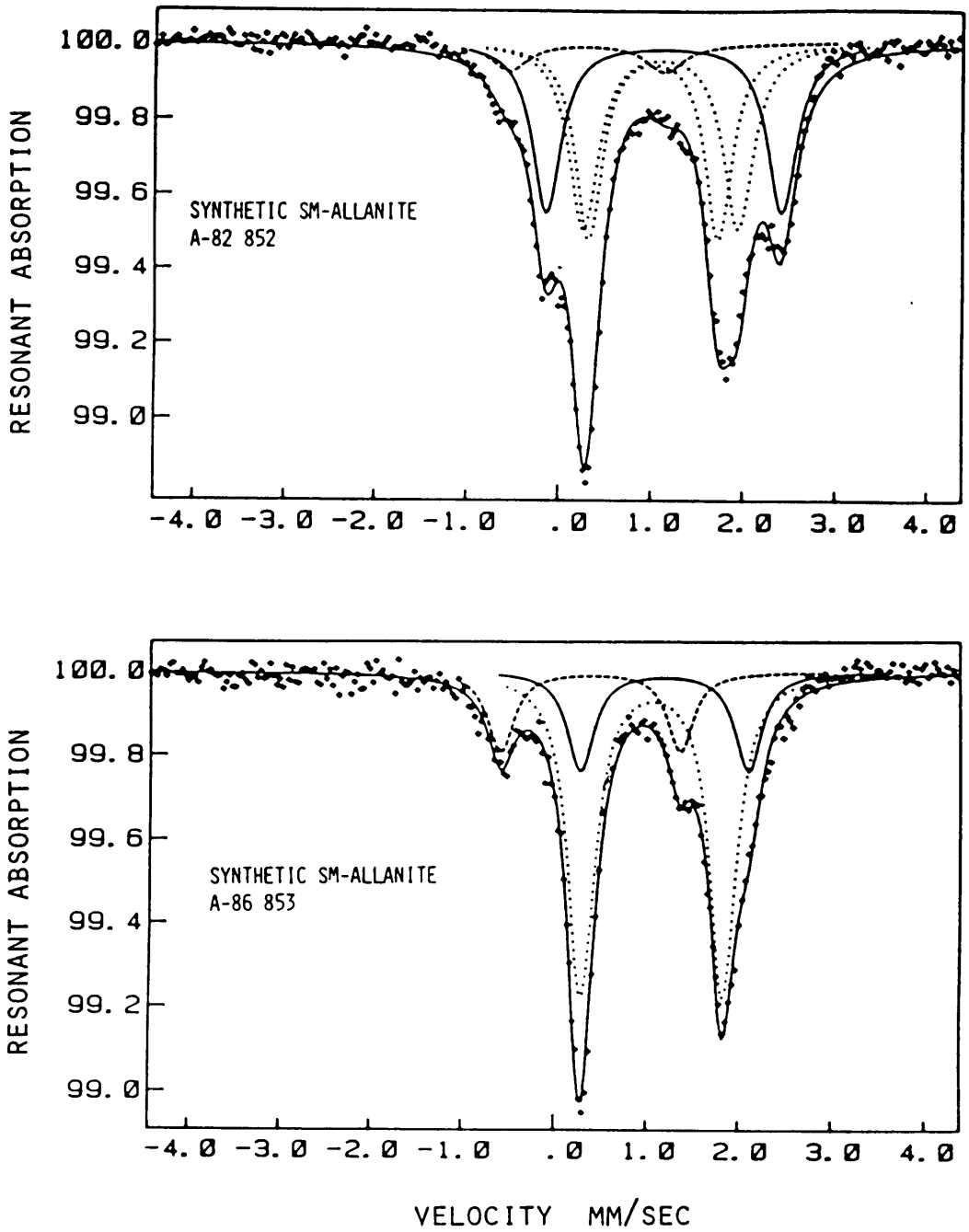
100.0
99.8
99.6
99.4
99.2
99.0
RESONANT ABSORPTION
SYNTHETIC SM-ALLANITE
A-82 852
-4.0 -3.0 -2.0 -1.0 .0 1.0 2.0 3.0 4.0
100.0
99.8
99.6
99.4
99.2
99.0
RESONANT ABSORPTION
SYNTHETIC SM-ALLANITE
A-86 853
-4.0 -3.0 -2.0 -1.0 .0 1.0 2.0 3.0 4.0
VELOCITY MM/SEC

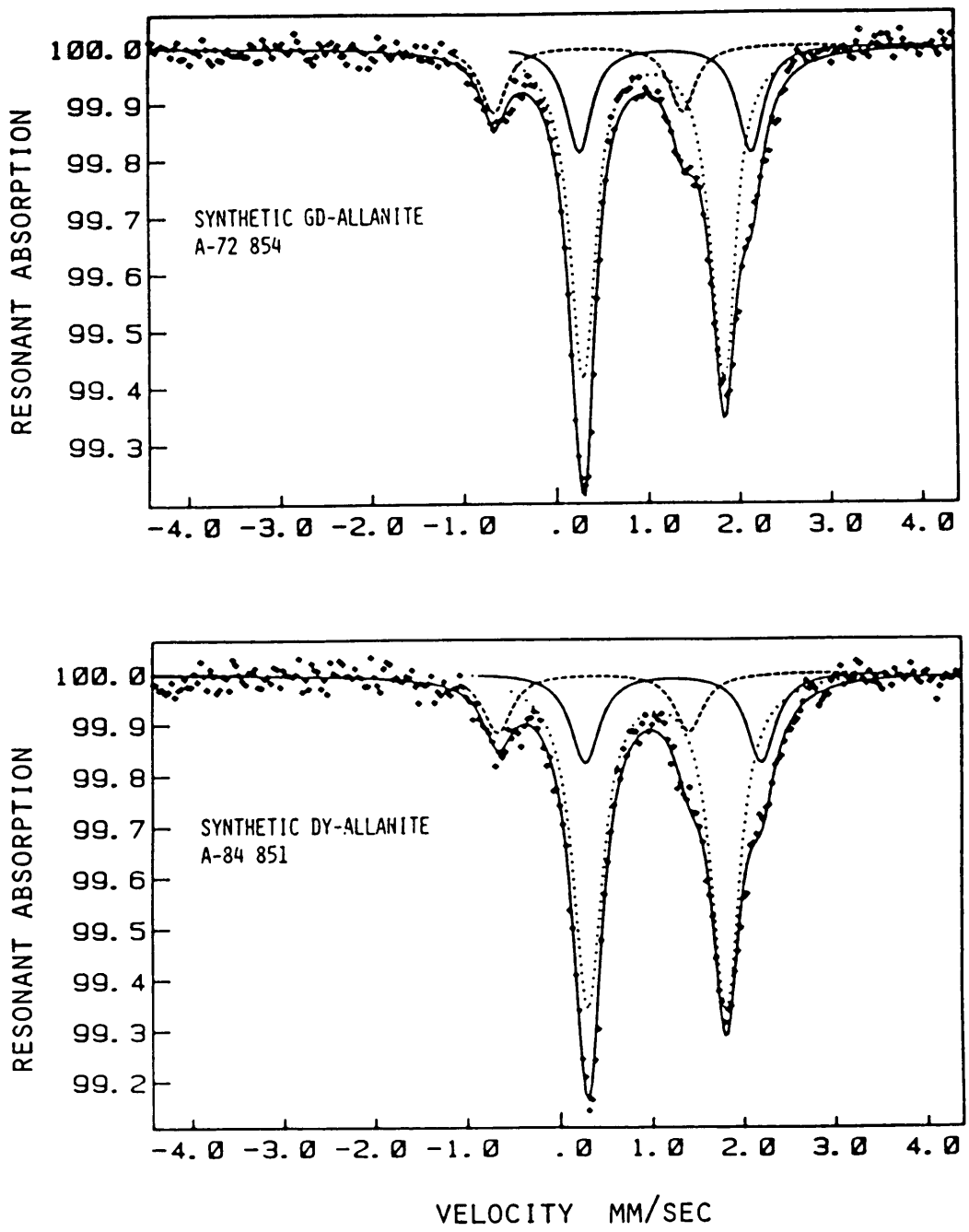
100.0
99.9
99.8
99.7
99.6
99.5
99.4
99.3
RESONANT ABSORPTION
SYNTHETIC GD-ALLANITE
A-72 854
-4.0 -3.0 -2.0 -1.0 .0 1.0 2.0 3.0 4.0
100.0
99.9
99.8
99.7
99.6
99.5
99.4
99.3
99.2
RESONANT ABSORPTION
SYNTHETIC DY-ALLANITE
A-84 851
-4.0 -3.0 -2.0 -1.0 .0 1.0 2.0 3.0 4.0
VELOCITY MM/SEC

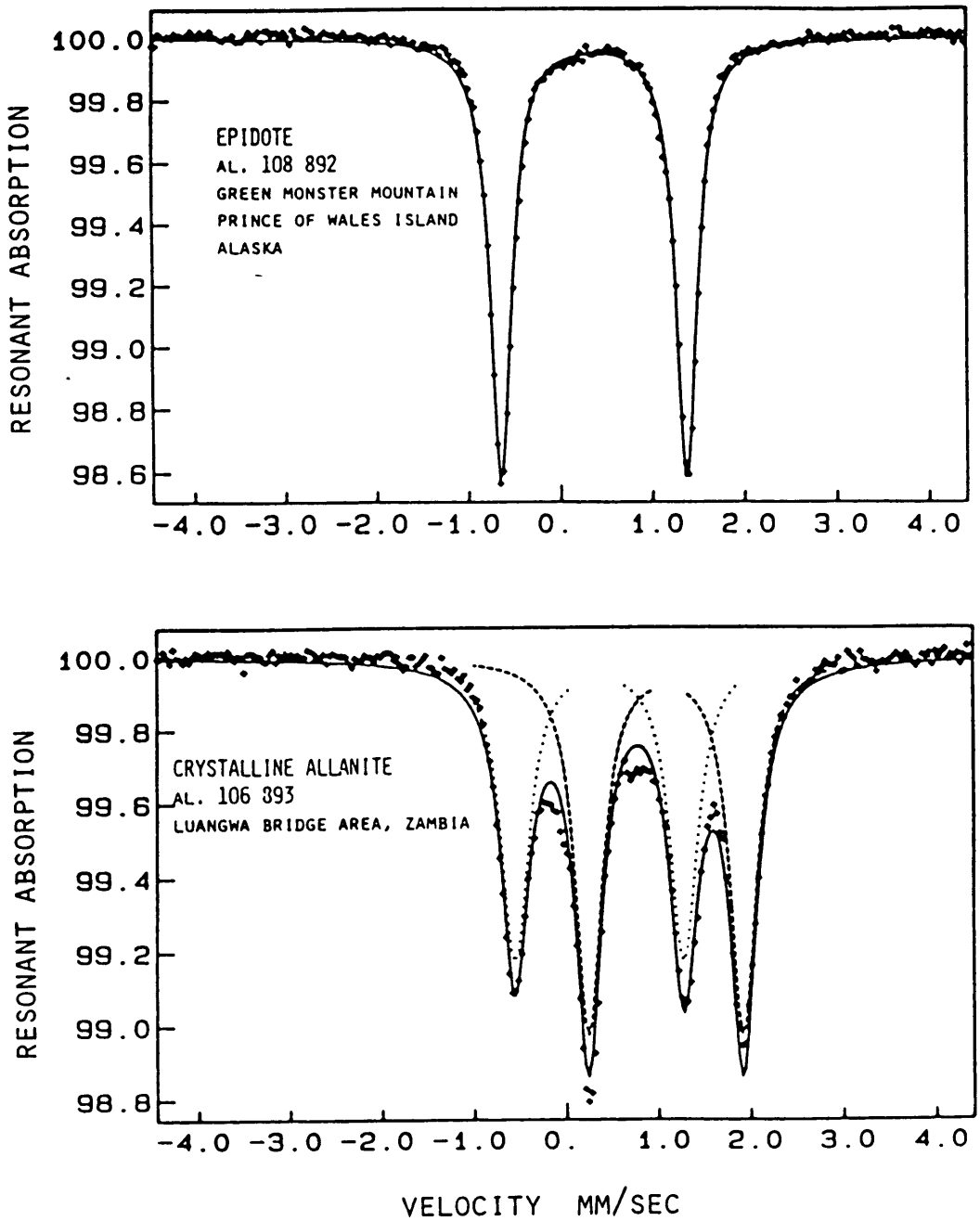
EPIDOTE
AL. 108 892
GREEN MONSTER MOUNTAIN
PRINCE OF WALES ISLAND
ALASKA
CRYSTALLINE ALLANITE
AL. 106 393
LUANGWA BRIDGE AREA, ZAMBIA
RESONANT ABSORPTION
100.0
99.8
99.6
99.4
99.2
99.0
98.8
98.6
-4.0 -3.0 -2.0 -1.0 0. 1.0 2.0 3.0 4.0
VELOCITY MM/SEC

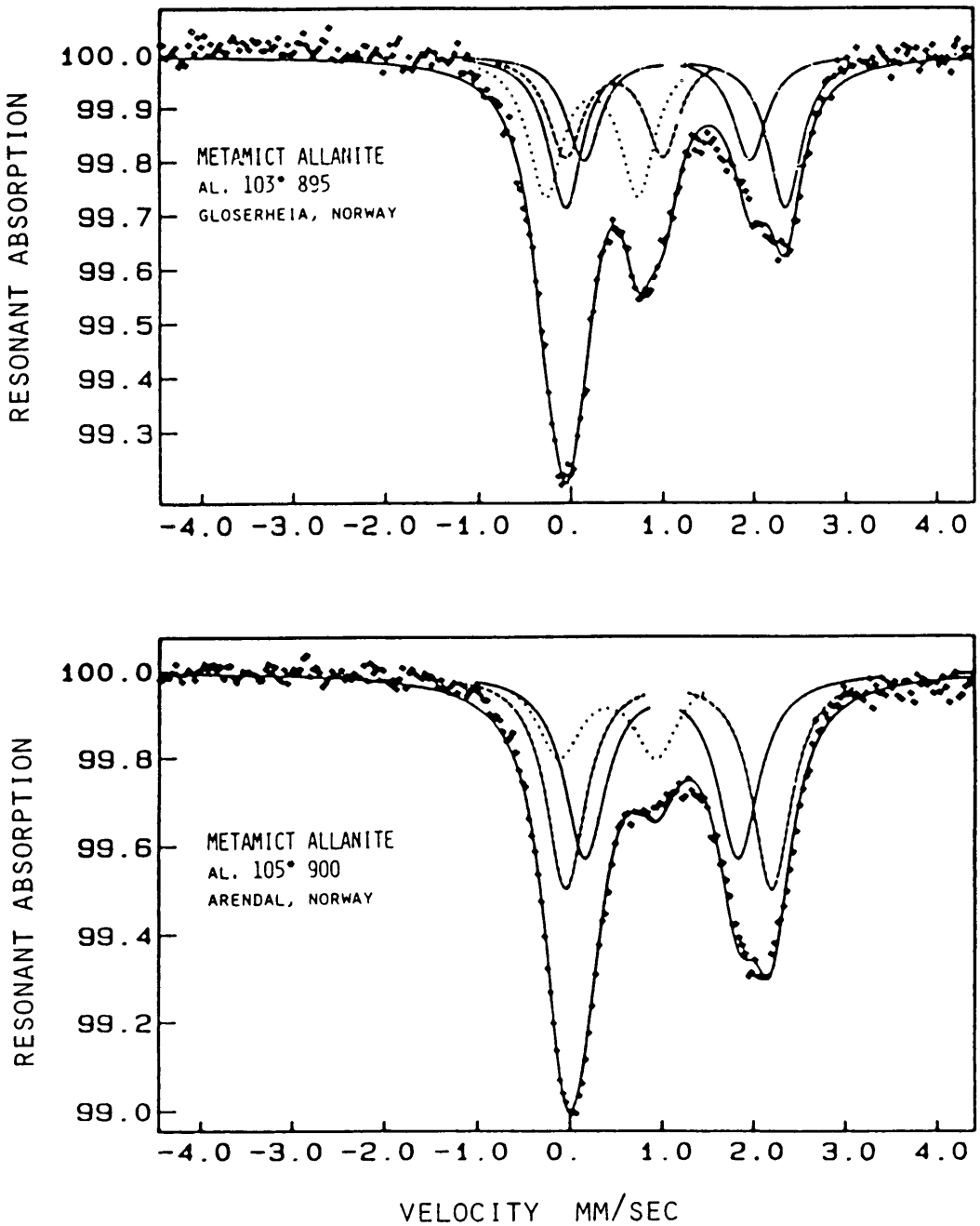
RESONANT ABSORPTION
100.0
99.9
99.8
99.7
99.6
99.5
99.4
99.3
METAMICT ALLANITE
AL. 103° 895
GLOSERHEIA, NORWAY
-4.0 -3.0 -2.0 -1.0 0. 1.0 2.0 3.0 4.0
RESONANT ABSORPTION
100.0
99.8
99.6
99.4
99.2
99.0
METAMICT ALLANITE
AL. 105° 900
ARENDAL, NORWAY
-4.0 -3.0 -2.0 -1.0 0. 1.0 2.0 3.0 4.0
VELOCITY MM/SEC

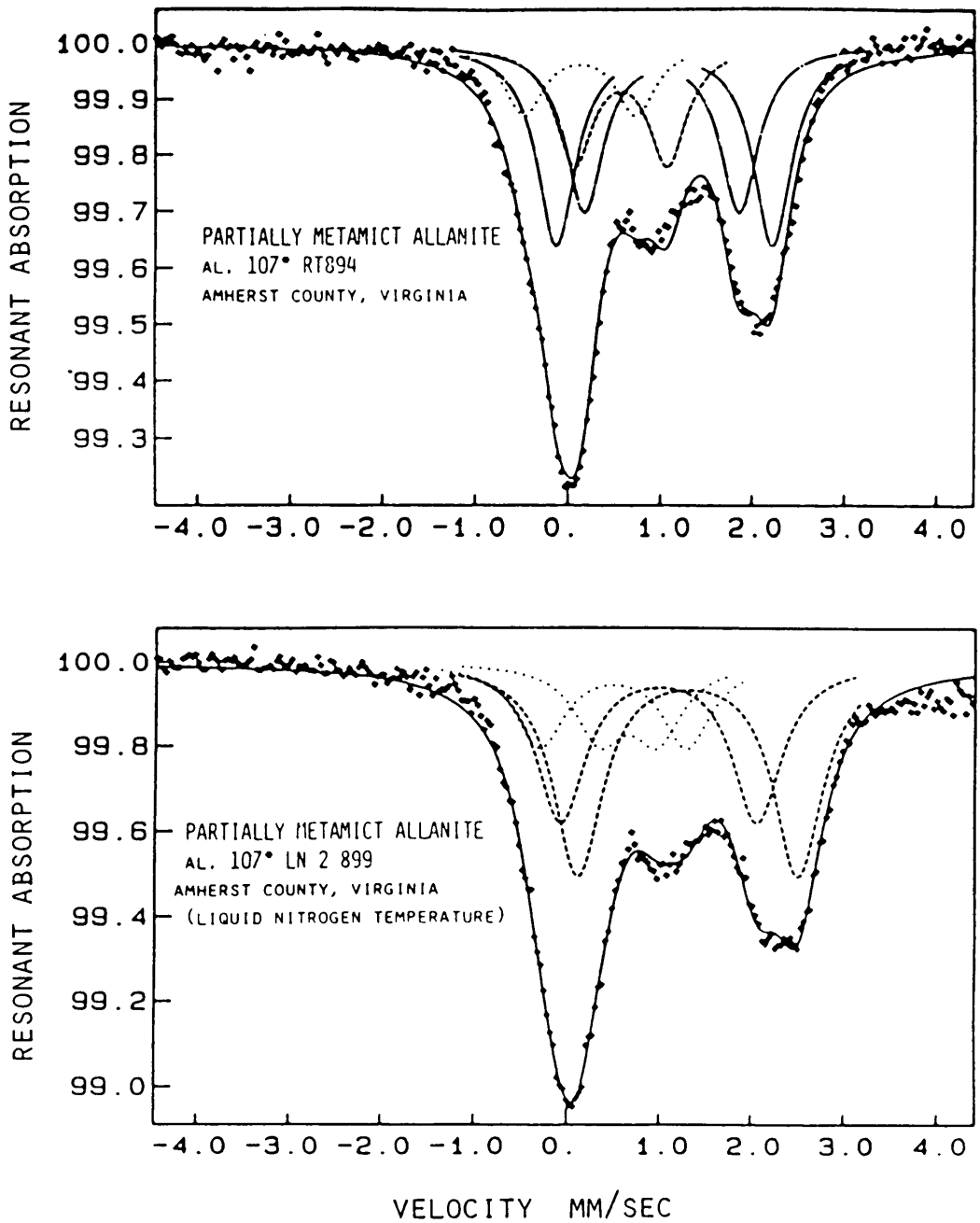
RESONANT ABSORPTION
100.0
99.9
99.8
99.7
99.6
99.5
99.4
99.3
PARTIALLY METAMICT ALLANITE
AL. 107° RT894
AMHERST COUNTY, VIRGINIA
-4.0 -3.0 -2.0 -1.0 0. 1.0 2.0 3.0 4.0
RESONANT ABSORPTION
100.0
99.8
99.6
99.4
99.2
99.0
PARTIALLY METAMICT ALLANITE
AL. 107° LN 2 899
AMHERST COUNTY, VIRGINIA
(LIQUID NITROGEN TEMPERATURE)
-4.0 -3.0 -2.0 -1.0 0. 1.0 2.0 3.0 4.0
VELOCITY MM/SEC

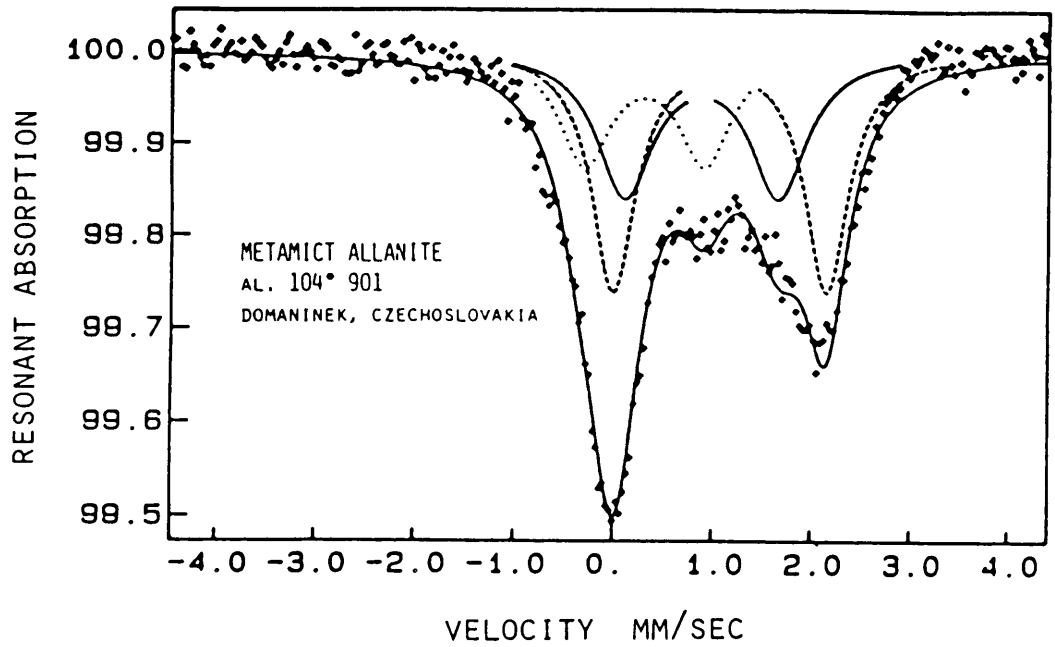
100.0
99.9
99.8
99.7
99.6
99.5
RESONANT ABSORPTION
METAMICT ALLANITE
AL. 104° 901
DOMANINEK, CZECHOSLOVAKIA
-4.0 -3.0 -2.0 -1.0 0. 1.0 2.0 3.0 4.0
VELOCITY MM/SEC

Table E1. ^{57}Mössbauer parameters for natural allanites. Absorber temperature 300 K.

Name Locality	Sample Number	Fe^{3+} IS mm/s	Fe^{3+} ΔEQ mm/s	Fe^{3+} FWHH mm/s	Fe^{3+} Int %	Fe^{2+}. IS mm/s	Fe^{2+}. ΔEQ mm/s	Fe^{2+}. FWHH mm/s	Fe^{2+}. Int %
metamict allanite Gloserheia, Norway	al. 103* 895	1.10	2.10	0.44	53.0	0.32	1.03	0.44	47.0
metamict allanite Domaninek, Czechoslovakia	al. 104* 901	0.98	1.85	0.61	67.0	0.30	1.21	0.63	23.0
metamict allanite Arendal, Norway	al. 105* 900	1.03	1.95	0.53	82.0	0.40	1.05	0.58	18.0
partially crystalline allanite Amherst Co., VA	al. 107* RT 894	1.02	2.00	0.50	66.0	0.28	1.20	0.50	33.0
partially crystalline allanite Amherst Co., VA	al. 107* LN2 899	1.16	2.26	0.64	71.0	0.57	1.11	0.64	29.0

*Mean of two doublets.

IS, EQ and FWHH are isomer shift, quadrupole splitting and full width at half height and given in mm/s (±0.01 mm/s). Int is the area under the absorption doublet and given in percent of the total absorption (±2%) IS relative to iron.

The vita has been removed from the scanned document